Sheffield Hallam University

A Sheffield Hallam University thesis

101 893 072 8

REFERENCE

Return to Learning Centre of issue
Fines are charged at 50p per hour

ProQuest Number: 10700915

ProQuest 10700915

Published by ProQuest LLC (2017). Copyright of the Dissertation is held by the Author.

ProQuest LLC.
789 East Eisenhower Parkway
P.O. Box 1346
Ann Arbor, MI 48106 – 1346

Investigation of ADAMTS-9 Expression in Models of Central Nervous System Inflammation

Martin James Reid

A thesis submitted in partial fulfilment of the requirements of
Sheffield Hallam University for the degree of Doctor of Philosophy

October, 2007

Abstract

The ADAMTSs (a disintegrin and metalloproteinase with thrombospondin type 1-like motifs) are a group of peptidases with important roles in normal physiology and pathology. ADAMTS-9 is expressed in the central nervous system (CNS) and has been reported to cleave aggrecan and versican, which are chondroitin sulphate proteoglycans (CSPGs) with critical roles in the extracellular matrix (ECM) of the brain. CSPGs are structural components of the glial scar, which forms in response to destructive CNS inflammation, inhibiting axonal outgrowth but protecting neurones against inflammatory infiltrates. Therefore, ADAMTS-9 has the potential to be involved in normal processing of the brain ECM as well as contributing to or protecting against pathology. In this study the expression of ADAMTS-9 was analysed in CNS-derived cells *in vitro* under basal conditions and following treatment with factors pertinent to CNS inflammatory disorders. ADAMTS-9 expression was also analysed in rat brains following transient middle cerebral artery occlusion (tMCAo), a model of focal cerebral ischaemia.

Real-time RT-PCR data demonstrated that ADAMTS-9 mRNA was constitutively expressed by human astrocytic (U373-MG, U87-MG and B327-01), microglial (CHME3) and neuronal (SHSY-5Y) cell lines *in vitro*, under basal conditions. In U373-MG cells, ADAMTS-9 mRNA expression was increased 25 and 8-fold following treatment with 1 ng/mL interleukin-1 beta (IL-1β) and tumour necrosis factor (TNF) respectively. In B327-01 cells, IL-1β (100 ng/mL) modulated a 6-fold increase in ADAMTS-9 mRNA expression. In contrast, treatment with 1 ng/mL interferon-gamma (IFN-γ) led to a decrease in ADAMTS-9 expression in B327-01 cells. The effect of IFN-γ in CHME3 cells differed to that observed in B327-01 in that 10 ng/mL increased expression of ADAMTS-9 mRNA 2-fold in the astrocytic cells. The study also demonstrated that ADAMTS-9 mRNA expression was modulated by retinoic acid in SHSY-5Y cells. Immunocytochemical analysis of U373-MG cells indicated that ADAMTS-9 protein is localised in the nucleus under basal conditions.

Real-time RT-PCR analysis of ADAMTS-9 mRNA expression demonstrated it was up-regulated in tMCAo tissue compared to sham-operated at 6, 24 and 120 h post-procedure. In addition ADAMTS-9 mRNA levels were higher in ipsilateral (occluded) hemispheres when compared to contralateral (non-occluded) hemispheres in tMCAo

i

brains. Western blotting indicated that the mature form of the ADAMTS-9 protein was only detected in brains subjected to tMCAo at 24 h. An ADAMTS-9-specific riboprobe was generated by subcloning and expression of a plasmid containing ADAMTS-9 cDNA in the XL-1 blue strain of *E. coli* followed by *in vitro* transcription and labelling with digoxigenin (DIG). The probe was utilised to perform *in situ* hybridisation, which showed that neurones were the predominant cell-type expressing ADAMTS-9 mRNA in tMCAo tissue.

Preliminary bioinformatical analysis of the putative human and rat ADAMTS-9 promoter regions demonstrated that consensus binding sites for transcription factors (nuclear factor kappa B [NFκB], activator protein 1 [AP-1], hypoxia inducible factor-1 [HIF-1] and interferon regulatory factor 1 [IRF-1]) pertinent to CNS inflammation were present in the sequence. Such transcription factors are potentially involved in activating the expression of ADAMTS-9 expression. Consequently, this study confirms that ADAMTS-9 is expressed by endogenous CNS cells and its expression is modulated by CNS inflammatory conditions both *in vitro* and *in vivo*.

Contents

List of Figures

Chapter 1

Chapter 2

Chapter 3

Chapter 4

Chapter 5

Chapter 6

Chapter 7

List of Tables

List of Abbreviations

AD Alzheimer's disease

ADAM a disintegrin and metalloproteinase

ADAMTS a disintegrin and metalloproteinase with thrombospondin type 1-like motifs

Adamts ADAMTS gene

AGE agarose gel electrophoresis

AP alkaline phosphatase

AP-1 transcription factor activator protein 1

BBB blood-brain barrier

BCA bicinchonic acid

BCIP/NBT 5-bromo-4-chloro-3'-indolyphosphate p-toluidine salt/nitro-blue tetrazolium chloride

BM basement membrane

bp base pair

BSA bovine serum albumin

cDNA complementary DNA

CH contralateral hemisphere

CJD Creutzfeldt-Jakob disease

CNS central nervous system

CRD cysteine-rich domain

CSPG chondroitin sulphate proteoglycan

CUB cubulin

DAPI 4'-6-Diamidino-2-phenylindole

dNTP deoxynucleotide triphosphate

ddNTP dideoxynucleotide triphosphate

dsDNA double stranded DNA

DTT dithiothreitol

EAE experimental autoimmune encephalomyelitis

EC endothelial cell

ECM extracellular matrix

EDTA ethylenediamine tetraacetic acid

ER endoplasmic reticulum

FCS foetal calf serum

GAG glycosaminoglycan

GEP glutamyl endopeptidase

GF growth factor

GFAP glial fibrillary acidic protein

H&E stain haematoxylin and eosin stain

HIF-1 hypoxia inducible factor 1

HRP horseradish peroxidase

HSPG heparan sulphate proteoglycan

ICC immunocytochemistry

IFN-γ interferon-γ

IFN-γR IFN-γ-receptor

Ig immunoglobulin

IGD interglobular domain

IH ispilateral hemisphere

IHC immunohistochemistry

IL interleukin

IL-1R interleukin-1 receptor

IL-1ra interleukin-1 receptor antagonist

IOD integrated optical density

IRF-1 interferon regulatory factor 1

*IV*T *in vitro* transcription

KO knock-out (mice)

LDS lithium dodecyl sulphate

MAPK mitogen activated protein kinase

mBSA methylated bovine serum albumin

MMP matrix metalloproteinase

*M*r molecular mass

mRNA messenger RNA

MS multiple sclerosis

NF-κB nuclear factor-kappa B

NGF nerve growth factor

NK natural killer (cells)

NT-3/4 neurotrophin 3/4

NTF neurotrophic factor

OA osteoarthritis

PC proprotein convertase

PBS phosphate-buffered saline

PD Parkinson's Disease

PFA paraformaldehyde

PLAC proteinase and lacunin

PNN perineuronal nets

RA rheumatoid arthritis

RetA retinoic acid

RetAR retinoic acid receptor

RPE retinal pigment endothelium

RT reverse transcriptase

RT-PCR reverse transcriptase-polymerase chain reaction

SDHA succinate dehydrogenase complex, subunit A

SDS-PAGE sodium dodecyl sulphate-polyacrylamide gel electrophoresis

siRNA short interfering ribonucleic acid

SLCD subtilisin-like catalytic domain

SSC sodium chloride-sodium citrate in distilled H_2O

ssDNA single stranded DNA

SVD snake venom disintegrin

TBS Tris-buffered saline

TBST Tris-buffered saline/0.05% Tween 20

TGF transforming growth factor

TGN trans-Golgi network

TIMP tissue inhibitor of metalloproteinase

TM transmembrane (domain)

tMCAo transient middle cerebral artery occlusion

TNF tumour necrosis factor

TNFR tumour necrosis factor receptor

TSP1 thrombospondin type 1-like motif

UBC ubiquitin C

UL-vWF 'unusually large'-von Willebrand Factor

WT wild-type

YWHAZ tyrosine 3-monooxygenase activation protein, zeta polypeptide

ZBM zinc-binding motif

Publications Relevant to this Thesis

Manuscript in Preparation

Reid, MJ, Cross, AK, Haddock, G, Allan, SM, Stock, CJ, Apte, SS, Woodroofe, MN, Buttle, DJ, Bunning, RAD (2007). ADAMTS-9 Expression is Up-Regulated following Transient Middle Cerebral Artery Occlusion (tMCAo) in the Rat and its Cellular Origin is Predominantly Neuronal. **In Preparation**

Published Abstracts

Reid, MJ, Cross, AK, Haddock, G, Woodroofe, MN, Buttle, DJ, Bunning, RAD (2005). Pro-Inflammatory Cytokines Modulate ADAMTS-9 mRNA Expression in Human CNS-Derived Cell Lines. International Journal of Experimental Pathology **86**; A57-A94

Reid, MJ, Cross, AK, Haddock, G, Allan, SM, Stock, CJ, Apte, SS, Woodroofe, MN, Buttle, DJ, Bunning, RAD (2006). ADAMTS-9 is Up-Regulated at the mRNA Level following Middle Cerebral Artery Occlusion (MCAo) in Rats. International Journal of Experimental Pathology **87**; A1-A58

Reid, MJ, Cross, AK, Haddock, G, Allan, SM, Stock, CJ, Apte, SS, Woodroofe, MN, Buttle, DJ, Bunning, RAD (2007). Studies of the Expression of ADAMTS-9 in the Middle Cerebral Artery Occlusion (MCAo) Model of Stroke. International Journal of Experimental Pathology **88**; A1-A45

Acknowledgements

1.1 The ADAMTSs

1.1.1 Overview of Peptidases

Peptidases are enzymes that hydrolyse peptide bonds. In the human genome, 1.6 % (over five-hundred) of all genes encode for peptidases and their inhibitors (Rawlings *et al*, 2006). Exopeptidases are peptidases that hydrolyse a bond close (within three residues) to either the N-terminus or C-terminus (or both). Alternatively, the hydrolysis of internal (away from N-terminus or C-terminus) α-peptide bonds is the hallmark of endopeptidases, which includes oligopeptidases that act on substrates smaller than proteins (peptides) (Rawlings *et al*, 2004). Endopeptidases vary in the type of catalysis they perform and examples include the serine-, aspartic-, threonine- and metallo-proteinases.

The term given to a peptide bond which is hydrolysed by a peptidase is 'scissile bond'. Many peptidases have substrate specificity for certain amino acids that make up scissile bonds as well as the location within the substrate. The active site of peptidases is located in a structural groove along which a substrate can bind at different sites (subsites). A method of representing the substrate specificity taking into account subsites as well as the location of the scissile bond within the substrate was originally described by Schechter & Berger (1967) and is shown below:

<div align="center">

scissile
bond
↓

Substrate: - P3 - P2 - P1 + P1' - P2' - P3' -

Peptidase: - S3 - S2 - S1 * S1' - S2' - S3' -

</div>
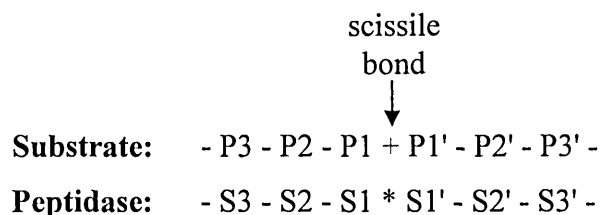
Where: + = scissile bond, * = catalytic site, S/Pn = subsite/peptide numbered from catalytic site/scissile bond to N-terminus, S/Pn' = subsite/peptide numbered from catalytic site/scissile bond to C-terminus.

The MEROPS database is a valuable resource, providing a hierarchical system of classification of about three-thousand peptidases and their inhibitors in many different organisms (Rawlings *et al*, 2006). MEROPS classifies into families; peptidases with

relationships in amino acid sequence in the part of the molecule termed the 'peptidase unit' (catalytic site). MEROPS also classifies peptidases into clans, which contain families with common ancestry. Sets of families in which all the peptidases have diverged from a single gene over time are grouped into clans, of which there are about forty.

1.1.2 The M12 Peptidase Family

The M12 family contains peptidases with a metallopeptidase catalytic site: His-Glu-Xaa-Xaa-His-Xaa-Xaa-Gly-Xaa-Xaa-His (where His residues are ligands of a zinc atom). Members of the M12 family have been shown to be expressed in bacteria, protozoa, fungi and animals and include; ADAMs (a disintegrin and metalloproteinase) (also known as adamalysins), the snake venom metalloproteinases (reprolysins) and the ADAMTSs (a disintegrin and metalloproteinase with thrombospondin type 1-like motifs).

The M12 family, along with a variety of other metallopeptidases is contained within clan MA. The families in clan MA all contain the motif Xaa-Xbb-Xcc-His-Glu-Xbb-Xbb-His-Xbb-Xdd (where Xaa is hydrophobic or Thr, Xbb is uncharged, Xcc is any amino acid except Pro, and Xdd is hydrophobic) (Jongeneel et al, 1989). Clan MA peptidases also possess a third zinc ligand towards the C-terminus, the nature of which varies depending on the subclan to which the peptidase belongs. The M12 family is categorised as being in subclan MA(M). The other subclan of clan MA is MA(E).

All secreted proteinases including those belonging to both MA(E) and MA(M) subclans are synthesised as proenzymes. The general difference between the two is that some MA(E) subclan peptidases are activated by removal of an N-terminal propeptide (e.g. by furin-cleavage) (Kessler & Safrin, 1994). Alternatively, peptidases in some families of the MA(M) subclan are secreted as latent proenzymes requiring activation by proteolytic cleavage of an amino terminal domain to expose the active catalytic site ('cysteine-switch' mechanism) (Van Wart & Birkedal-Hansen, 1990). Virtually all the peptidases in the MA(M) subclan that lack the 'cysteine switch' contain a Tyr located 2 residues beyond Met of the Met-turn (described in Section 1.1.4.2). Peptidases in subclan MA(M) are termed metzincins because of the presence of zinc-binding segments and a Met-turn in the catalytic domain.

The M12 family can be divided into two subfamilies. The M12A subfamily is also known as the Astacin family, so named after the crayfish metalloproteinase astacin. The M12B subfamily (Adamalysin) contains a total of thirty-two peptidases found in *Homo sapiens* including the ADAMs and ADAMTSs. Figure 1.1 shows the phylogenetic (evolutionary) tree of the human members of the M12B family. A phylogenetic tree displays the evolutionary relationship between the different peptidases by aligning the sequences and calculating the percentage difference.

1.1.3 Overview of ADAMTSs

In 1997, Kuno *et al* transplanted colon adenocarcinoma cells into mice and screened the resultant tumour for genes which were expressed *in vivo* to further understand cancer cachexia pathogenesis. One novel complementary DNA (cDNA) clone was identified which encoded a cysteine-rich protein related to the ADAMs in that it contained a prodomain, a metalloproteinase domain and a disintegrin-like domain. The protein possessed thrombospondin type 1-like motifs (TSP-1) absent in the ADAMs, hence the name ADAMTS-1 was given to the protein and ADAMTS was used subsequently to describe a new group of peptidases with sequence similarity to the reprolysins. ADAMTSs lack the transmembrane (TM) domain present in ADAMs and thus have generally been considered to be secreted as opposed to membrane-bound, until recently (Koo *et al*, 2007).

Since ADAMTS-1 was discovered, eighteen more ADAMTS genes and the proteins they encode have been identified in humans. It is now believed that all the human ADAMTSs have been discovered, mainly due to the work of Cal *et al* (2002) who cloned the final seven members following a bioinformatics screen of the human genome. The complete list and phylogenetic tree of the ADAMTSs is displayed in Figure 1.2. All ADAMTSs have the same basic domain organisation as the prototype ADAMTS-1 with the main differences between the peptidases existing at the C-terminus. In addition to the ADAMTSs, three ADAMTS-like genes have been identified which encode proteins called ADAMTSL-1 (punctin), ADAMTSL-2 and ADAMTSL-3, containing ancillary ADAMTS domains but lacking obvious metalloproteinase domains and a disintegrin-like module (Wang *et al*, 2007).

Figure 1.1 *Homo Sapiens* Members of the M12B Family: Phylogenetic Tree
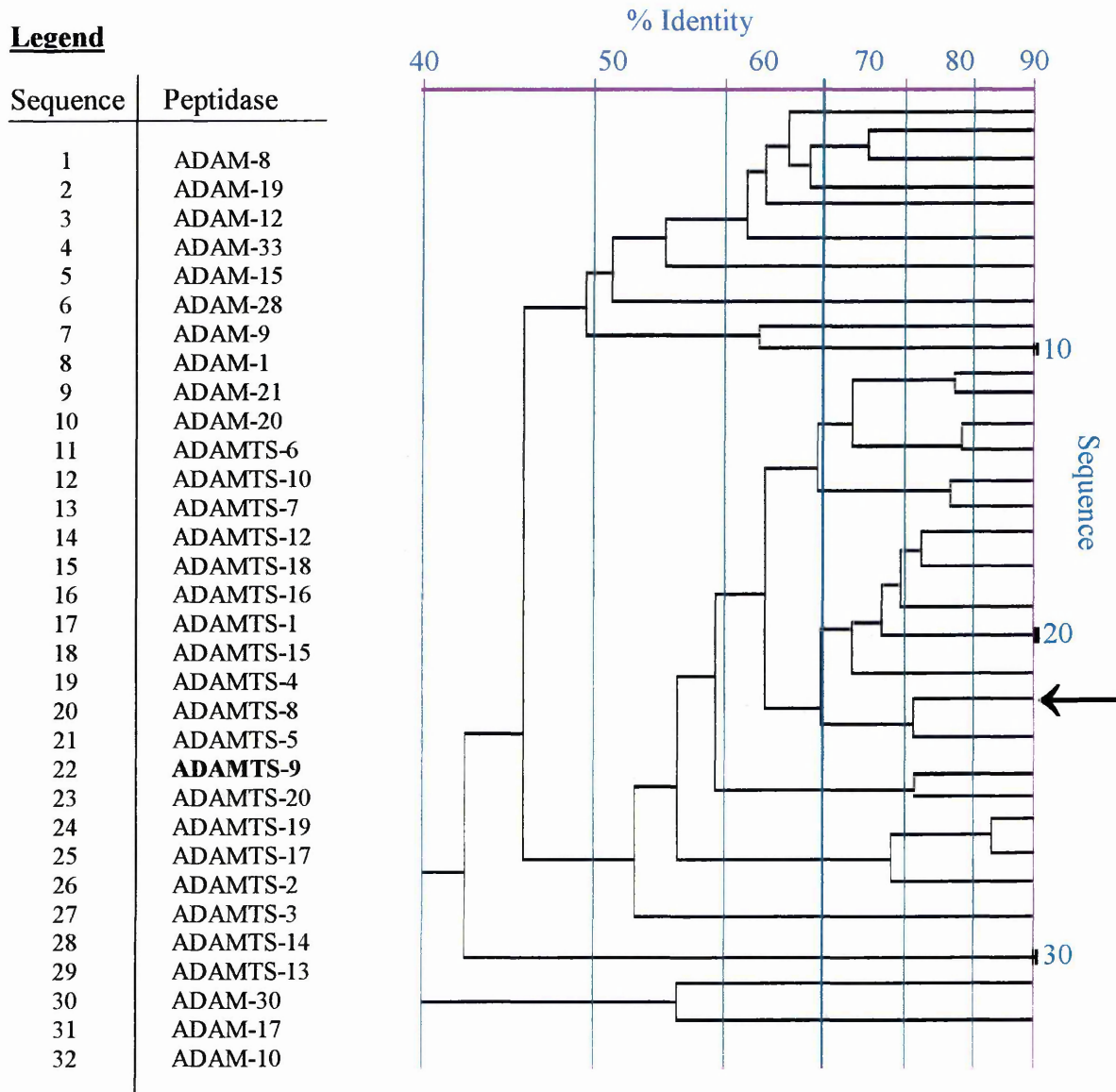
Legend

Sequence	Peptidase
1	ADAM-8
2	ADAM-19
3	ADAM-12
4	ADAM-33
5	ADAM-15
6	ADAM-28
7	ADAM-9
8	ADAM-1
9	ADAM-21
10	ADAM-20
11	ADAMTS-6
12	ADAMTS-10
13	ADAMTS-7
14	ADAMTS-12
15	ADAMTS-18
16	ADAMTS-16
17	ADAMTS-1
18	ADAMTS-15
19	ADAMTS-4
20	ADAMTS-8
21	ADAMTS-5
22	**ADAMTS-9**
23	ADAMTS-20
24	ADAMTS-19
25	ADAMTS-17
26	ADAMTS-2
27	ADAMTS-3
28	ADAMTS-14
29	ADAMTS-13
30	ADAM-30
31	ADAM-17
32	ADAM-10

Tree adapted from MEROPS Peptidase Database. % identity relates to how similar the primary sequences are following a multiple sequence alignment of peptidase units. The peptidase unit is defined as 'the part of the protein sequence that is directly responsible for peptidase activity' i.e. aligns with the smallest mature peptidase molecule in the family (Rawlings *et al*, 2006). ADAMTS-9 represented by '←'.

Figure 1.2 ADAMTS Phylogenetic Tree

Sequence	ADAMTS
1	ADAMTS-6 (*H. sapiens*)
2	ADAMTS-10 (*H. sapiens*)
3	ADAMTS-10 (*M. musculus*)
4	ADAMTS-10 (*R. norvegicus*)
5	ADAMTS-7 (*G. gallus*)
6	ADAMTS-7 (*H. sapiens*)
7	ADAMTS-7 (*R. norvegicus*)
8	ADAMTS-12 (*M. musculus*)
9	ADAMTS-12 (*H. sapiens*)
10	ADAMTS-12 (*R. norvegicus*)
11	ADAMTS-18 (*M. musculus*)
12	ADAMTS-18 (*H. sapiens*)
13	ADAMTS-16 (*M. musculus*)
14	ADAMTS-16 (*H. sapiens*)
15	ADAMTS-16 (*C. intestinalis*)
16	ADAMTS-1 (*H. sapiens*)
17	ADAMTS-1 (*E. caballus*)
18	ADAMTS-1 (*M. musculus*)
19	ADAMTS-1 (*R. norvegicus*)
20	ADAMTS-15 (*H. sapiens*)
21	ADAMTS-15 (*R. norvegicus*)
22	ADAMTS-4 (*P. troglodytes*)
23	ADAMTS-4 (*H. sapiens*)
24	ADAMTS-4 (*M. musculus*)
25	ADAMTS-4 (*R. norvegicus*)
26	ADAMTS-4 (*C. porcellus*)
27	ADAMTS-8 (*M. musculus*)
28	ADAMTS-8 (*R. norvegicus*)
29	ADAMTS-8 (*H. sapiens*)
30	ADAMTS-5 (*R. norvegicus*)
31	ADAMTS-5 (*M. musculus*)
32	ADAMTS-5 (*H. sapiens*)
33	**ADAMTS-9 (*H. sapiens*)**
34	ADAMTS-9 (*R. norvegicus*)
35	ADAMTS-9 (*G. gallus*)
36	ADAMTS-20 (*M. musculus*)
37	ADAMTS-20 (*H. sapiens*)
38	ADAMTS-19 (*H. sapiens*)
39	ADAMTS-19 (*M. musculus*)
40	ADAMTS-17 (*H. sapiens*)
41	ADAMTS-3 (*G. gallus*)
42	ADAMTS-3 (*H. sapiens*)
43	ADAMTS-14 (*H. sapiens*)
44	ADAMTS-13 (*M. musculus*)
45	ADAMTS-13 (*R. norvegicus*)
46	ADAMTS-13 (*H. sapiens*)
47	ADAMTS-13 (*G. gallus*)

Tree adapted from MEROPS Peptidase Database. % identity relates to how similar the primary sequences are following a multiple sequence alignment of peptidase units (Rawlings *et al*, 2006). ADAMTS-9 represented by '←'.

Documented roles of ADAMTSs include processing of procollagens (ADAMTS-2, -3 and -14), von Willebrand factor (ADAMTS-13) and extracellular matrix (ECM) components such as chondroitin sulphate proteoglycans (CSPGs) (ADAMTS-1, -4, -5, -8 and -9) (reviewed by Flannery, 2006). ADAMTSs have also been demonstrated to mediate connective tissue organisation, coagulation, inflammation, arthritis, angiogenesis and cell migration (reviewed by Tang, 2001).

1.1.4 Basic Domain Structure/Function

ADAMTS peptidases have the same basic domain organisation as illustrated in Figure 1.3, in that they all possess (from N-terminus to C-terminus) a signal peptide, prodomain, metalloproteinase domain, disintegrin-like domain, central TSP-1 motif, cysteine-rich domain (CRD), spacer region and C-terminal TSP-1 motifs. The 'proteinase domains' (from signal peptide up to and including metalloproteinase domain) are highly conserved between ADAMTSs (except ADAMTS-13). The main structural difference between ADAMTSs occurs at the C-terminal ancillary domains, where the number of TSP-1 motifs varies. Many ADAMTSs also contain additional domains (e.g. a cubulin [CUB] motif) at the C-terminus which (as described in Section 1.1.4.3) potentially influences the function of the peptidase (Tao *et al*, 2005).

1.1.4.1 Signal Peptide and Prodomain

The amino-terminal signal peptide of ADAMTSs directs the post-translational transport of the peptidase into the secretory pathway via the endoplasmic reticulum (ER), involving a signal recognition particle. The size of the signal peptide varies in length between ADAMTSs (~5-30 amino acids) and is removed prior to the secretion of the protein from the cell (Dunn *et al*, 2006).

The prodomain displays a high level of sequence similarity between the ADAMTSs and is generally of a comparable length throughout (220-300 amino acids). The exception to this rule is ADAMTS-13, which has a significantly smaller prodomain (74 amino acids). In fact this is the only notable structural variability between all the ADAMTSs within the 'proteinase domains' (N-terminus). It has been widely reported that the prodomain of ADAMTSs contain highly conserved residues, which are of importance in the maturation, protein folding and secretion of these peptidases (Longpré and Leduc, 2004;

7

Figure 1.3 Basic Domain Structure of the ADAMTSs
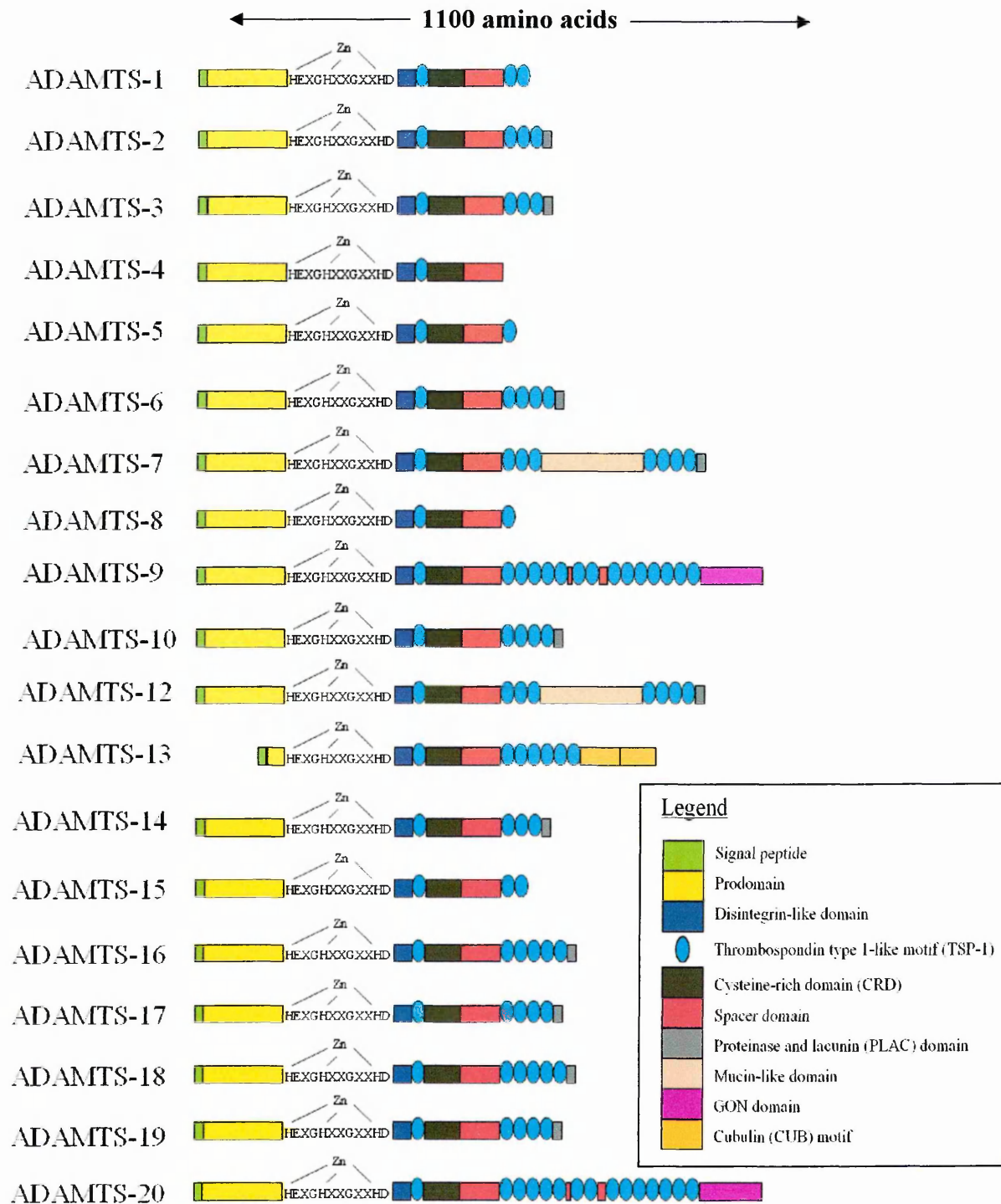
The ADAMTSs have the same general structure in that they all contain a signal peptide, prodomain, metalloproteinase domain, disintegrin-like domain, central TSP-1, CRD, spacer domain and variable numbers of C-terminal TSP-1 motifs. Additional domains are present at the C-terminus of specific ADAMTSs including PLAC, mucin-like, GON and CUB domains. Note: HEXGHXXGXXHD ('X' = any amino acid residue) represents the zinc-binding motif of metalloproteinase domain (not the full sequence of domain). Adapted from Porter *et al* (2005).

Cao *et al*, 2000). Most ADAMTSs contain three cysteine residues in the prodomain with the exception of ADAMTS-2, -3, -14 (which contain two) and -13 (one). The presence of a prodomain is generally considered to confer latency on ADAMTS enzymatic activity as it has been shown to do for other members of the MA clan (Hijova, 2005).

1.1.4.2 Metalloproteinase Domain

A 193-249 residue metalloproteinase domain as shown in Figure 1.4 enables ADAMTSs to function as peptidases. There is a high level of sequence similarity between the catalytic domains of the different ADAMTSs with an average sequence identity (ASI) of 43%. It is worth noting that the catalytic domain of ADAMTSs is also highly similar to that of the ADAMs with an ASI of 24% between the two types of peptidases (Andreini *et al*, 2005). The domain consists of a reprolysin-type zinc-binding motif (ZBM) containing three conserved His in the C-terminal region, HEXGHXXGXXHD ('X' = any amino acid residue). The conserved aspartic acid residue (D) distinguishes the ADAMTSs (and ADAMs) from other metalloproteinases (Porter *et al*, 2005).

In order for ADAMTSs to be catalytically active, it is essential for a zinc ion to be bound to the His residues within the ZBM. The zinc activates a water molecule by removal of a hydrogen, rendering it a reactive nucleophile with the ability to attack peptide carbonyl groups (Berg *et al*, 2002). The glutamate (E) has been shown to have an important role in this mechanism by polarising (deprotonation) the water molecule through hydrogen bonding (Andreini *et al*, 2005). Yiallouros *et al* (2000) performed site directed mutagenesis to substitute glutamate for alanine in astacin, the prototype member of the metzincin superfamily. The resultant mutant was unable to cleave known substrates of astacin, whereas the wild-type (WT) was.

In common with other members of subclan MA(M), ADAMTS metalloproteinase domains have a conserved methionine residue within the sequence V/IMA/S C-terminal to the ZBM (10-20 amino acids after 3rd His), which forms the 'Met-turn'. The crystallographic structure of the Met-turn was characterised by Bode *et al* (1993) and it is known to provide a hydrophobic environment for the zinc ion and the three His residues in the catalytic site. It is thought that the presence of the Met-turn also

Figure 1.4 Catalytic (Metalloproteinase) Domain of ADAMTSs
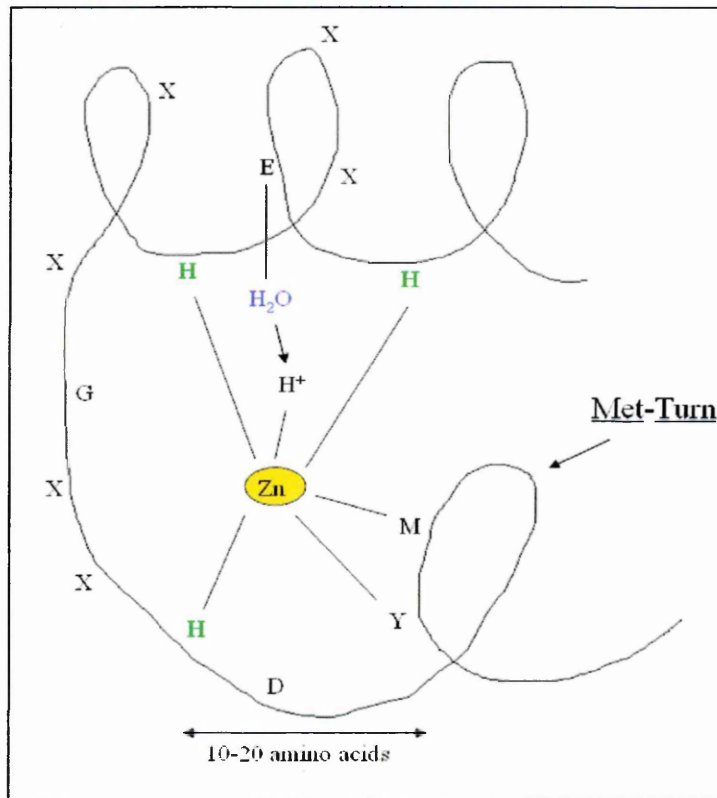
Simplified interpretation of the 'peptidase unit' of ADAMTSs showing the binding of the zinc ion to the His residues. Note the importance of the interaction of the glutamate with the H_2O molecule in the catalytic mechanism. G, E, H, M, Y, D represent amino acids (single-letter code). X = any amino acid. Adapted from Bode *et al* (1993).

contributes to the catalytic properties of the ADAMTSs because of the presence of a tyrosine residue. Using methods described above, Yiallouros *et al* (2000) showed that the presence of the Tyr residue increased astacin catalytic activity 40-fold. The group proposed that the Tyr stabilised the substrate binding to the zinc ion during hydrolysis.

1.1.4.3 Ancillary Domains

The domains C-terminal to the metalloproteinase domain are known as the ancillary domains. All ADAMTSs have a highly conserved 60-90 amino acid domain with primary sequence similarity to snake venom disintegrins (SVD), hence the name 'disintegrin-like domain'. SVDs are low molecular mass (M_r), cysteine-rich peptides which bind to cell-surface adhesion molecules; the integrins (Huang, 1998). Some SVDs contain a characteristic arginine/glycine/aspartic acid (RGD) integrin-recognition sequence, although this is lacking from the disintegrin-like domain and there is no evidence to suggest ADAMTSs adhere to integrins. This differs from many ADAM enzymes where the corresponding region is involved in integrin-mediated adhesion e.g. the binding of ADAM-2 to $\alpha_6\beta_1$ during sperm passage through oviducts (Kim *et al*, 2005).

C-terminal to the disintegrin-like domain is a highly conserved 48-54 amino acid central TSP-1, homologous to type I motifs seen in thrombospondins 1 and 2. The thrombospondins are glycoproteins proven to have a role in platelet function, wound healing, inflammation and angioinhibition (Bornstein, 2001). As well as having a single central TSP-1, ADAMTSs have additional TSP-1s at the C-terminus, ranging from zero (ADAMTS-4) to fourteen (ADAMTS-9, -20). The motifs of the C-terminal TSP-1s are far more variable than the highly conserved central TSP-1 and are usually arranged singly or in groups of two, three or four (except ADAMTS-9, -20 [both have TSP-1s in groups of four and seven] and -13 [a group of six]) separated by short linker peptides (reviewed by Jones & Riley, 2005).

Rather than have linker peptides between TSP-1s, ADAMTS-12 and -7 have a longer mucin-like domain between the third and fourth of their seven C-terminal TSP-1s, a region which is heavily O-glycosylated (Somerville *et al*, 2004). Similarities are drawn between mucin and the mucin-like domain because both are high in threonine, proline and serine residues (Porter *et al*, 2005). ADAMTS-7 has a glycosaminoglycan (GAG)

attached to the mucin-like domain, hence it can be described as a 'proteoglycan', a fact that could have profound effects on the peptidase's localisation and function (Somerville *et al*, 2004).

Immediately adjacent to the central TSP-1 is a highly conserved CRD containing ten cysteine residues. The next domain downstream to the CRD is a cysteine-free spacer region of 127-221 amino acids containing a conserved N-terminal region of hydrophobic amino acids and a highly variable C-terminal region (Hurskainen *et al*, 1999). Additional C-terminal domains are present in some ADAMTSs e.g. ADAMTS-13 contains two CUB domains, perhaps involved in binding to ligands such as an 'unusually large' multimer of von Willebrand factor (UL-vWF) (Zheng *et al*, 2001; Tao *et al*, 2005). The C-termini of ADAMTS-2, -3, -10, 14, -17 and -19 terminate with a forty-residue PLAC (proteinase and lacunin) domain containing six cysteines, originally observed in lacunin. As yet the function of the PLAC domain in ADAMTSs is largely unknown, although lacunin is an important ECM protein in basal lamina formation in lepidopteron *Manduca sexta* wing morphogenesis (Nardi *et al*, 2001).

The ancillary domains are highly important in terms of ADAMTS function, activation, localisation and substrate specificity. Rodríguez-Manzaneque *et al* (2000) demonstrated this by deleting two TSP-1s from the C-terminus of ADAMTS-1. The resulting protein had a decreased ability to inhibit endothelial cell (EC) proliferation as well as reducing the enzyme's affinity for sulphated GAG, heparin and EC cultures. Therefore it appears that the TSP-1s contribute to the angio-inhibitory properties displayed by recombinant full-length ADAMTS-1, reported in a study by Vazquez *et al* (1999). Further evidence implicating TSP-1s in the angio-inhibitory process came from the same study because thrombospondin-1 protein also inhibited vascular endothelial growth factor (VEGF)-mediated vascularisation. In fact thrombospondin-1 is now well known to be anti-angiogenic (Bocci *et al*, 2003).

1.1.4.4 Binding of ADAMTSs via the Ancillary Domains

It became apparent from early work on ADAMTSs that they sequester themselves into the ECM and that it is the ancillary domains that are responsible for this. The first observation of this property came from Kuno *et al* (1997) who demonstrated that the TSP-1 of ADAMTS-1 is functional for binding to heparin and almost certainly to the

structurally related heparan sulphate. Both molecules are composed of repeating disaccharide units, the difference being that only heparan sulphate GAG-side chains connect to core proteins to form proteoglycans (HSPGs) such as in syndecans, perlecan and the glypicans (glycosylphosphatidylinositol [GPI]-anchored protein) (Capila & Linhardt, 2002).

There have been further studies characterising the binding of ADAMTSs to substrates via the ancillary domains. When compared to the zymogen, isoforms of ADAMTS-4 (lacking cysteine-rich and/or spacer domains) (Flannery *et al*, 2002) and truncated ADAMTS-9 (lacking all domains C-terminus to the central TSP-1 motif) (Zeng *et al*, 2006) displayed a reduction in binding with heparin. Also full-length ADAMTS-4 and -5 bound to chondroitin sulphate with higher affinities than the autocatalytically produced isoforms. In contrast, the loss of these domains did not have an important effect on the heparin-binding affinity of ADAMTS-5 (Zeng *et al* 2006). It therefore appears that the binding properties of the ancillary domains vary between ADAMTSs and that removal of them alters the interactions of the peptidase with different ECM components.

It has become apparent that such binding of ADAMTSs to the ECM has a profound impact on catalytic activity. The fact that ADAMTSs can localise themselves to the ECM via GAGs is likely to be a contributing factor in their ability to cleave specific substrates e.g. proteoglycans containing GAG side-chains (lecticans). On the other hand the binding of ADAMTSs to ECM ligands may have an inhibitory effect on proteolytic activity by immobilising/sequestering the peptidase. For example, Hashimoto *et al* (2004) showed that the binding of ADAMTS-4 to the adhesion molecule fibronectin inhibited its cleavage of aggrecan.

1.1.5 Activation and Control of ADAMTSs

In contrast to the matrix metalloproteinases (MMPs), there is no conclusive evidence to suggest that ADAMTS activation occurs extracellularly via the 'cysteine-switch' mechanism. Despite an unpaired cysteine being present in the prodomain (XXCGVXD) of ADAMTSs, it has not been reported that it forms an inactivating bridge to the zinc atom forming the active site. Instead, ADAMTSs are synthesised as inactive 'full-length' zymogens prior to intracellular cleavage of the prodomain and subsequent

secretion as an active mature peptidase. It has been well documented that a ubiquitously expressed 794 amino acid proprotein convertase (PC) named furin is responsible for such activation in the secretory pathway. In fact all ADAMTSs (except ADAMTS-10, -12) have a furin cleavage consensus site (RXR/KR) located at the C-terminal end of the prodomain (reviewed by Porter *et al*, 2005).

Furin was the first PC to be identified (Bresnahan *et al*, 1990) and it has been shown to have important roles in many diseases as well as in protein trafficking (Thomas, 2002). It belongs to the subtilisin superfamily of serine peptidases which includes six other PCs (PC2, PC1/PC3, PC4, PACE4, PC5/PC6 and PC7). All the PCs contain a signal peptide, propeptide, subtilisin-like catalytic domain (SLCD), homo B domain and a CRD. In addition, furin, PC7 and an isoform of PC5/PC6 each contain a single TM domain (Nakayama, 1997). There is a level of amino acid sequence identity between all the PCs, the most similarity occurring in the SLCD (Thomas, 2002).

1.1.5.1 Evidence for Furin-Mediated Activation of ADAMTSs

The first report of furin-mediated activation of ADAMTSs was by Kuno *et al* (1999). The group transfected an ADAMTS-1 expression vector (X5) into a human colon carcinoma cell line (LoVo) which does not express functional furin. Western blotting showed that only the precursor (zymogen) form of ADAMTS-1 was detected in the culture supernatant. However, in a cell line expressing furin (COS-7), both the precursor and mature forms of ADAMTS-1 were detected. Furthermore, following the co-transfection of LoVo with furin cDNA and X5, the precursor form of ADAMTS-1 was not detected but the mature form was. Following on from these data, evidence for furin-cleavage activation was obtained for other ADAMTSs, with particular emphasis on ADAMTS-4. Gao *et al* (2002) reported that proADAMTS-4 (100 kDa) in media from a cell line transfected with ADAMTS-4 was converted to a smaller form (75kDa) by digestion with recombinant furin.

Following on from these preliminary experiments, Wang *et al* (2004) conducted an in-depth analysis of the processing of intracellular ADAMTS-4 by furin. Initially, ADAMTS-4 transfected cells (HEK293 and SQ1253) were used to show that cleavage of the prodomain was blocked by chloromethylketone (CMK), an inhibitor of furin. It was demonstrated that endogenous furin was responsible for the processing of

14

ADAMTS-4 by using siRNA (short interfering RNA) to block furin expression within the cells. The result was an increase in the levels of proADAMTS-4 protein when compared to cells that were not subjected to siRNA. The group also characterised three potential furin recognition sites between the prodomain and catalytic site of ADAMTS-4 (^{206}RPRR^{209}, ^{209}RAKR^{212}, ^{211}KR^{212}) as well as performing important studies to ascertain the location within the cell where furin cleavage of ADAMTS-4 occurred. By conducting experiments to block protein trafficking, it was shown that the processing of pro-ADAMTS-4 occurred in the trans-Golgi network (TGN) and not the ER (where furin is synthesised) or cell surface (where furin is also localised). The group also demonstrated by confocal microscopy that ADAMTS-4 was colocalised with furin in the TGN.

It has been demonstrated that furin-cleavage can occur at locations other than the TGN. Activation of ADAMTS-7 appeared to involve a multi-step mechanism with partial processing in the TGN prior to further removal of the prodomain at the cell surface (extracellular) by membrane-bound furin (Somerville *et al*, 2004). Another study showed that ADAMTS-9 was processed exclusively extracellularly at the cell surface by furin (Koo *et al*, 2006). The authors extended their analysis of ADAMTS-9 to show that the peptidase has unique properties in terms of activation and secretion. Experiments in HEK293F cells suggested that a) ADAMTS-9 requires the presence of the propeptide to be secreted, b) the ADAMTS-9 propeptide must be *N*-linked glycosylated in order for ADAMTS-9 to be secreted and it remains highly-resistant to furin cleavage throughout the secretory pathway, c) propeptide fragments and the catalytic domain of ADAMTS-9 remain non-covalently associated following furin processing, and surprisingly d) ADAMTS-9 cleaved versican more efficiently when the propeptide was still attached as opposed to it being cleaved by furin (Koo *et al*, 2007). However, these data are subject to conjecture as many of the experiments were performed with transfected mutants of ADAMTS-9 lacking many domains, which may influence peptidase maturation.

In a furin-deficient cell line (RPE.40), Wang *et al* (2004) showed that ADAMTS-4 was processed to a smaller form indicating that a furin-independent activation pathway exists for this peptidase. Following on from this evidence, Tortorella *et al* (2005) investigated five of the PCs, serine proteases (trypsin, chymotrypsin and plasmin) as well as twelve MMPs and ADAM-17 in respect to ADAMTS-4 activation. Out of this

comprehensive list of enzymes, it was shown that only PACE4, PC5/6B, furin (all by cleavage at Arg^{212}-Phe^{213}), MMP-9 and trypsin had the capacity to remove the prodomain. This work indicated that ADAMTS-4 activation occurs by a limited number of mechanisms and activators, a conclusion supported by the fact that MMP-9-processed ADAMTS-4 did not show aggrecanase activity.

1.1.5.2 Activation of ADAMTSs by C-Terminal Processing

It is clear that ADAMTSs are not solely cleaved at the N-terminus, but also at the C-terminus and that such processing has a significant effect on enzyme activity, substrate specificity and localisation. There are a number of mechanisms by which C-terminal processing of ADAMTSs is likely to occur including proteolysis by MMPs and autocatalysis.

There have been a number of studies that have implicated MMPs in ADAMTS C-terminal processing. Rodríguez-Manzaneque *et al* (2000) transfected kidney cells with the complete ADAMTS-1 cDNA prior to detecting only a 110 kDa unprocessed form in the cell layer. In contrast an 87 kDa and 65 kDa form was detected in the conditioned media. It was shown that the 87 kDa form was a result of prodomain cleavage by furin whereas the 65 kDa form was a result of additional processing events at the C-terminus (following initial furin-cleavage to produce p87). The group showed that MMP-2, MMP-8 and MMP-15 had the ability to cleave p87 to form p65. ADAMTS-4 has also been shown to be processed by MMPs (MMP-17) at the C-terminus (Gao *et al*, 2004).

Evidence that C-terminal processing has a direct effect on activation of ADAMTS catalytic activity was shown by Gao *et al* (2002). Only isoforms of ADAMTS-4 generated by C-terminal truncation (shown by domain-specific antisera) displayed aggrecanase and versicanase activity. Consistent with data by Rodríguez-Manzaneque *et al* (2000), C-terminal cleavage appeared to have occurred following initial prodomain removal by furin. Importantly, both studies identified the C-terminal cleavage site as being close to the same amino acid residue (744).

Another mechanism of ADAMTS C-terminal activation that has been described is autocatalysis. Flannery *et al* (2002) incubated purified recombinant full-length ADAMTS-4 at 37°C without the presence of any PCs or MMPs. The presence of

ADAMTS-4 isoforms that displayed aggrecanase activity suggested that autocatalytic activation by C-terminal clipping (showed by sequencing) had taken place. Autocatalysis has also been described for ADAMTS-1 generating N- and C-terminal cleavage fragments (Liu *et al*, 2005). When compared to full length ADAMTS-1, these fragments inhibited pulmonary metastasis in carcinoma cells by inhibiting cell signalling pathways, proliferation, survival and angiogenesis. An important observation was that autocatalysis was inhibited by HSPGs, suggesting that the interaction of ADAMTSs with the ECM has a bearing on activation.

Further evidence that ADAMTS activation occurs by removal of ancillary domains came from Kashiwagi *et al* (2004) who constructed ADAMTS-4 C-terminal domain deletion mutants. The results showed that deleting each of the ancillary domains had a profound effect on ADAMTS-4 activity and specificity. These data appeared to suggest that the spacer domain acts as an 'intramolecular suppressor', deletion of which coincided with ADAMTS-4 being able to cleave different substrates including carboxymethylated transferrin, fibromodulin and decorin. Further deletions of C-terminal domains created mutants that varied in ability to cleave different bonds within the aggrecan molecule and with different efficiencies. For example the spacer domain deletion mutant cleaved the Glu^{373}-Ala^{374} and Glu^{1480}-Gly^{1481} inter-globular bonds more effectively than a mutant lacking just the CRD.

Another study utilising domain deletion mutants showed that the CRD and spacer region are required for ADAMTS-13 to cleave UL-vWF (Soejima *et al*, 2003). This is an important finding because a lack of ADAMTS-13 and thus insufficient UL-vWF breakdown causes thrombotic thrombocytopenic purpura (TTP) which is characterised by thrombus formation, renal failure and neurological dysfunction (Zheng *et al*, 2001). The spacer region has also proved crucial for ADAMTS-1 to cleave aggrecan as shown by domain deletion studies (Kuno *et al*, 2000). The potential processing of ADAMTS-9 by removal of the signal peptide, prodomain and C-terminal domains is summarised in Figure 1.5.

1.1.5.3 Alternative Splicing of ADAMTSs

Another potential mechanism of ADAMTS regulation is pre-transcriptional via the generation of multiple isoforms. This phenomenon is caused by alternative splicing,

Figure 1.5 Potential Processing of ADAMTS-9
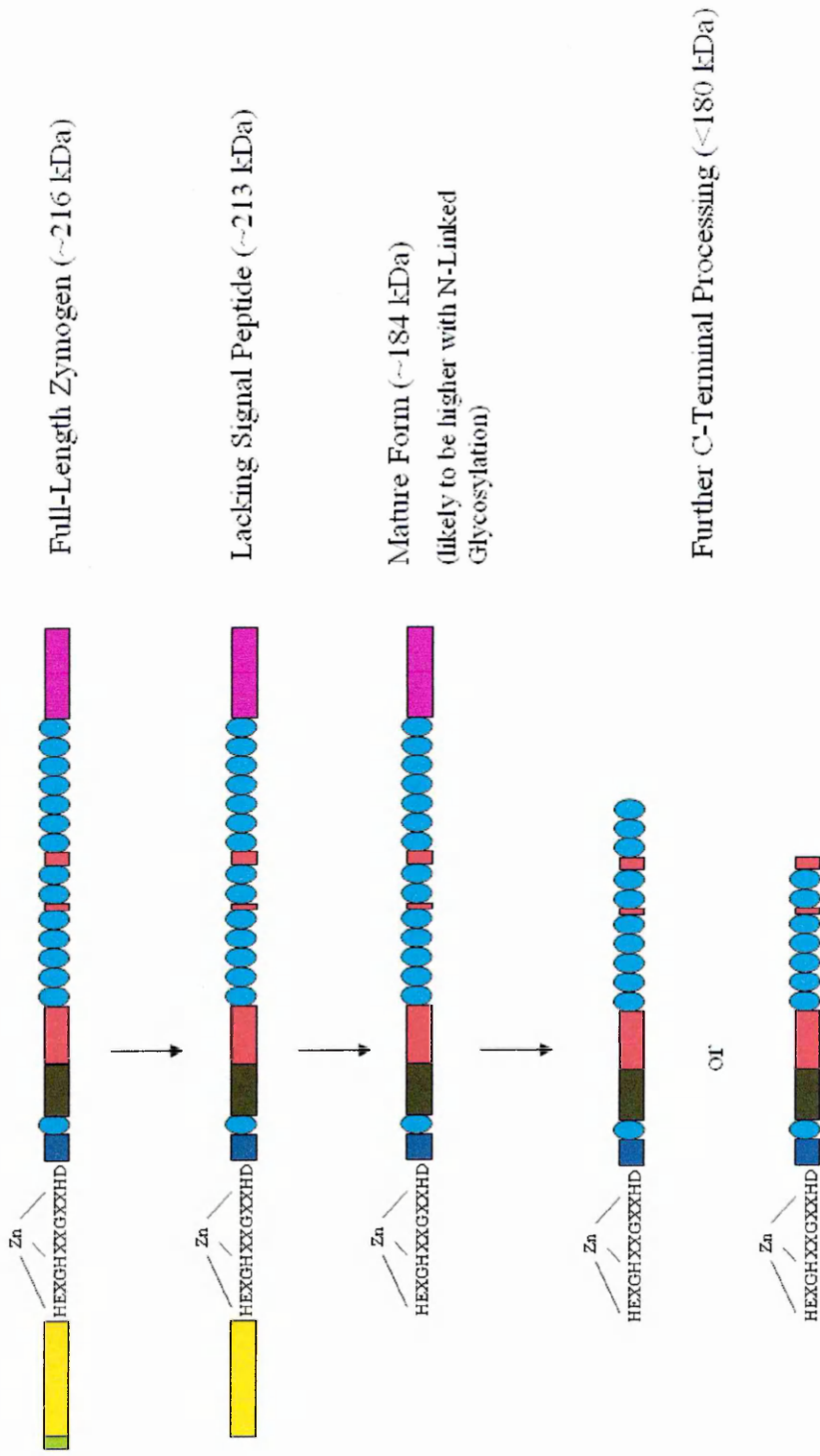
The various species of ADAMTS-9 following potential processing of the signal peptide, prodomain and C-terminal domains. Predicted $\underline{M}_r$ values from Somerville *et al* (2003). See Figure 1.3 for legend of ADAMTS-9 domains.

whereby pre-RNA exons are arranged in various ways to yield slightly different messenger RNA (mRNA) and hence proteins. Splice variants have been demonstrated for ADAMTS-6, -7, -9 and potentially -16 and -18 (reviewed by Jones & Riley, 2005). The generation of proteins with different C-terminal domain structures could be a mechanism of controlling the function of ADAMTSs.

1.1.6. Inhibitors of ADAMTSs

The ADAMTSs are important in many normal physiological roles such as angiogenesis, wound healing and development. It is important that ADAMTS activity is controlled to prevent the shift in balance from normal physiology to destructive pathological conditions. ADAMTSs are controlled at many levels including: transcriptional (e.g. cytokine modulation of transcription initiation), post-transcriptional (e.g. alternative splicing) and post-translational (e.g. prodomain or C-terminal cleavage) regulation. As is the case with all secreted eukaryotic proteinases, it is apparent that in order to counteract the destructive potential of ADAMTSs, endogenous inhibitors are present in the body as another form of regulation.

1.1.6.1 Tissue Inhibitors of Metalloproteinases (TIMPs)

Tissue inhibitors of metalloproteinases (TIMPs), of which there are four (TIMP-1, -2, -3 and -4), are the major endogenous inhibitors of the MMPs. Recent studies indicate that TIMP-3 is the main inhibitor of ADAMTSs, although TIMP-1 and TIMP-2 also show slight inhibitory capacity when used in higher concentrations *in vitro* (Hashimoto *et al*, 2001). Compared to ADAMTSs, TIMPs are relatively small proteins of between 21 and 34 kDa, with twelve conserved cysteine residues. The proteins are folded into two domains, with all the TIMPs containing a conserved binding site for proteinases (VIRAK amino acid sequence), in the domain responsible for the inhibitory activity, the N-terminal domain (Lambert *et al*, 2004).

There have been a number of studies implicating TIMP-3 in the inhibition of ADAMTSs. Hashimoto *et al* (2001) showed that TIMP-3 blocked aggrecan cleavage by ADAMTS-4 at a significantly lower concentration than TIMP-1 and TIMP-2 whereas TIMP-4 had no effect. Kashiwagi *et al* (2001) observed similar results with the N-terminal domain of TIMP-3 (N-TIMP-3), which blocked ADAMTS-4 and -5

cleavage of aggrecan *in vitro*. In contrast, N-TIMP-1 and TIMP-2 had no effect on aggrecanase activity of both ADAMTSs whereas TIMP-4 showed 35% inhibition when added in higher concentrations to ADAMTS-4 but not to ADAMTS-5. These data obtained by Kashiwagi *et al* would perhaps have been more conclusive if the full length TIMP-3 protein was utilised as opposed to the truncated construct lacking the C-terminus, which is perhaps crucial in directing the inhibitory effect of TIMP-3 *in vivo*. In fact the C-terminus is thought to be involved in binding to proenzymes as opposed to active metalloproteinases (Lambert *et al*, 2004).

TIMP-3 was also shown to inhibit ADAMTS-1 although in contrast to its action on ADAMTS-4 (as described above) not all activity was blocked (Rodríguez-Manzaneque *et al*, 2002). Further evidence that ADAMTSs have varying inhibitor profiles came from the same study, with TIMP-2 having a similar effect on ADAMTS-1 activity as TIMP-3. The question of where inhibition of ADAMTSs is occurring is an important one. TIMP-3 is the only TIMP known to bind to the ECM (via GAGs) (Yu *et al*, 2000), suggesting it has the potential to inhibit ADAMTSs in matrix-rich tissue e.g. cartilage or brain. Inhibition of ADAMTSs may also be taking place in the circulatory system because α_2-macroglobulin which is present in the blood (~2-4 mg/mL) has been shown to inhibit ADAMTS-4 and -5 (Tortorella *et al*, 2004).

1.1.6.2 Inhibition of ADAMTSs as Potential Therapies

The field of 'ADAMTS inhibition' is important in that potential therapies could be developed based on such studies. One such treatment could involve the augmentation or activation of endogenous TIMP-3. Another potential approach could be to use molecules/drugs to inhibit ADAMTSs directly. Therefore, as well as studying the TIMPs, Rodríguez-Manzaneque *et al* (2002) performed a comprehensive analysis of the effects of a number of synthetic inhibitors on ADAMTS-1 activity. Partial or total inhibition was observed with monoclonal antibodies (raised against ADAMTS-1 epitopes), metal (zinc) chelators such as ethylenediamine tetraacetic acid (EDTA), 1,10-phenanthroline and doxycycline, hydroxamates e.g. BB94, MMP inhibitor I and heparin. It has also been shown that catechin gallate esters, present in green tea inhibit ADAMTS-1, -4 and -5 (Vankemmelbeke *et al*, 2003).

With such a variety of roles for the ADAMTS peptidases in normal turnover, it could prove difficult to achieve beneficial tissue-specific inhibition *in vivo* to treat diseases where ADAMTS-induced proteolysis is a factor. There is a complex balance in all systems between inhibitors and enzymes which is lost during pathological conditions. Further understanding of the inhibitory mechanism of endogenous TIMPs as well as the pathways by which ADAMTS expression is modulated prior to activation is required before any ADAMTS-related therapeutic interventions can be contemplated.

1.2 Glutamyl Endopeptidase ADAMTSs

1.2.1 Overview

The glutamyl endopeptidases (GEPs) are defined as enzymes that cleave proteins at the carboxyl end of glutamate residues. ADAMTSs which are GEPs are among the most extensively studied because of their ability to cleave aggrecan, the major CSPG of cartilage, thus implicating them in arthritic disorders including osteoarthritis (OA) and rheumatoid arthritis (RA). For this reason the ADAMTS GEPs are also known as the aggrecanases and include ADAMTS-1, -4, -5, -8, -9 and -15 (and possibly ADAMTS-20 due to similar domain structure to ADAMTS-9) (reviewed by Porter *et al*, 2005). OA is characterised by progressive degeneration of articular cartilage ECM by an increase in proteinase activity and insufficient synthesis of new matrix components (reviewed by Hedbom & Häuselmann, 2002). Rheumatoid arthritis (RA) is a systemic autoimmune inflammatory disorder, caused by autoreactive T cells, cytokines, chemokines and proteinases, resulting in joint destruction (reviewed by Lee & Weinblatt, 2001).

The GEPs do not have greatly similar domain structures or primary sequences that are as highly conserved as the pro-collagen convertases. This suggests that the breakdown of collagen requires stringent structural requirements whereas aggrecan breakdown can be achieved with structurally diverse ADAMTSs. GEPs are expressed in a large number of tissue-types within the body and degrade substrates other than aggrecan e.g. the lectican; versican and cartilage oligomeric matrix protein (COMP, processed by ADAMTS-4), thus they are likely to have roles other than in cartilage turnover (reviewed by Flannery, 2006).

1.2.2 Chondroitin Sulphate Proteoglycans

The main substrates of ADAMTS GEPs are the proteoglycans, which are important components of the ECM, found in all tissue types including cartilage and the brain. Some of the functions of proteoglycans were summarised by Rhodes & Fawcett (2004) including; cellular adhesion and growth, binding to receptors, formation of barriers and interactions with other ECM constituents. Proteoglycans are comprised of a core protein carrying covalently bound, negatively charged GAG chains of ~20-200 residues in length. GAGs are unbranched chains of repeating disaccharide units usually consisting of an uronic acid and an amino sugar. The main types of proteoglycan known to be cleaved by GEPs all have chondroitin sulphate GAGs (CSPGs), although aggrecan also has keratan sulphate GAGs attached (Roughley, 2006).

The disaccharide unit of chondroitin sulphate GAGs is glucuronic acid which is linked to N-acetyl galactosamine via a β-glycosidic bond. Polymerisation into the long GAG chains is facilitated by human chondroitin synthase and chondroitin sulphate polymerising agent. The serine residues of proteoglycan core proteins are linked to GAGs by the sugar xylose (by xylosyltransferase). The position on the core protein where GAGs bind has a profound influence on the ability of the proteoglycan to bind to other molecules (Galtrey & Fawcett, 2007).

1.2.2.1 The Lecticans

A group of CSPGs that have been shown to be GEP substrates are the lecticans, which are structurally related in that they have similar N and C-terminal domains but vary in the size of core protein as well as the length and number of GAGs attached as shown in Figure 1.6. The lecticans are also known as the hyalecticans (or hyaladherins) because of their ability to bind non-covalently to hyaluronan, a GAG residing in the ECM and on cell-surfaces. This interaction is stabilised by a link protein, to which lecticans also bind. In mammals, there are four members of the lectican family, two of which are expressed throughout the body; aggrecan (cartilage, notochord, central nervous system [CNS]) and versican (virtually all connective tissue, blood vessels, mesenchyme, brain, kidney, cartilage) and two which are only found in the CNS; brevican and neurocan (reviewed by Viapiano & Matthews, 2006; Bandtlow & Zimmermann, 2000).

Figure 1.6 The Structure of the Lecticans
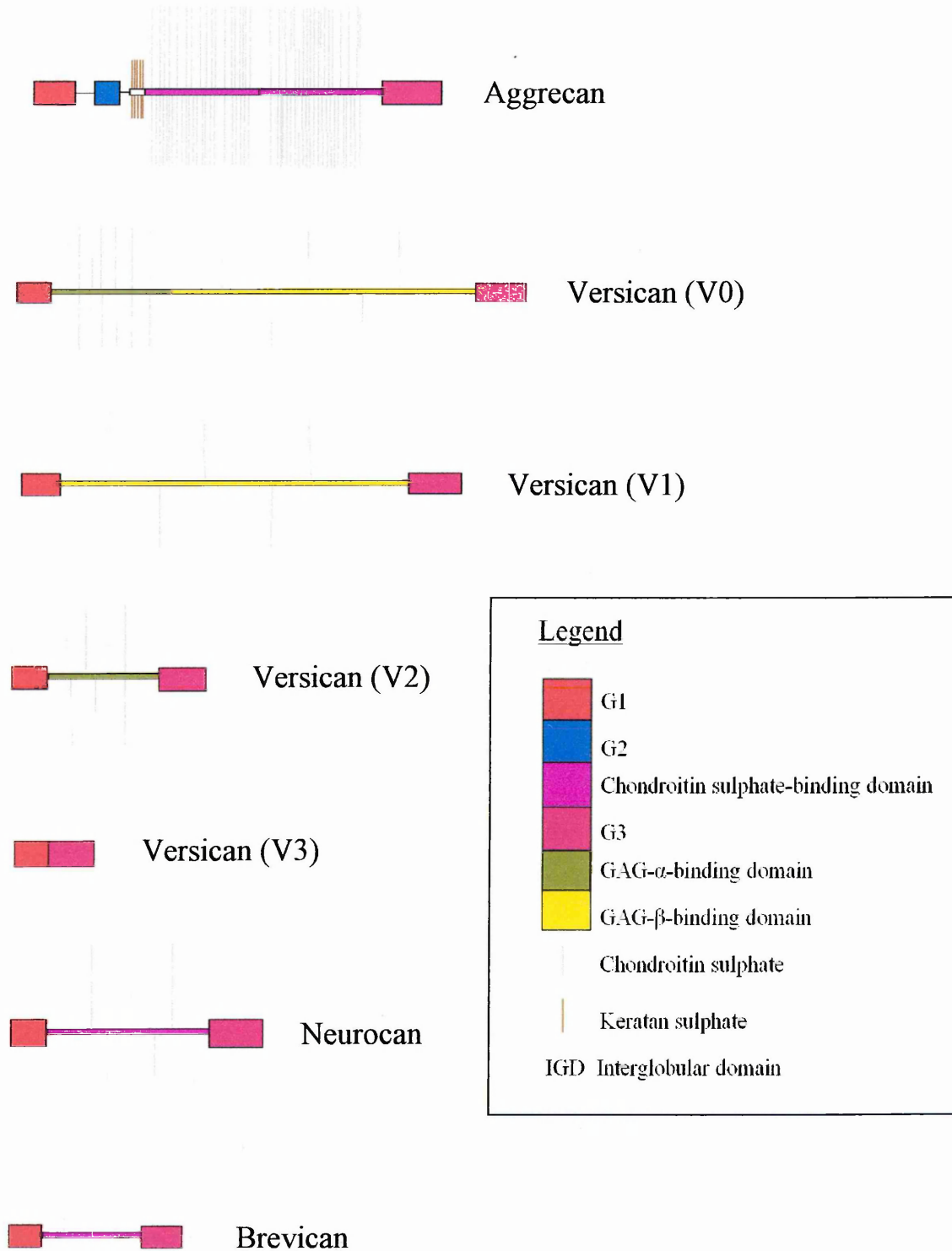
The figure demonstrates the similarities and differences between the lecticans. All lecticans contain G1 and G3 domains whereas the size of the core protein is variable as well as the number of GAGs, which are attached. Note aggrecan has both chondroitin sulphate and keratan sulphate GAGs attached to the core protein. Adapted from Roughley (2006).

The core protein of aggrecan consists of three globular domains; G1, G2 and G3 with an interglobular domain (IGD) between G1 and G2 and a GAG-attachment region between G2 and G3. Aggrecan exists in the ECM as aggregates, forming structural complexes with hyaluronan and link proteins and it is the G1 domain at the N-terminal end of the protein which is important for such interactions (Knudson & Knudson, 2001). The function of G2 has yet to be deciphered but no interactions with hyaluronan have been observed. At the C-terminus of aggrecan is G3, which can be alternatively spliced, producing aggrecan variants, the implications of which are as yet unknown (Roughley, 2006).

The GAG-binding region of aggrecan can be divided into three domains, one binding keratan sulphates (next to G2) and two binding chondroitin sulphates. The GAG-attachment domain is considerably larger in aggrecan than the other lecticans with ~100 chondroitin sulphates attached compared with ~20 in versican, ~3-7 in neurocan and ~1-3 in brevican (Viapiano & Matthews, 2006). It is this large GAG-attachment region which gives aggrecan a high anionic charge density, rendering the protein with crucial osmotic properties required for cartilage function (Roughley, 2006). Aggrecan prevents compression of cartilage by hydrating and swelling against the type II collagen scaffold. Proteolytic liberation of the GAG-attachment region may initiate a series of cellular responses that cumulate in the loss of load-bearing properties (reviewed by Arner, 2002).

Brevican, versican and neurocan lack the G2 domain but contain highly similar G1 and G3 domains to aggrecan. As a result of alternative splicing four different isoforms of versican have been identified; V0, V1, V2 (major species in adult brain) and V3. The four isoforms vary in terms of GAG-binding domains, with V0 having two (GAG-α and GAG-β), V1 (GAG- β) and V2 (GAG-α) having one and V3 lacking both (just the globular domains).

1.2.3 ADAMTS Proteoglycanase Activity

Sandy et al (1991) discovered a novel aggrecan cleavage-site which was not a target for MMPs, thus triggering an eight-year search for the unknown aggrecanases. The bond was Glu^{373}-Ala^{374} and similarly to the characteristic-cleavage site of MMPs (Asn^{341}-Phe^{342}) was located in the IGD, cleavage of which liberated the G2, GAG-binding and G3 domains of aggrecan from hyaluronan (G1 still attached). A group at DuPont

Pharmaceuticals (USA) were the first to show that ADAMTS-4 (aggrecanase-1) and ADAMTS-5 (aggrecanase-2) cleaved at the Glu^{373}-Ala^{374} bond and as a result aggrecanases have become the focus of intensive research (Tortorella *et al*, 2000; Abbaszade *et al*, 1999).

The same group further characterised ADAMTS-4 cleavage of aggrecan by identifying two more cleavage-sites, both within the GAG-binding domain. Purified ADAMTS-4 was incubated with bovine aggrecan (the cleavage-sites of which are highly similar to human aggrecan) over a period of time and antibodies were used to detect breakdown products. It was demonstrated that the preferred cleavage-site for ADAMTS-4 was the Glu^{1667}-Gly^{1668} bond followed by Glu^{1480}-Gly^{1481} bond with Glu^{373}-Ala^{374} bond the least preferred. However, these data did not answer the question of whether Glu^{1667}-Gly^{1668} is the first to be targeted or whether it is the bond which is just cleaved the fastest (i.e. all sites are initially targeted at the same time). Problems with varying antibody reactivity for different breakdown products were also cited by the authors (Tortorella *et al*, 2000). Since this study it is understood that ADAMTS-4 and ADAMTS-5 generally cleave at the same sites and further bonds have been characterised or proposed as targets for these aggrecanases (Glu^{1545}-Gly^{1546}, Glu^{1819}-Ala^{1820} and Glu^{1919}-Leu^{1920}) (reviewed by Flannery, 2006).

ADAMTS-1 has also been demonstrated to cleave aggrecan at the Glu^{373}-Ala^{374} site (Kuno *et al*, 2000) as well as all the bonds cleaved by ADAMTS-4 and -5, as shown by N-terminal sequencing of fragments, a more objective approach than using antibodies (Vankemmelbeke *et al*, 2003). Other aggrecanases, which cleave aggrecan far less efficiently than ADAMTS-1, -4 and -5 include ADAMTS-8, major cleavage site at Glu^{373}-Ala^{374}, which is expressed in human articular cartilage (Collins-Racie *et al*, 2004), ADAMTS-15, major cleavage site at Glu^{373}-Ala^{374} (Yamaji *et al*, 2004) and ADAMTS-9 at Glu^{441}-Ala^{442} (Somerville *et al*, 2003).

1.2.3.1 Aggrecanase ADAMTSs in Arthritis

In arthritic disorders, ADAMTS-4 and -5 are considered to be the most important. ADAMTS-1$^{-/-}$ mice challenged with methylated bovine serum albumin (mBSA), which induced arthritis-like pathology, displayed no protection against 'accelerated aggrecanolysis' when compared to WT animals (Little *et al*, 2005). A recent study

utilising siRNA techniques to knockdown ADAMTS-1, -4 and -5 genes in human cartilage explants showed further the redundancy of ADAMTS-1 in arthritis. A marked reduction in aggrecan degradation was observed in ADAMTS-4 and -5-suppressed explants. However no reduction in aggrecan catabolism was observed in explants transfected with ADAMTS-1 siRNA (Song *et al*, 2007). These findings backed up earlier data which demonstrated that ADAMTS-4 and -5 were the predominant aggrecanases in OA cartilage, based on the detection of aggrecan-neoepitopes cleaved at target sites for these enzymes (Malfait *et al*, 2002).

An in-depth *in vivo* analysis of aggrecan processing in human knee cartilage and synovial fluid was conducted by Sandy & Verscharen (2001). These data showed an important role for both ADAMTSs and MMPs. In normal, injured and late stage OA knee joint cartilage, five (>50% of total aggrecan present) of the seven major aggrecan breakdown products resulted from MMP processing and not ADAMTS activity. The major product detected that was a result of ADAMTS proteolysis was formed by cleavage at the Glu^{373}-Ala^{374} site. In contrast to the results obtained in cartilage tissue, aggrecan breakdown products in the normal synovial fluid and fluid-obtained from injured knee joints are a result of cleavage by ADAMTSs as opposed to MMPs (Sandy & Verscharen, 2001).

Recently the question of which aggrecanase is the most important in arthritis has been addressed by studies in ADAMTS-4 and ADAMTS-5 knock-out (KO) mice. There is substantial evidence demonstrating that ADAMTS-5 (not ADAMTS-4) is the crucial aggrecanase mediating OA and RA-like pathology in mice. Glasson *et al* (2004) originally showed that ADAMTS-4 KO mice showed no difference in progression or severity of OA-like pathology (induced surgically by transecting the meniscotibial ligament) compared to WT. Following on from this study, Glasson *et al* (2005) deleted the catalytic domain of ADAMTS-4 and -5 prior to inducing the same joint instability. In contrast to the ADAMTS-4 data, ADAMTS-5$^{-/-}$ mice displayed a reduction in aggrecan-cleavage product production compared to WT *in vivo* (showed by immunostaining technique). Furthermore, cartilage obtained from ADAMTS-5$^{-/-}$ mice and cultured in the presence of interleukin-1β (IL-1β) and RetA *in vitro* showed minimal release of proteoglycan fragments. This was in contrast to tissue from WT and ADAMTS-4$^{-/-}$ tissue.

Similar methods were adopted to ascertain the key aggrecanase in a RA mouse model, whereby ADAMTS-4 and -5 KO mice knee joints were injected with mBSA. In a similar pattern to the study undertaken by Glasson *et al* (2005), ADAMTS-5$^{-/-}$ cartilage tissue explants displayed no release of aggrecan *in vitro* following inflammatory stimulus when compared to ADAMTS-4$^{-/-}$ and WT. Furthermore, *in vivo* studies showed that ADAMTS-5$^{-/-}$ mice had less aggrecan loss and cartilage erosion as showed by toluidine blue staining (Stanton *et al*, 2005).

1.2.3.2 Versican and Brevican Processing by Glutamyl Endopeptidase ADAMTSs

Aggrecanases have the potential to cleave lecticans other than aggrecan, although many have still to be tested. When incubated with brevican *in vitro*, ADAMTS-4 generated two major fragments thus demonstrating that only one cleavage site was targeted (Glu^{395}-Ser^{396}) (Nakamura *et al*, 2000). This same result was obtained by another group who conducted similar incubations following the observation that a glioma cell line synthesised and cleaved brevican at the same site (Matthews *et al*, 2000). Furthermore, Nakada *et al* (2005) showed that glioblastoma cells transfected with ADAMTS-4 and -5 produced brevican cleavage products, whereas ADAMTS-1 and un-transfected cells displayed no cleavage.

ADAMTS-1 and ADAMTS-4 have been shown to cleave V1 versican in the GAG-β binding domain at Glu^{441}-Ala^{442} in a study which demonstrated that the resultant fragment (70 kDa) was detected in human aorta (Sandy *et al*, 2001). Additionally ADAMTS-4 has been shown to process V2 versican at the Glu^{405}-Gln^{406} site within the GAG-α binding domain (Westling *et al*, 2004). ADAMTS-9 has also been described as having the ability to cleave versican (Somerville *et al*, 2003).

1.2.4 ADAMTS-9

ADAMTS-9 was originally cloned by Clark *et al* (2000), who localised the gene to chromosome 3p14.2-p14.3. The aggrecanase was characterised as having one central TSP-1 motif and three TSP-1s at the C-terminus. However, Somerville *et al* (2003) described a much longer form that is considered to be the full-length product of the ADAMTS-9 gene (*Adamts9*), containing fourteen TSP-1s at the C-terminus.

ADAMTS-9 has an identical domain organisation and exon structure to ADAMTS-20 (Somerville *et al*, 2003; Llamazares *et al*, 2003). In addition, both enzymes have similar primary sequences with ADAMTS-9 (1935) containing twenty-five amino acids more than ADAMTS-20 (1911). An important difference between the two enzymes is that they do not have identical zinc-binding catalytic site motifs. The catalytic site of ADAMTS-9 is identical to ADAMTS-1 and -15 in that a proline residue precedes the third zinc-binding histidine. In contrast, the catalytic site of ADAMTS-20 is not identical to that of any other ADAMTS but most closely resembles that of ADAMTS-7 and ADAMTS-12 (8/12 matched amino acids) (Somerville *et al*, 2003). ADAMTS-20 has been shown to be sparingly expressed in all tissues studied, when compared to ADAMTS-9 (except in leukocytes where ADAMTS-20 levels are higher than ADAMTS-9) (Somerville *et al*, 2003). Hence ADAMTS-9 has been far more extensively studied, especially in the field of development and embryogenesis.

1.2.4.1 ADAMTS-9 in Embryogenesis and Development

It is not surprising that the ADAMTSs have been implicated in development considering the need for remodelling of the ECM to allow for growth. Somerville *et al* (2003) and Llamazares *et al* (2003) demonstrated that human ADAMTS-9 and -20 have comparable domain organisations and primary sequences to GON-1, a proteinase required for gonadal morphogenesis in *Caenorhabditis elegans* nematode, by migration of distal tip cells. In fact ADAMTS-9, ADAMTS-20 and GON-1 have a unique 200 residue GON domain containing several conserved cysteine residues at the C-terminus, which defines these enzymes as being in their own subgroup. Furthermore, either human ADAMTS-9 or -4 can substitute for GON-1 in GON-1 KO mice (Hesselson *et al*, 2004). Preliminary evidence implicating ADAMTS-9 in such processes came from reverse transcriptase polymerase chain reaction (RT-PCR) data showing that the peptidase was expressed in all foetal tissue tested (brain, heart, kidney, liver, lung, skeletal muscle, spleen and thymus) by Clark *et al* (2000). Somerville *et al* (2003) also detected *Adamts9* in the same tissues as well as detecting it in foetal cartilage. *Adamts9* is also widely expressed during mouse embryo development (Jungers *et al*, 2005).

1.2.4.2 Novel Activation Mechanisms of ADAMTS-9

ADAMTS-9 has recently attracted much interest because it appears to be retained at the cell-surface as opposed to being secreted into the ECM (Somerville *et al*, 2003; Koo *et al*, 2006; Koo *et al*, 2007), which is unusual for ADAMTSs because they lack a TM domain. In addition, novel mechanisms exist for ADAMTS-9 secretion and activation (described in Section 1.1.5.1), which the authors postulate; 'ensures that ADAMTS-9 activity is maximal at the cell-surface', perhaps implicating the enzyme in cell migration and growth by clearing a path through the ECM.

1.2.4.3 ADAMTS-9 Expression and Substrate Profile

In addition to being expressed in foetal tissue, *Adamts9* is widely expressed throughout the adult body including brain, heart, placenta, lung, liver, skeletal muscle, kidney, pancreas, spleen, thymus, prostate, testis, ovary, small intestine, colon and skin fibroblasts (Somerville *et al*, 2003). The role(s) of ADAMTS-9 in such tissues can be speculated to some extent based on a very limited amount of substrate specificity data.

ADAMTS-9 is considered to be an aggrecanase and is categorised in this way in a number of reviews based on data by Somerville *et al*, 2003. However, there is some doubt as to whether ADAMTS-9 does in fact function as an active aggrecanase. COS-1 cells were transfected with ADAMTS-9 or ADAMTS-4 (positive control) expression plasmids and incubated overnight with aggrecan or versican. Antisera and antibodies raised against aggrecan or versican catabolites generated by cleavage at known sites were utilised for western blotting. A V1 versican neoepitope of approximately 75 kDa was detected with sera raised against the C-terminus resulting from cleavage at Glu^{441}-Ala^{442} generated by ADAMTS-9-transfected cells. The same band was detected with ADAMTS-4-transfected cells whereas no band was observed with cells expressing the plasmid but lacking the insert (negative control). Therefore, from these findings ADAMTS-9 can be considered a versicanase.

The amount of aggrecan (20 µg) that was incubated with the transfected cells was four-fold greater than the amount of versican utilised. Intense immunoreactivity (band at 100 kDa) to antisera raised against an aggrecan neoepitope generated by cleavage at Glu^{1771}-

Ala^{1772} bond was observed following incubation with ADAMTS-4-transfected cells. However, a very faint band is observed with ADAMTS-9-transfected cells.

The conclusion that can be drawn from these data is that ADAMTS-9 cleaves aggrecan less effectively than it cleaves versican *in vitro*. However, the investigators do not report that they tested antibodies or antisera raised against other neoepitopes, consequently there is no evidence to suggest that ADAMTS-9 does not cleave aggrecan at sites other than those tested, such as at the Glu^{373}-Ala^{374} bond. Another limitation with the work was that only the signal peptide, prodomain and catalytic domain of ADAMTS-9 was expressed and not the full-length protein. The ancillary domains of many ADAMTSs are crucial for activity/substrate specificity, therefore the fourteen C-terminal TSP-1s (and other domains) of ADAMTS-9 may contribute to a more efficient cleavage of aggrecan. A direct comparison between ADAMTS-9 and ADAMTS-4 activity cannot be drawn because of variations in transfection efficiencies, expression levels and secretion levels (Somerville *et al*, 2003). It is likely that ADAMTS-9 has substrates other than aggrecan and V1 versican, such as other isoforms of the latter and the structurally similar brevican.

1.2.4.4 ADAMTS-9 in Arthritis and Inflammation

In light of this study demonstrating that ADAMTS-9 has the potential to cleave cartilage proteoglycans, arthritis is an area of research in which it has been investigated. Expression of *Adamts9* was shown to be synergistically induced by IL-1β and tumour necrosis factor (TNF) in OUMS-27 chondrosarcoma cells and in human chondrocytes. In the same study, Demircan *et al* (2005) showed that p38 and p44.42 mitogen activated protein kinases (MAPKs) played a role in regulating some responses of *Adamts9* to IL-1β. These data indicate that ADAMTS-9 is potentially involved in physiology and/or pathology as a result of cytokine-induced inflammation. ADAMTS-9 may not be as critical in OA, in which inflammation is a less significant aspect when compared to RA. *Adamts9* levels were shown to be decreased in hip joints and synovium from patients with OA when compared to samples from the same region displaying normal physiology (Davidson *et al*, 2006).

Further evidence that ADAMTS-9 is involved in inflammation came from a study utilising a retinal pigment epithelium (RPE) derived cell line ARPE-19. The RPE is a

cell layer that plays an important role in the regulation and development of the photoreceptors in the vertebrate retina. It lies adjacent to Bruch's membrane, a region of ECM containing numerous CSPG species. Treatment of ARPE-19 with TNF resulted in an up-regulation of *Adamts9* expression (as well as *Adamts1* and *Adamts6*) (Bevitt *et al*, 2003).

Analysis of *Adamts9* expression levels in response to an anti-inflammatory stimulus shed further light on its role in inflammation. Cross *et al* (2005a) showed that transforming growth factor-β1 (TGF-β1) initiated a down-regulation (~3-fold decrease compared to control) of *Adamts9* (as well as other ADAMTSs) in prostatic stromal cells. Treatment with TGF-β1 also initiated a ~7-fold increase in the expression of versican. The authors speculated that the increased levels of versican observed in benign prostatic hyperplasia (BPH) is a result of both decreased ADAMTS expression and increased versican expression modulated by TGF-β1.

1.2.4.5 ADAMTS-9 in other Pathologies

Recent work has identified *Adamts9* as a potential tumour suppressor gene in oesophageal cancer. The group used microcell-mediated chromosome transfer to introduce chromosome 3 into an oesophageal cell line prior to identifying the ADAMTS-9 gene within the tumour suppressive critical region. Furthermore, levels of ADAMTS-9 were lower in 94% of oesophageal cell lines tested as well as in over 40% of primary tumours in high-risk regions (Far East) (Lo *et al*, 2007). In another study, Keating *et al* (2006) demonstrated by gene-silencing approaches that ADAMTS-9 could be involved in the pathogenesis of lung fibrosis. Despite ADAMTS-9 mRNA being abundantly expressed within the adult and developing brain, as of yet no studies have focussed on ADAMTS-9 within the CNS from a functional or pathological view point.

1.3 Central Nervous System

1.3.1 Organisation/Structure

The CNS consists of the brain and spinal cord which are made up of a complex meshwork of a variety of cell-types, structural proteins, vasculature and circuits that relay electrical signals; triggering neural functions such as memory, cognition, emotion

and movement. The human brain weighs ~1-1.5 kg and can be divided into regions, each with generally specific functions and structures (Purves *et al*, 2001).

The cerebrum is concerned with conscious thoughts such as memory and emotions and can be separated into two hemispheres; right (controls left side of body) and left (controls right). Each cerebrum hemisphere consists of four lobes; frontal, parietal, temporal and occipital. The cerebellum is located at the back of the brain and is important for balance and coordination. The cerebral cortex (grey matter) is a thin layer of tissue that forms the outer surface of the cerebrum and cerebellum and has long been considered responsible for perception/cognition. Two hippocampuses are located in medial temporal lobes, located on either side of the brain and are involved in memory and spatial recognition. The brain stem is at the bottom of the brain, connecting it to the spinal cord and ultimately the rest of the body and is crucial for sustaining important processes such as blood pressure, heart beat and breathing (Purves *et al*, 2001).

The brain receives blood from four arteries; two vertebral arteries (which join to form the basilar artery) and two internal carotid arteries. The vasculature within the brain is arranged around the circle of Willis from which the main arteries branch off including posterior cerebral artery (serves the midbrain and superior cistern), internal carotid artery (delivers to the optic chiasm), middle cerebral artery (MCA, feeds lateral sulcus and entire lateral surface of cerebral hemisphere and temporal pole) and anterior cerebral artery (leads to the optic nerve). In general it has been established that arteries dictate cerebral blood pressure and the much smaller more branched capillaries control CNS nutrition and waste removal (Farkas & Luiten, 2001).

A number of problems exist when studying the human brain including: a) samples are difficult to obtain from the tissue (because of the skull), b) volunteers are reluctant to be involved in studies, c) its 3-D structure is easily distorted during handling (due to its high state of hydration and loose connections), d) post-mortem tissue is often not stored (frozen) quickly enough, leading to tissue degradation and e) there is a lack of post-mortem tissue (few donors). Consequently, the brain is perhaps the least understood organ in the human body and animal-models are relied upon for experimental analysis.

1.3.2 Neurones

The role of neurones (nerve/neuronal cell) as the information processors/transmitters of the body is well established. The basic mechanism by which 'messages' are passed from neurone to neurone and ultimately to other regions of the brain/target-tissues can be termed 'synaptic transmission'. The process involves the generation of an action potential in an electrically excited axon prior to the influx of Ca^{2+} ions and the passage of neurotransmitter molecules across the synaptic cleft (Siegel et al, 1999).

1.3.2.1 Neuronal Structure

All neurones have the same basic structure consisting of a soma (perikaryon), an axon and dendrites. The neuronal soma (cell body) contains organelles common to most cells of the body including the nucleus, smooth ER, Golgi apparatus and lysosomes. The axon can extend a great distance from the soma and can be divided into four morphologically distinct regions: 1) the ribosome-abundant 'axon hillock', 2) the 'initial segment', containing axolemma, responsible for action potential generation, 3) the 'axon proper' (also contains axolemma), which is surrounded by insulating myelin sheath, aiding in smooth nerve-impulse propagation and 4) the 'axon terminal', which interacts with other neurones by extending out from the axon proper and releasing neurotransmitters. Dendrites are arranged around the neuronal soma in many branches, hence the term 'dendritic tree'; they are responsible for the nerve impulse entering the cell prior to transmittance down the axon (Siegel et al, 1999).

1.3.2.2 Types of Neurones

Within the CNS different types of neurones exist with subtle structural variations and functions. Some neurones are widespread throughout the brain whereas others are specific to a particular region. The most abundant neuronal cell type in the CNS is the granular neurone (granule cells), present in the cerebellum (granular layer), cerebral cortex, dentate gyrus of hippocampus and the olfactory bulb (forebrain). Granular neurones are the smallest neurones in the CNS and are characterised by a round soma (Yamasaki et al, 2001).

Another neuronal-type is the pyramidal neurone, which is characterised by a conical (triangular) soma, one large apical dendrite and numerous, distinctly large basal dendrites, which extend over vast regions of the cerebral cortex and the hippocampus (Tsiola, 2003). Elston (2003) proposed that the evolution of the specialised structure of pyramidal neurones within the cerebral cortex is a major factor in how humans have developed such a complex level of cognition. Furthermore, there is evidence to suggest that pyramidal neurones in the hippocampus play a key role in environmental and spatial responses by becoming active and changing their orientation (O'Keefe, 1999).

The presence of Purkinje cells is a characteristic morphological feature of the cerebellum. Purkinje cells have multiple postsynaptic dendritic spines which change morphology in different experimental conditions e.g. mushroom-shaped spines are more dynamic and have different signalling mechanisms than branched spines (Lee *et al*, 2005). Another morphological feature of Purkinje cells is an extremely large soma (Purves *et al*, 2001). Other types of neurones include Renshaw cells, medium spiny neurones and Basket cells.

1.3.3 Glial Cells

Spindle-shaped glial cells are the most abundant (~90% of all cells) cell-type in the CNS, consisting of astrocytes, microglia and oligodendrocytes, which are all smaller than neurones. Glia possess no synaptic contacts and were originally considered to play supporting roles for neurones with no real functions, other than structural hence they were named after the Greek word for 'glue' (He & Sun, 2007). However, it has become apparent that glial cells perform essential roles in neuronal function and maintenance as well as in response to injury (Siegel *et al*, 1999).

Astrocytes are the most abundant cell-type in the brain, providing physical support, chemicals and nourishment to neurones. These star-shaped cells form a matrix which keeps neurones in place and isolates synapses, thus aiding in transmission of neural messages (Bear *et al*, 2001). Other functions of astrocytes in normal CNS physiology include; glycogen storage and export of metabolites, uptake of unutilised neurotransmitters (glutamate), neurotrophic factor (NTF) and cytokine production/secretion, synapse genesis and maintenance (Flynn *et al*, 2003; Farina *et al*, 2007).

Microglia, the smallest of the glial cells, are the resident immune cells of the CNS, whose roles include immune surveillance and phagocytosing debris from damaged nerves. They belong to the same phagocytic lineage as other tissue macrophages e.g. Kupffer cells, a liver-specific macrophage population. Morphologically, microglia are similar to dendritic cells in that they have many 'spiky' outgrowths from the cell body, however an amoeboid shape is adopted in response to injury (Vilhardt, 2005). In the healthy brain, microglia are supportive cells but are also extremely motile suggesting they are 'busy and vigilant housekeepers' (Nimmerjahn *et al*, 2005). There is evidence to suggest microglia are kept in a quiescent state in the healthy brain by signalling from neurones. The mechanism is thought to involve the interaction of the neuronally expressed CD200 membrane glycoprotein with the CD200 receptor, present on microglia (Hoek *et al*, 2000). Noted functions of microglia in normal physiology include stimulating migration of neuronal precursor cells by releasing soluble factors including chemokines (Aarum *et al*, 2003), axonal growth (via the release of NTFs) (Batchelor *et al*, 2002) and synthesis of ECM components (Vilhardt, 2005).

The cells responsible for manufacturing myelin sheaths around axons are oligodendrocytes (Schwann cells are principle myelinating cells in the peripheral nervous system [PNS]) as first described by Hortega & del Rio (1921). The process of myelination initially involves the migration of the oligodendrocyte precursors to the axons where adherence takes place. Next, the cells proceed to differentiate and spiral their processes around the axon via a poorly understood mechanism. One theory is that the timing of oligodendrocyte differentiation and thus myelination is controlled by the developmentally regulated decrease in the expression of Jagged1 in axons (Stangel & Hartung, 2002). Jagged1 is thought to inhibit oligodendrocyte differentiation by interacting with the Notch1 receptor; therefore the down-regulation of Jagged1 potentially increases oligodendrocyte maturation and thus myelination (Wang *et al*, 1998).

Glial precursor cells have become the focus of extensive study in recent years because of their ability to differentiate into various cell-types. During embryogenesis, radial glial cells can differentiate into neuronal, oligodendrocyte and astrocyte precursor cells. Furthermore, astrocyte precursor cells can also differentiate into neuronal and oligodendrocyte precursor cells as well as astrocytes in the perinatal period. It has been described that MAPK1/2 and extracellular signal-regulated kinase 1/2 (ERK1/2) are

important signalling pathways within radial glial cells, which contribute to the proliferation of these cells (Vaccarino *et al*, 2007).

1.3.4 CNS Extracellular Matrix

The ECM is a complex structure which surrounds and supports cells in all tissue-types in the body. It is made up of diverse proteins and proteoglycans which are secreted into the extracellular space by numerous cell-types. The composition and form of ECM varies greatly between tissue types and has a large impact on its different functions. CNS ECM lacks fibrillar collagen, fibronectin and laminin, giving the brain a soft consistency when compared to other proteoglycan-rich tissues (e.g. cartilage). The matrix has a critical role in a wide variety of physiological brain processes such as development (migration of precursor cells), repair, proliferation and cell signalling (via integrins) (Bellail *et al*, 2004).

A significant percentage (~20%) of the normal brain volume is occupied by the ECM, forming both general 'loosely-defined' matrices as well as perineuronal nets (PNN) which surround and support neurones in a tightly packed, condensed manner. PNNs have been shown to stabilise/limit synaptic plasticity (cellular adaptation to the environment) and support ion homeostasis of neurones (Galtrey & Fawcett, 2007). It is known that neurones and glial cells contribute to the secretion of PNN components; principally hyaluronan, proteoglycans, tenascin-C (adhesive molecule related to laminin and fibronectin) and thrombospondins (Yamaguchi, 2000; He & Sun, 2007).

The GAG hyaluronan is a major component of the cerebral ECM. It is comprised of long chains of up to 25,000 repeating non-sulphated disaccharide units (made of glucuronic acid and N-acetylglucosamine) forming molecules of up to 10^6 Da in size (Galtrey & Fawcett, 2007). It is highly anionic, electrostatically attracting Na^+ and inducing an osmotic influx of H_2O into the extracellular space (Bellail *et al*, 2004). Many ECM components are attached non-covalently to hyaluronan, which acts as the 'back-bone' to form complex ECM structures with lecticans, tenascins, link proteins and carbohydrates.

The lecticans have been described as 'organisers of the brain ECM' and 'molecular bridges' because they bind to two key ligands; hyaluronan via the N-terminus and to

36

tenascin-C/-R via the C-terminus (Yamaguchi, 2000) as shown in Figure 1.7. Lecticans are the most abundant CSPGs in the brain and are important because they a) provide structural support to the hyaluronan scaffold and b) influence matrix function by interacting with cell-surface molecules of other ECM components. Link proteins are small glycoproteins thought to secure the interactions of lecticans with hyaluronan. Bral2/Hapln4 is a link protein which is colocalised with brevican in PNNs, whereas Bral2/Hapln2 is colocalised with V2 versican (Aono & Oohira, 2006).

Examples of lectican molecular interactions in the CNS ECM include neurocan with members of the cell adhesion molecule superfamily (CAM), brevican with sulphated glycolipids and aggrecan/versican with fibulin family members. In addition all lecticans have the potential via their GAG-side chains to interact with NTFs, cytokines and cell-surface signalling receptors (e.g. tyrosine kinases, CD44) (Viapiano & Matthews, 2006).

The ECM of the CNS contains proteoglycans other than the lecticans; including phosphacan, which interacts with tenascin-R but is unable to bind to hyaluronan (Galtrey & Fawcett, 2007). Another PNN component is thrombospondin-1, which binds to HSPGs via its C-terminus and promotes platelet aggregation and cell adhesion (De Fraipont *et al*, 2001).

In normal physiological conditions the ECM of the brain is a dynamic structure which undergoes constant remodelling. In brevican$^{-/-}$ mice, neurocan expression was found to be up-regulated because there were more binding sites for it within the matrix (Brakebusch *et al*, 2002). Furthermore, mice lacking neurocan, brevican, tenascin-C and -R were healthy and fertile because aggrecan and versican compensated for the absent molecules. Also, fibulin-1 and -2 increased in expression to neutralise the loss of tenascin-C and -R (Rauch *et al*, 2005).

1.4 CNS Inflammation

1.4.1 Immunology of the CNS

Inflammation is the body's innate response to injury or microbial infection involving white blood cells (leukocytes) and plasma enzyme systems, which generate inflammatory mediators. If it is localised correctly with limited severity and duration it

Figure 1.7 Structure of the CNS Extracellular Matrix
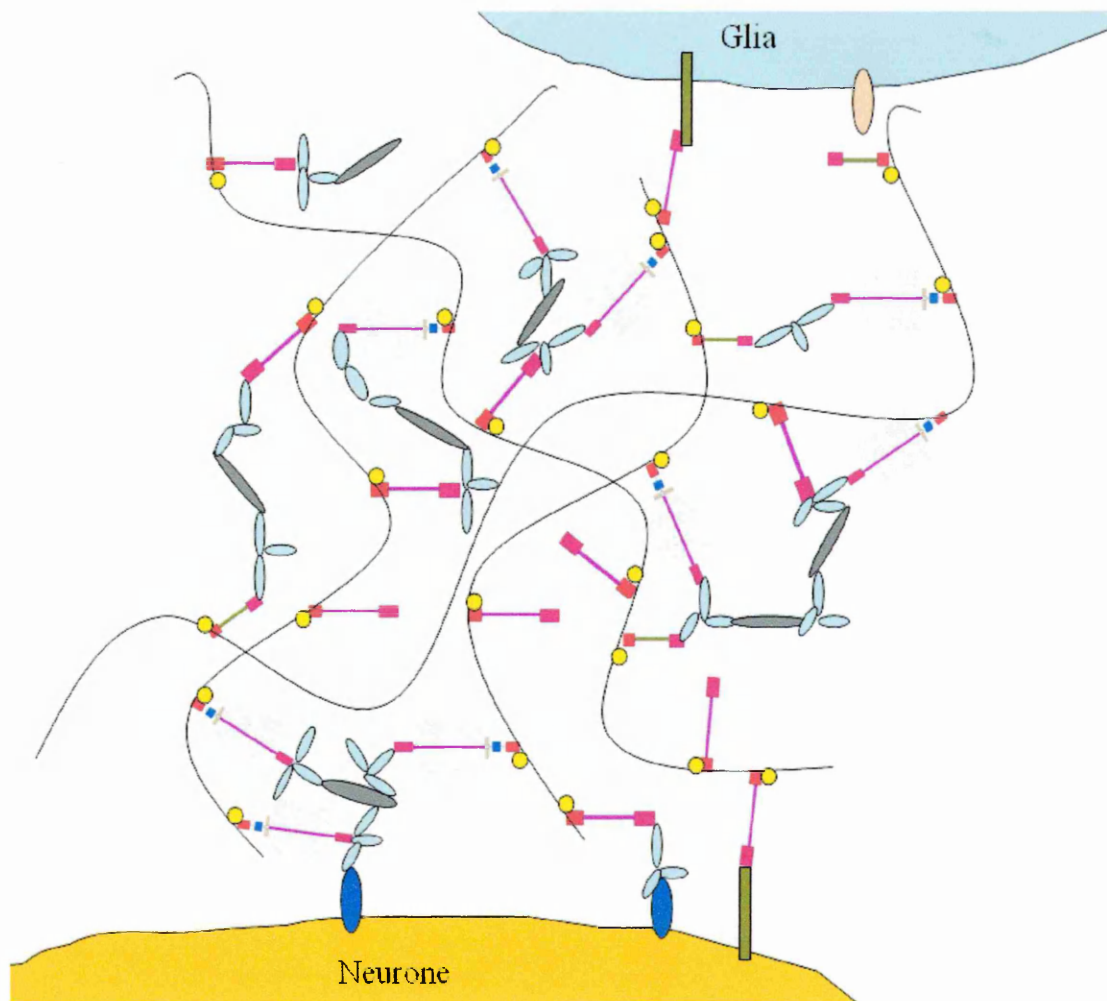
Simplified interpretation of the ECM of the CNS showing how lecticans act as anchors between the hyaluronan scaffold (via the N-terminus) and tenascins (via the C-terminus). Note how neurocan does not bind with tenascins yet can anchor to the CAM family on the cell surface. Adapted from Galtrey & Fawcett (2007); Viapiano & Matthews (2006).

can be effective at returning the host to a state of normality by eliminating pathogens, repairing damaged tissue and preventing further destruction (Allan & Rothwell, 2003). A complex series of pro-inflammatory pathways promote inflammation in the body. However if it is not controlled effectively or is triggered inappropriately, devastating damage can occur. To counteract detrimental inflammation, the body has a cohort of anti-inflammatory responses/mediators.

It was not long ago that the brain was considered an 'immunologically privileged' environment, which did not respond to inflammatory stimuli. It is true to a certain extent that the brain guards against self-damage by having a scaled down immune system. However, the brain still possesses many features which facilitate an immune response including oedema, immune cell invasion, endogenous glial cell (especially microglia) activation, complement activation, acute phase proteins and cytokines (Allan & Rothwell, 2003; Aktas *et al*, 2007). It is when the balance of inflammatory mediators, inhibitors, receptors and immune cells becomes disturbed that destructive CNS inflammation can lead to neuronal damage characteristic of CNS inflammatory disorders.

1.4.1.1 The Blood-Brain Barrier

The blood-brain barrier (BBB) protects the fragile ECM of the neuronal parenchyma from chemicals and variations in blood composition. A simplified interpretation of the BBB structure is displayed in Figure 1.8. The BBB is comprised of three main structures; capillary ECs, astrocytic end-feet and pericytes. Tight junctions and adherens junctions are present between the ECs allowing selective permeability of molecules/nutrients, which are ~0.5 kDa or less (e.g. glucose, amino acids, insulin and leptin), into the brain (Petty *et al*, 2002; Ballabh *et al*, 2004). Capillary ECs of the BBB are phenotypically different from those found on non-cerebral capillaries and contain a greater amount of mitochondria required for the mechanisms involved in transporting larger molecules across the BBB (Rubin & Staddon, 1999). The astrocytic end-feet are in close proximity to the ECs and are thought to provide support to the structure as well as intercellular signals (Ballabh *et al*, 2004).

The blood vessel endothelium is surrounded by a 30-40 nm thick matrix known as the basement membrane (BM/basal lamina). The ECM components of the BM are thought

Figure 1.8 Structure of the Blood-Brain Barrier (BBB)
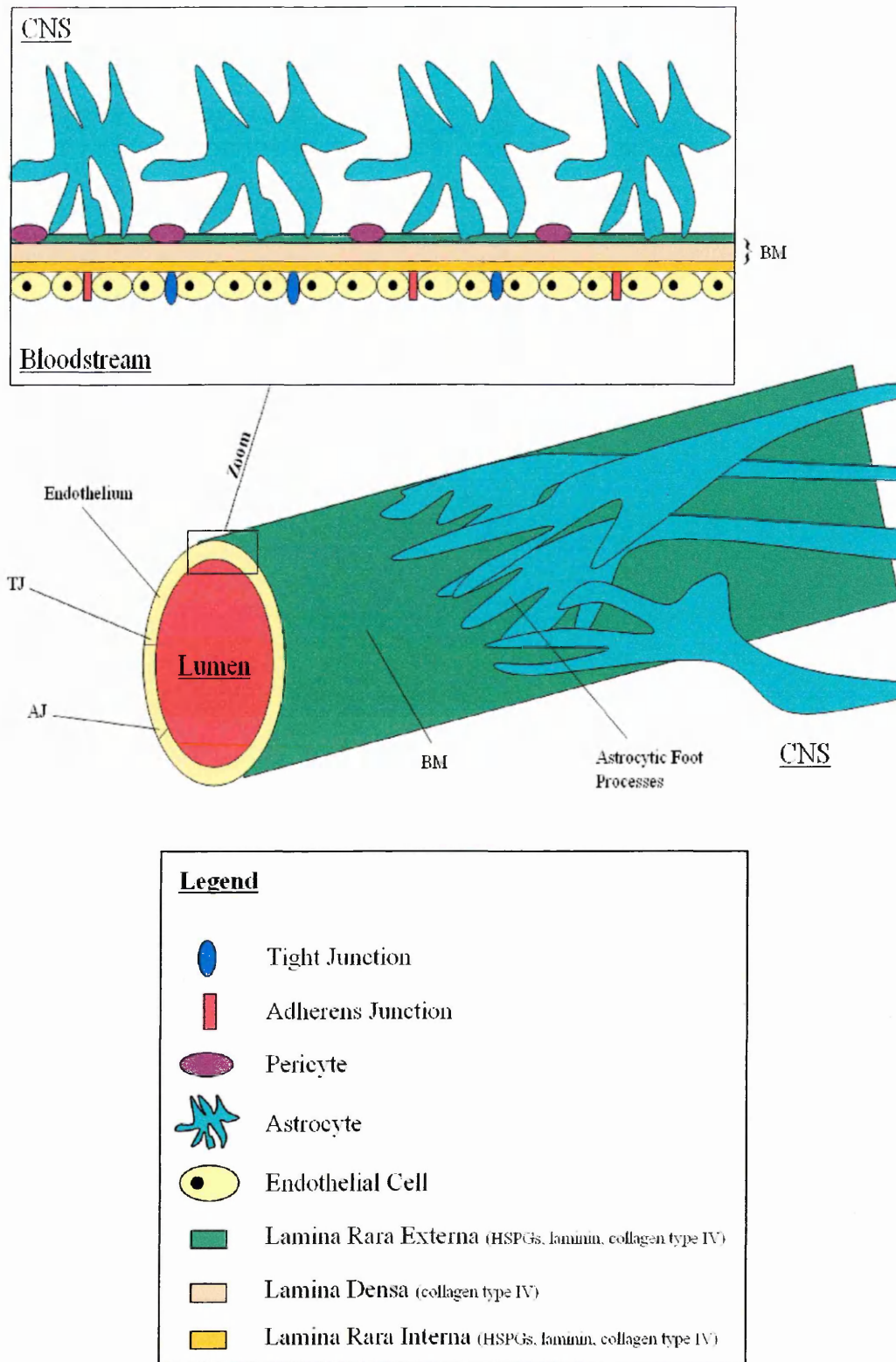
The barrier that prevents the passage of inflammatory cells into the CNS from the blood. In health, the barrier is effective. However, in many CNS inflammatory disorders the integrity of the BBB is compromised. BM = basement membrane, TJ = tight junction, AJ = adherens junction. Adapted from Ballabh *et al* (2004).

to be produced by capillary cell-types (Farkas & Luiten, 2001). It is arranged into a trilaminar structure, the layer in closest proximity to the ECs being the 'lamina rara interna' which is made up of HSPGs (especially perlecan), laminin and collagen type IV (both comprise the BM 'scaffold'). A layer of similar structure, the 'lamina rara externa' is in contact with astrocytic end-feet, thus linking the BM to the rest of the BBB. A collagen type IV layer (lamina densa) separates the two lamina rara layers. The BM has many functions such as support of microvessels, providing a route for cell migration, selective permeability of molecules, modulation of EC function, adhesion and general protection of neurones from inflammatory cells (Farkas & Luiten, 2001).

Pericytes are embedded into the BM and have been shown to have a role in regulating a) CNS vascular diameter and capillary blood flow (by their ability to contract), b) BBB EC differentiation/proliferation and c) phagocytosis (Rucker *et al*, 2000). It has been demonstrated that pericytes synthesise HSPGs, which have a high level of hydration and therefore fill the gaps in the BM. HSPGs have also been implicated as 'molecular sieves' within the BBB, blocking leukocyte extravasation as well as having a role in binding growth factors (GFs) and cytokines (Parish, 2006).

In normal physiological conditions, the BBB limits the entry of monocytes, lymphocytes and other cells of the immune system preventing cellular damage caused by autoimmunity and destructive inflammatory responses. However, disruption of the BBB in pathological conditions such as multiple sclerosis (MS) and stroke allows the entry of activated, inflammation-inducing leukocytes which initiate CNS damage.

1.4.2 CNS Inflammatory Disorders - Overview

CNS inflammatory disorders can be characterised into two main types; acute and chronic. The aetiology of chronic CNS inflammatory disorders are far less understood than acute disorders but they generally present and worsen with age and are likely to involve environmental factors triggered in a genetically susceptible host. Multiple sclerosis (MS) presents at an earlier age than most chronic CNS diseases, with most sufferers, of which there are ~85,000 in the UK, first experiencing symptoms between the ages of twenty and forty (Burridge *et al*, 2007). Symptoms of MS include; weakness, lack of coordination and impaired vision/speech because autoimmune responses destroy myelin (demyelination) resulting in axonal damage and ultimately death. MS is

characterised by inflammatory cascades thought to be triggered by the immune system mistakenly recognising myelin antigen as 'foreign', although this theory has not yet been proven (reviewed by Hafler, 2004).

MS pathogenesis is complex and not fully understood although it is considered to be initiated in the periphery by the presentation of myelin derivative-like antigens on antigen presenting cells (e.g. macrophages) by major histocompatibility complex class II (MHC II) molecules (Compston, 2004) to $CD4^+$ T lymphocytes (T helper cells), which are thus activated (Sospedra & Martin, 2005). The activated lymphocytes pass through the BBB via expression of adhesion molecules and chemokines (chemo-attractant cytokines) (Bar-Or *et al*, 1999). It has been reported that the release of MMP-2 and -9 facilitates the infiltration of activated cells through the BBB (Sospedra & Martin, 2005). Following migration into the CNS, T cells re-encounter myelin antigen, and initiate delayed-type hypersensitivity reactions, resulting in the release of inflammatory-mediators leading to the activation of microglia/macrophages and cytotoxic T cells. The resultant auto-pathogenic responses target critical myelin-components, which are broken down by oxygen/nitrogen free radicals and proteinases, mediated by pro-inflammatory cytokines (Markovic-Plese *et al*, 2004).

Chronic inflammatory disorders of the aged population are areas of intense research activity due to the increased life expectancy. Alzheimer's disease (AD) is characterised by neuronal cell death in the hippocampus and frontal cortex leading to poor memory and disorientation. The pathogenesis of AD involves the abnormal processing of amyloid β protein (Aβ), leading to the production of insoluble forms, resulting in senile plaques. Parkinson's disease (PD) is a chronic inflammatory disease characterised by loss of neurones from substantia nigra causing shaking and sporadic muscle contraction. Other long-term inflammatory CNS disorders include the motor neurone disease; amyotrophic lateral sclerosis (ALS) and the prion disease Creutzfeldt-Jakob disease (CJD) (reviewed by Aktas *et al*, 2007).

Acute CNS inflammation is triggered by trauma such as a blow to the head, seizure caused by discharging neurones (epilepsy) or blocking of the blood supply to the brain (stroke). The resultant loss of nerve cells can have a significant impact on brain function either permanently or temporarily. Acute traumatic brain injury (TBI) according to the International Brain Injury Association (IBIA) (2007) accounts for one million hospital

admissions per year in the European Union. The inflammatory response following head trauma can be delayed and may have varying degrees of severity or symptoms. There is evidence to suggest that pro-inflammatory cytokines, COX-2 and complement components have a role in the ensuing inflammation (Lucas *et al*, 2006).

Cerebral ischaemia (stroke) is triggered when a blood vessel carrying O_2 and nutrients to the brain is either blocked by a clot or bursts. The ischaemia usually arises from clots in cerebral arteries (thrombotic) but can also be embolic (an embolus elsewhere in circulation, which moves to the brain) causing symptoms such as speech-loss and impaired mobility. In 2005, cerebrovascular disease accounted for 12.9% of all female and 7.9% of all male deaths in the UK according to the government-issued national statistics (http://www.statistics.gov.uk/pdfdir/hsq0506.pdf). The damage caused to neurones post-stroke involves a highly complex pathway of inflammatory events and counter-events.

1.4.3 Inflammatory Response to Cerebral Ischaemia

The role of inflammation in stroke is a complex one and our understanding is limited because of the lack of data obtained within the early stages of stroke onset. Also, it has proved difficult differentiating between inflammation stimulated by cerebral infarction and that of pre-existing infective processes (Emsley *et al*, 2003). However, it is clear that stroke inflammatory responses are unique when compared to many other CNS disorders in that necrosis is a key stimulatory event (Esiri, 2007).

Necrosis is caused by the depletion of cerebral blood flow to the CNS, which starves the tissue of O_2 and glucose and thus causes a breakdown in the energetics required to sustain ionic gradients. This results in a disruption in the regular neuronal uptake and release of Ca^{2+}, Na^+, Cl^-, K^+, amino acids and H_2O, causing oedema and excitotoxicity (nerve damage by excess glutamate). As well as necrosis, cell death can also occur by apoptosis, particularly in the ischaemic penumbra, an intermediate region which surrounds cells that have permanently lost their membrane potential (the ischaemic core) (Dirnagl *et al*, 1999; Esiri, 2007). A number of mechanisms stemming from such events have been speculated to trigger the inflammatory response to stroke. In a review on stroke pathobiology, Dirnagl *et al* (1999) highlighted key events that trigger the transcription of pro-inflammatory genes including Ca^{2+} activation of intracellular

secondary messenger systems contributing to tissue damage by proteolysis and free radical generation.

In addition, hypoxia itself can also induce synthesis of transcription factors including nuclear factor-κB (NF-κB), interferon regulatory factor 1 (IRF-1) and signal transducer and activator of transcription 3 (STAT3). However, perhaps the most important transcription factor in stroke is hypoxia inducible factor 1 (HIF-1) because a) many studies have shown it is only expressed in hypoxic conditions (unlike the above mentioned factors) (Hirota, 2002), b) it has been shown to be up-regulated in animal models of cerebral ischaemia (Ke & Costa, 2006) and c) many of the characterised HIF-1-target genes are involved in the body's response to O_2 depletion i.e. they encode for pro-erythropoiesis and pro-angiogenic proteins (Bracken et al, 2003). HIF-1 exists as a heterodimer comprising of a HIF1α and a HIF1β (aryl hydrocarbon nuclear translocater [ARNT]) subunits, which bind to the consensus sequence 5'-R(A/G)CGTG-3' (Semenza et al, 1996; Bracken et al, 2003; Choi et al, 2004) in the promoter regions of target genes to trigger transcription.

Transcription can be triggered in this manner in endogenous cells such as glial cells and neurones as well as inflammatory cells, which migrate to the site of the infarct (damaged tissue). Inflammation is not considered to be an event which occurs directly following ischaemia due to a 4-6 h delay in leukocyte migration through the BBB via adhesion molecules, selectins and integrins (Wang et al, 2007). In the minutes following ischaemia, excitotoxicity and neurone depolarisation are the main causes of necrosis. The inflammatory cells postulated to be involved in such secondary damage of potentially salvageable tissue are polymorphonuclear leukocytes, monocytes, neutrophils and macrophages with little evidence for lymphocyte involvement (Huang et al, 2006). Many pro-inflammatory mediators are released by such cell-types including cytokines.

It has been documented that proteinases are implicated in stroke pathogenesis but as yet their role is poorly understood. There is strong experimental evidence that cytokine-induced MMPs (mainly MMP-2 and -9) have an important role in post-stroke damage, potentially by compromising the integrity of the BBB (Wang et al, 2007). Microglia have been shown to a) produce MMPs following ischaemia and b) stimulate astrocytes to secrete MMPs (del Zoppo et al, 2007). Furthermore, following ischaemia, neurones

44

and brain ECs express MMPs (Rosenberg *et al*, 2001). The role of MMPs in the early stages following ischaemia seems to be a harmful one because MMP inhibitors have been shown to reduce infarct size, oedema and haemorrhage (Pfefferkorn & Rosenberg, 2003) whilst MMP-9$^{-/-}$ mice also displayed smaller infarcts when compared to WT (Asahi *et al*, 2000). However, MMPs may be mediators of repair in the latter stages of stroke recovery by inducing angiogenesis and hence increased blood supply to necrotic regions (Wang *et al*, 2007).

1.4.4 Glial Cells in CNS Inflammation

In the CNS, microglia are the 'protectors' of neurones from pathogens and damage from trauma, their processes rapidly extend to sites of injury (Nimmerjahn *et al*, 2005). In the healthy brain, microglia function as resident macrophages carrying out classical innate immune functions seen in other organs such as phagocytosis of apoptotic cells and forming the first line of defence against microbes. They also have the ability to contribute to an inflammatory, antibody-mediated response which can be beneficial if localised and controlled. However, these protecting cells can also 'betray' neurones and contribute to inflammation characteristic of autoimmune disorders and CNS inflammatory diseases (Kim & de Vellis, 2005; Block & Hong, 2005).

When microglia become activated they can present antigen to lymphocytes as well as express a range of pro-inflammatory mediators such as the cytokines TNF and IL-1β, chemokines, proteinases, reactive oxygen species and nitrogen intermediates (Vilhardt, 2005). The role of microglia in pathology is complex because they have also been shown to secrete anti-inflammatory products such as IL-10 and TGF-β. In fact it is very difficult to say whether activated microglia are neuroprotective or neurotoxic.

In MS, it has been shown that microglial cells take part in the removal of myelin debris due to cytokine/chemokine interactions (Ayers *et al*, 2004) as well as associating with damaged axons (Werner *et al*, 2001). Furthermore, Cipriani *et al* (2003) showed that in guinea pigs sensitised for experimental autoimmune encephalomyelitis (EAE), a model of MS, the majority of cells migrating to lesions were microglia. Zhang *et al* (1997) showed in a rat model of focal cerebral ischaemia; transient MCA occlusion (tMCAo), microglial morphological changes (from resting to active) correlated with injury severity. A number of reviews have further highlighted the importance of microglia in CNS inflammatory disorders (Wang *et al*, 2007; Kim & de Vellis, 2005).

45

As components of the BBB, astrocytes are the first glial cell-type to be confronted by inflammatory infiltrates but similarly to microglia, their role in CNS inflammation is a complex one because they too release anti- as well as pro-inflammatory mediators such as chemokines (e.g. CCL3) (Ambrosini *et al*, 2005). During cerebral ischaemia there is evidence to suggest that astrocytes contribute to ionic concentration changes which trigger inflammatory pathways (Dronne *et al*, 2007).

1.4.4.1 Astrogliosis

In response to CNS tissue damage, reactive astrocytes partake in the formation of glial scars (reactive gliosis, astrogliosis), which protects the injured area from inflammatory cells but also forms an inhibitory barrier to neuronal regeneration and prevents plasticity (reviewed by Rhodes & Fawcett, 2004; Silver & Miller, 2004; Galtrey & Fawcett, 2007; Viapiano & Matthews, 2006). Many reports suggest that the main mediators of the inhibitory effect of astrogliosis are GAGs of CSPGs, which are tightly-packed within the glial scar (reviewed by Properzi *et al*, 2003). Treatment with chondroitinase ABC, which specifically cleaves chondroitin sulphate side chains from CSPGs, promoted functional recovery in the CNS following injury (Barritt *et al*, 2006).

Alternatively, there is evidence to suggest that glial scars may have a protective role in CNS inflammatory disorders by sealing off the damaged region and thus preventing secondary damage from pro-inflammatory mediators (Silver & Miller, 2004). Glial scars could serve as a 'bandage' around the damaged blood-brain barrier (BBB) preventing more inflammatory infiltrates from entering the CNS as indicated by the findings of Bush *et al* (1999) who ablated reactive astrocytes in mice and observed an increase of infiltrating CD-45-positive leukocytes, poor BBB repair and substantial neuronal degeneration. The blood clotting proteinase, thrombin, has been proposed to stimulate astroglial scar formation following extravasation through the compromised BBB by promoting astrocyte proliferation via MAPK signalling (Wang *et al*, 2002). Following a stroke, glial scars are usually formed after a few days as opposed to occurring in the early stages post-ischaemia (Trendelenburg & Dirnagl, 2005).

1.4.5 CNS Inflammatory Mediators

In the normal CNS, inflammation is not a phenomenon that spontaneously occurs. It requires a stimulus (e.g. infection or trauma) triggering pathways involving intercellular communication via pro-inflammatory mediators. One such family of mediators is the cytokines, which are secreted by many cell-types and bind to specific cytokine receptors (on target cells) triggering intracellular signalling pathways which modulate transcription of specific genes (reviewed by Wang & Shuaib, 2002). Consequently, much attention has focused on unravelling the role of cytokines in the innate and adaptive immune response in CNS inflammatory disorders. This has proven challenging because a complex balance exists between pro- and anti-inflammatory cytokines.

1.4.5.1 Interleukin-1 (IL-1) Family

Perhaps the most extensively studied cytokines in CNS inflammation is the IL-1 family of which IL-1α and IL-1β are members (both 17 kDa). IL-1 binds to IL-1 receptor I (IL-1RI) through which signal transduction is initiated within the cell. Another IL-1 receptor, IL-1RII acts as a molecular trap, inactivating IL-1 by binding it to the cell-surface with no effect on the cell because of the absence of a cell signalling domain (decoy receptor) (López-Castlejón et al, 2007). A third member of the IL-1 family is IL-1 receptor antagonist (IL-1ra), the only function of which seems to be the blocking of IL-1 action by competitively binding to IL-1 receptors without initiating a signalling cascade (Gibson et al, 2004).

IL-1α and IL-1β are expressed at low levels in the healthy brain with levels rising in response to local injury and minor infections. In contrast, a rapid up-regulation of mRNA and protein following clinical or experimental ischaemia, injury, neurotoxicity or inflammatory stimuli has been observed (Gibson et al, 2004). The mature form of IL-1β is secreted whereas IL-1α largely remains intracellular (although it can be released via calpain-mediated activation pathways), thus IL-1β is widely considered to be more important in mediating CNS inflammation (Gosselin & Rivest, 2007). IL-1ra has proven to be a useful experimental tool to study the effects of IL-1. The antagonist reduced the damage caused by focal or global ischaemia by 50% following administration into the cerebral ventricles of rodents. These early results indicated that IL-1 present in the brain

contributes to CNS insults and that IL-1ra could prove to be useful for therapeutic intervention (Relton & Rothwell, 1992).

Toulmond & Rothwell (1995) utilised tMCAo in the rat to show that IL-1ra is effective when given 3 h post-operation. Importantly, the results were not as positive after 8-12 hours suggesting a critical time-window for therapeutic intervention post-stroke. Another study showed that damage caused by tMCAo in mice lacking either IL-1α or IL-1β was similar in severity suggesting the two types of IL-1 were implicated. This seems likely because brain damage is reduced by 80% when both IL-1α and IL-1β are deleted (Boutin et al, 2001). IL-1β is elevated in the cerebrospinal fluid (CSF) of MS patients as well as being localised in the plaque region. The expression of the cytokine was also noted to be increased in the CSF of EAE animals (Wang & Shuaib, 2002). In addition to acute CNS injury, IL-1 has been implicated in chronic inflammatory diseases such as PD, AD and CJD (Lucas et al, 2006).

1.4.5.2 Tumour Necrosis Factor (TNF)

Another pro-inflammatory cytokine heavily implicated in CNS pathology is TNF. It is a 17 kDa polypeptide, which initiates intracellular signalling by binding to two TNF receptors (TNFRI [p55] and TNFRII [p75]). Binding to the p55 form has been demonstrated to induce cytotoxicity and arachidonic acid release whereas binding to p75 induces cell proliferation (Viviani et al, 2004). With the exception of red blood cells, virtually all cells in the body express TNF receptors (Wang & Shuaib, 2002). Furthermore, most cells within the CNS express and secrete TNF in pathological conditions. Studies in mice subjected to tMCAo showed that astrocytes as well as neurones produced TNF in the brain (Wang & Shuaib, 2002), whereas, in situ hybridisation (ISH) illustrated that TNF mRNA was localised to microglial cells in mice post-ischaemia (Gregersen et al, 2000). In chronic and active MS lesions, TNF was expressed by macrophages, astrocytes, microglia and ECs (Wang & Shuaib, 2002).

In a mouse model of global ischaemic CNS injury, TNF-protein was shown to be increased in the brain 1 h post-injury (Uno et al, 1997). Importantly, the protein expression levels went down before increasing again after 3 days, a result which was replicated in gerbils (Saito et al, 1996). In ischaemic rats, TNF neutralising antibodies significantly reduced infarct volume and MMP-9 expression, suggesting that TNF-induced expression of MMP-9 plays a role in post-stroke CNS damage (Hosomi et al,

2005). Studies in MS patients demonstrated that elevation in TNF levels correlated with disease severity. Additionally, at the peak of EAE symptoms, TNF levels were demonstrated to be elevated in serum and the CSF (Munoz-Fernandez & Fresno, 1998).

1.4.5.3 Interferon-Gamma (IFN-γ)

Interferon-gamma (IFN-γ) is not normally produced in the healthy CNS but is expressed by T and NK cells during CNS inflammation making it a noteworthy cytokine to study (Owens *et al*, 2004). Transgenic CNS expression of IFN-γ has been shown to increase expression of TNF, further demonstrating the complex interactions of many mediators in pro-inflammatory pathways (Jensen *et al*, 2000). There is evidence that IFN-γ may induce and control chemokine responses. Studies in IFN-γ KO mice induced with EAE have shown that IFN-γ has a profound effect on the chemokine profile in the disease model. Expression of chemokines CCL5 and CXCL10 were down-regulated whereas CXCL2 was up-regulated. Furthermore, the usual T cell and macrophage infiltration observed in WT mice was replaced by neutrophil infiltration (Tran *et al*, 2000).

1.4.5.4 Anti-Inflammatory Mediators

To counteract such powerful and prolific pro-inflammatory instigators, cells in the CNS synthesise a host of anti-inflammatory cytokines such as TGF-β and IL-10. TGF-β has traditionally been known as a suppressor of the immune system. However recent evidence suggests it may also attract inflammatory cells (Wahl, 2007). Three 25 kDa isoforms of TGF-β exist in humans: TGF-β1, -β2 and -β3, which bind as dimers to type II membrane receptors on cells. Following binding, a type I receptor is recruited, which undergoes phosphorylation triggering Smad-protein signal pathways. This can trigger apoptosis in a variety of cell-types (Chen *et al*, 1998).

1.4.5.5 Neurotrophic Factors

An important family of neuronal protective proteins are the NTFs, of which there are four members: nerve growth factor (NGF), brain-derived NTF (BDNTF), neurotrophin 3 (NT-3) and NT-4. NTFs bind to cell signalling receptors; tyrosine kinase TrKA and pan-neurotrophin receptor p75, promoting differentiation and proliferation of neurones by stimulating outgrowth and preventing degeneration (Boyd & Gordon, 2003; Allen &

Dawbarn, 2006). NGF is considered the prototype NTF and its critical role in neuronal development, adult cholinergic system protection, response to neurotoxic injury, prevention of neuronal loss, synaptic plasticity and beneficial effects in the aged brain are well established (Connor & Dragunow, 1998; Williams *et al*, 2006; Allen & Dawbarn, 2006).

1.5 ADAMTSs in the CNS

1.5.1 Studies of ADAMTSs in the CNS

Proteinases such as tissue plasminogen activator (tPA) and MMPs are up-regulated in a host of CNS inflammatory disorders suggesting that proteolysis is a key event in such pathologies (reviewed by Galtrey & Fawcett, 2007). To date, a limited number of reports have indicated that not only are ADAMTS proteinases expressed in the CNS but they also have potentially important roles within the tissue. The most extensively studied of the ADAMTSs within the brain are the GEPs because they have been shown to cleave CSPGs, which are key components of the CNS ECM. The expression levels of the GEP ADAMTSs have been studied in specific disorders of the CNS, producing some potentially important findings.

A previous study by our laboratory suggested that ADAMTSs may have a role in cerebral ischaemia by showing that ADAMTS-1 and -4 (mRNA and protein) were up-regulated following tMCAo in rats (Cross *et al*, 2006). Importantly, TIMP-3 levels remained constant between sham-operated and tMCAo brains, suggesting ADAMTS activity was not sufficiently inhibited. In the same study, TNF modulated an increase in ADAMTS-4 expression (mRNA and protein) in B327-01 human astrocytes *in vitro* indicating that inflammation is a trigger for the ADAMTSs in the CNS.

Studies in our laboratory with human and EAE tissue have demonstrated a potential role for GEP ADAMTSs in MS. In post-mortem MS brain tissue, ADAMTS-1, ADAMTS-5 and TIMP-3 mRNA was decreased compared to control tissue. In addition, ADAMTS-4 protein expression was raised in MS tissue when compared to healthy brain (demonstrated by western blotting) and was associated with astrocytes (shown by immunohistochemistry [IHC]) (Haddock *et al*, 2006). In EAE, our group detected differential expression of ADAMTS-1, -4, -5 and TIMP-3 at various stages of disease

progression (Cross *et al*, 2005b). It has also been demonstrated that there is a genetic association between polymorphisms in the ADAMTS-14 gene and MS; however the functional reasons for this are unclear (Goertsches *et al*, 2005).

There have been a limited number of reports in other CNS disorders focussing on ADAMTS involvement. Following hypoglossal nerve (in lower brain stem [medulla oblongata]) injury in rats, ADAMTS-1 mRNA was shown to be up-regulated (Sasaki *et al*, 2001). ADAMTS-1 (but not ADAMTS-5) expression was also shown to be raised in Down syndrome (genetic, congenital mental illness), AD and Pick's disease (degeneration of frontal and temporal lobes) tissue (Miguel *et al*, 2005).

1.5.2 Why Study ADAMTS-9 in the CNS?

The first preliminary indication of ADAMTS-9 expression in the CNS came from Clark *et al* (2000) who cloned a splice variant of the enzyme from a β amyloid-treated rat astrocyte cDNA library. There is evidence that the group cloned ADAMTS-9 from partially processed pre-RNA (Somerville *et al*, 2003) and therefore it is highly likely that the authentic mRNA encoding for full-length ADAMTS-9 was also present in the CNS-derived library that was screened. Any doubt that the authentic product of the ADAMTS-9 gene was expressed in the human brain (foetal and adult) was removed by RT-PCR analysis (Somerville *et al*, 2003). Further evidence of ADAMTS-9 CNS expression came from *ISH* studies of mouse brain embryo development. *Adamts9* was detected in the floorplate of the diencephalon, cerebral cortex, dorsal root ganglia, choroid plexus and neuroepithelium (Jungers *et al*, 2005).

Despite the fact ADAMTS-9 is clearly abundantly expressed in the CNS, no studies have focussed specifically on the peptidase in the brain. Clearly ADAMTS-9 has the potential to contribute to a host of physiological and pathological processes in the CNS because it has been shown to cleave aggrecan (albeit with limited efficiency) and versican, which are major structural components of the CNS ECM (Somerville *et al*, 2003). ADAMTS-9 may also degrade other proteins including other CNS ECM CSPGs brevican and neurocan, on which the peptidase has yet to be tested. Therefore, ADAMTS-9 may be involved in normal ECM turnover e.g. clearing a path for the migration of endogenous cells.

As well as having a role in normal physiology, studies in non-CNS tissue point towards ADAMTS-9 expression being modulated by mediators, important in CNS inflammatory disorders. It has been demonstrated that ADAMTS-9 is up-regulated in response to pro-inflammatory cytokines, in particular IL-1β, TNF and oncostatin M (Demircan *et al*, 2005; Hui *et al*, 2005). Whereas, anti-inflammatory mediators such as TGF-β1 have been shown to down-regulate ADAMTS-9 expression (Cross *et al*, 2005a). Such data indicate that the proteinase could be part of inflammatory pathways in which control of expression is a key regulatory event.

In CNS pathology, ADAMTS-9 could mediate the opening of the BBB following binding to BM HSPGs because the peptidase has a BBXB (where B = a basic amino acid [Lys or Arg], X = any amino acid) consensus site for binding to heparin (Somerville *et al*, 2003). If the metalloproteinase domain is accessible to substrates following binding, ADAMTS-9 could have a similar role to MMP-2 and -9, which have been shown to compromise the integrity of the BBB (Sospedra & Martin, 2005). Following astrogliosis which accompanies neuronal injury, ADAMTS-9 has the potential to be bound to HSPGs present in glial scars (Trendelenburg & Dirnagl, 2005). CSPGs, which are substrates of ADAMTS-9, are the main inhibitory component of glial scars (reviewed in Properzi *et al*, 2003) thus the peptidase could have a profound impact on post-neuronal damage responses.

ADAMTS-9-mediated degradation of the glial scar could be either protective or detrimental to the damaged CNS. It could enable the migration of neuronal precursor cells to damaged regions and allow for neurite outgrowth thus restoring neuronal function. In contrast, CSPG-processing may allow for the passage of inflammatory cells, activated microglia and pro-inflammatory mediators e.g. cytokines to access susceptible neurones and mediate further damage. As well as cleavage of CSPGs within the glial scar, ADAMTS-9 may also compromise the structure of more general ECM regions away from injured sites thus aiding in the migration of infiltrating inflammatory cells from the BBB to areas of damage.

The BBXB motif is also a consensus site for binding to sulphatide, a sulphated glycosphingolipid, which is a membrane protein predominantly expressed in the CNS on oligodendrocytes and neurones. Sulphatide is also found in myelin and is a target for autoimmune responses in MS (Halder *et al*, 2006). Thus binding of ADAMTS-9 to

sulphatide may have implications in MS by either aiding or inhibiting myelin breakdown. Alternatively, sulphatide may be another binding site for ADAMTS-9 within the CNS. With such a wealth of potential roles for ADAMTS-9 in the normal and inflamed CNS, this study of the expression profile and modulation of ADAMTS-9 in the brain is both timely and relevant.

1.6 Aims and Objectives of the Study

Despite having the potential to be involved in CNS inflammatory disorders and normal brain physiological processes, a study of ADAMTS-9 in this field has not been reported.

Hypothesis: ADAMTS-9 is an important enzyme in the normal and inflamed CNS.

Overall Aim: To establish the expression profile of ADAMTS-9 in CNS-derived cells and a model of CNS inflammation, to provide preliminary evidence that the peptidase is modulated by inflammatory conditions in the brain.

Objectives:

1. To develop, optimise and validate methods (real-time RT-PCR, *IS*H, western blotting) to test ADAMTS-9 mRNA and protein expression by cells of the CNS *in vivo* and *in vitro*.

2. To analyse the modulation of ADAMTS-9 expression by factors (e.g. cytokines) pertinent to CNS inflammation in astrocytic, microglial and neuronal cells *in vitro*.

3. To establish the expression profile and cellular origin of ADAMTS-9 in tMCAo, a rat model of focal cerebral ischaemia.

Chapter 2

Materials and Methods

All procedures were performed at ambient temperature (~20°C) and atmospheric pressure (~0.1 MPa) unless otherwise stated.

2.1 Cell Culture

The isolation of a particular CNS-derived cell-type in culture allows the analysis of target protein/mRNA (e.g. ADAMTS-9) expression levels under a) basal conditions and b) experimental conditions, which mimic a particular physiological or pathological state. By controlling or modifying the culture medium, the effect on the cell of one variable or molecule from a complex disease process can be analysed e.g. a cytokine. There are two main types of cell culture: primary and secondary (cell lines). Primary human cells are separated and purified from the body tissues and cultured directly with limited modifications and are utilised over a small number of passages. Cell lines are often immortalised but still have density inhibition and anchorage-dependant growth. Alternatively, cell lines can be obtained from tumours which are already immortalised.

Human CNS-derived cells were obtained in accordance with international ethical requirements, guidelines and legislation. The cell-types, origins, where they were obtained and the media in which they were cultured are listed in Table 2.1. Foetal calf serum (FCS) was heat-inactivated prior to addition to the media by incubation at 56°C for 30 min to destroy complement components and prevent cell lysis by antibody binding. All cells were incubated at 37°C in a humidified atmosphere of 5% (v/v) CO_2 (in air) in a Hera Cell incubator (Heraeus Instruments, Kandro Laboratories Products, Germany). All plasticware (flasks, tubes) was purchased from BD Falcon Biosciences (Oxford, UK).

Cells were passaged when they became confluent by disposal of the medium and the addition of 0.05% trypsin/0.53 mM EDTA (Gibco, Invitrogen Co, Paisley, UK). Once cells dissociated from the flask, they were centrifuged in a Sorvall RT7 Plus centrifuge (Kendro Laboratory Products, Newtown, USA), which was used throughout the cell culture work, at 200 x g and the pellet was re-suspended in fresh media. Cells were either divided into new flasks or counted on a haemocytometer for plating in experiments. Alternatively, the pellet was resuspended in freezing medium consisting of 10% cryopreservative dimethyl sulfoxide (DMSO, Sigma Aldrich, Poole, UK), 90% (v/v) growth media prior to depositing 1 x 10^6 cells in cryovials, which were placed in a

56

Table 2.1 Human Cell Lines used in this Study and the Composition of Media

Name	Origin	Obtained From	Culture Media
U373-MG astrocytoma cell line	61 year-old Caucasian male, malignant grade 3 glioma	European Cell Culture Collection	- minimum essential media (MEM) (Sigma) - 10% (v/v) heat inactivated foetal calf serum (HIFCS) - 2 mM L-glutamine (L-glut) - 100 U/mL penicillin/100 μg/mL streptomycin (1% [v/v] P/S) - 1% (v/v) non-essential amino acids - 1 mM sodium pyruvate
U87-MG astrocytoma cell line	44 year-old caucasian female, grade 3-4 malignant glioma	European Cell Culture Collection	as above
CHME3 microglia cell line	foetal microglia transfected with SV40 large T antigen (Janabi et al, 1995)	Prof. Tardieu, Université Paris Sud, France	- Dulbecco's Modification of Eagle's medium (DMEM) containing Glutamax II (L-glycyl-L-glutamine) and 4500 mg/L glucose - 10% HIFCS - 1% (v/v) P/S - 1% non-essential amino acids - 1 mM sodium pyruvate
SHSY-5Y neuroblastoma cell line	4 year-old Caucasian female, metastasised to the bone marrow	American Type Culture Collection (ATCC)	- DMEM - 10% HIFCS - 1% v/v P/S - 2 mM L-glut
B327-01 astrocytes	temporal lobe resections from an epilepsy patient (Flynn et al, 2003)	Dr. I. Romero, The Open University, Milton Keynes, UK	Differentiated for 7 days with 10^{-5} M retinoic acid (Sigma) - 50% (v/v) MEMα - 50% (v/v) F10 - 250 U/mL fungizone Utilised up to passage 6 - 1% (v/v) P/S - 1% (v/v) human serum - 10% (v/v) HIFCS

All reagents purchased from Gibco, Invitrogen Co. unless otherwise stated.

57

Cryo 1°C (temperature decreases -1°C/min) freezing container (Nalgene, Rochester, USA) containing isopropanol in -80°C freezer. Once cells were at -80°C, cryovials were transferred to liquid N_2 storage. Cells were thawed by placing cryovials in a 37°C incubator before depositing cells in 10 mL of growth media prior to centrifugation at 200 x g to remove DMSO. Pellets were resuspended in fresh growth medium prior to depositing in a cell culture flask.

Through binding to RetA receptors (RetARα, RetARβ and RetARγ), RetA regulates the expression of hundreds of genes in the CNS (Clagett-Dame et al, 2005). Treatment with physiological concentrations (10^{-5} M) of RetA has been shown to decrease proliferation of SHSY-5Y cells and promote extension of neuritic processes resulting in a morphologically neuronal population of cells (Encinas et al, 2000). Therefore, to differentiate the SHSY-5Y neuroblastoma cells to a phenotype comparable to in $vivo$ neurones, the cells were treated with RetA (vitamin A). A 10^{-2} M RetA stock solution was prepared in 100% molecular grade ethanol. Cells were cultured in 10^{-5} M RetA diluted in culture media for one week prior to either passaging or plating for experiments. For comparative studies, SHSY-5Y cells were additionally cultured in parallel without RetA. Neuronal morphology of the SHSY-5Y cells was confirmed by visualisation under a light microscope (Leica Microsystems, Wetzlar, Germany) prior to image capture and analysis with the USB 2.0 camera/XLi-Cap software (XL Imaging Ltd. Swansea, UK).

2.2 Treatment of Cells with Cytokines/Growth Factors

Cells were seeded into 24-well plates at a density of 1×10^5 cells/well in 1 mL of medium and left for 24 h to adhere. IL-1β, IFN-γ, TNF (all Tebu-Bio Laboratories, Peterborough, UK), TGF-β1 and NGF (both PeproTech) were diluted in serum-free media at concentrations of 0.2 ng/mL (4×10^{-8} M), 0.4 ng/mL (8×10^{-8} M), 0.8 ng/mL (1.6×10^{-7} M), 1 ng/mL (2×10^{-7} M), 10 ng/mL (2×10^{-6} M) or 100ng/mL (2×10^{-5} M). Medium was removed prior to the addition of 1 mL of each cytokine/GF in triplicate wells. Combinations of these concentrations were prepared for IL-1β and TNF prior to analysis of the synergistic effect of both cytokines added together. Cells were incubated with cytokines/GFs for 24 h after which the media was removed and replaced with 333 μL of TRI Reagent (Sigma) per well (1 mL per treatment). All experiments were repeated a minimum of three times independently.

2.3 Transient Middle Cerebral Artery Occlusion (tMCAo) Rat Model of Focal Cerebral Ischaemia

All animal procedures were carried out at The University of Manchester by Dr. Stuart Allan and Dr. Chris Stock. Male Sprague-Dawley rats (290-320 g, Charles River, UK) were subjected to halothane anaesthesia (Fluorothane, Zeneca, UK, 1-2% in a mixture of oxygen and nitrous oxide [1:2 ratio]). Body temperature was maintained at 37.0 ± 0.5°C throughout anaesthesia by means of a homoeothermic blanket (Harvard Apparatus, UK). All surgical procedures were carried out in accordance with the 'Guidance on the Operation of Animals (Scientific Procedures) Act' (1986).

Transient focal cerebral ischaemia was induced in rats by luminal thread occlusion of the MCA, as described previously (Longa *et al*, 1989; Mulcahy *et al*, 2003) and illustrated in Figure 2.1. The thread was withdrawn to allow reperfusion at 90 min post-occlusion. Sham-operated animals were exposed to the same surgical procedure, with the exception that the thread was inserted only briefly and not to its full extent. Six, 24 and 120 h after tMCAo or sham-operation, the animals were sacrificed by exposure to a rising concentration of CO_2 and the brains removed and frozen on dry ice. Brains were dissected into ipsilateral (occluded in tMCAo) and contralateral (non-occluded in tMCAo) hemispheres prior to each hemisphere being cut in half again coronally (all dissecting performed on dry ice). Frozen sections of each quarter of each brain (10 μm thickness) were cut on a cryostat (Leica) and collected on polylysine slides (VWR International, Belgium) for *IS*H and IHC analysis. For extraction of protein and RNA, 5 x 30 μm sections of each quarter of each brain were cut and deposited into Eppendorf tubes prior to the addition of 1 mL TRI reagent. Table 2.2 shows the number of animals included in the study.

Figure 2.1 Procedure of Inducing tMCAo in the Rat
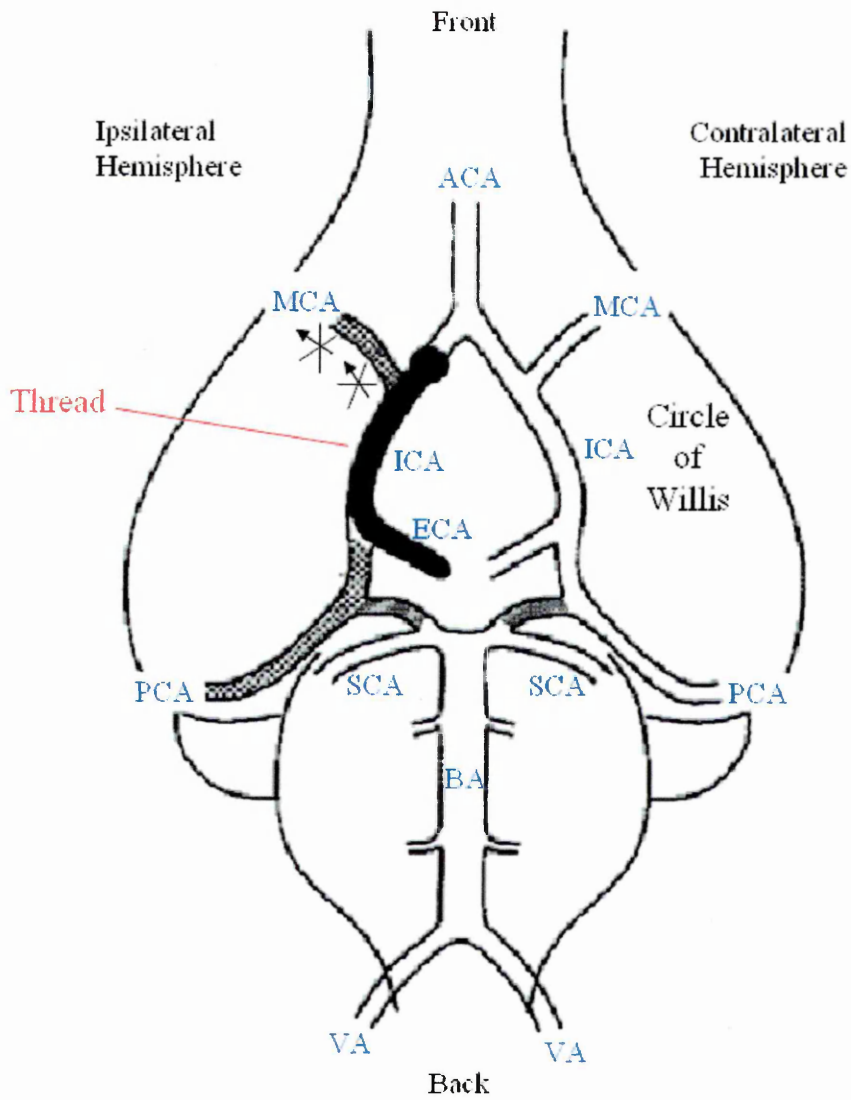
The diagram shows the route of luminal thread insertion and resultant occlusion of the middle cerebral artery (MCA). Thread is inserted via the external carotid artery (ECA) and internal carotid artery (ICA) prior to reperfusion after 90 min. ACA = anterior cerebral artery, SCA = superior cerebral artery, BA = basilar artery, PCA = posterior cerebral artery, VA = vertebral artery. Crossed-out arrows indicate blocked blood-flow. Image courtesy of Dr. Peter Thornton (Manchester, UK).

Table 2.2 Numbers of Animals Utilised in the tMCAo Study

Hours Post-Operation	Procedure	Number of Animals
6	sham	2
6	tMCAo	5
24	sham	4
24	tMCAo	4
120	sham	3
120	tMCAo	3

2.4 RNA/Protein Extraction

RNA and protein were extracted from cells and tMCAo tissue using TRI Reagent in accordance with the manufacturer's protocol. TRI Reagent is a mixture of guanidine thiocyanate and phenol in a mono-phase solution. Briefly, TRI Reagent was added to cells and tissue prior to homogenisation (pippeting up and down). Upon addition of chloroform and centrifugation the mixture separated into three phases: 1) an aqueous RNA phase, 2) an interphase containing DNA and 3) an organic protein phase. RNA was isolated by a series of washes in molecular grade isopropanol and ethanol with intervening centrifugation steps. Protein was isolated by a series of washes in molecular grade ethanol and 0.3 M guanidine hydrochloride, 95% (v/v) ethanol with intervening centrifugation steps.

2.5 Bicinchonic Acid (BCA) Protein Assay

Protein concentration was determined by bicinchonic acid (BCA) protein assay, in which protein reduces Cu^{2+} to Cu^{+} in an alkaline medium (Biuret reaction). The binding of Cu^{+} to BCA yielded a purple-coloured product, the intensity of which was proportional to the amount of protein present. Protein concentration was subsequently calculated by plotting a standard curve of known protein concentrations. Protein samples (20 µL) were added to 96-well plates in duplicate as well as 20 µL bovine serum albumin (BSA) standards (0-20 mg/mL) in triplicate. To each well, 200 µL of working BCA reagent (50:1 BCA : 4% [w/v] copper [II] sulphate) was added and the plate incubated for 30 min prior to analysing the absorbance by spectrophotometry (570

nm) on a Wallac Victor^2 1420 Multilabel Counter (PerkinElmer, Turku, Finland). The protein assay allowed the calculation of the correct volume of protein to load for SDS-PAGE (sodium dodecyl sulphate-polyacrylamide gel electrophoresis).

2.6 cDNA Synthesis

Extracted mRNA cannot serve as a template for real-time PCR and therefore it is used to synthesise cDNA with the enzyme reverse transcriptase (RT). The synthesis of the first strand of cDNA requires a primer in order for the RT to extend. The cDNA copy is produced by the addition of deoxynucleotide triphosphates (dNTPs) to the 3' end of the extending primer. There are three main priming approaches to perform the cDNA synthesis reaction, yielding different products depending on the purpose of the experiment. The primers can either be: 1) oligo (dT) primers, which prime all mRNAs simultaneously, yielding complete cDNA, 2) sequence specific primers, which target one mRNA sequence or 3) random hexanucleotides (hexamers), which are short (~8 nucleotides long) single stranded DNA (ssDNA) of every combination of bases that copy mRNA scattered from all over the sequence. In this study, random hexamers were utilised because the synthesised cDNAs are shorter thus there is an increased probability that the 5' ends of the mRNA are copied because RT is rarely able to extend the full length of the mRNA molecule (Turner *et al*, 2001).

The cDNA synthesis was performed with RNAse/DNAse free tips, tubes and gloves following the de-contamination of surfaces with alcohol wipes. The total reaction volume for each RNA sample was 19 µL including: Superscript II RT (1 µL), 5x 1st strand buffer (4 µL), preservative dithiothreitol (DTT) (2 µL), RNAseOut ribonuclease inhibitor (0.5 µL), random hexamers (0.5 µL) (all Invitrogen) and 1 µL dNTPs mix containing 12.5% dATP, 12.5% dCTP, 12.5% dGTP and 12.5% dTTP in 50% H_2O (all v/v) (Bioline, London, UK), RNA sample (1 µL) and molecular grade H_2O (10 µL). The reaction was performed at 42°C for 2 h in a heat block. The reaction was stopped by incubating the samples at 95°C for 5 min in a heat block, to inactivate the enzyme. For each cDNA synthesis preparation two samples were included as negative controls, one lacking RT and the other RNA (replaced by water). The resulting cDNA was used as a template for real-time RT-PCR.

2.7 Agarose Gel Electrophoresis

Throughout this thesis, agarose gel electrophoresis (AGE) was routinely performed to visualise nucleic acids e.g. to assess the quality of an RNA sample prior to cDNA synthesis. AGE works on the principle that nucleic acids are negatively charged and thus migrate to the positive pole in an electric field. The size of the molecule dictates the speed at which it migrates through the pores in the agarose gel resulting in a separation of different sized nucleic acid chains. Within the agarose is ethidium bromide (EtBr), which intercalates between the base pairs (bps) of DNA/RNA and fluoresces under UV light. DNA ladders were loaded in order to ascertain the size of the nucleic acid.

Agarose (2% or 4%) was dissolved in Tris-boric acid-EDTA (TBE) buffer (89 mM Tris, 89 mM boric acid, 2 mM EDTA, pH 8.3) prior to addition of 5 mg/mL EtBr. Nucleic acids were mixed 1:1 (3 μL:3 μL) with 2x loading buffer (50% glycerol, 0.1% bromophenol blue, 1x TBE) prior to loading in agarose wells with a DNA ladder (10, 100 or 500 bp) (Promega, Madison, USA). Electrophoresis was performed at 100 V for approximately 1 h prior to visualisation under a UV light in a BioChemi system (UVP Bioimaging System, USA) and subsequent analysis with LabWorks Image Acquisition and Analysis Software (UVP, USA).

2.8 Real-Time RT-PCR

2.8.1 Real-Time RT-PCR Theory

Real-time RT-PCR is a powerful tool for quantifying relative differences in amounts of mRNA of the same gene between different samples e.g. control versus treated. Conventional PCR analysis occurs at the end of the reaction process, the amount of product and starting material theoretically being proportional at any cycle number. However, replicate reactions yield different amounts of PCR products (due to undetected deviations from normal amplification) and therefore results cannot be considered quantitative, merely qualitative. Real-time RT-PCR was developed by Higuchi *et al* (1992) as a technique which allows the measurement of the reaction whilst the amplification is taking place as opposed to the end-point.

Classical PCR can amplify minute amounts of DNA using a pair of oligonucleotide primers each complementary to one end of the DNA target sequence. Primers are extended towards each other by a thermostable polymerase in a reaction cycle of denaturation (~95°C), primer annealing (~55°C) and polymerisation (~72°C). Real-time RT-PCR adheres to these basic principles but the monitoring of accumulating amplicon has been made possible by utilising fluorescent molecules to label primers, oligoprobes or the amplicon itself. The change in signal which occurs when these labels directly interact or hybridise to the amplicon is proportional to the amount of amplicon present during each cycle (Wong & Medrano, 2005).

Data obtained from a real-time RT-PCR run yields a sigmoidal curve when fluorescence intensity is plotted against cycle number as shown in Figure 2.2A. The initial amplification is not taken into account because the signal does not significantly rise above background noise. The rate of amplification occurs in three phases; a log-linear phase (LP) where exponential progress is observed, a transitional phase (TP) where reagents become limiting (e.g. primers and enzyme) and finally a plateau phase (PP) where no further product is formed (Mackay, 2004). The point where the fluorescence is clearly higher than the background is known as the cycle threshold (C_T), which is reached at a lower cycle number if a higher level of target template is present in the reaction, thus the curve is shifted to the left.

There are a number of different detection chemistries currently available which can be categorised as 'specific' or 'non-specific' for the amplicon target sequence. All chemistries are based on fluorogenic detection and have generally the same level of sensitivity. SYBR green is a non-specific double stranded DNA (dsDNA)-binding fluorogenic molecule which was utilised in this project. The unbound dye exhibits negligible fluorescence in solution but during LP it intercalates to the minor groove of dsDNA and an increasing signal is observed upon light excitation and amplicon amplification. Measurements are taken at the end of the elongation step of every cycle to monitor the increasing amount of the amplicon (Bustin, 2000).

The main advantage of using SYBR green over fluorogenic oligoprobes is that the dye can be utilised for different genes assays and only specific primers are required. Also SYBR green offers a lower cost detection system than oligoprobes. Unfortunately, SYBR green binds to any dsDNA which may form, thus fluorescing because of non-

Real-Time PCR amplification plot (A) with GAPDH and ADAMTS-9 primers showing log-linear phase (LP), transitional phase (TP) and plateau phase (PP). Cycle-threshold (C_T) is represented by the red line. ΔRn = fluorescence signal - residual background fluorescence (fluorescence intensity). Note that ADAMTS-9 (C_T values ~23-28) expression levels vary under different experimental conditions, in contrast to the stable expression of GAPDH (C_T values ~16-17). GAPDH expression > ADAMTS-9 expression, hence GAPDH plots are shifted to the left.

Figure B represents a typical melt curve analysis showing specific melt curves with ADAMTS-9 and GAPDH primers. Derivative '-dF/dT' = fluorescence as a function of temperature against time. Note the lack of smaller peaks, which represent primer dimer formation (non-specific amplification).

Figure 2.2 Representative Real-Time PCR Amplification and Melt Curves
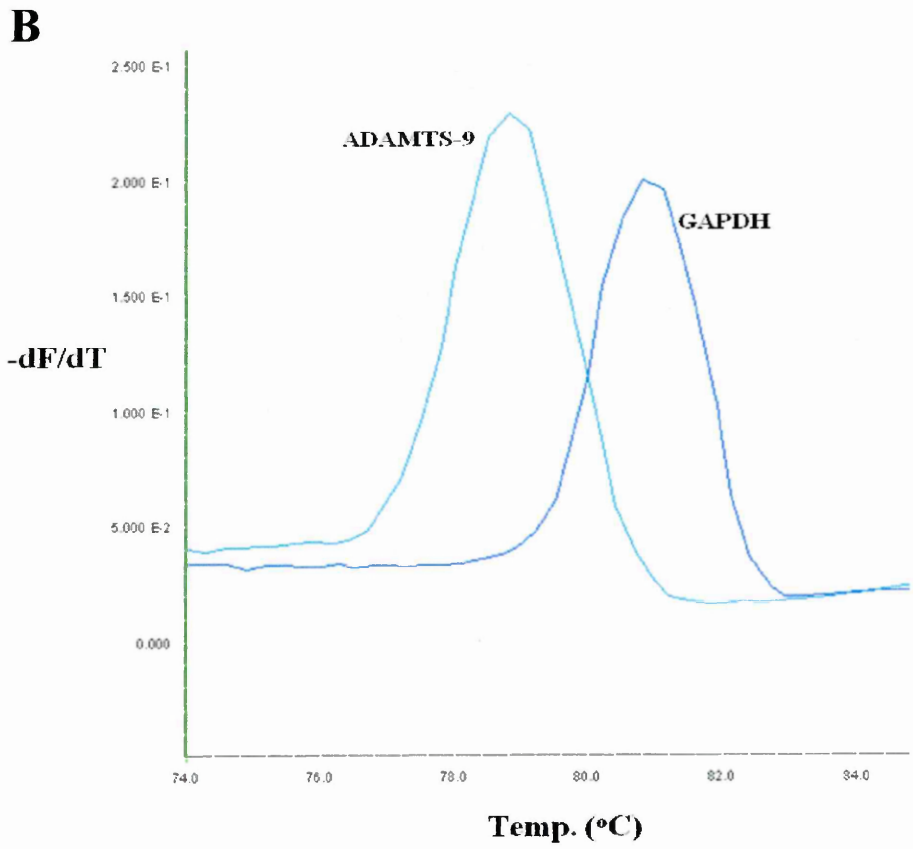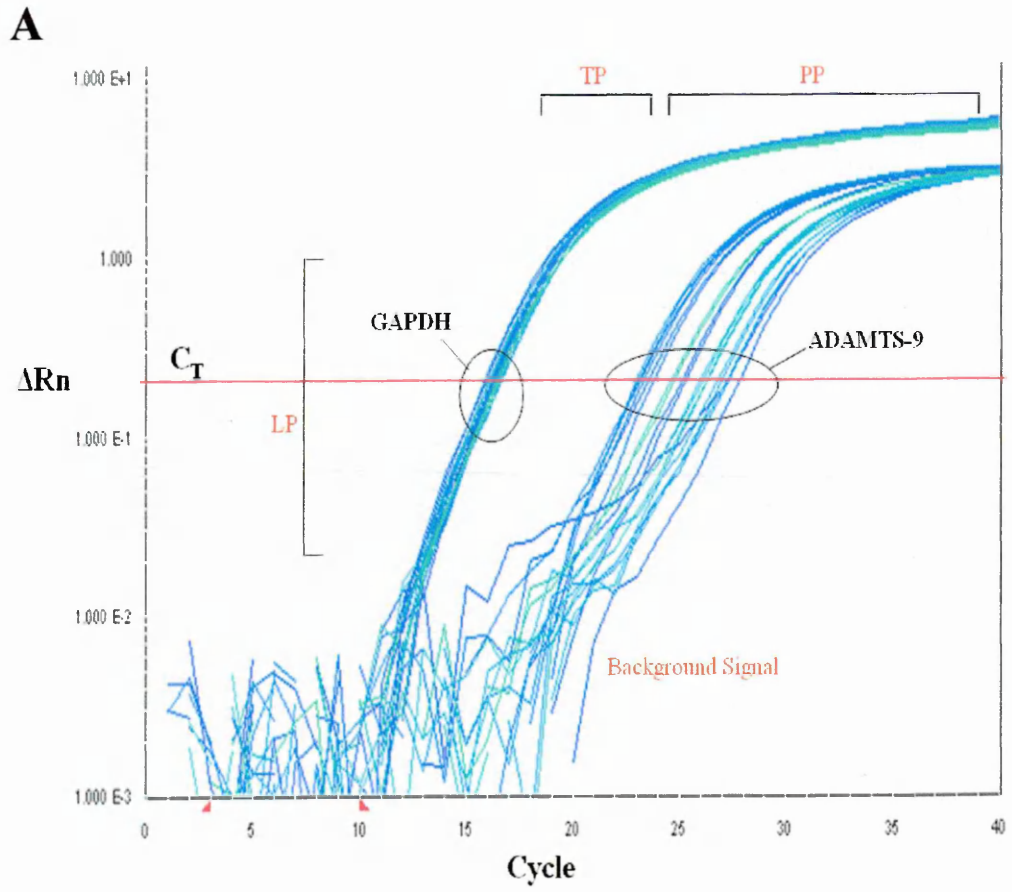
specific products (i.e. primer-dimer) and generating inaccurate data. To counteract this problem a short additional step is included after the extension step whereby the temperature is increased and non-specific products are denatured prior to detection of fluorescence (Mackay *et al*, 2002).

To verify that no non-specific products are contributing to the signal, melt curve analysis must be performed. Each amplicon product has its own specific nucleotide composition and thus a specific melting temperature (*T*m). Melt curve analysis involves increasing the temperature above the *T*m of the amplicon and utilising software (ABI Prism 7900 HT Sequence Detection System, Applied Biosystems, Warrington, UK) to plot fluorescence as a function of temperature against time to produce a melt curve as shown in Figure 2.2B. The small primer-dimer and amplification artefacts melt at a much lower temperature than the amplicon and when analysing are easily distinguishable from the characteristic melt curves of the amplicon product (Mackay *et al*, 2002).

There are two main types of applications for real-time RT-PCR, the first one being 'absolute quantification' whereby a standard curve is constructed from known standards, which is used to determine the concentration (copy number) of the starting template (Bustin, 2000). In this study a standard curve was not required because 'relative quantification' compares the amount of template between samples using a mathematical formula (e.g. $2^{-\Delta\Delta C_T}$) to calculate relative fold increases/decreases in expression.

In parallel to detecting the target gene, it is critical to analyse the expression levels of at least one housekeeping gene in all samples tested. This compensates for introducing varying amounts of total mRNA into the RT reaction and thus producing different concentrations of starting template cDNA between samples. Housekeeping genes are consistently expressed at moderately abundant levels and their products are crucial for preserving cellular function and completing the cell-cycle (Butte *et al*, 2001). In any real-time RT-PCR analysis, it is critical that the expression of the normalising housekeeping gene is not altered by the experimental conditions being tested.

2.8.2 Primer Design and General Real-Time RT-PCR Protocol

The real-time RT-PCR primers were designed to span intron/exon boundaries in order to preclude the amplification of contaminating genomic DNA, which can lead to false positives. This eradicated the need for treating RNA samples with DNase prior to cDNA synthesis (Bustin, 2002). Primers had a G/C content of 20-75% and had an optimal length of 15-20 bp (long enough for high-specificity, short enough for high annealing-efficiency). Primers generated a product which did not exceed 150 bp (for optimal amplification efficiency) (Gunson et al, 2006). A key property was that the Tm of the primer pairs were similar (within 1-2°C), in the range of 58-60°C.

The primers utilised in this study were designed using Primer Express (Applied Biosystems), which is a powerful tool that generates primers based on the above requirements (Bustin, 2000). Synthesis of primers was performed by MWG-Biotech AG (Ebersberg, Germany). Table 2.3 lists the details of all fully optimised and validated primers utilised in this study. Human and rat GAPDH as well as human ADAMTS-1, -4, -5 and -9 primers were validated and optimised previously (by Dr. Alison Cross). In this study it was necessary to design and validate rat ADAMTS-9 primers as well as human YWHAZ primers (housekeeping gene used with B327-01 and SHSY-5Y cells). All real-time RT-PCR products were visualised by 4% AGE to confirm the correct size prior to sending for sequencing (Core Genetics Service, The University of Sheffield, UK) to confirm that primers were specific to the correct target gene. In preparation for sequencing, PCR-clean-up was carried out on the product with QIAquick kit (Qiagen) in accordance with the manufacturer's protocol. The clean-up removed components of the PCR reaction (primers, nucleotides and polymerase enzyme) by a series of binding, washing and eluting steps from a silica membrane column. The reverse complement of the sequence obtained with the reverse primer was obtained by utilising The Sequence Manipulation Suite (http://www.bioinformatics.org/sms/) and was subjected along with the sequence obtained with the forward primer to a nucleotide-nucleotide BLASTn search (basic local alignment search tool) (http://www.ncbi.nlm.nih.gov/BLAST/). All RT-PCR product sequences were a 100% match with the sequence from which the primers were designed.

All real-time RT-PCR experiments were performed using the ABI Prism 7900 sequence detection system (Applied Biosystems). Real-time RT-PCR was carried out with 10 μL

Human ADAMTS-9 primers were utilised with all human cell lines (U373-MG, U87-MG, B327-01, CHME3 and SHSY-5Y). Human ADAMTS-1, -4 and -5 primers (as used in Haddock *et al*, 2006) were utilised to study expression of these enzymes in the SHSY-5Y cell line. Human GAPDH primers were used with human U373-MG, U87-MG, SHSY-5Y (under basal conditions only) and CHME3 cells except. For details of YHWAZ primers, which was utilised as the housekeeping gene with B327-01 and SHSY-5Y (under experimental conditions e.g. treatment with factors) cells, see Table 2.4. Rat ADAMTS-9 and GAPDH primers were utilised with tMCAo rat model of stroke. Note all products were <150 bp.

69

Table 2.3 Primers Utilised in Real-Time RT-PCR Experiments for Analysis of ADAMTS mRNA Expression Levels

Gene	Species	Accession Number	Forward Sequence (Concentration used at)	Reverse Sequence (Concentration used at)	Location	Product Size (bp)
ADAMTS-9	human	NM_182920	5' GCACCCGAGGCAAGTGAA 3' (3.3 pmol/μL)	5' TCGGATGGGAGACACGATTT 3' (3.3 pmol/μL)	Forward: 7 Reverse: 86	79
ADAMTS-9	rat	NM_001107877	5' GAAGTACATCACCGAGTTCTTAGACACT 3' (10 pmol/μL)	5' AGAAGGGCCGGGCAGTTG 3' (3.3 pmol/μL)	Forward: 1092 Reverse: 1193	101
ADAMTS-1	human	NM_006988	5' GCACTGCAAGGGCGTAGGAC 3' (3.3 pmol/μL)	5' AAGCATGGTTTCCACATAGCG 3' (0.5 pmol/μL)	Forward: 945 Reverse: 1034	89
ADAMTS-4	human	NM_005099	5' TCACTGACTTCCTGGACAATGG 3' (0.5 pmol/μL)	5' GGAAAGTCACAGGCAGAGATGCA 3' (10 pmol/μL)	Forward: 1641 Reverse: 1721	80
ADAMTS-5	human	NM_007038	5' CACTGTGGCTCACGAAATCG 3' (0.5 pmol/μL)	5' CGCTTATCTTCTGTGGAACCAAA 3' (3.3 pmol/μL)	Forward: 1340 Reverse: 1432	92
GAPDH	human	NM_002046	5' GCTCCTCCTGTTCGACAGTCA 3' (10 pmol/μL)	5' ACCTCCCCATGGTGTCTGA 3' (3.3 pmol/μL)	Forward: 7 Reverse: 86	79
GAPDH	rat	M_17701	5' TGATTCTACCCACGGCAAGT 3' (3.3 pmol/μL)	5' AGCATCACCCCATTTGATGT 3' (3.3 pmol/μL)	Forward: 171 Reverse: 295	124

reactions in duplicate and each experiment was repeated three times. The reaction consisted of 5 μL 2x SYBR green master-mix (containing SYBR green dye, AmpliTaq Gold DNA polymerase, dNTPs and dUTPs) (Applied Biosystems), 2 μL H_2O, 1 μL each of forward and reverse primers (made up to optimised concentrations, see Tables 2.3 and 2.4) and 1 μL cDNA sample.

2.8.3 Comparative C_T Method of Data Analysis

Relative fold increases/decreases in mRNA expression levels of test samples (treated) compared to control samples (untreated) were calculated using the comparative C_T ($2^{-\Delta\Delta C_T}$) method using the formula and calculation below (Livak & Schmittgen, 2001). Levels of target gene mRNA expression in untreated samples are expressed as '1'. The fold differences in treated samples are expressed as values relative to the untreated samples.

$$2^{-\Delta\Delta C_T}$$

Calculation:

Step 1: $\Delta C_T = C_T$ of target gene - C_T of housekeeping gene

Step 2: $\Delta\Delta C_T = \Delta C_T$ of test sample - ΔC_T control sample

Step 3: $2^{-\Delta\Delta C_T}$ = relative fold increase

For the $2^{-\Delta\Delta C_T}$ method to be valid, the amplification efficiencies of the target gene and housekeeping gene must be approximately equal (Livak & Schmittgen, 2001). In order to ascertain that the ADAMTS-9 human and rat primers had similar efficiencies to the housekeeping genes, a primer efficiency comparison test was conducted. Real-time RT-PCR was performed on serially diluted cDNA (1:2, 1:3, 1:4, 1:5, 1:10, 1:100, 1:1000, 1:10,000) prior to plotting the ΔC_T value of each sample against $\log_{10}$(cDNA concentration) (Ginzinger, 2002). A slope close to zero (0±0.1) indicated that the target gene and housekeeping gene primer efficiencies were approximately equal (Wong & Medrano, 2005).

In this study, relative levels of ADAMTS-9 expression were also analysed between test samples i.e. comparison of target gene expression between different cell-types under

basal conditions. In order for this approach to be valid, the efficiencies of the target gene and housekeeping gene primers must also be close to 100% (and ~equal). To compare the expression levels of test samples (as opposed to comparing treated with control) the following formula was utilised:

$$2^{-\Delta C_T}$$

Note: $2^{-\Delta C_T}$ values represent the relative levels of target gene expression between samples in a particular experimental system, normalised to a housekeeping gene. Hence $2^{-\Delta C_T}$ values have no units. Values can only be compared across experiments if the same housekeeping gene is utilised and the experimental procedure was comparable (i.e. cells cultured in the same manner).

2.8.4 Real-Time RT-PCR Primer Concentration and Efficiency Tests

If the concentration of real-time RT-PCR primers is too high, mis-priming is a more likely occurrence, leading to the amplification of non-specific regions of DNA (Bustin, 2000). To ascertain the optimal concentration of forward and reverse rat ADAMTS-9 primers, a primer concentration test was performed. Three concentrations of the forward and reverse primers were prepared (0.5, 3.3 and 10 pmol/μL) yielding nine different combinations (10F/0.5R, 10F/3.3R, 10F/10R, 3.3F/0.5R, 3.3F/3.3R, 3.3F/10R, 0.5F/10R, 0.5F/3.3R, 0.5F/0.5R). Each primer pair combination was used to amplify the same amount of rat tMCAo cDNA sample and a negative sample (no cDNA) prior to analysis of melt-curve, ΔRn (amplification efficiency) and C_T value.

Wong & Medrano (2005) stated the importance of having high amplification efficiency in real-time RT-PCR reactions. The efficiency of the rat ADAMTS-9 and GAPDH primers was determined by performing a primer efficiency test. Real-time RT-PCR was performed on serially diluted cDNA (as in Section 2.8.3) and C_T value was plotted against $\log_{10}$(cDNA concentration). Efficient primers (~100%) would expect to yield a gradient close to -3.2 on a graph of C_T value against $\log_{10}$(cDNA concentration) because 3.2 is the number of cycles it would take for 1 unit of DNA to be amplified to 10 units.

It is possible that primers can appear 'too efficient' i.e. >100% (slopes steeper than -3.2) as caused by too much template, which is inhibitory to PCR (Ginzinger, 2002) or too little template (i.e. 1:10,000 dilutions) being present in the reaction. Thus acceptable primer efficiencies range from 85-115% (Hamatani *et al*, 2004; Sohn *et al*, 2006; Germann *et al*, 2006; Aidinis *et al*, 2005). Primer efficiencies were calculated using the formula below:

$$\% \text{ Efficiency} = 10^{-1/\text{slope}} - 1$$

2.8.5 Housekeeping Gene Validation

Real-time RT-PCR is far more sensitive than conventional PCR, which has led to the observation that some widely used housekeeping genes do change their expression levels in certain experimental conditions and therefore it is crucial to validate the choice of housekeeping gene for each experimental condition tested in a study (Bustin, 2002). The fact that one housekeeping gene is suitable for one cell-type does not mean it is suitable for another. Also, a housekeeping gene which is stably expressed in cell-lines treated with factors *in vitro* may be up- or down-regulated *in vivo* (e.g. animal models), where many other factors are present, which potentially influence expression.

Housekeeping genes for use with U373-MG, U87-MG, CHME3 cells and the tMCAo models were optimised and validated previously by Dr. Alison Cross. For the B327-01 and SHSY-5Y cells, the following seven genes were analysed for suitability as normalisers for real-time RT-PCR; hypoxanthine phosphoribosyl-transferase I (HRPT1), β-actin, ribosomal protein L13a (RPL13A), tyrosine 3-monooxygenase activation protein, zeta polypeptide (YWHAZ), ubiquitin C (UBC), glyceraldehyde-3-phosphate dehydrogenase (GAPDH) and succinate dehydrogenase complex, subunit A (SDHA), details of which are in Table 2.4.

SHSY-5Y and B327-01 cells were subjected to each experimental condition studied prior to RNA being extracted and quantified accurately with the Experion automated electrophoresis system (BioRad, Richmond, USA). RNA (1 µg) was reverse transcribed and the resulting cDNA was used as a template for real-time RT-PCR. For each sample,

Table 2.4 Primer Pairs Utilised for Real-Time RT-PCR Analysis of Suitable Housekeeping Genes for use with SHSY-5Y and B327-01 Cells

Gene	Accession Number	Location	Function	Forward Sequence (Concentration used at)	Reverse Sequence (Concentration used at)
β-actin	NM_001101	7p15-p12	Cytoskeletal protein	5' CTGGACGGTGAAGGTGACA 3' (3.3 pmol/μL)	5' AAGGGACTTCCTGTAACAATGCA 3' (0.5 pmol/μL)
GAPDH	NM_002046	12p13	Glycolysis and gluconeogenesis	5' TGCACCACCAACTGCTTAGC 3' (10 pmol/μL)	5' GGCATGGACTGTGGTCATGAG 3' (3.3 pmol/μL)
HRPT I	NM_000194	Xq26	Purine synthesis	5' TGACACTGGCAAAACAATGCA 3' (10 pmol/μL)	5' GGTCCTTTTCACCAGCAAGCT 3' (3.3 pmol/μL)
RPL13A	NM_012423	19q13	Component of large 60S ribosomal subunit	5' CCTGGAGGAGAAGAGGGAAAGAGA 3' (3.3 pmol/μL)	5' TTGAGGGGACCTCTGTGTATTTGTCAA 3' (3.3 pmol/μL)
SDHA	NM_004168	5p15	Electron transporter	5' TGGGAACAAGAGGGCATCTG 3' (3.3 pmol/μL)	5' CCACCACTGCATCAAATTCATG 3' (3.3 pmol/μL)
UBC	M26880	12q24	Protein degradation	5' ATTTGGGTCGCGGGTTCTTG 3' (3.3 pmol/μL)	5' TGCCTTGACATTCTCGATGGT 3' (3.3 pmol/μL)
YWHAZ	NM_003406	2p25	Signal transduction	5' ACTTTTCCTACATTGTGGCTTCAA 3' (10 pmol/μL)	5' CCGCCAGGACAAACCAGTAT 3' (3.3 pmol/μL)

Details of primers were published previously (Vandesompele *et al*, 2002). From the genes detailed above, the most suitable housekeeping genes were confirmed by geNorm. YWHAZ was the most suitable housekeeping gene for use with the B327-01 and SHSY-5Y cells under all experimental conditions tested. All primers yielded products which were <150 bp.

$2^{\Delta C_T}$ values were calculated and analysed using Microsoft Excel based GeNorm software (http://medgen.ugent.be/~jvdesomp/genorm/). Since its development in 2002, geNorm has been cited in 590 papers and has proven to be an accurate and reliable tool for determining the best housekeeping genes in many sets of tissues (Vandesompele *et al*, 2002). Note: GAPDH was used as the housekeeping gene for the original preliminary study of ADAMTS-1, -4, -5 and -9 mRNA expression in SHSY-5Y cells under basal conditions. The same cDNA samples were tested for expression of these aggrecanases without being subjected to differing experimental conditions.

2.8.6 Statistical Analysis of Real-Time RT-PCR Data

The statistical significance of relative fold increases/decreases ($2^{-\Delta\Delta C_T}$) in ADAMTS-9 mRNA expression between untreated cells and cells treated with cytokines/GFs was determined by performing a single-factor ANOVA followed by a Dunnett's test (Wallenstein *et al*, 1980). Initially, ANOVA analysed the variance between the full data set from all concentrations of a particular cytokine/GF. If the ANOVA test showed that variance existed within these data set (null hypothesis rejected) then a Dunnett's test was performed, which allowed for the analysis of each particular treatment relative to the control sample to ascertain whether the values were statistically significant. If the ANOVA test showed no variance between a data set then Dunnett's was not conducted and treatment with the particular cytokine/GF was considered to have a null effect on ADAMTS-9 expression. Both ANOVA and Dunnett's test were performed using GraphPad Prism Software Inc. (San Diego, USA).

To ascertain whether the difference in relative ADAMTS-9 mRNA expression levels between RetA differentiated and undifferentiated SHSY-5Y cells were statistically significant an unpaired, 2-tailed T-test was performed. In the tMCAo study, a 2 sample T-test assuming unequal variance, was performed to ascertain whether differences in relative ADAMTS-9 mRNA expression levels between CHs/IHs from tMCAo/sham brains were statistically significant. T-tests were performed using Microsoft Excel software.

Statistically significant differences are represented in figures by *** = $p < 0.001$, ** = $p < 0.01$, * = $p < 0.05$.

2.9 SDS-PAGE and Western Blotting

Proteins in a sample (i.e. cell lysates) can be separated by SDS-PAGE on the basis of M_r by migrating through a polyacrylamide gel in the presence of a current via electrostatic attraction of the negative charge (caused by SDS binding) to the anode. Smaller proteins are resolved further along the gel than larger proteins and a sample with known M_r markers is run in parallel to determine the M_r of the test sample.

Following SDS-PAGE, the presence of a particular protein within a sample can be confirmed by western blotting with a specific primary antibody raised against the target antigen. Enzyme-labelled secondary antibodies are used to bind to the resulting antigen-primary antibody complex prior to detection by chemiluminescence or coloured-precipitate formation. Western blotting offers the advantage over real-time RT-PCR in that different species of a protein can be detected. Bands can represent mature or processed enzyme/protein as opposed to detecting the mRNA which codes for the zymogen. Furthermore, mRNA is not always translated to protein.

In order to achieve reproducible separation by SDS-PAGE, protein extracted from tMCAo tissue and CNS-cell lysates were denatured to their primary structures by dilution in 4x NuPAGE lithium dodecyl sulphate (LDS) (cf SDS) sample buffer (pH 8.4) and 5x reducing agent (DTT) (both Invitrogen). The denaturation process involves the breaking of S-S bonds by DTT and the amino acids gaining negative charges (from LDS) which repel against each other forcing all proteins into a comparable extended linear structure. The process occurs most efficiently at high temperature; therefore samples were heated to 100°C for 5 min.

SDS-PAGE was performed in Novex Minicell tanks (Invitrogen) with 10% NuPAGE Novex Bis-Tris gels (pH 7.0) in the presence of NuPAGE 1x 3-(N-Morpholino)propanesulfonic acid (MOPS) SDS running buffer (pH 7.7) or Novex 4% Tris-Glycine gels (pH 8.6) in the presence of Novex Tris-Glycine SDS running buffer (pH 8.3) (all Invitrogen) with 6 μg of protein/well (as loaded previously by our laboratory: Cross et al, 2005b, Cross et al, 2006, Haddock et al, 2006, Plumb et al, 2005) for approximately 1.5 h at 150 V (300 mA). Determination of protein M_r was achieved by running 8 μL SeeBlue Plus2 pre-stained M_r markers (Invitrogen). SDS-PAGE 4%

gels were only utilised for preliminary testing of commercial anti-ADAMTS-9 antibodies.

Protein was transferred to Hybond-C nitrocellulose membrane (Amersham Biosciences, Amersham, UK) at 150 V (300 mA) for 1 h in the presence of 1x NuPAGE transfer buffer (Invitrogen) (with 10% methanol). All western blot incubations were performed with agitation to allow solutions to wash over the surface of the nitrocellulose. Details of the primary and secondary antibodies utilised in this study are displayed in Table 2.5. The anti-ADAMTS-9 (raised against the linker 2 domain) antibody (ADAMTS-9L2 antibody) was a kind gift from Dr. Suneel Apte (Cleveland, USA) and its generation and characterisation was reported previously (Demircan et al, 2005). Membranes were blocked in 5% (w/v) Marvel low-fat skimmed milk powder (Premier Brands, Spalding, UK) in Tris-buffered saline (20 mM Tris, 0.9% [w/v] NaCl, pH 7.4) (TBS) (Sigma) with 0.05% Tween 20 (Sigma) (TBST) for 1.5 h prior to 3 x 10 min washes with TBST and incubation of primary antibody for 18 h at 4°C. Unbound antibody was washed with TBST (3 x 10 min) prior to incubation with horseradish peroxidase (HRP)-conjugated secondary antibody for 1.5 h. A further 3 x 10 min wash in TBST was followed by 2 x 5 min washes in TBS to remove excess Tween 20 prior to detection with the ECL Plus Western Blotting Detection Reagent (Amersham Biosciences) in accordance with the manufacturer's protocol. The HRP catalyses a photon-generating chemical reaction involving the generation of acridinium ester intermediates, which react with peroxide under slight alkaline conditions to result in intense light emission (chemiluminescence) (Kricka, 1991). Intensity of bands was quantified by densitometry in a Biochemi system, measuring the integrated optical density (IOD) using LabWorks software. An identical procedure was performed in parallel but with primary antibodies omitted to serve as negative controls.

To confirm that equal concentrations of protein (as calculated by BCA assay) were loaded between samples, western blotting with an anti-β-actin antibody (see Table 2.5) was routinely performed. β-actin is a ubiquitously expressed cytoskeletal protein, the levels of which remain relatively stable in most experimental conditions and thus the signal generated between protein extracts of the same concentration should be highly comparable. Our laboratory has previously validated the use of β-actin as a protein loading control in the tMCAo model (Cross et al, 2006). The antibody has been extensively characterised and the protocols for its use have been well established.

77

Table 2.5 Antibodies Utilised for Western Blotting in the Study

Primary Rabbit Antibodies	Obtained from	Dilution	Goat anti-Rabbit-HRP-Conjugated Secondary Antibody Concentration
anti-human ADAMTS-9 (ADAMTS-9L2 Antibody) (targeting linker 2 domain between 8th and 9th TSP-1s) (Demircan et al, 2005)	Dr. Suneel Apte (Cleveland, USA)	1:1,000 (2μg/mL) in TBS	1:80,000 in TBST
anti-human ADAMTS-9 (targeting catalytic domain)	CedarlaneLaboratories Ltd, Canada (cat no. CL3ADAMTS9) (also supplied by TriplePoint Biologics, Inc)	attempted 1:5,000 (recommended), 1:2,500, 1:1,000, 1:500 in TBS and PBS	attempted 1:80,000 and 1:40,000 in TBS and TBST
anti-human ADAMTS-9 (targeting propeptide domain)	Affinity BioReagents, USA (cat no. PA1-8401)	attempted 1:1,000 and 1:500 in TBS and PBS	1:80,000 in TBS and TBST
anti-human ADAMTS-9 (targeting carboxy end of propeptide domain) (Koo et al, 2006)	TriplePoint Biologics, Inc, cat no. RP4ADAMTS9) (also supplied by Abcam, UK, cat no. ab28276)	attempted 1:500 and 1:1,000 in TBS	attempted 1:80,000 in TBST
anti-GFAP	DakoCytomation, Denmark (cat no. Z0334)	1:2,500 (U373-MG), 1:1,000 (B327-01) in TBS	1:80,000 (U373-MG), 1:50,000 (B327-01) in TBST
anti-β-actin (20-33) IgG	Sigma (cat no. A5060)	1:1,000 im TBS, 5% milk	1:80,000 in TBST, 5% milk powder

The table details the antibodies utilised in this thesis for western blotting. Note: goat anti-Rabbit-HRP-Conjugated Secondary Antibody was purchased from Sigma (cat no. A9169).

Therefore β-actin was chosen as the normalising control for western blotting with the tMCAo study as opposed to GAPDH (housekeeping gene for real-time RT-PCR).

Peptide blocking of anti-ADAMTS-9 antibodies was performed to determine antibody specificity. In theory a specific antibody should have its reactivity blocked by binding to the 'immunising' peptide. Any bands observed with an antibody following peptide blocking are considered to be non-specific. Peptides were only available for Triple Point RP4 antibody (sequence undisclosed) and anti-ADAMTS-9L2 antibody (H-CQHPFQNEDYRPRSASPSRTH-OH, synthesised by Invitrogen). Antibodies (15 mL) were incubated with peptides (30 µg for ADAMTS-9L2, 100 µg for RP4) for 30 min prior to western blotting.

2.10 Immunocytochemistry and Immunohistochemistry

Immunocytochemistry (ICC) relies on antibody specificity to locate the distribution of a cellular antigen in the cell. The antigen-antibody complex can be detected by either direct or indirect methods. Direct methods of staining involve the use of primary antibodies that have fluorescent molecules or dyes attached. Indirect methods utilise secondary antibodies, which bind to the primary antibody and fluoresce or have enzymatic activity to form a coloured product when a substrate is added (Strachan & Read, 1999). Fixatives are utilised prior to antibody incubation to preserve and stabilise samples, thus protecting them from the rigours of the staining and washing techniques.

Cells were seeded into Nunc 8-well chamber slides (Lab-Tek, Wiesbaden, Germany) at a density of 5×10^4 cells/500 µL media/well and left to adhere for 24 h. The media were discarded and the excess washed off with phosphate-buffered saline (0.138 M NaCl, 0.0027 M KCl, pH 7.4) (PBS) prior to fixation with 4% (w/v) paraformaldehyde (PFA), 0.2 M sodium phosphate pH 7.2 (100 µL/chamber) for 10 min. The fixative was prepared by dissolving PFA powder in 0.2 M sodium phosphate by heating to 60°C in a fume cupboard. Drops of 1 M NaOH were added until the PFA went into solution. The solution was filtered using a funnel and filter paper (Whatman, Maidstone, UK) prior to adjusting the pH to 7.2 with 1 M HCl. PFA forms cross-links between proteins, creating a 'gel' which retains the cellular constituents in their *in vivo* relationship to each other by rendering proteins insoluble via fixation to structural proteins. The resultant structure is high in mechanical strength, enabling it to withstand the ICC procedure.

After 2 x 5 min washes in PBS, cells were blocked in the normal serum (10%) of the animal in which the secondary antibody (goat) (Sigma) was produced for 30 min to prevent non-specific binding of the secondary antibody. Primary antibody (diluted in PBS) incubation was performed for 18 h at 4°C in a humidified chamber before washing slides for 3 x 10 min in PBS. Secondary antibody (diluted in PBS) was applied for 1 h at 37°C before being washed 3 x 10 min in PBS. Samples were mounted with Vectashield mounting media (Vector Laboratories, Inc, Burlingame, USA), containing 4'-6-Diamidino-2-phenylindole (DAPI), which forms fluorescent complexes with dsDNA, enabling nuclei visualisation. This serves as a control to confirm that cells have remained on the chamber slide during the process and also allows for comparison of cell number between chambers. Furthermore, it enables the visualisation of proteins distributed around the nucleus. Images were taken on a Zeiss 510 CSLM confocal scanning laser microscope and/or an Olympus BX60 fluorescent microscope with Cool Snap Pro colour digital camera (Media Cybernetics, Silver Spring, USA). Confocal images were analysed with the Zeiss LSM5 software whereas fluorescent microscope images were analysed with LabWorks Image Acquisition and Analysis Software.

In this study ICC was utilised to characterise cultured astrocytes prior to performing further experiments. ICC staining for astrocytic marker glial fibrillary protein (GFAP) was performed on U373-MG and B327-01 cells (U87-MG characterisation was performed previously by our laboratory) with rabbit anti-GFAP polyclonal primary antibody (see Table 2.5) at 1:100 dilution, which was detected by Alexa Fluor 488-conjugated goat anti-rabbit IgG (H+L) (Molecular Probes, Eugene, USA) at 1:500 dilution. Detection of astrocytic marker S-100β was performed by ICC with mouse anti-S-100β-subunit IgG1 monoclonal primary antibody (Sigma, cat no. S-2532) at a dilution of 1:50 prior to incubation with FITC-conjugated rabbit anti-mouse immunoglobulins (Ig) secondary antibody (DakoCytomation, Glostrup, Denmark) at a dilution of 1:200. ICC detection of ADAMTS-9 protein was performed with ADAMTS-9L2 antibody at a dilution of 1:50 followed by incubation with Alexa Fluor 488-conjugated goat anti-rabbit IgG (H+L) (Molecular Probes) at 1:500 dilution.

IHC adheres to the same basic principles as ICC except that it allows for the detection and visualisation of a protein within tissue sections as opposed to in cultured cells. To analyse the localisation of ADAMTS-9, tMCAo tissue sections were subjected to IHC for the detection of well characterised CNS-cell-specific markers for comparison with

*IS*H ADAMTS-9 images. Details of primary and corresponding secondary antibodies used in IHC of tMCAo are in Table 2.6. Sections were warmed to ambient temperature for 30 min after removal from the -80°C freezer. Tissue was fixed for 10 min with 4% PFA prior to 2 x 5 min washes in PBS and was blocked in 1% BSA for 30 min before an 18 h incubation with primary antibody (100 μL) at 4°C. Unbound antibody was washed off with PBS/0.05% Tween 20 for 3 x 5 min prior to incubation with secondary antibody (100 μL) for 1.5 h. Unbound secondary antibody was removed with PBS/0.05% Tween 20 for 3 x 5 min. Sections were mounted, imaged and analysed using the same protocol as described for ICC.

2.11 *In Situ* Hybridisation

2.11.1 *In Situ* Hybridisation Theory

*IS*H relies on antisense probes designed to bind to unique sequences of target mRNA in tissue sections, thus giving a clearer indication as to the cellular origin of a protein of interest as well as to whether it is being expressed at any point in time. In comparison to IHC, *IS*H can confirm which cells actually synthesise a protein which is particularly useful if the protein is secreted or sequestered into the ECM. Also, protein detected by IHC could be mistaken as being synthesised by the cell when in fact it has been phagocytosed or adsorbed onto it.

The choice of probe-type is a crucial aspect of *IS*H experimental design and there are a number of options available including oligonucleotide probes, ssDNA probes, dsDNA probes and riboprobes (cRNA, ssRNA). Oligonucleotide probes are highly resistant to RNAses as well as being small (40-50 bp) so can easily penetrate into a cell to access the target sequence. Another advantage is that they can be produced commercially by well established methods by automated chemical synthesis utilising deoxynucleotides. The problem with oligonucleotide probes is that they are more likely to bind non-specifically because they are composed of a small number of bases (Luehrsen *et al*, 2000). However, riboprobes, ssDNA and dsDNA probes offer the advantage over oligonucleotide probes in that they are far longer (200-500 bp) and hence more specific (Goldsmith *et al*, 2007).

Table 2.6 CNS Cell Marker Antibodies utilised for Immunohistochemical Analysis of tMCAo Rat Sections

Cell-Type	Primary Antibody	Secondary Antibody
astrocytes	mouse anti-GFAP monoclonal 1:200 (0.005mg/mL) (Chemicon International, Temecula, USA)	rabbit anti-mouse Ig FITC-conjugated 1:100 (DakoCytomation)
neurones (nuclei)	mouse anti-NeuN AlexaFluor 488-conjugated monoclonal 1:1000 (0.001mg/mL) (Chemicon)	N/A
macrophages/ monocytes	mouse anti- ED1 monoclonal (AbD Serotec, Oxford, UK), attempted 1:50, 1:100	**Attempted:** 1) goat anti-mouse-AP-conjugated 1:1000 (CalBiochem, San Diego, USA) 2) rabbit anti-mouse FITC 1:100 and 1:50 (DakoCytomation) 3) rabbit anti-mouse AlexaFluor 488-conjugated 1:50 and 1:100 (Dakocytomation)
endothelial cells	rabbit anti-human von Willebrand factor 1:200 (DakoCytomation)	goat anti-rabbit AlexaFluor 568-conjugated 1:500 (Molecular Probes)

The preparation of ssDNA probes usually involves PCR amplification of a DNA fragment (followed by a second round of PCR, with only one set of primers to produce DNA that is single stranded) or reverse transcription of RNA. The lesser used dsDNA probes can be mass-produced in bacteria or alternatively by PCR. However, dsDNA probes have low sensitivity because they have to be denatured prior to hybridisation and both strands can have a tendency to rehybridise together. Both ssDNA and dsDNA probes are highly specific but have the disadvantage that DNA-RNA hybrids are not as thermostable as RNA-RNA hybrids, the main advantage of riboprobes (McNicol & Farquharson, 1997; Hicks et al, 2004). Hence, it is possible to reduce non-specific binding by treating sections that have been hybridised with riboprobes with RNase to eliminate false-positive signals obtained with any non-specifically bound probe. The main disadvantage of riboprobes and dsDNA probes is that generation involves subcloning in bacteria and a number of molecular biological techniques. Also, riboprobes are relatively unstable so have to be utilised promptly or new batches prepared regularly (Hicks et al, 2004).

There are a number of ways in which ISH probes can be labelled and detected. Traditionally, probes have been radiolabeled (i.e. [35]S) and detected with photographic film or emulsion. This method is widely used in laboratories in which the containment and waste disposal procedures are already well established. A non-radioactive approach is to use digoxigenin (DIG), offering the advantage of no signal decay (^{35}S has a half-life of 80 days) and quicker experimental procedure. DIG is a steroid only found in the digitalis plant (foxglove) (LeWinn, 1984) so anti-DIG antibodies can be used to detect bound probe without non-specific binding to an endogenous signal. A spacer arm of 11 carbon atoms links DIG and the uridine nucleotides of the probe. DIG-labelled oligonucleotide probes and riboprobes have been shown in many experiments to generate less background signal and higher resolution than corresponding ^{35}S-labelled probes (Komminoth et al, 1992) but are less conducive to quantitation.

RNA is highly susceptible to degradation by RNAses and limiting this is an important aspect of any ISH experiment. Steps to prevent RNAse degradation include freezing of freshly cut sections (-80°C), baking of glassware, use of RNAse free buffers (by treatment with 0.001% diethyl pyrocarbonate [DEPC]), gloves, tubes and tips. A method of ascertaining the quality of RNA in a tissue sample is to use a poly(dT) (p[dT]) positive control probe, which binds to the poly A tails of all mRNA in the tissue. A poor

signal with this probe indicates that the tissue is of a low quality and RNA degradation has occurred.

To ascertain whether probes are binding specifically to the target mRNA, hybridisation is performed not only with the antisense probe but also the sense strand. The signal obtained with the sense strand should be nothing more than background noise caused by the chemical properties of the probe. Consequently, if the signal obtained with the antisense probe rises above the background noise of that obtained with the sense probe, it is likely to be due to sequence-specific binding to mRNA and not other constituents of the tissue (Strachan & Read, 1999).

2.11.2 Oligonucleotide Probe Method

2.11.2.1 ADAMTS-9 Oligonucleotide Probe Details

The ADAMTS-9 antisense oligonucleotide probe was designed and synthesised to be specific to a unique sequence located in rat ADAMTS-9 sequence NM_001107877 (confirmed by BLAST and FastA) by GeneDetect.com (Auckland, NZ). The probe was complementary to nucleotides 6375-6422 with a Tm of 104.1°C. The sense probe was also synthesised to serve as a negative control. A 48mer p(dT) probe was used as a positive control (Gene.Detect.com). All probes were labelled with DIG, added to the 3' end.

Below is the 48mer antisense DIG-labelled probe sequence (the sense negative control probe was the reverse complement of this sequence):

6422 TGGCCACAGGACACAGAGCACTGACTCCATGCGCGAGCCTTCCATCGG **6375**

2.11.2.2 *In Situ* Hybridisation Protocol with Oligonucleotide Probes

All reagents were purchased from Novagen (Madison, USA) unless otherwise stated.

Pre-hybridisation steps were performed with buffers and baked-glassware treated with 0.001% (v/v) DEPC in H_2O. Tissue sections (tMCAo) were taken out of the -80°C

freezer and allowed to warm to ambient temperature for 30 min prior to treatment with chloroform (Sigma) for 10 min. The tissue was fixed with 4% PFA for 10 min prior to washing for 3 x 5 min with PBS. PFA was used because it prevents loss of material but is mild enough to allow the probe to penetrate into the cell (Nilsson et al, 1996). Sections were treated with 100 μL proteinase K (PK) (2 μg/mL in dH$_2$O) for 10 min. PK is used to digest cross-linked proteins, thus allowing access of the probe to the target mRNA (Rheinhardt & Finkbeiner, 2001). A further PBS wash (3 x 5 min) was followed by a post-fixation step with 4% PFA prior to rinsing the sections in H$_2$O. The tissue was dehydrated with an alcohol series of 70, 80, 95 and 100% molecular grade ethanol (Sigma) for 2 min each prior to air drying.

Slides were incubated at 39°C in pre-hybridisation buffer (Biochain, Hayward, USA) for 1 h in a humidified chamber. Probes were diluted (attempted 1:25, 1:50, 1:100 and 1:500) in hybridisation buffer (Ambion, Applied Biosystems). The same concentration of antisense and sense probes was used. Probes were denatured at 70°C for 10 min prior to cooling on ice and incubation of 100 μL/slide in a humidified chamber for 18 h at 39°C as calculated by the following formula (http://www.genedetect.com/Merchant2/Ol igoHandling.pdf):

$$\textbf{Hybridisation temp.} \ (°C) = 24.21 + 0.41(\%GC) - 500/n$$

Where:
n = probe length, %GC = % of probe that is composed of G or C bases.

The positive control p(dT) probe was used at 1:50 at ambient temperature (inc. pre-hybridisation buffer incubation). Unbound probe was removed by incubating slides in the following wash solutions for 30 min at 60°C for antisense/sense probes and 34°C for p(dT) unless otherwise stated:

1. 20x NaCl-sodium citrate in distilled H$_2$O (SSC, 15 mM sodium citrate, 150 mM NaCl, pH 7.0), 0.01 M β-mercaptoethanol.
2. 20x SSC, 0.01 M β-mercaptoethanol, 10 mg/mL RNAse A at 37°C.
3. 20x SSC, 50% (v/v) deionised formamide, 0.01 M β-mercaptoethanol.

4. 20x SSC, 1% (v/v) sodium pyrophosphate, 0.014 M β-mercaptoethanol.

5. Repeated Step 4.

Slides were air-dried for 10 min prior to washing in 100 mM Tris-HCl, 150 mM NaCl (pH 7.5) (Buffer 1) for 1 min prior to incubation in 100 μL 10% (v/v) normal sheep serum (NSS) (Sigma Immuno Chemicals)/PBS. Sheep anti-DIG-alkaline phosphatase (AP) antibody (Roche Diagnostics, Mannheim, Germany) was diluted 1:100 in 5% (v/v) NSS/PBS and 100 μL was applied to each slide prior to incubation for 18 h at 4°C in a humidified chamber. Slides were washed in buffer 1/0.05% (v/v) Tween 20 for 10 min before being washed in 100 mM Tris-HCl, 100 mM NaCl (pH 9.5) for 10 min. One tablet of SIGMA FAST BCIP/NBT (5-bromo-4-chloro-3'-indolyphosphate p-toluidine salt/nitro blue tetrazolium chloride) (Sigma) was dissolved in 10 mL H_2O prior to incubation on slides until a purple precipitate was formed where hybridisation had occurred (~ 2-3 h). AP cleaves the phosphate from the BCIP, resulting in the formation of an indole (C_8H_7N), which undergoes a redox reaction with NBT to produce the coloured product. The reaction was stopped by incubation in 10 mM Tris-HCl, 1 mM EDTA (pH 8.0) (Buffer 2). EDTA chelates Zn^{2+}/Mg^{2+} (required in the active site) making it unavailable to the AP. Sections were mounted with 50% PBS/50% glycerol (v/v) and visualised/captured with an Olympus BX60 microscope in bright-field mode prior to subsequent analysis with LabWorks Image Acquisition and Analysis Software.

2.11.3 Riboprobe Method

2.11.3.1 Riboprobe Generation Strategy

A second *IS*H approach, which was adopted, was to generate a riboprobe from ADAMTS-9 plasmid DNA. ADAMTS-9 cDNA (715 bp) encoding for the CRD, spacer region and TSP-1s 2-4 was previously cloned into a pBluescript KS+ plasmid, as illustrated in Figure 2.3, and was a kind gift from Dr. Suneel Apte (Cleveland, USA). The cDNA clone was generated by the Apte laboratory during attempts to clone full-length mouse ADAMTS-9 as described previously (Jungers, *et al*, 2005). Cloning of cDNA allows the production, isolation and utilisation of DNA that encodes for the mRNA of a protein of interest. Incorporation of cDNA into a multiple cloning site (MCS) of a vector involves a number of steps, which would have been performed previously by the Apte laboratory. The ADAMTS-9 cDNA was engineered so that it

Figure 2.3 ADAMTS-9 Plasmid DNA and pBluescript KS+ Vector
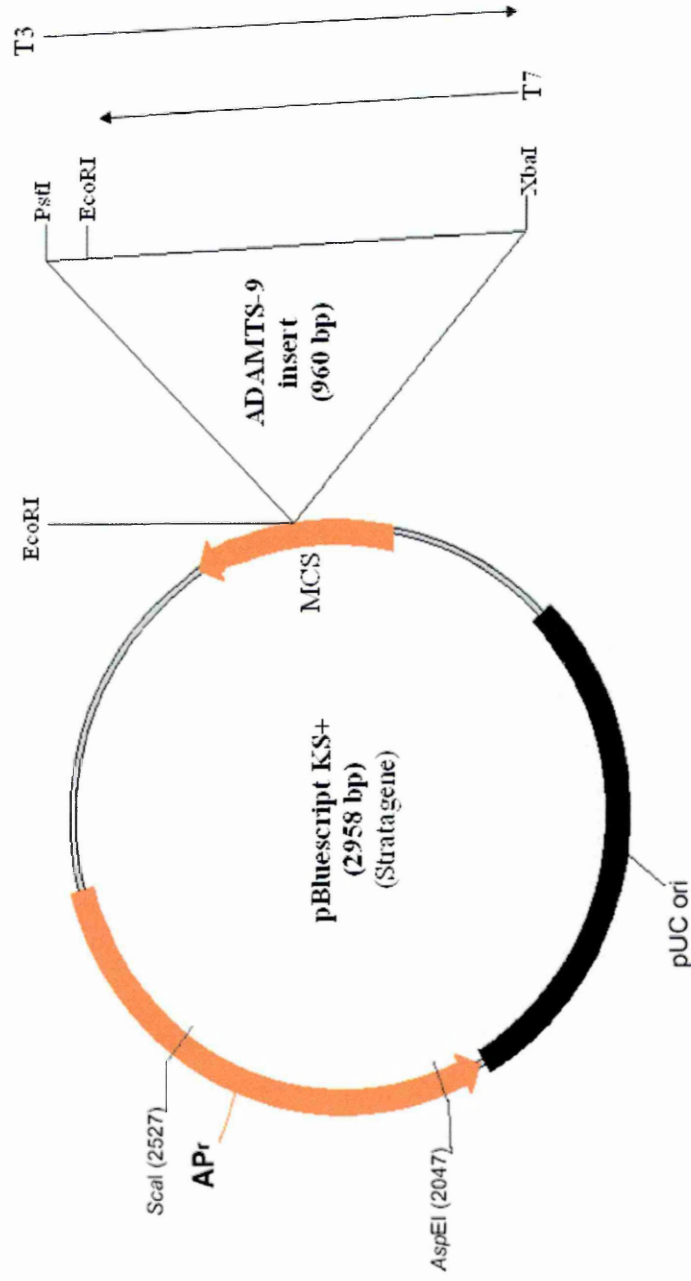
ADAMTS-9 cDNA was cloned with PstI and XbaI ends into multiple cloning site (MCS) of pBluescript KS+ expression vector containing ampicillin resistance (APr) and origin of replication for propagation in *E. coli* (pUC ori). 'T7' and 'T3' represent location of promoter regions for these RNA polymerases and the straight black arrows depict direction of polymerisation to 5' overhang (generated by digestion with EcoRI and XbaI restriction enzymes respectively).

contained unique restriction sites (XbaI and PstI) at each end (Fig. 2.3). Synthetic oligonucleotides are usually ligated to ends of the cDNA to act as 'linkers' in the correct alignment for specific restriction enzymes to target. Further modifications of the cDNA are necessary in order to make it accessible to the vector including generation of overhangs which are complementary to overhangs within the vector. Such modifications resulted in the insert and contents increasing in size to 960 bp.

Generation of the riboprobe from the plasmid involved a number of cloning steps, which were performed as part of this study. Transformation in *E. coli* was possible because pBluescript KS+ vector contained an origin of replication for propagation in *E. coli* (pUC ori). The plasmid was expressed in the host on ampicillin plates because of an ampicillin resistance gene in the vector (APr). Plasmid DNA was isolated from the host cell suspension by miniprep. Next, plasmid DNA was linearised prior to performing *in vitro* transcription (*IVT*) with suitable RNA polymerases to generate RNA antisense and sense strands. A DIG-labelling mix was utilised so that the RNA strands were labelled during the transcription reaction, thus generating riboprobes.

2.11.3.2 Transformation of ADAMTS-9 Plasmid DNA

The uptake of foreign DNA (usually plasmids) by an organism (e.g. bacteria), is termed 'transformation'. *E. coli* can be rendered 'competent' (having the ability to take up plasmid DNA) by treatment with Ca^{2+} or by increasing the temperature (heat-shock). Transformation of the plasmid was carried out utilising aseptic technique. ADAMTS-9 plasmid DNA (10 μL) was added to 200 μL XL-1 blue strain of *E.coli* (which was thawed on ice) prior to incubation on ice for 30 min. Cells were made competent by 'heat shocking' in a 42°C water bath for 45 sec prior to returning the cells to ice for 2 min. Next, 800 μL of SOC media (20 g tryptone, 5 g yeast extract, 0.5 g/L NaCl, 1% glucose, 20 mM $MgCl_2$, pH 7.5) was added to the competent cells prior to 30 min incubation at 37°C. Cells were plated at a range of densities (50 μL, 100 μL, 200 μL, and 500 μL/plate) onto LB (Luria-Bertani) agar/ampicillin plates (0.5% yeast extract, 0.5% NaCl, 1% tryptone, 1.5% agar, 50 μg/mL ampicillin) with a sterile spreader. Plates were incubated at 37°C for 24 h. Single colonies were picked and added to 5 mL of LB and 1 μg/mL ampicillin prior to shaking at 37°C for 18 h to grow a bacterial cell suspension.

2.11.3.3 Preparation of Plasmid DNA

A miniprep is a technique for preparing plasmid DNA from a bacterial cell suspension on the basis that plasmid DNA is far smaller than bacterial chromosomal DNA. The QIAprep Spin Miniprep Kit (Qiagen) was used to perform the miniprep in this study. Exact buffer compositions were undisclosed by the manufacturer and all centrifugation steps were performed in a microfuge. The overnight-cultured XL-1 blue cell suspension (3 mL) was centrifuged (1.5 mL in 2 Eppendorf tubes) at 8000 x g for 1 min and the supernatant was discarded prior to resuspension in 250 µL Buffer P1 (containing RNAse A). Buffer P2 (contains NaOH) (250 µL) was added to the solution and the tube was inverted 4-6 times prior to the addition of 350 µL Buffer N3 (contains guanidine hydrochloride, acetic acid). The tube was inverted 4-6 times prior to centrifugation at 11,000 x g for 10 min. Next, the supernatant (~ 800 µL) was deposited (by pipetting) in a QIAprep spin column prior to centrifugation at 11,000 x g for 1 min. The flow-through was discarded and the column was washed by addition of 500 µL Buffer PB (contains guanidine hydrochloride, isopropanol) and centrifugation at 11,000 x g for 1 min prior to discarding the flow-through. The column was additionally washed in 750 µL Buffer PE by centrifugation at 11,000 x g for 1 min and the flow-through was discarded prior to an additional centrifugation step at 11,000 x g for 1 min to remove the residual wash buffer. The column was placed in a fresh Eppendorf tube and Buffer EB (10 mM Tris-Cl, pH 8.5) (50 µL) was added to the centre of the column and left to stand for 1 min. Finally, the plasmid DNA was eluted from the column by centrifugation at 11,000 x g for 1 min and was stored at -20°C.

A diagnostic restriction digest was performed with PstI and XbaI to confirm that the correct ADAMTS-9 insert was inserted in the pBluescript KS+ vector. The restriction digestion reaction consisted of 5 µL minipreped plasmid DNA, 1 µL PstI (20 U), 1 µL XbaI (20 U), 2 µL NEBuffer 3 (100 mM NaCl, 50 mM Tris-HCl, 10 mM MgCl$_2$, 1 mM DTT, [pH 7.9]), 11 µL ddH$_2$O in an Eppendorf tube. Efficient digestion was achieved without the supplementation of NEBuffer 3 with BSA. Digestion was performed at 37°C for 2 h prior to visualisation of insert by 2% AGE. All restriction enzymes and restriction enzyme buffers used in the generation of riboprobes were purchased from New England Biolabs, Ltd (Beverly, USA).

2.11.3.4 Linearisation of Plasmid DNA and *In Vitro* Transcription

Digestion of the plasmid DNA with either XbaI or EcoRI downstream of the RNA polymerase promoter region (at the opposite end of the insert to the promoter region) resulted in 5' overhangs and thus terminated the T7 or T3 polymerase reaction. Despite there being an EcoRI site 5' to the cDNA fragment within the MCS, it was the EcoRI site within the insert where T7 RNA polymerase termination occurred as shown in Figure 2.4. Fresh batches of riboprobes were generated regularly from a stock of linearised plasmid DNA. This was because cRNA is highly susceptible to degradation from RNAses whereas plasmid DNA is relatively stable.

Plasmid DNA (including ADAMTS-9 insert) was linearised by restriction digestion with XbaI (for sense probe) or EcoRI (for antisense probe) restriction enzymes. The reaction consisted of 10 µL 10x NEBuffer 2 (10 mM Tris–HCl [pH 7.9], 10 mM $MgCl_2$, 50 mM NaCl, 1 mM DTT), 10 µg minipreped plasmid DNA, 100 U XbaI or EcoRI (5 µL), 75 µL sterile dH_2O. The digestion was performed at 37°C for 3 h prior to visualisation by 2% AGE. Uncut plasmids typically contain two forms of DNA (supercoiled and nicked circles), which migrate more rapidly by AGE (displaying two bands relatively close together). Linear plasmid DNA was concentrated by ethanol precipitation. Brifely, 100 µL DNA was added to 300 µL 95% (v/v) ethanol/0.12 M sodium acetate (pH 5.0) prior to mixing by inversion and incubation on ice for 10 min. The sample was centrifuged in a microfuge at 9000 x *g* for 15 min at 4°C prior to discarding of the supernatant and addition of 80% ethanol (200 µL). After 10 min, the sample was centrifuged at 9000 x *g* for 15 min at 4°C and the supernatant discarded before the sample was air dried in a vacuum concentrator 5301 (Eppendorf, Hamburg, Germany) for 10 min at 4°C. The pellet was dissolved in 10 mM Tris-HCl (pH 7.6-8), 0.1 mM EDTA.

DIG-labelled antisense and sense probes were generated by *IVT* with T7 and T3 RNA polymerases respectively as demonstrated by the schematic in Figure 2.4. All reagents were purchased from Roche Diagnostics unless otherwise stated. The following was added to a tube on ice: 1 µg linear plasmid DNA (cut with either EcoRI or XbaI) (1 µL), 10x DIG labelling mix (10 mM ATP, 10 mM CTP, 10 mM GTP, 6.5 mM UTP, 3.5 mM DIG-11-UTP, pH 7.5) (2 µL), 10x transcription buffer (400 mM Tris-HCl, pH 8.0, 60 mM $MgCl_2$, 100 mM DTT (2 µL), RNase Out (Invitrogen) (1 µL), 20 U RNA

Figure 2.4 Schematic Representation of Linearisation of ADAMTS-9 Plasmid DNA and *In Vitro* Transcription
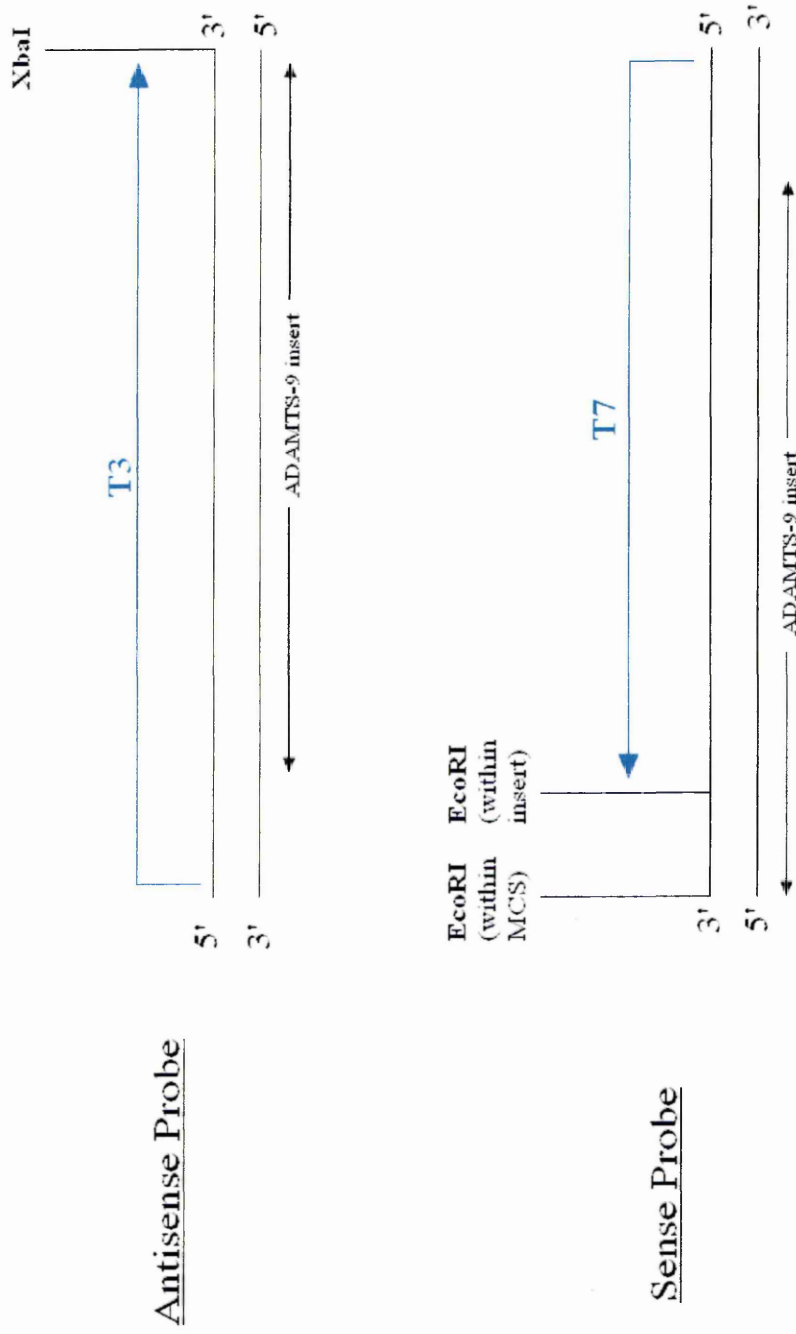
Not to scale. Note that T3 and T7 RNA polymerase promoter regions initiate outside of the ADAMTS-9 insert sequence. The blue arrows depict RNA polymerase activity.

polymerase (T7 or T3) (2 μL), sterile H_2O (12 μL). The reaction components were mixed prior to incubation at 37°C for 2 h. Template DNA was removed by incubation with DNAse I (2 μL) (Sigma) for 15 min at 37°C. The reaction was stopped by addition of 0.2 M EDTA (pH 8.0) (2 μL) prior to removal of unincorporated DIG with MEGAclear purification kit (Ambion) in accordance with the manufacturer's protocol. Briefly, ssRNA (riboprobe) was bound to a glass fibre filter membrane prior to removal of contaminants and elution in a low salt buffer by centrifugation. Riboprobe purity and yield was assessed by 2% AGE.

2.11.3.5 Dot Blot and Calculation of Riboprobe Dilution

Merely deducing the concentration of the riboprobes (by spectrophotometry) is not sufficient because it does not take into account DIG-labelling efficiency i.e. antisense and sense probes with the same cRNA concentration may vary in the amount of bound DIG. Therefore, the probes were subjected to dot blotting with an anti-DIG antibody prior to measuring the IOD by densitometry. By using the ratio of antisense:sense IODs, the required dilution of riboprobes was calculated to give the same concentration of DIG for each probe. The optimal dilution of the riboprobes where non-specific binding was at a minimum and the antisense probe gave a good signal (whilst keeping the concentration of DIG equal) was determined by experimental *IS*Hs. This technique was performed each time new probes were generated because the *IV*T/DIG-labelling reactions will have varying efficiencies across batches.

The positive controls for the dot blot were; DIG-labelled control RNA (Roche Diagnostics) and commercially purchased DIG-labelled p(dT) (GeneDetect.com). Controls were diluted to concentrations of 0-10 ng/μL in RNA dilution buffer consisting of 50% H_2O, 30% SSC and 20% formaldehyde (v/v). Control dilutions, antisense (undiluted) and sense (undiluted) probes were blotted (1 μL) onto nitrocellulose membrane and air dried prior to UV cross-linking for 1 min (both sides of membrane). Membranes were washed in PBS for 1 min prior to blocking in 1% (w/v) BSA/PBS for 30 min and incubation with sheep anti-DIG antibody conjugated to AP (1:5,000 in PBS) (Roche Diagnostics) for 30 min. Unbound antibody was removed by washing twice in PBS prior to incubation in SIGMA FAST BCIP/NBT substrate until a precipitate was visible. The reaction was stopped by incubation with Buffer 2. Dots were visualised in a

BioChemi system prior to densitometry with LabWorks software to assess DIG-labelling efficiency.

2.11.3.6 *In Situ* Hybridisation Protocol with Riboprobes

The *IS*H protocol (pre-hybridisation, hybridisation, detection and visualisation) with riboprobes was identical to that adopted for the oligonucleotide probes (see Section 2.10.2.2) with the exception that the pre-hybridisation buffer incubation and hybridisation of the riboprobes was performed at 60°C. Furthermore, the unbound riboprobes were washed utilising a different protocol as described below.

The following washing steps were followed at 60°C for ADAMTS-9 (antisense and sense probes) and 39°C for p(dT) unless otherwise stated:

1. 1x SSC for 10 min.
2. 1.5x SSC for 10 min.
3. Twice in 2x SSC at 37°C.
4. 2x SSC 0.2 µg/mL RNAse A (Qiagen) at 37°C. RNAse treatment prevents background binding of excess probe.
5. 2x SSC at ambient temperature for 10 min.
6. Twice in 0.2x SSC for 30 min each.

2.12 Haematoxylin and Eosin Staining

The haematoxylin and eosin (H&E) stain is routinely performed in histological diagnosis. It is a method of detecting (and differentiating between) basophilic (stained blue/purple by haematoxylin) and eosinophilic (stained pink by eosin) structures within a tissue section. Basophilic structures include nucleic acids, therefore cell nuclei and ribosomes are stained. Eosinophilic structures are generally proteins which can be extracellular or intracellular. In this study H&E staining was performed on tMCAo tissue sections and compared with ADAMTS-9 *IS*H to aid in determining which cells were *Adamts9*-positive.

H&E staining was performed in Coplin jars. Tissue sections (tMCAo) were taken out of the -80°C freezer and allowed to warm for 30 min prior to fixation in 4% PFA for 10

min. Sections were rinsed in PBS for 1 min prior to treatment with filtered Harris' haematoxylin (Sigma) for 1 min before being rinsed under a running tap of H_2O until the solution was clear. Water was drained and sections were incubated in eosin stain (Sigma) for 2 min prior to rinsing in H_2O (as above). Dehydration of the tissue sections was performed with 50, 70, 80, 95 and 100% (v/v) ethanol for 2 min each. Next, sections were rinsed in xylene (Sigma) for 4 min prior to mounting with DPX mountant (Fluka, Buchs, Switzerland) and visualisation under an Olympus BX60 microscope in bright-field mode prior to analysis with the LabWorks Image Acquisition and Analysis Software.

Chapter 3

Development, Optimisation and Validation of Methods to Study ADAMTS-9 Expression in the CNS

3.1 Background

This chapter describes the thorough development, optimisation and validation of methods to study ADAMTS-9 expression in CNS inflammation at the mRNA level (real-time RT-PCR and *IS*H) and the protein level (western blotting and ICC). This was conducted in order to apply the methods to the cell culture and rat model in Chapter 4 and Chapter 5 respectively.

3.2 Real-Time RT-PCR Optimisation

3.2.1 Overview of Optimisation Steps

For this study, rat ADAMTS-9 primers were designed for use with the tMCAo model. Although primers were designed using Primer Express, it was critical to optimise and validate them prior to analysing rat tMCAo samples. Three putative primer pairs were generated for rat ADAMTS-9 and the pair which gave a clean melt curve with no primer-dimer was optimised further by conducting primer concentration and efficiency tests. It was essential to validate that the rat ADAMTS-9 primers were amplifying the correct target gene. Analysis of the real-time RT-PCR product was performed with AGE to confirm the correct size. Next, the product was sequenced prior to running a BLASTn search to ascertain that the sequence was unique and that of rat ADAMTS-9.

As is the case with most mathematical models, the $2^{-\Delta\Delta C_T}$ method of real-time RT-PCR data analysis relies on assumptions in order for it to be valid. As well as requiring stable housekeeping gene expression, the target gene and housekeeping gene primer efficiencies must be approximately equal (Livak & Schmittegen, 2001). Therefore, a primer efficiency comparison test was conducted to validate the use of the $2^{-\Delta\Delta C_T}$ method in this study. Also, geNorm analysis was conducted to determine the most stable housekeeping genes for the B327-01 and SHSY-5Y cells.

3.2.2 Results

3.2.2.1 Rat ADAMTS-9 Primer Concentration Test

Figure 3.1 shows the rat ADAMTS-9 primer combinations of 10F/3.3R, 10F/0.5R, 3.3F/3.3R and 0.5F/3.3R displayed no non-specific signal in negative samples (lacking cDNA). The same combinations also displayed low C_T values indicating high amplification efficiency i.e. fluorescent signal rose above the background noise at an earlier cycle number. The primer pair combination which was chosen and utilised throughout the tMCAo study was 10F/3.3R because it yielded the cleanest melt-curve, with no primer-dimer and the highest ΔRn (fluorescence intensity) (not shown). Throughout the tMCAo rat model study, the ADAMTS-9 primers used at this concentration did not display primer dimer i.e. negative samples were not resolved.

3.2.2.2 Rat ADAMTS-9 and GAPDH Primer Efficiency Test

Figure 3.2 demonstrates that the slope of the line when C_T was plotted against $\log_{10}$(cDNA concentration) with ADAMTS-9 rat primers was -3.29 whereas the slope with GAPDH was -3.04. Based on these gradients, the calculated efficiencies of the primers were 101.4% for ADAMTS-9 and 113.2% for GAPDH thus validating their use in this study (within 85-115% range).

3.2.2.3 Confirmation of Real-Time RT-PCR Product Size

The real-time RT-PCR amplicon obtained from a reaction with the ADAMTS-9 rat primers was the same size as the expected product (101 bp, see Table 2.3) as demonstrated in Figure 3.3. The real-time RT-PCR product was confirmed as being specific to rat ADAMTS-9 by sequencing at a central DNA sequencing service (not shown).

3.2.2.4 Validation of $2^{-\Delta\Delta C_T}$ Method

The results of the primer efficiency comparison tests for human and rat GAPDH and ADAMTS-9 primers are shown in Figure 3.4. The slope generated by plotting ΔC_T values against $\log_{10}$(cDNA concentration) for the human primers (Fig. 3.4A) was -0.05

97

Figure 3.1 Rat ADAMTS-9 Primer Concentration Test
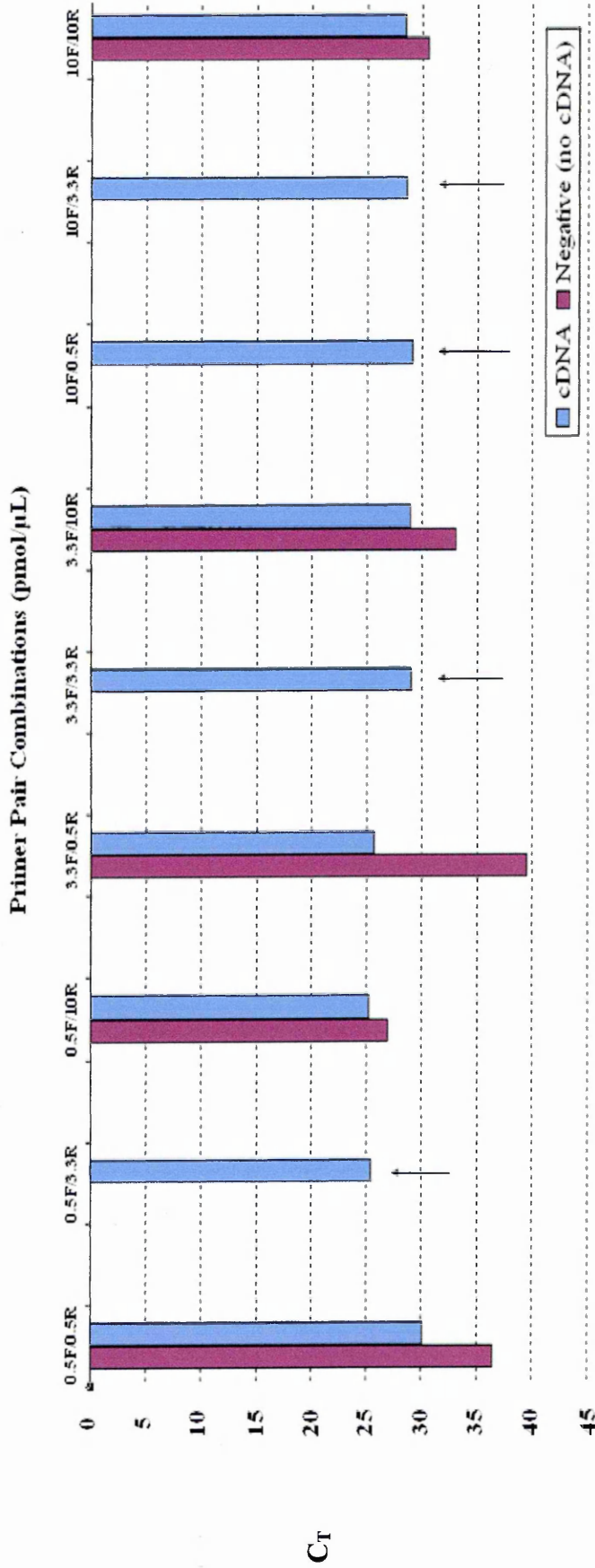
Real-time RT-PCR analysis assessing the optimal concentration of forward and reverse rat ADAMTS-9 primer combinations. Nine combinations were prepared and used to amplify identical amounts of starting template (rat EAE cDNA) or no cDNA (negative). Optimal combinations would expect to have an 'undetermined' signal when no cDNA is added to the reaction or have a C_T value of >35 (not returned). Arrows depict suitable primer combinations based on a) the lack of non-specific amplification in reactions lacking cDNA and b) the low C_T values in samples containing cDNA i.e. high amplification efficiency. Three independent experiments were conducted, figure is representative of these.

Figure 3.2 Rat ADAMTS-9 and GAPDH Primer Efficiency Tests

A

ADAMTS-9

$y = -3.2886x + 35.225$
$R^2 = 0.9323$

$Log_{10}(cDNA\ Concentration)$

% Efficiency $= 10^{-1/slope} -1$
$= 10^{-1/-3.2886} -1$
$= \mathbf{101.4\%}$

B

GAPDH

$y = -3.0411x + 25.958$
$R^2 = 0.9994$

$Log_{10}(cDNA\ Concentration)$

% Efficiency $= 10^{-1/slope} -1$
$= 10^{-1/-3.0411} -1$
$= \mathbf{113.2\%}$
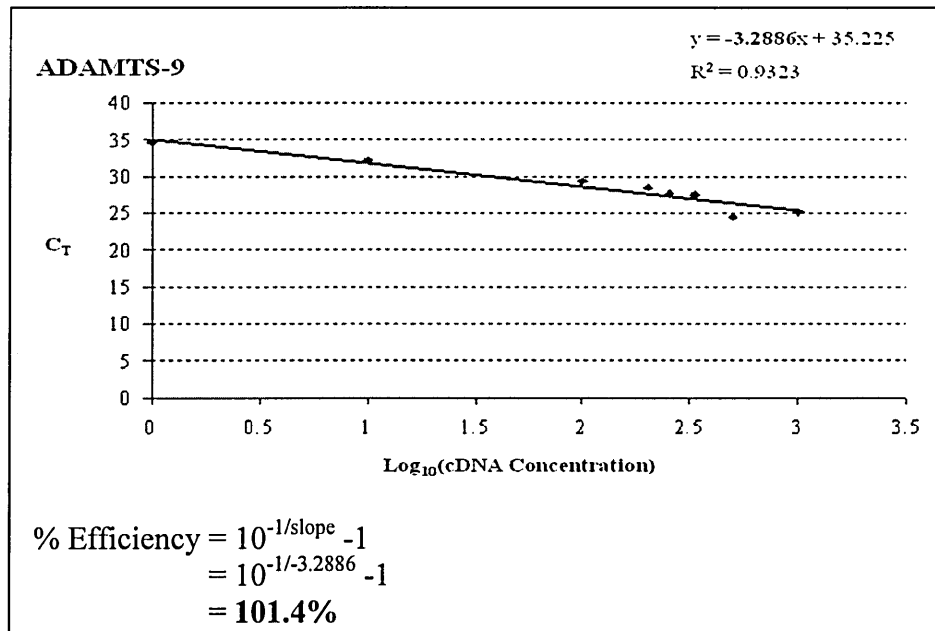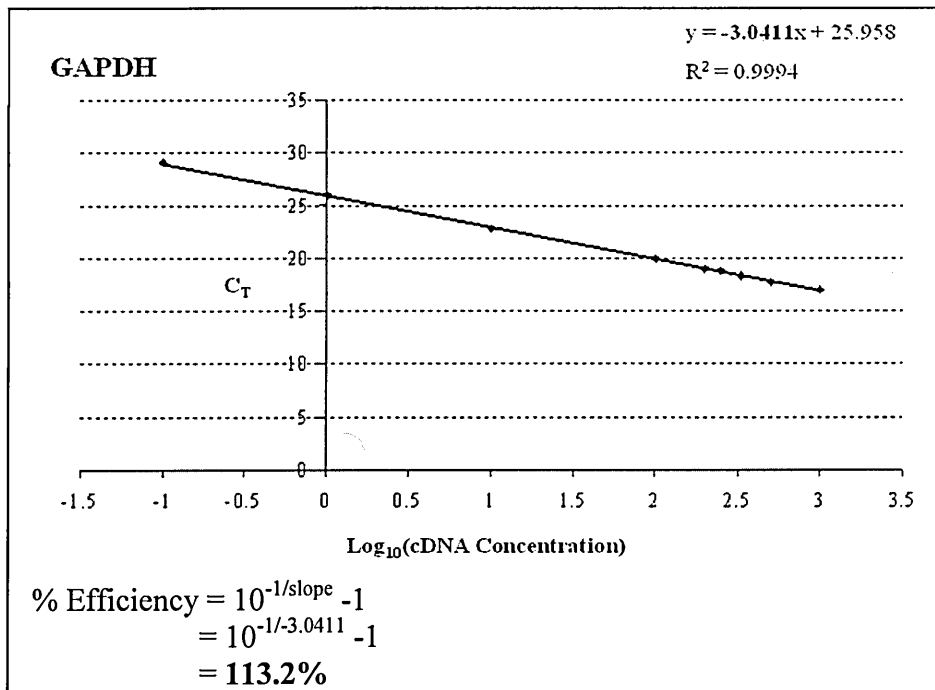
Real-time PCR analysis of serially diluted cDNA with rat ADAMTS-9 (A) and GAPDH (B) primers to assess primer efficiencies. RNA was extracted from rat EAE tissue prior to cDNA synthesis. Serial dilutions of the cDNA were prepared (1:2, 1:3, 1:4, 1:5, 1:10, 1:100, 1:1,000 and 1:10,000) and used as templates for real-time RT-PCR with ADAMTS-9 and GAPDH primers. Real-time RT-PCR was performed in duplicate and the experiment was repeated 3 times (independently). Note: Some cDNA dilutions were not amplified (template concentration was too low) and were omitted from the graphs.

Figure 3.3 Analysis of Real-Time RT-PCR Product Obtained with Rat ADAMTS-9 Primers
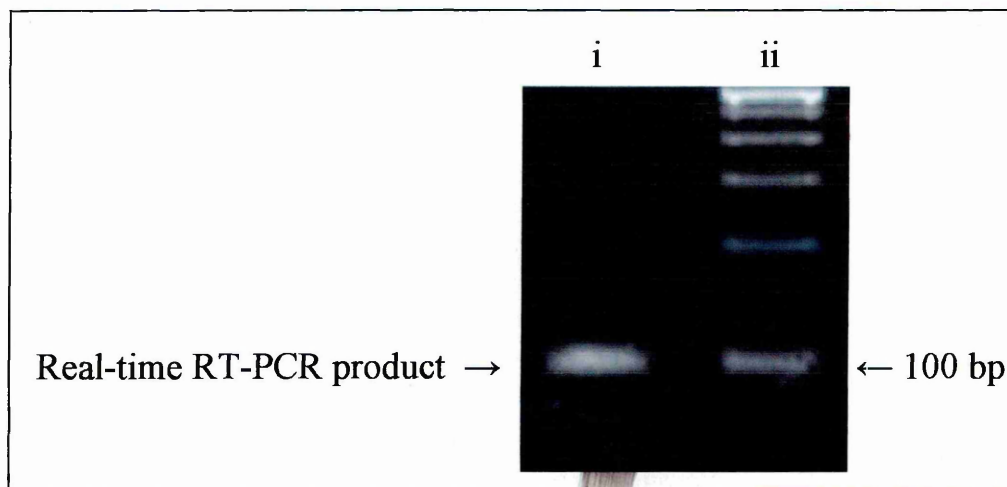
The real-time RT-PCR product obtained with the rat ADAMTS-9 primers was analysed by 4% AGE to confirm the correct size. Real-time RT-PCR was performed (as described in Section 2.8.2) on cDNA, which was synthesised from RNA extracted from rat EAE tissue. The real-time RT-PCR product from 6 x 10 µL reactions was pooled and PCR clean-up performed with the QIAquick kit (Qiagen) prior to loading 10 µL DNA in an agarose gel. i = product, ii = 100 bp marker.

Figure 3.4 Primer Efficiency Comparison Tests to Validate use of $2^{-\Delta\Delta C_T}$ Method
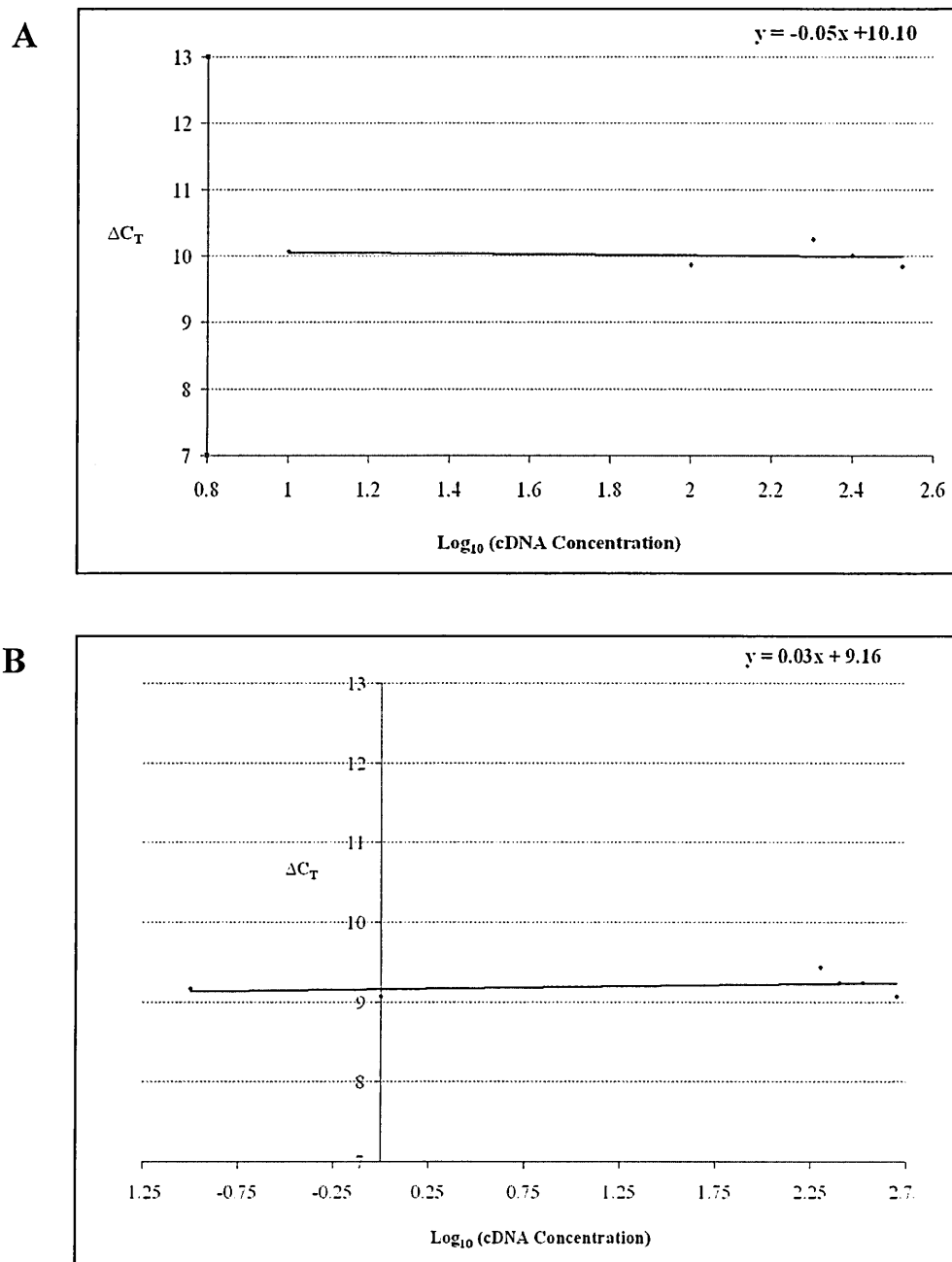
Real-time RT-PCR analysis of serially diluted cDNA with ADAMTS-9 and GAPDH human (A) and rat (B) primers to ascertain whether efficiencies of target gene and housekeeping gene primers are ~ equal (slope ~ zero) thus validating the use of $2^{-\Delta\Delta C_T}$ method. RNA extracted from (A) human U373-MG astrocytoma cells (untreated) and (B) rat tMCAo tissue (24 h) was reverse transcribed to cDNA, which was serially diluted (1:2, 1:3, 1:4, 1:5, 1:10, 1:100, 1:1,000, 1:10,000) prior to real-time RT-PCR (performed in duplicate) with ADAMTS-9 and GAPDH. Note: Some cDNA dilutions were not amplified (template concentration was too low) and were omitted from the graphs.

whereas the slope with the rat (Fig. 3.4B) primers was 0.03. Therefore, the $2^{-\Delta\Delta C_T}$ method was valid for this study because the slopes were 0 ± 0.1. Comparable slopes were obtained with YWHAZ/ADAMTS-9 to validate the use of the $2^{-\Delta\Delta C_T}$ method in the B327-01 and SHSY-5Y cells (not shown).

3.2.2.5 B327-01 and SHSY-5Y Housekeeping Gene Validation

It was demonstrated that both YWHAZ and SDHA were the most stable housekeeping genes for use with both the B327-01 and SHSY-5Y cells under the experimental conditions studied as calculated by geNorm and illustrated in Figure 3.5. YWHAZ primers produced cleaner melt-curves and were more efficient than the SDHA primers (not shown). Therefore, YWHAZ was the housekeeping gene utilised with the B327-01 and SHSY-5Y cells to normalise expression levels of ADAMTS-9 following treatment with factors (e.g. cytokines). YWHAZ primers were optimised and validated similarly to the rat ADAMTS-9 primers as described in this study (not shown).

3.2.3 Real-Time RT-PCR Optimisation Discussion

For this study, real-time RT-PCR primers were designed to detect ADAMTS-9 mRNA in tMCAo rat tissue. AGE and sequencing analysis of the real-time RT-PCR product obtained with the primers confirmed they were specific to ADAMTS-9. However, it was important to ascertain that the primers had a high amplification efficiency percentage, which was comparable to that of the housekeeping gene primers. Primer efficiency and primer efficiency comparison tests were conducted on serially diluted cDNA to assess these primer parameters. A problem encountered whilst conducting these tests was that highly diluted cDNA (e.g. 1:1,000 and 1:10,000) was not amplified (or had very high C_Ts of >40). Having extensively repeated the tests it was decided that there simply was not enough starting template in these samples for amplification to be initiated efficiently. This was substantiated by the fact that template doubled with each cycle for the lesser diluted cDNA samples. Therefore, these data for the highly diluted samples were not plotted in the graphs for these tests.

Figure 3.5 GeNorm Validation of Real-Time RT-PCR Housekeeping Genes for use with SHSY-5Y and B327-01 Cells
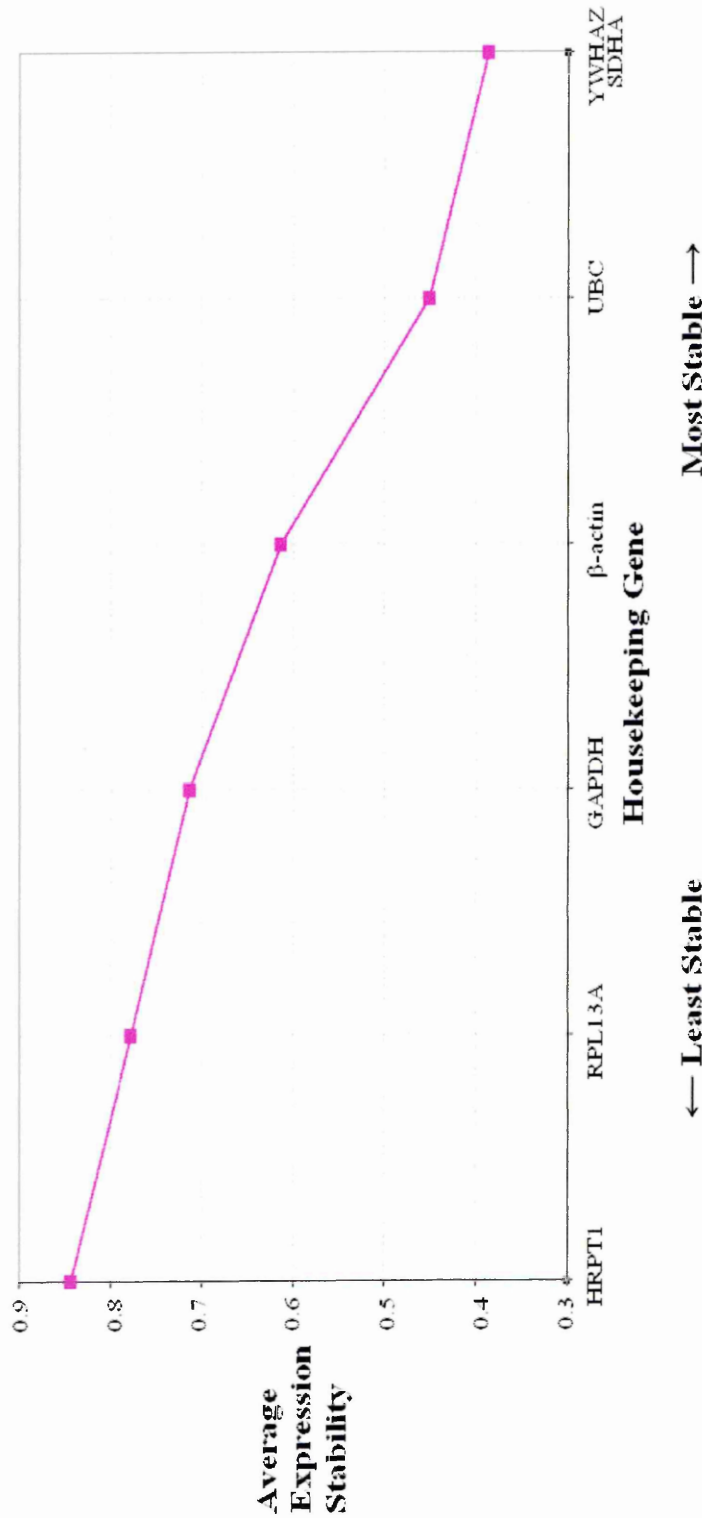
SHSY-5Y and B327-01 cells were treated with all factors tested in the study (B327-01: IL-1β, IFN-γ and TNF, SHSY-5Y: IL-1β, IFN-γ, TNF, NGF, TGFβ1 and dual treatments with IL-1β/TNF) prior to extraction of RNA and cDNA synthesis. Real-time RT-PCR was performed with seven housekeeping genes and an analysis of the $2^{\Delta C_T}$ values was conducted using geNorm to calculate the most stable genes across both cell types under all conditions tested. The graph shows the result of the geNorm validation when all data was inputted simultaneously (both cell types, all treatments). Analysis was also conducted with each cell line separately, yielding the same result (not shown).

3.3 *In Situ* Hybridisation - Oligonucleotide Probe Approach

3.3.1 Overview of Optimisation Steps

Oligonucleotide probes were initially adopted to detect ADAMTS-9 mRNA in tMCAo tissue sections by *ISH*. Unfortunately, non-specific binding of the probes was a common problem throughout the study. This was demonstrated by the strong signal obtained with the negative control sense probe. Therefore, the general *ISH* protocol was adapted in a number of ways in an attempt to reduce the non-specific binding as described below:

1. Included a pre-hybridisation acetylation step (treatment with 0.1 M Triethanolamine-acetic anhydride) to block reactive amine groups (have positive charges that associate with nucleic acids), which bind to probes non-specifically.

2. Increased the probe hybridisation temperature (39-60°C) (to increase the stringency) and decreased the hybridisation incubation time (1-18 h).

3. Decreased the probe concentration (1:50-1:500) (keeping antisense and sense concentrations equal) because excess DIG may have led to false-positives.

4. Increased post-hybridisation washing temperature (up to 60-80°C) and intensity (vigorous shaking of slides in the wash buffers) to remove non-specifically bound probe.

5. Increased NSS blocking concentration (1-20%) and incubation time (1-5 h) because non-specific binding of the anti-DIG antibody was a potential source of the problem.

6. Incubated SigmaFast BCIP/NBT in the presence of 1 mM levamisole to block endogenous AP, which the substrate may have been binding to.

7. Decreased incubation time with SIGMA FAST BCIP/NBT (10 min-18 h) because non-specific binding of the substrate to the tissue may have been a reason for the signal on the negative control sections.

8. Attempted fluorescent detection (F*ISH*) as opposed to colourmetric AP/BCIP/NBT method to ascertain whether specificity was improved.

3.3.2 Results

3.3.2.1 Oligonucleotide Probe Specificity

None of the optimisation attempts noticeably decreased non-specific binding with the oligonucleotide probes. A representative series of images obtained with these probes are shown in Figure 3.6. The signal displayed with the sense probe (Figs 3.6D, 3.6E, 3.6F) was not considerably different from that obtained with the antisense probe (Figs 3.6A, 3.6B and 3.6C). Evidence that the antisense and sense probes were binding non-specifically came from using a 'no probe' control (Fig. 3.6G), which did not generate a signal. A p(dT) positive control confirmed tissue integrity because total mRNA expression was detected (Figs 3.6H, 3.6I). Therefore, it was impossible to say with any certainty with oligonucleotide probes, which cells were expressing ADAMTS-9.

3.4 *In Situ* Hybridisation - Riboprobe Approach

3.4.1 Overview of Development and Optimisation Steps

A great deal of time and work in this study was directed at optimising the *ISH* method using oligonucleotide probes. Unfortunately, it was decided that the oligonucleotide probes were not appropriate for specifically detecting ADAMTS-9 in tMCAo CNS sections. A different *ISH* approach was to utilise riboprobes. As opposed to the oligonucleotide probes purchased from GeneDetect.com, the ADAMTS-9 riboprobe has been characterised and utilised previously for *ISH* (Jungers *et al*, 2005). Generation of the ADAMTS-9 antisense and sense probes from the DNA plasmid involved a number of molecular biological steps. The subsequent data in this section demonstrate the results of the various stages of riboprobe generation, validation and optimisation.

Figure 3.6 *In Situ* Hybridisation of tMCAo Tissue Sections with Oligonucleotide Probes showing Non-Specific Binding
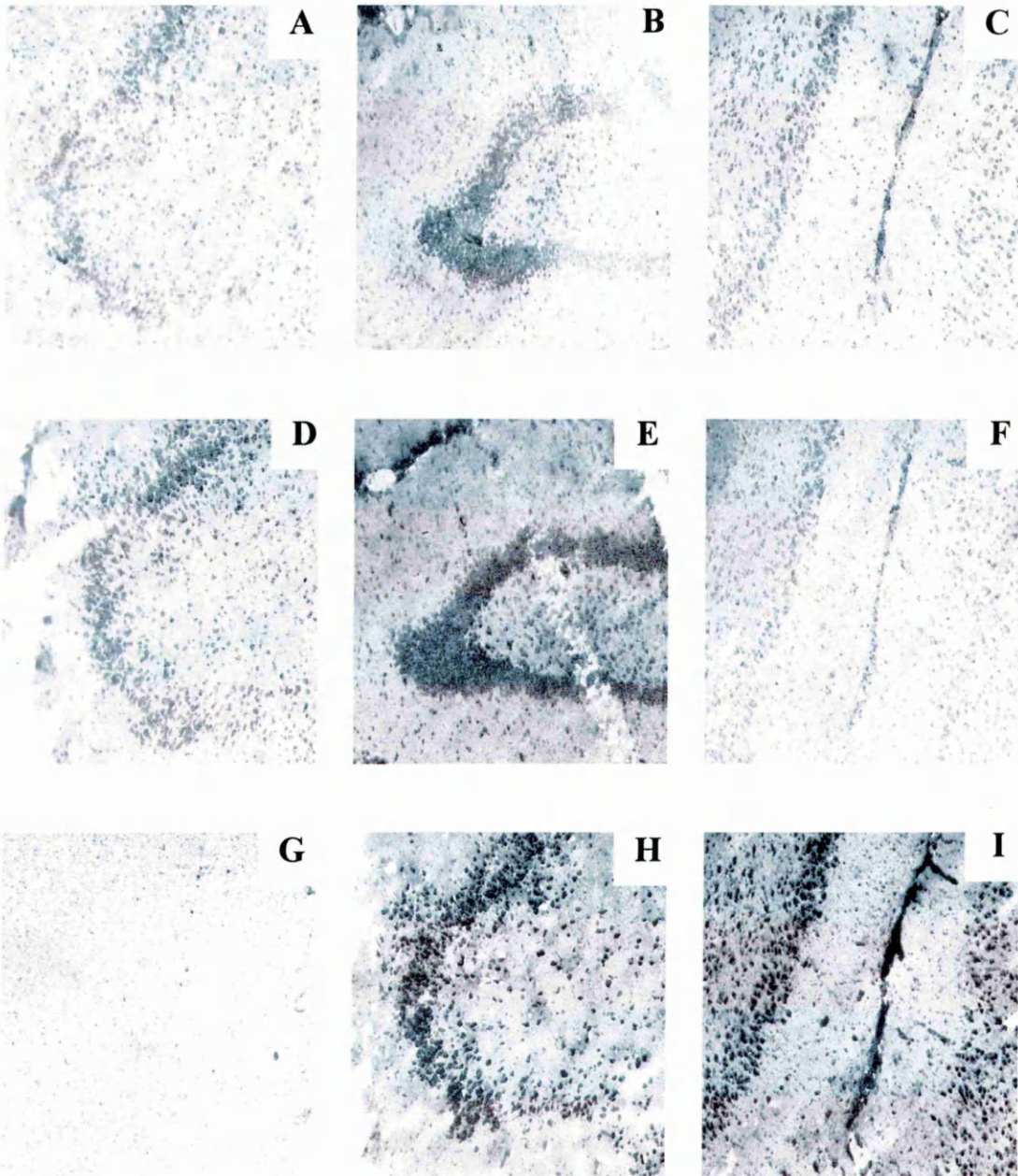
Hybridisation with; oligonucleotide ADAMTS-9 antisense probe (A, B, C), sense probe (D, E, F), no-probe (G), p(dT) probe (H, I). Images of A, D and H are from same region, images of B and E are from the same region, images of C, F, G and I are from the same region. Images taken on a fluorescent microscope in bright-field mode (x100).

3.4.2 Results

3.4.2.1 Riboprobe Generation

Diagnostic restriction digest of pBluescript KS+ plasmid to verify ADAMTS-9 cDNA insert identity

Two bands were visualised by AGE following a restriction digest of pBluescript KS+ (containing an ADAMTS-9 insert) with PstI and XbaI as shown in Figure 3.7A. The larger of the bands was the size of the vector (~2958 bp), whereas the smaller band was the size of the ADAMTS-9 insert (~960 bp). This data confirmed that the insert within the pBluescript KS+ vector was that of the correct ADAMTS-9 cDNA clone.

Linearisation of plasmid DNA in preparation for *IV*T/DIG-labelling

Figure 3.7Bii shows that XbaI cut at one site within the plasmid because one band of the size of the plasmid and insert (~3918 bp) was observed. Figure 3.7Biii demonstrates that EcoRI cut at two locations close together within the plasmid (see Fig. 2.4) thus generating two pieces of linear plasmid DNA (one large, one small). The size of the EcoRI-EcoRI fragment was ~130 bp which was the approximate difference between the size of the larger band in Figure 3.7Biii and the only band in Figure 3.7Bii. This confirmed that the antisense probe is slightly shorter than the sense probe following *IV*T/DIG-labelling.

Assessment of *IS*H Riboprobe Purity following *In Vitro* Transcription/DIG-Labelling and DNAse I Treatment

For both the antisense and sense riboprobes, only one band was observed by AGE, suggesting the probes were pure (no template DNA), as demonstrated by the representative image in Figure 3.7C. The antisense probe was ~450 bases (Fig. 3.7Cii), whereas the sense probe was ~580 bases (3.7Ciii). The smaller size of the antisense probe was expected because of the presence of the EcoRI-EcoRI fragment seen in Figure 3.7B.

A: Diagnostic Restriction Digest of pBluescript KS+ Plasmid to Verify ADAMTS-9 cDNA Insert Identity. A miniprep was performed to obtain plasmid DNA from XL-1 blue *E. coli* colonies, which were picked following ampicillin resistance selection. Plasmid DNA was cut with diagnostic restriction enzymes PstI and XbaI (see Figure 2.3 for schematic of pBluescript KS+ plasmid) to release the ADAMTS-9 fragment prior to 2% AGE analysis (Aii).

B: Linearisation of Plasmid DNA in Preparation for *IV*T/DIG-Labelling. Plasmid DNA was linearised with XbaI (Bii) and EcoRI (Biii) prior to 2% AGE. The single band observed following digestion with XbaI demonstrates the plasmid DNA was cut at one site. The two bands observed following digestion with EcoRI suggests the plasmid DNA was cut at two sites (close together given the small size of EcoRI-EcoRI fragment) (see Figure 2.4 schematic).

C: Assessment of *IS*H Riboprobe Purity following *In Vitro* Transcription/DIG-Labelling and DNAse I Treatment. Riboprobes were subjected to 2% AGE following *IV*T/DIG-labelling and treatment with DNase I. Cii = linearisation with EcoRI and subsequent transcription with T7 polymerase (antisense probe). Ciii = Linearisation with XbaI and subsequent polymerisation with T3 polymerase (sense probe). Note: representative image of one batch of probes, these procedures were performed each time a new batch of probes were produced.

Ai and Bi = 500 bp DNA ladder, Ci = 100 bp DNA ladder.

Figure 3.7 ADAMTS-9 Riboprobe Generation
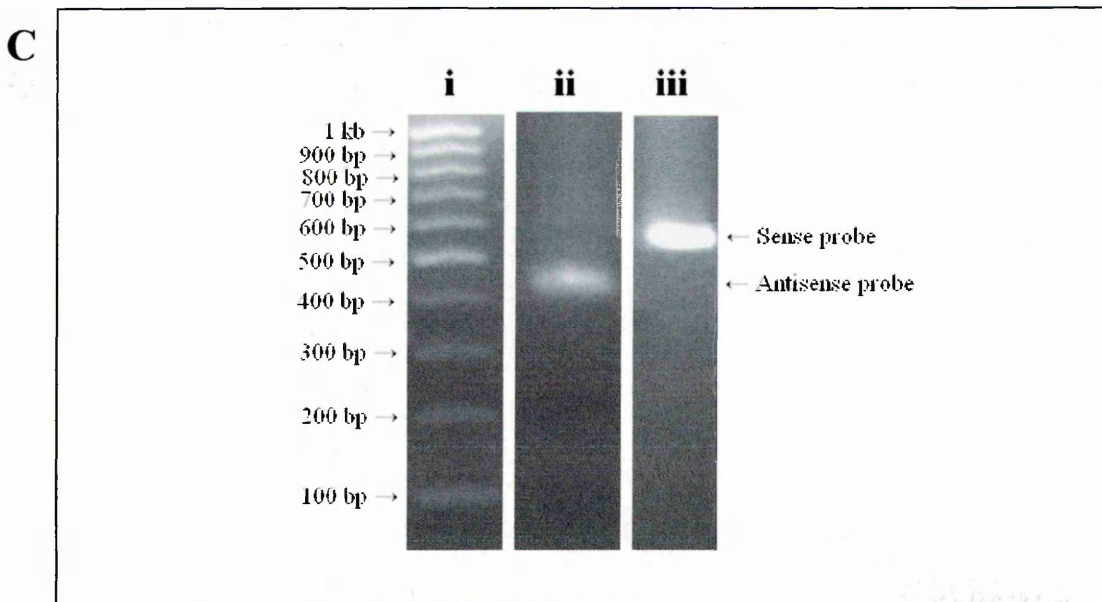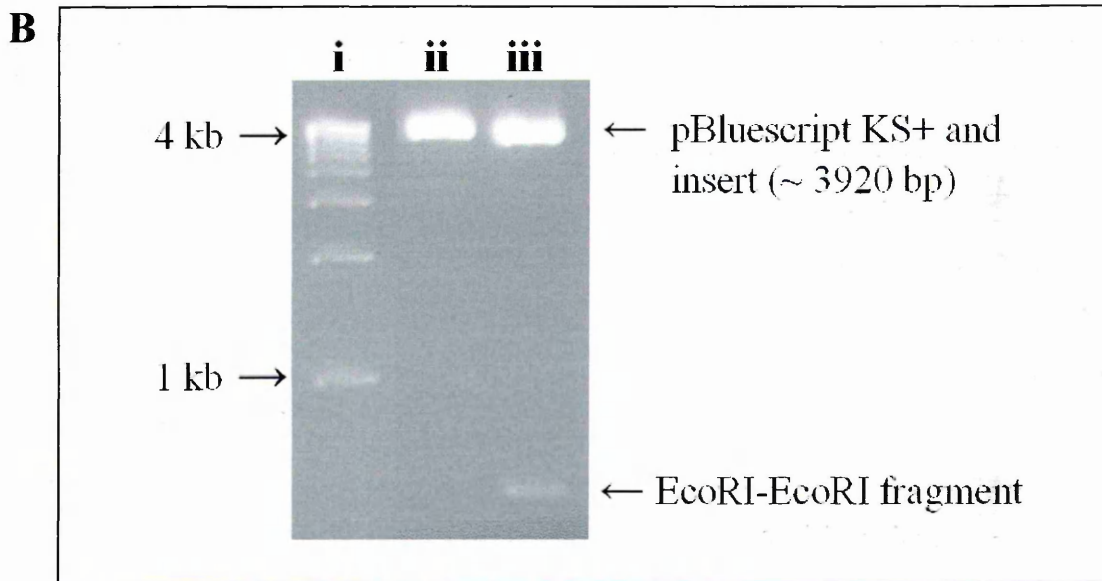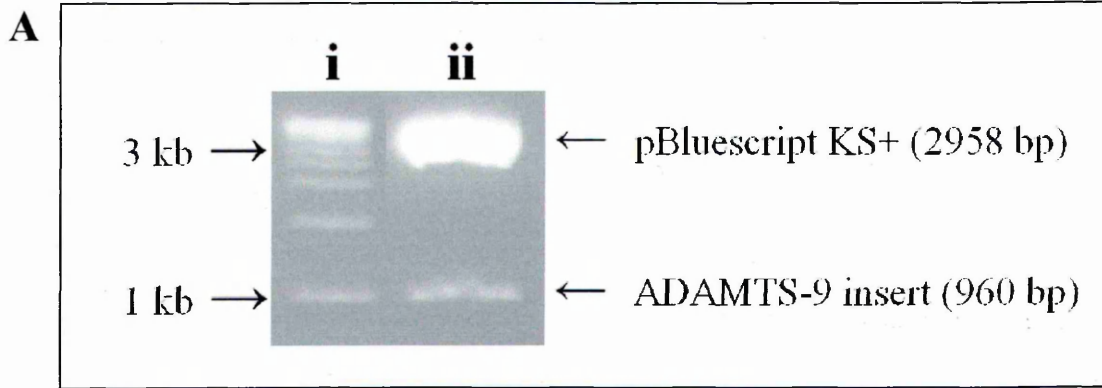
3.4.2.2 Verification of Riboprobe DIG-Labelling/Dilution Calculation

The serial dilutions of the commercial p(dT) and DIG-labelled RNA controls demonstrated that the dot blotting technique was sensitive enough to differentiate between different concentrations of DIG as demonstrated in Figure 3.8A. The strong signal observed with the p(dT) dot blot (Fig. 3.8A) confirmed that this probe could be utilised as the positive control in *IS*H experiments.

The representative blot in Figure 3.8B shows that both the antisense and sense probes were labelled with DIG. The IOD of the batch of antisense probe represented in Figure 3.8B was ~100 whereas the sense probe was ~57 (note IOD varied with each batch due to variations in *IV*T/DIG-labelling reaction). Therefore the ratio of DIG-labelling of antisense to sense with this batch of probes was ~2:1 thus using the antisense probe at a dilution of 1:50 and the sense probe at 1:25 would give approximately the same concentration of DIG in *IS*H experiments. The concentrations at which the probes were utilised throughout the study were between 500-1500 ng/mL (depending on the batch).

3.4.2.3 ADAMTS-9 Riboprobe Specificity

The representative *IS*Hs in Figure 3.9 demonstrate that the ADAMTS-9 riboprobe was specific. The intense cellular signal shown in 3.9A and B was not replicated with the sense probe (Figs 3.9C and D), which gave only background staining. Furthermore, with the antisense probe, the difference in signal between the positive cells and the background signal was clear. Negligible signal was obtained with the no-probe negative control (Fig. 3.9E). The high-affinity hybridisation of the riboprobe demonstrates that it is suitable for detecting ADAMTS-9 in rat tissue despite its generation from a mouse cDNA clone and previous use in mouse tissue (Jungers *et al*, 2005).

3.4.3 *In Situ* Hybridisation Optimisation Discussion

The fact that the ADAMTS-9 oligonucleotide probes were only 48 bases in length is proposed to be the main reason for the *IS*H non-specific binding. The ADAMTS-9 riboprobe was far longer (~450 bases), making the binding to the complementary sequence much tighter, thus allowing stringent washes to be performed. In support of these findings, a study by Komminoth *et al* (1992) demonstrated that DIG-labelled

110

Figure 3.8 Determination of DIG-Labelling Efficiency of ADAMTS-9 Riboprobes
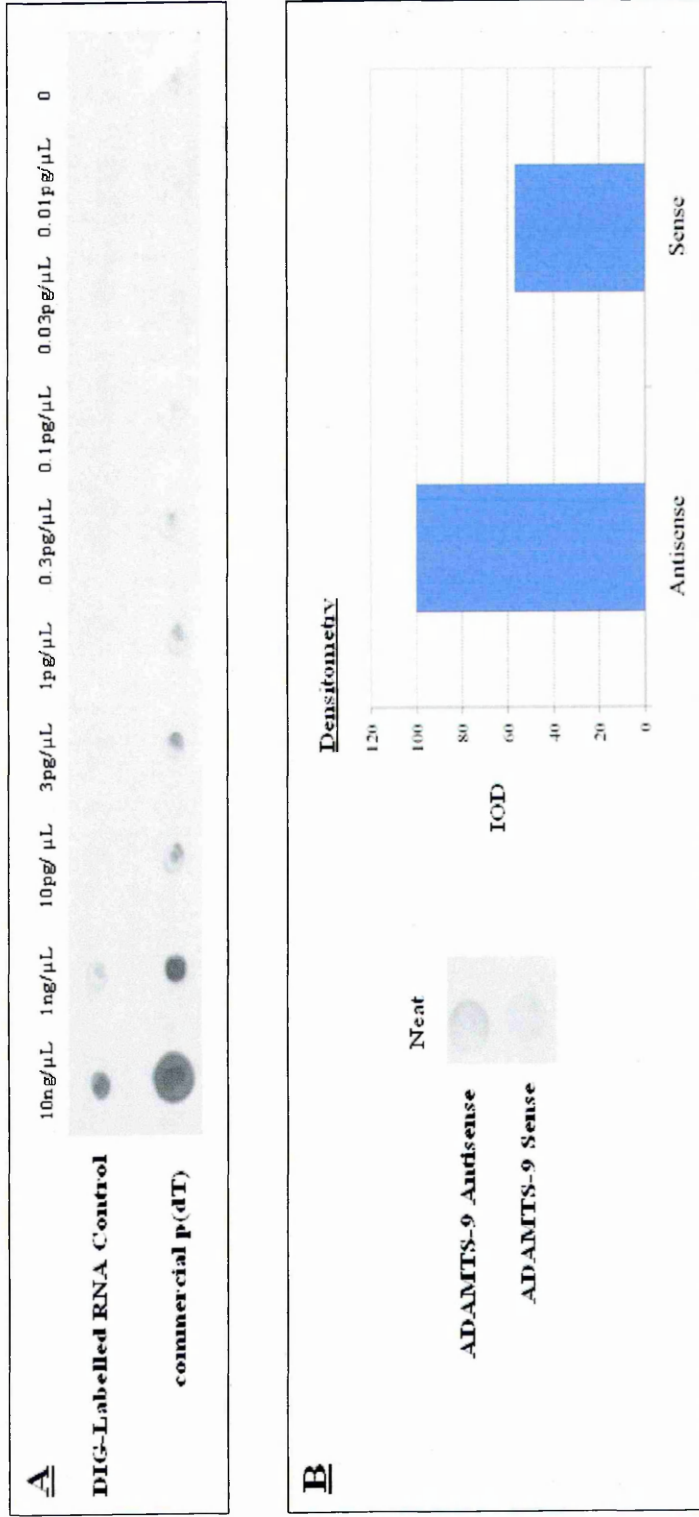
Dot blot analysis of ADAMTS-9 riboprobe DIG-labelling efficiency. Box A shows dot blot of serially diluted positive control DIG-labelled RNA and commercial p(dT). Box B shows dot blot of antisense and sense probes and densitometry which was utilised to confirm probe dilutions for *ISH*. Images are representative; this technique was applied to different batches of probes (generated from a stock of linearised plasmid DNA) to confirm correct dilutions of antisense and sense probes so they were utilised with ~ equal concentrations of DIG. IOD = integrated optical density.

111

Figure 3.9 *In Situ* Hybridisation of 5 Day tMCAo Tissue Sections Showing Specific Binding of ADAMTS-9 Riboprobe
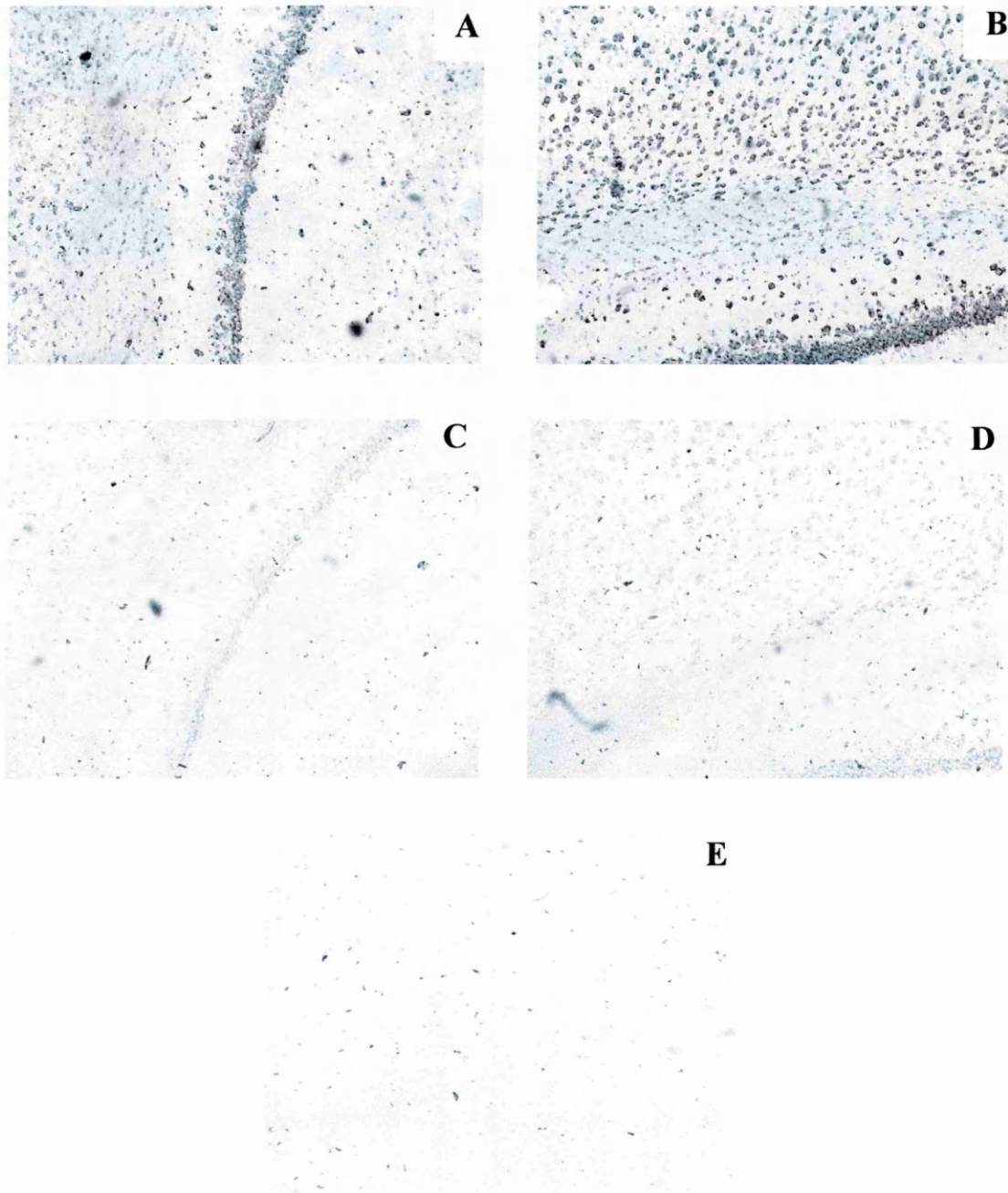
Representative *IS*Hs of tMCAo tissue sections with; ADAMTS-9 antisense riboprobe (A and B), sense riboprobe (C and D) and no-probe (E). Images of A and C are from same region, images of B, D and E are from the same region. Images taken on an Olympus BX60 microscope in bright-field mode (x100).

riboprobes were more sensitive and displayed less background reactivity than DIG-labelled oligonucleotide probes. The original method would perhaps have been more specific and sensitive if a cocktail of oligonucleotide probes had been used as opposed to the one 48-mer probe. The antisense cocktail would comprise of a number of oligonucleotides with specificity to bases in different regions of the target sequence, thus a positive signal would be more intense because of the increased concentration of DIG being present.

Following digestion of the plasmid DNA with EcoRI in preparation for *IVT*/DIG-labelling, two bands were observed by AGE, which was not surprising given that there is a restriction site within the insert as well as in the MCS as shown in Figure 2.4. Having the EcoRI site within the insert offered the advantage that the 3' end of the antisense probe was more specific to ADAMTS-9 as opposed to being the transcript of the cDNA sequence, which was engineered into the insert to ligate the cDNA into the vector.

3.5 Optimisation of Anti-ADAMTS-9 Antibodies

3.5.1 Overview of Antibody Optimisation Steps

In order to study the expression of ADAMTS-9 at the protein level, specific and sensitive antibodies needed optimising and validating. A number of commercially purchased antibodies as well as the ADAMTS-9L2 antibody were tested for their ability to detect ADAMTS-9. Western blotting is the preferred technique to assess an antibody's specificity because it allows the visualisation of different processed forms of protein(s) which are being detected. Prior to testing antibodies by western blotting, it is impossible to say an ICC or IHC is specifically detecting the target antigen i.e. staining may be a result of the antibody binding non-specifically.

3.5.2 Results

3.5.2.1 Analysis of Anti-ADAMTS-9 Antibody Specificity and Efficacy

The Cedarlane (anti-catalytic domain) and BioReagents (anti-propeptide) anti-ADAMTS-9 antibodies displayed negligible reactivity to ADAMTS-9 protein as shown by the representative western blot in Figure 3.10A and 3.10C. The representative western blot shown in Figure 3.10B, demonstrates that the RP4 antibody (anti-propeptide) was not specific to ADAMTS-9 because the same reactive band was observed with (3.10Bii) and without (3.10Bi) peptide blocking. These outcomes were replicated in numerous repeat experiments with different samples i.e. both CNS-cell and tMCAo brain protein extracts under different western blotting conditions (not shown). Consequently, the Cedarlane, RP4 and Affinity BioReagents antibodies were not further utilised further to study ADAMTS-9.

Figure 3.10D indicates that the ADAMTS-9L2 antibody (anti-linker 2 domain) was specific to ADAMTS-9. In the representative blot shown, reactive bands were observed at ~188 and (to a lesser extent) ~100 kDa and ~50 kDa (Fig. 3.10Di). These bands were absent following blocking of the antibody with the 'immunising' peptide (Fig. 3.10Dii). Other bands were observed at ~38, ~62-64, ~80 and ~140 kDa when other tMCAo protein extracts were blotted (not shown). These bands were absent following blocking of the antibody with the immunising peptide. Therefore, this antibody was used to study ADAMTS-9 in CNS inflammatory disorders in further work.

3.5.3 Antibody Optimisation Discussion

Prior to analysing ADAMTS-9 at the protein level, it was essential to validate antibodies raised against the peptidase. There are problems when analysing protein levels of ADAMTS-9. Firstly, the fact that the ADAMTS-9 zymogen is ~216 kDa (Somerville *et al*, 2003) means it is the largest of the ADAMTSs, making it difficult to resolve on SDS-PAGE, as described by Koo *et al*, 2007. Secondly, experiments are limited by the availability and quality of commercial antibodies as highlighted in a recent study analysing proteolytic cleavage of versican in the heart, in which the author states, 'the lack of adequate antibodies to murine ADAMTS-9 precluded us from investigating its expression' (Kern *et al*, 2007).

Representative western blots showing the analysis of anti-ADAMTS-9 antibody specificity. Figure shows blotting with Cedarlane anti-ADAMTS-9 antibody (Ai), RP4 anti-ADAMTS-9 antibody (Bi), Affinity BioReagents anti-ADAMTS-9 antibody (Ci) and ADAMTS-9L2 anti-ADAMTS-9 antibody (Di). As a negative control for non-specific binding of the secondary antibodies, the protocol was adhered to in an identical fashion but for the omission of the primary antibodies. Such negative controls are shown following omission of the Cedarlane antibody (Aii) and the Affinity BioReagents antibody (Cii). The negative blots obtained by omission of the ADAMTS-9L2 and RP4 antibodies are not shown. As controls to ascertain the specificity of the RP4 (Bii) and ADAMTS-9L2 (Dii) antibodies, the immunising peptides were incubated with the antibodies prior to blotting. Peptides were not available for Cedarland and BioReagents antibodies. The representative images show western blotting of B327-01 astrocytic cell extracts (A), protein extracted from 24 h tMCAo brains (B and D) and protein extracted from a 5 day tMCAo stroke brain (C). All antibodies were tested on CNS cell-lysates and tMCAo (all time-points) brain protein extracts with similar results (not all blots shown). Note the same M_r markers are depicted in C and D for comparative purposes. Blot A is following protein separation via 4% SDS-PAGE, whereas B-D were 10% gels.

115

Figure 3.10 Analysis of Anti-ADAMTS-9 Antibody Specificity and Efficacy
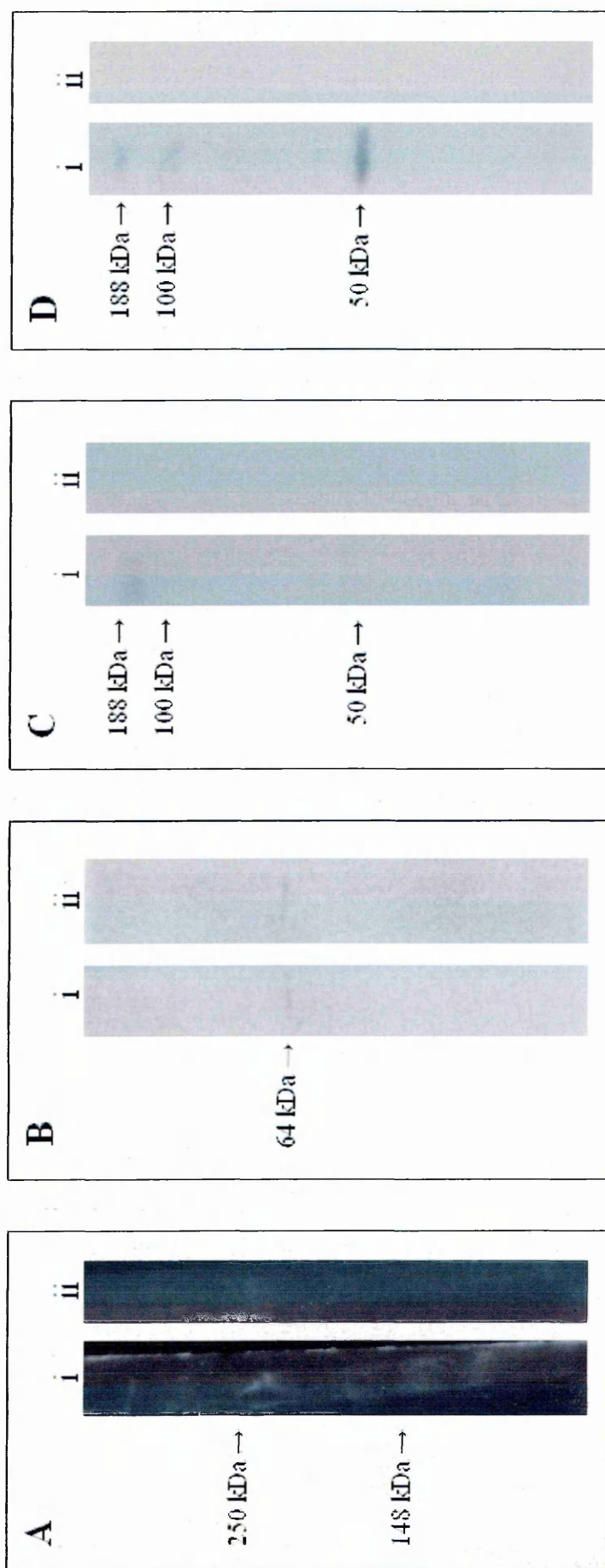
It was demonstrated in this study that none of the commercial antibodies were suitable for generating meaningful data because they were either a) non-specific or b) lacking efficacy. Unsuccessful attempts were made to block out the non-specific binding of the RP4 antibody by incubating membranes in a higher concentration (up to 20%) of milk prior to application of the primary antibody. Also, the immunising RP4 peptide was used at a high concentration (100 μg). The antibodies which displayed low binding affinities (Cedarlane and BioReagents) were used at increased concentrations (1:500) but efficacy was not improved. To support these findings, no papers have been published with either the Cedarlane or Affinity BioReagents anti-ADAMTS-9 antibodies. However, data have been published with the RP4 antibody previously (Koo *et al*, 2006; Koo *et al*, 2007); although, the authors do not report the use of peptide blocking or the performing of any experiments to determine the specificity of the antibody. The same western blotting protocol adopted by Koo *et al*, was applied to this study but non-specific binding was not eradicated.

In contrast to the commercially purchased antibodies, the ADAMTS-9L2 antibody was shown to label ADAMTS-9 with high efficacy. All commercial antibodies were raised against peptides with amino acid sequence homology to the human form of ADAMTS-9, which is a potential reason for their poor reactivity with rat protein extracted from tMCAo brains. However, this problem was not replicated with the ADAMTS-9L2 antibody, which displayed high affinity to rat ADAMTS-9 protein in tMCAo extracts despite targeting the human form.

The bands detected in this study with the ADAMTS-9L2 antibody appear to be specific to ADAMTS-9 because they were absent on blots following incubation with peptide-blocked antibody. However, it is difficult to conclude whether the antibody is detecting numerous species of ADAMTS-9 protein present in the extracts or whether some of the smaller bands are a result of the extraction protocol (degradation). Dissolving of the protein pellet following extraction with TRI Reagent involved increasing the temperature to ~70°C and vigorous vortexing and mixing by pippetting. This may have disrupted the structure of the proteins, which were present in the original sample thus generating fragments (still containing the 2nd linker domain) that are not pathophysiologically relevant e.g. the smaller bands at ~35-39 and ~62-64. The larger proteins detected (e.g. ~140 and ~188 kDa) are more likely to be ADAMTS-9 species, which were present in the cell and tMCAo extracts. Data obtained with the ADAMTS-

9L2 antibody were published previously (Demircan *et al*, 2005), showing a reactive band of similar size to the one detected in this study (~180-200 kDa). The authors detected bands at 75 and 100 kDa, which were described as being a result of 'cross-reactivity with non-ADAMTS-9 proteins'. No mention of testing the specificity of the antibody by peptide-blocking was reported.

Unfortunately, the Apte laboratory only produced a finite amount of the antibody, therefore it was only utilised extensively in the tMCAo model to analyse whether differences in ADAMTS-9 mRNA expression correlated with protein levels (Chapter 5). The antibody was also used to assess the cellular localisation of ADAMTS-9 in the U373-MG cells (Chapter 4).

3.6 Summary

These data presented in this chapter, demonstrate the successful development, optimisation and validation of methods (real-time RT-PCR, *ISH* and western blotting/ICC) to detect ADAMTS-9. This enabled the application of these methods to study expression levels and localisation of ADAMTS-9 mRNA and protein in CNS-derived cells (Chapter 4) and in the tMCAo rat model (Chapter 5).

Chapter 4

ADAMTS-9 Expression and Modulation in CNS-Derived Cells *In Vitro*

4.1 Background

There is limited evidence as to the cellular source of ADAMTS-9 in the human brain. Furthermore, little is known about transcriptional regulation of *Adamts9* in the CNS, though in other tissues it appears to be modulated by pro-inflammatory mediators (Bevitt *et al*, 2003; Demircan *et al*, 2005). In this study, the expression and modulation of *Adamts9* was analysed in human astrocytes (U373-MG, U87-MG astrocytomas and B327-01), microglia (CHME3 human foetal cell line) and neuronal cells (SHSY-5Y human neuroblastoma cell line) by real-time RT-PCR. To understand further the transcriptional initiators of ADAMTS-9 expression in the brain, cells were treated with factors implicated in the pathogenesis of CNS inflammatory disorders including pro-inflammatory cytokines IL-1β, IFN-γ and TNF and the anti-inflammatory cytokine TGF-β. In addition, SHSY-5Y cells were treated with NGF and RetA, which are both important in triggering neuronal differentiation and growth, to assess whether ADAMTS-9 is modulated by such factors. An analysis of the cellular localisation of ADAMTS-9 protein in U373-MG was also conducted by ICC.

4.2 ADAMTS-9 in Astrocytic Cells

4.2.1 Overview of Approach

A wealth of evidence implicates astrocytes in CNS inflammatory disorders as well as in normal physiological processes. It has been documented that astrocytes secrete many mediators of inflammation including cytokines as well as proteolytic enzymes (MMPs) (Yin *et al*, 2006). Therefore, cell culture methods were applied to analyse whether ADAMTS-9 is expressed by astrocytes *in vitro* and whether its expression can be modulated by inflammatory stimuli.

Despite using established cell-lines, it was important to characterise the U373-MG and B327-01 cells as astrocytic prior to using them in experiments (U87-MG cells were validated previously by Dr. Alison Cross). To do this western blotting and ICC were performed to detect GFAP, which is an intermediate filament protein found only in astrocytes. The M_r of GFAP as visualised by SDS-PAGE/western blotting varies between 47-55 kDa (Santos *et al*, 2005). Another marker which was detected was factor

S100β (~20 kDa), which is localised in the cytoplasm and nuclei of astrocytes. Functions of S100β include cell growth regulation, calcium homeostasis and cell structure (Mbele *et al*, 2002). B327-01 cell characterisation was performed in collaboration with Helen Denney and Antoine Fouillet (both Sheffield Hallam University)

As well as secreting cytokines, astrocytes have long been reported to express cytokine receptors including IL-1RI, IL-1RII, p75, p55, TNFR and IFN-γ-receptor (IFN-γR) (Tada *et al*, 1994; Carroll-Anzinger & Al-Harthi, 2006). Therefore, astrocytic cell cultures were treated with cytokines prior to real-time RT-PCR analysis to determine whether such mediators of CNS inflammation modulate the expression of *Adamts9* steady-state mRNA levels. Prior to treatment with cytokines an analysis of *Adamts9* expression levels for all the astrocytic cells under basal conditions was also conducted.

4.2.2 Results

4.2.2.1 Characterisation of Astrocytes

Figure 4.1Aiii illustrates strong GFAP staining of U373-MG cells by ICC with anti-GFAP antibody. Incubation with PBS instead of the primary antibody displayed a lack of staining (Fig 4.1Aiv). Figure 4.1Biii demonstrates detection of a protein with M_r of ~52 kDa by western blotting with anti-GFAP antibody. No bands were detected when anti-GFAP antibody was omitted (replaced by TBST) from the western blotting protocol as shown in Figure 4.1Biv.

ICC of the B327-01 cells with the anti-GFAP antibody produced unusual, diffuse (grainy) staining of the intermediate filaments (not shown). However, GFAP was shown by western blotting to be abundantly expressed by these cells as illustrated in Figure 4.1Bi. A protein with M_r of ~52 kDa was detected in B327-01 cells with the anti-GFAP antibody. No bands were detected when anti-GFAP antibody was omitted (replaced by TBS) from the western blotting protocol as shown in Figure 4.1Bii. To further confirm that the B327-01 cells were astrocytic, ICC was performed on these cells with an anti-S100β antibody. Figure 4.1Ai demonstrates strong ICC S100β staining of the B327-01 cells. No staining was observed when anti-S100β antibody was omitted (replaced with

Astrocytes were characterised by ICC staining (A) and western blotting (B). Ai = B327-01 ICC staining (green) with anti-S100β antibody. Aiii = U373-MG ICC staining (green) with anti-GFAP antibody. ICC was performed on B327-01 (Aii) and U373-MG (Aiv) with the omission of primary antibodies from the protocol (replaced by PBS), serving as a negative controls for non-specific binding of the secondary antibodies. Nuclear staining was with DAPI (blue) in all ICC images. Images were captured and analysed on a confocal microscope (x400). Western blotting was performed on B327-01 (Bi) and U373-MG (Biii) with anti-GFAP antibody. Primary antibodies were omitted (replaced by TBST) from western blots of B327-01 (Bii) and U373-MG (Biv), serving as negative controls for non-specific binding of the secondary antibodies. B327-01 characterisation was performed in collaboration with Helen Denney and Antoine Fouillet (both Sheffield Hallam University).

Figure 4.1 Characterisation of Human Astrocytic Cells

A
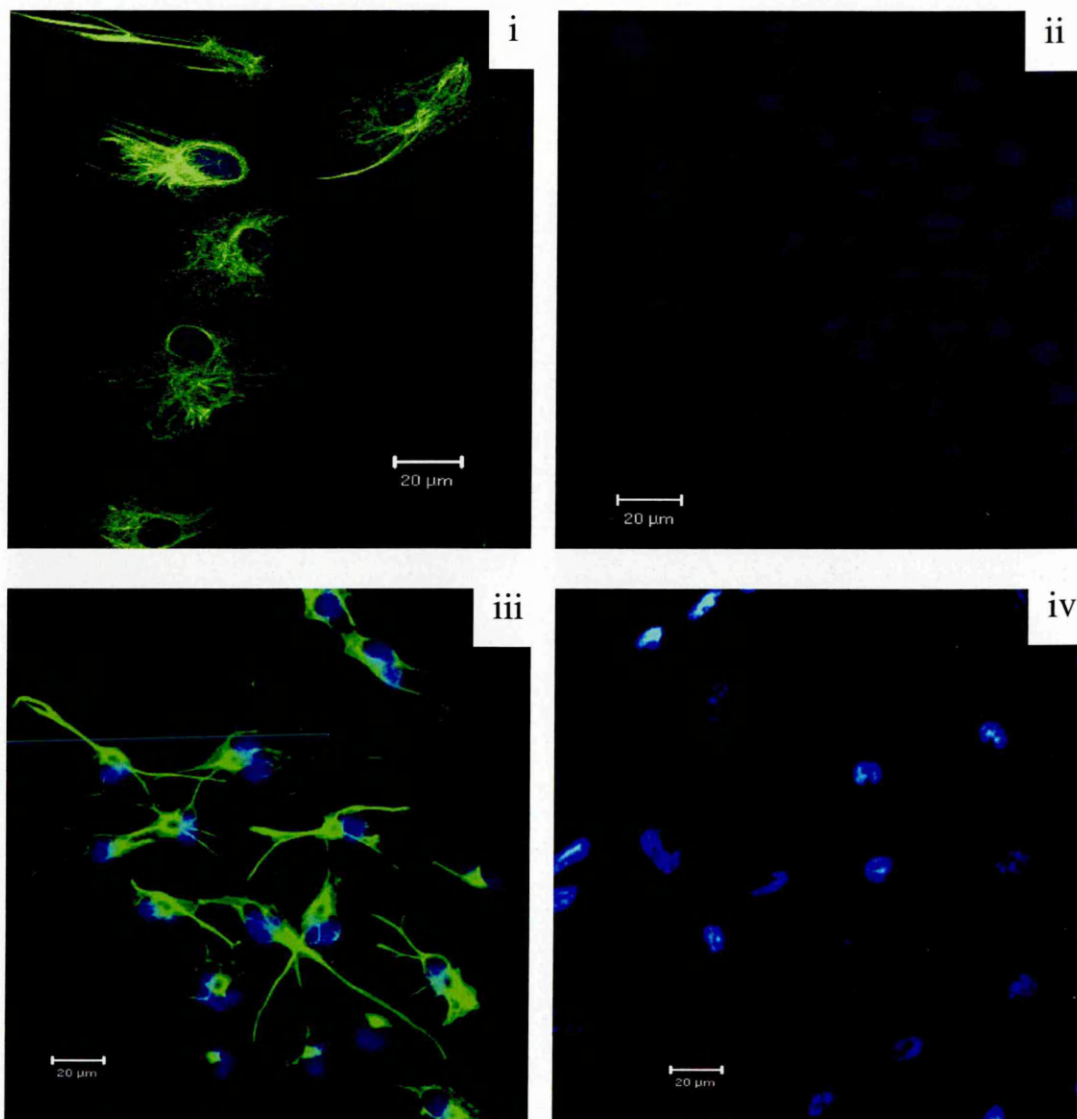
B
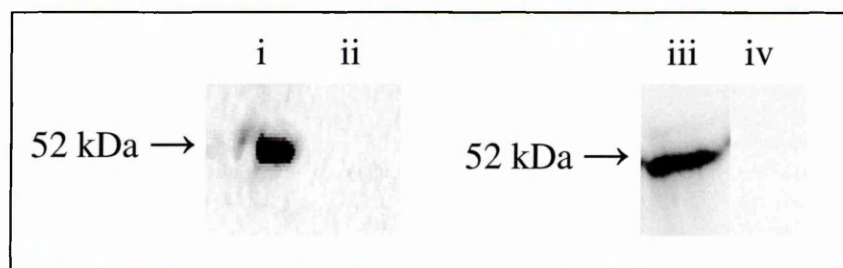
PBS) from the protocol (Fig. 4.1Aii). Therefore, both B327-01 and U373-MG were considered viable astrocytic cell populations.

4.2.2.2 Comparison of *Adamts9* Expression between different Astrocytic Cells under Basal Conditions

Figure 4.2 shows that all astrocytic cells analysed in the study expressed ADAMTS-9 mRNA. B327-01 astrocytes ($2^{-\Delta C_T} = 0.02$) expressed ~40 times more *Adamts9* than U373-MG astrocytoma (0.0005) and ~70 times more than U87-MG astrocytoma (0.0003) as detected by real-time RT-PCR.

4.2.2.3 Modulation of Astrocytic *Adamts9* Expression by Pro-Inflammatory Cytokines

U373-MG

Figure 4.3 demonstrates that treatment of U373-MG astrocytoma cells with 0.4-100 ng/mL IL-1β significantly ($p<0.01$) modulated expression of ADAMTS-9 mRNA. The average relative fold increase in *Adamts9* expression over control (0 ng/mL) when treated with IL-1β were ~5 (0.2 ng/mL), 14 (0.4 ng/mL), 19 (0.8 ng/mL), 25 (1 ng/mL), 27 (10 ng/mL) and 26 (100 ng/mL). From 0-1 ng/mL of IL-1β treatment, modulation of *Adamts9* expression was concentration-dependent. From 1-100 ng/mL expression of *Adamts9* was not dependent on increasing IL-1β concentration and a 'plateau' phase was reached.

Figure 4.3 also illustrates that ADAMTS-9 mRNA expression was modulated by treatment with TNF in U373-MG. The average relative fold increase in *Adamts9* expression over control when treated with TNF were ~2 (0.2 ng/mL), 5 (0.4 ng/mL), 4 (0.8 ng/mL), 8 (1 ng/mL), 10 (10 ng/mL) and 8 (100 ng/mL). *Adamts9* expression levels were statistically ($p<0.05$) greater than control levels at 1-100 ng/mL. However, treatment of U373-MG with IFN-γ displayed no statistically ($p>0.05$) significant modulation of ADAMTS-9 mRNA expression (Fig. 4.3).

Figure 4.2 Comparison of ADAMTS-9 mRNA Expression Levels in Astrocytic Cells under Basal Conditions
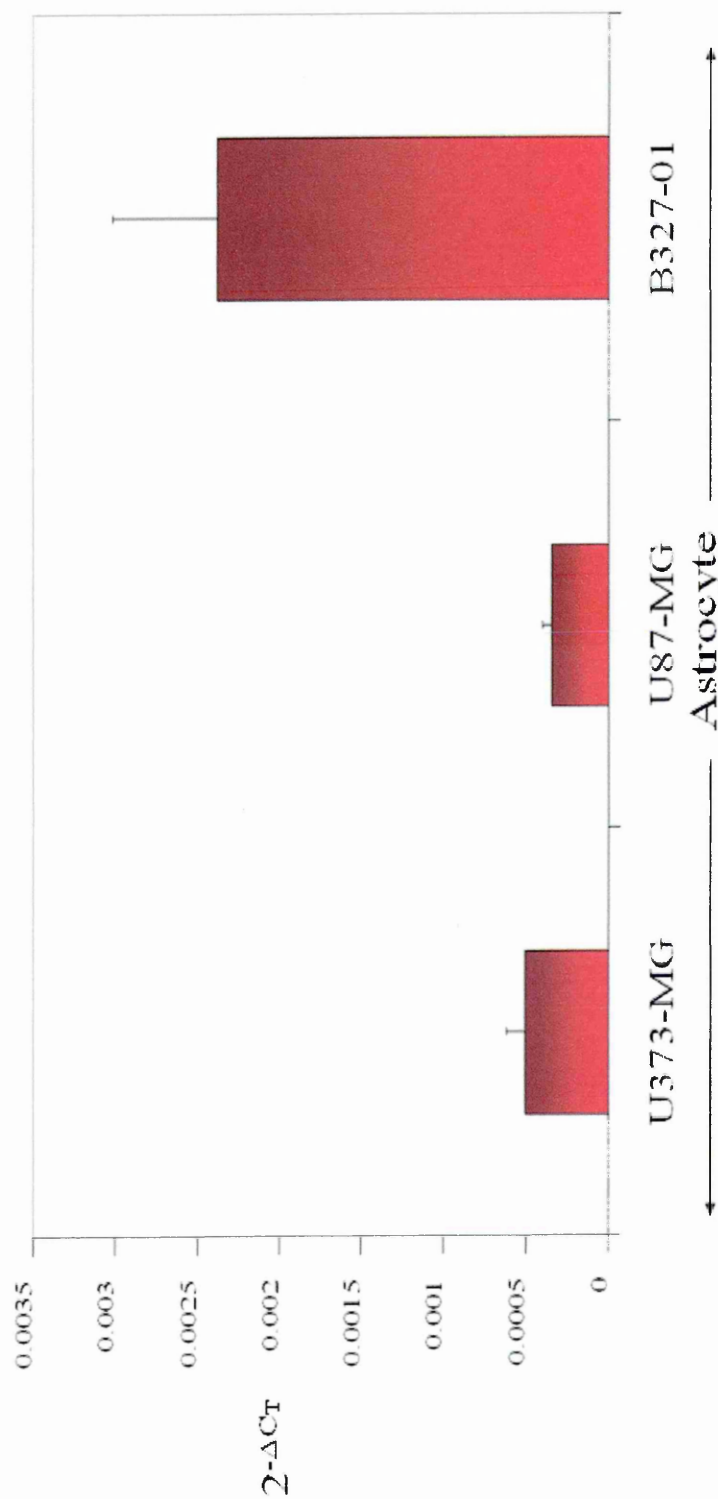
Real-time RT-PCR analysis of ADAMTS-9 mRNA relative expression levels under basal conditions ($2^{-\Delta C_T}$) in astrocytoma cell lines; U373-MG and U87-MG and B327-01 astrocytic cell line. Cells were seeded at a density of 1×10^5 cells/well and left for 24 h to adhere. Cells were incubated for a further 24 h in serum-free medium prior to extraction of RNA with TRI Reagent and cDNA synthesis and real-time RT-PCR. Real-time RT-PCR was performed in duplicate. Results expressed as ±SEM from 3 independent experiments of 48 h culture in 24-well plates.

Real-time RT-PCR analysis of ADAMTS-9 steady-state mRNA expression levels relative to control (0 ng/mL) ($2^{-\Delta\Delta C_T}$) following treatment with cytokines. Cells were seeded at a density of 1×10^5 cells/well and were left for 24 h to adhere prior to treatment with cytokine (1 mL/well in triplicate) in serum-free medium (for 24 h). RNA was extracted from cells with TRI Reagent (330 µL/well) prior to pooling (1 mL/treatment) of triplicate wells. Real-time RT-PCR was performed following cDNA synthesis. Real-time RT-PCR was performed in duplicate normalised to GAPDH housekeeping gene expression. Results expressed as ± SEM, n = 3 independent experiments. Statistically significant differences between control sample (expression expressed as 1) and treated represented by ** = p<0.01, * = p<0.05 (single-factor ANOVA, followed by Dunnett's test).

126

Figure 4.3 Effect of Pro-Inflammatory Cytokines on ADAMTS-9 mRNA Expression in U373-MG Astrocytoma Cell Line
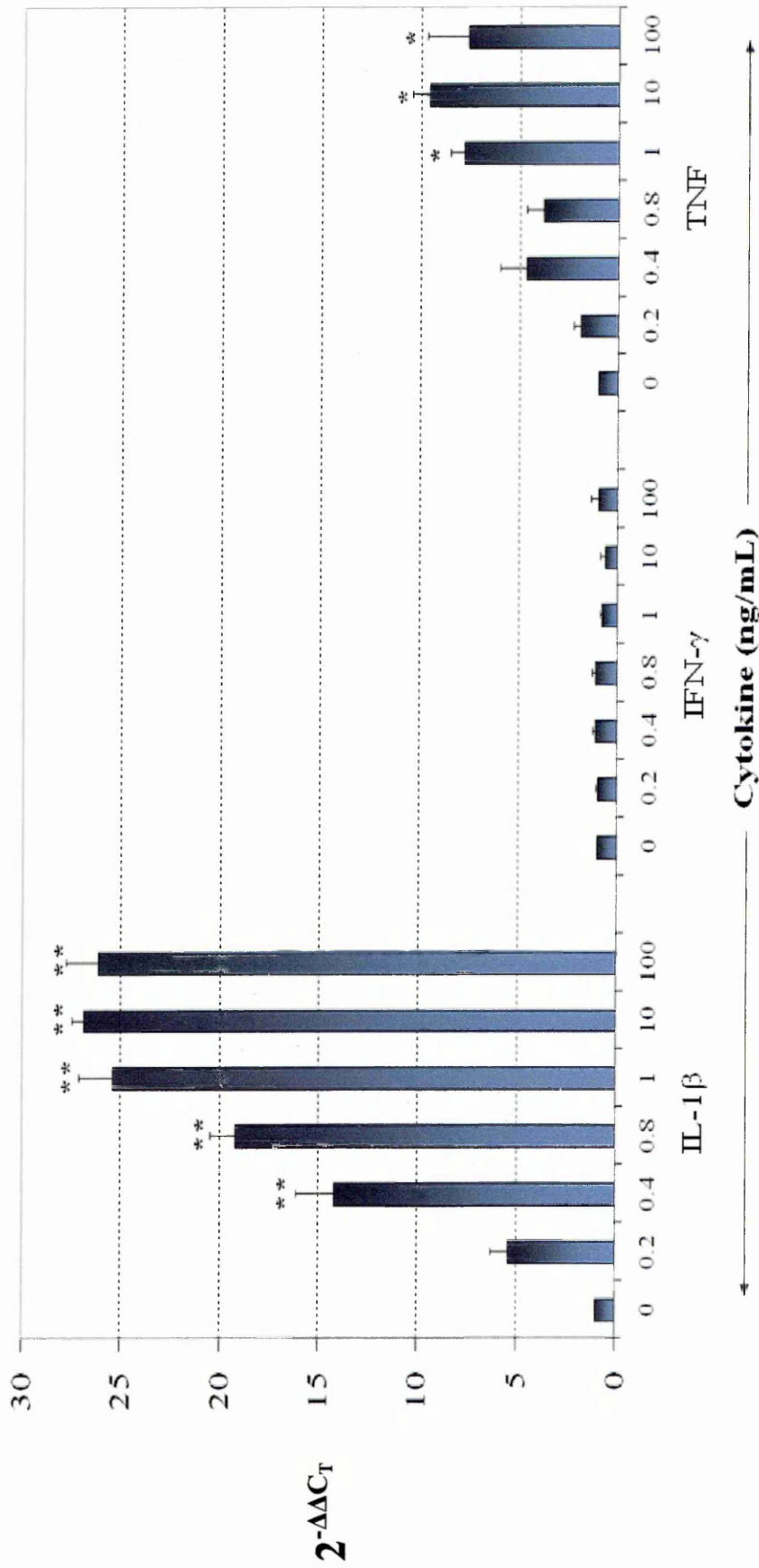
Treatment of U87-MG astrocytoma cell line with IL-1β, IFN-γ and TNF had no statistically (p>0.05) significant effect on ADAMTS-9 mRNA expression levels as detected by real-time RT-PCR. Cells were unresponsive to all concentrations tested (not shown). Culturing of cells, treatment of cells, RNA extraction, cDNA synthesis and real-time RT-PCR experimental procedures were identical to those adopted for the U373-MG cells.

B327-01 Astrocytes

Treatment of B327-01 astrocytes with IL-1β initiated a statistically (p<0.05) significant increase of ADAMTS-9 mRNA expression at 100 ng/mL as shown in Figure 4.4. The average relative fold increases of *Adamts9* expression over control when treated with IL-1β were ~5 (1 ng/mL), 5 (10 ng/mL) and 6 (100 ng/mL). In addition, Figure 4.4 demonstrates that IFN-γ caused a statistically (p<0.01) significant decrease in *Adamts9* expression. The average relative fold decrease in *Adamts9* expression over control when treated with IFN-γ were ~0.3 (1 ng/mL), 0.4 (10 ng/mL) and 0.3 (100 ng/mL). No statistically (p>0.05) significant effects on *Adamts9* expression levels were observed with TNF treatment in B327-01 astrocytes.

4.2.2.4 Cellular Localisation of ADAMTS-9 Protein

Intense nuclear staining of U373-MG cells with the ADAMTS-9L2 antibody is shown in Figure 4.5A. Figure 4.5B further confirmed nuclear staining by co-staining with DAPI. Figure 4.5D depicts intense-staining of ADAMTS-9 contained within the nucleus in small spherical organelles. Furthermore punctate, intense ADAMTS-9 expression was detected in the cytoplasm (potentially in the secretory pathway) (Fig. 4.5D). ADAMTS-9 was not detected in the ECM. ICC without the incubation of the primary antibody displayed no staining (Fig. 4.5C). Therefore, these data indicate that ADAMTS-9 is expressed in the nucleus and cytoplasm of U373-MG cells.

Real-time RT-PCR analysis of steady-state ADAMTS-9 mRNA expression levels relative to control (0 ng/mL) ($2^{-\Delta\Delta C_T}$) following treatment with cytokines. Cells were seeded at a density of 1×10^5 cells/well and were left for 24 h to adhere prior to treatment with cytokine (1 mL/well in triplicate) in serum-free medium (for 24 h). RNA was extracted from cells with TRI Reagent (330 µL/well) prior to pooling (1 mL/treatment) of triplicate wells. Real-time RT-PCR was performed following cDNA synthesis. Real-time RT-PCR was performed in duplicate normalised to YWHAZ housekeeping gene expression. Results expressed as $\pm$ SEM, n = 3 independent experiments. Statistically significant differences between control sample (expression expressed as 1) and treated represented by ** = p<0.01, * = p<0.05 (single-factor ANOVA, followed by Dunnett's test).

Figure 4.4 Effect of Pro-Inflammatory Cytokines on ADAMTS-9 mRNA Expression in B327-01 Human Astrocytic Cell Line
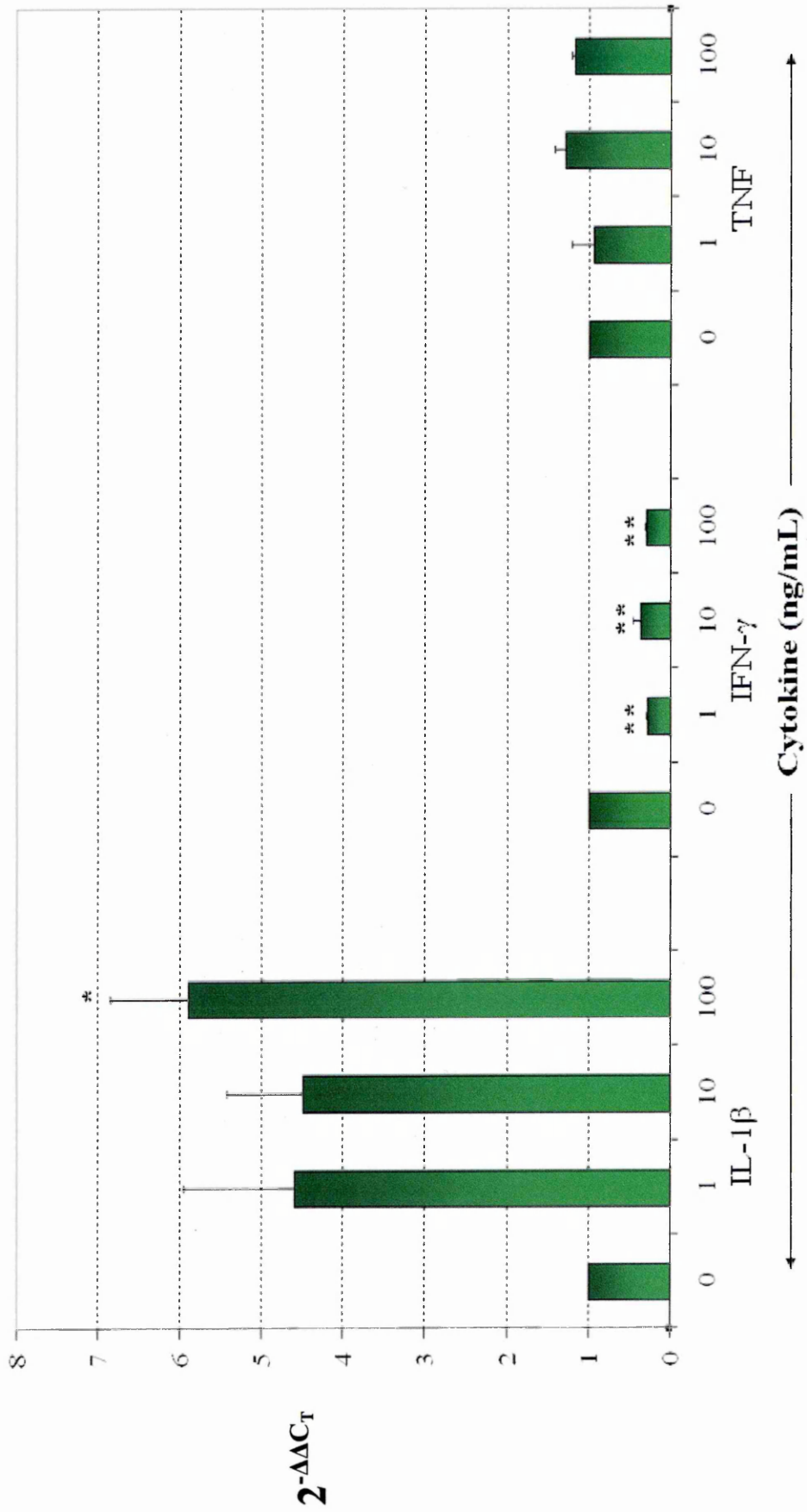
ICC staining of U373-MG astrocytoma cells with the ADAMTS-9L2 antibody visualised by (A and B) fluorescent microscopy (x200) and (D) confocal microscopy (x400). U373-MG cells were seeded in chamber slides at a density of 5×10^4 cells/500 µL media/well and left for 24 h to adhere. Medium was discarded and cells were fixed in 4% PFA prior to blocking, ADAMTS-9L2 antibody incubation (18 h at 4°C) and detection with the Alexa Fluor 488-conjugated goat anti-rabbit IgG (H+L) secondary antibody. Cells were not treated with any stimulus. Image B shows ADAMTS-9 and DAPI colocalisation. Image C is ICC with no primary antibody incubation (replaced by PBS) overlaid on image obtained with DAPI staining (serves as a control for non-specific binding of the secondary antibody) (fluorescent microscope x200). Arrows highlight intense nuclear organelle expression of ADAMTS-9. Arrowheads depict detection of punctate ADAMTS-9 expression in the cytoplasm. Due to having a finite quantity of ADAMTS-9L2 antibody, the repetition of this experiment was not possible.

Figure 4.5 Localisation of ADAMTS-9 in U373-MG Astrocytoma Cell Line

132
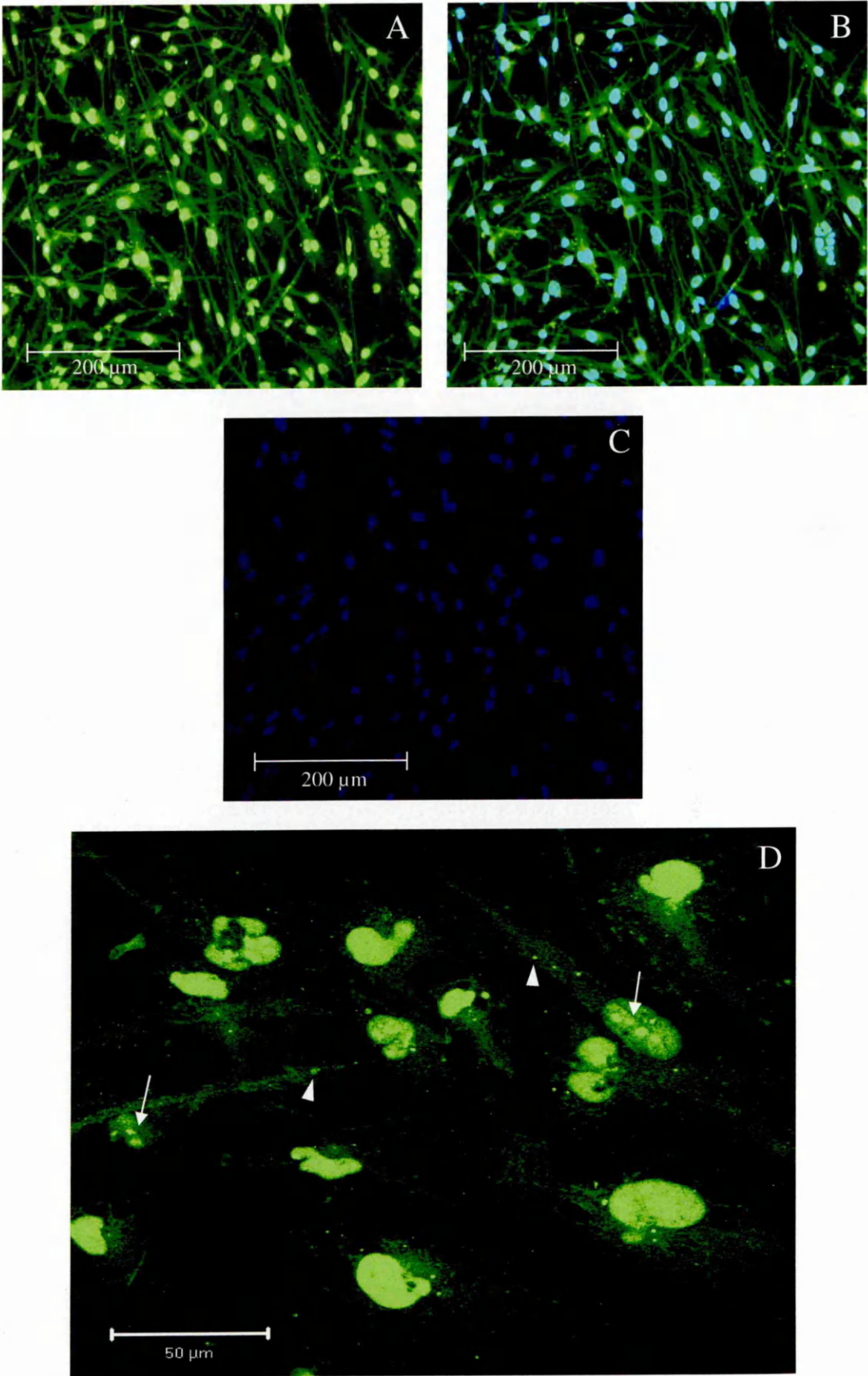
4.3 ADAMTS-9 in the CHME3 Microglial Cell Line

4.3.1 Overview of Approach

Activation of microglia is a key event in many CNS inflammatory disorders resulting in the release of pro-inflammatory mediators. Such activation is likely to be triggered in some capacity by pro-inflammatory cytokines because microglial cells express IL-1RI, IL-1RII (Lee *et al*, 2002), TNFRI, TNFRII and IFN-γR (Kim & de Vellis, 2005). Therefore, the effect of cytokines on *Adamts9* expression was analysed in a human foetal microglial cell line (CHME3) by real-time RT-PCR.

4.3.2 Results

4.3.2.1 Effect of Pro-Inflammatory Cytokines on *Adamts9* Expression Levels in CHME3 Microglial Cell Line

Figure 4.6 shows a statistically significant ($p < 0.05$) modulation of ADAMTS-9 mRNA expression in the CHME3 microglial cell line with 10-100 ng/mL IFN-γ. The average relative fold increases of *Adamts9* expression over control when treated with IFN-γ were ~1 (1 ng/mL), 2 (10 ng/mL) and 3 (100 ng/mL). From 1-100 ng/mL of IFN-γ treatment, modulation of *Adamts9* expression was concentration-dependent. Treatment of CHME3 with IL-1β and TNF had no statistically ($p > 0.05$) significant effect on ADAMTS-9 mRNA expression levels (Fig. 4.6).

4.4 ADAMTS-9 in the SHSY-5Y Neuroblastoma Cell Line

4.4.1 Overview of Approach

Neurones contribute to proteolysis in the brain by expressing MMPs (Liu *et al*, 2007). There is evidence that neurones require remodelling of glial scars to promote axonal outgrowth, a process which ADAMTSs have the potential to mediate by breakdown of CSPGs. ADAMTS-1 has been reported to be expressed in N1E-115; a mouse neuroblastoma cell line (Sasaki *et al*, 2001). However, a comprehensive investigation into whether human neurones express ADAMTSs with proteoglycanase activity has not

Real-time RT-PCR analysis of ADAMTS-9 mRNA expression relative to control (0 ng/mL) ($2^{-\Delta\Delta C_T}$) following treatment with cytokines. Cells were seeded at a density of 1×10^5 cells/well and were left for 24 h to adhere prior to treatment with cytokine (1 mL/well in triplicate) in serum-free medium (for 24 h). RNA was extracted from cells with TRI Reagent (330 µL/well) prior to pooling (1 mL/treatment) of triplicate wells. Real-time RT-PCR was performed following cDNA synthesis. Real-time RT-PCR was performed in duplicate and normalised to GAPDH housekeeping gene expression. Results expressed as ± SEM, n = 3 independent experiments. Statistically significant differences between control sample (expression expressed as 1) and treated represented by: * = p<0.05 (single-factor ANOVA, followed by Dunnett's test).

134

Figure 4.6 Effect of Treatment with Pro-Inflammatory Cytokines on ADAMTS-9 mRNA Expression in CHME3 Microglial Cell Line
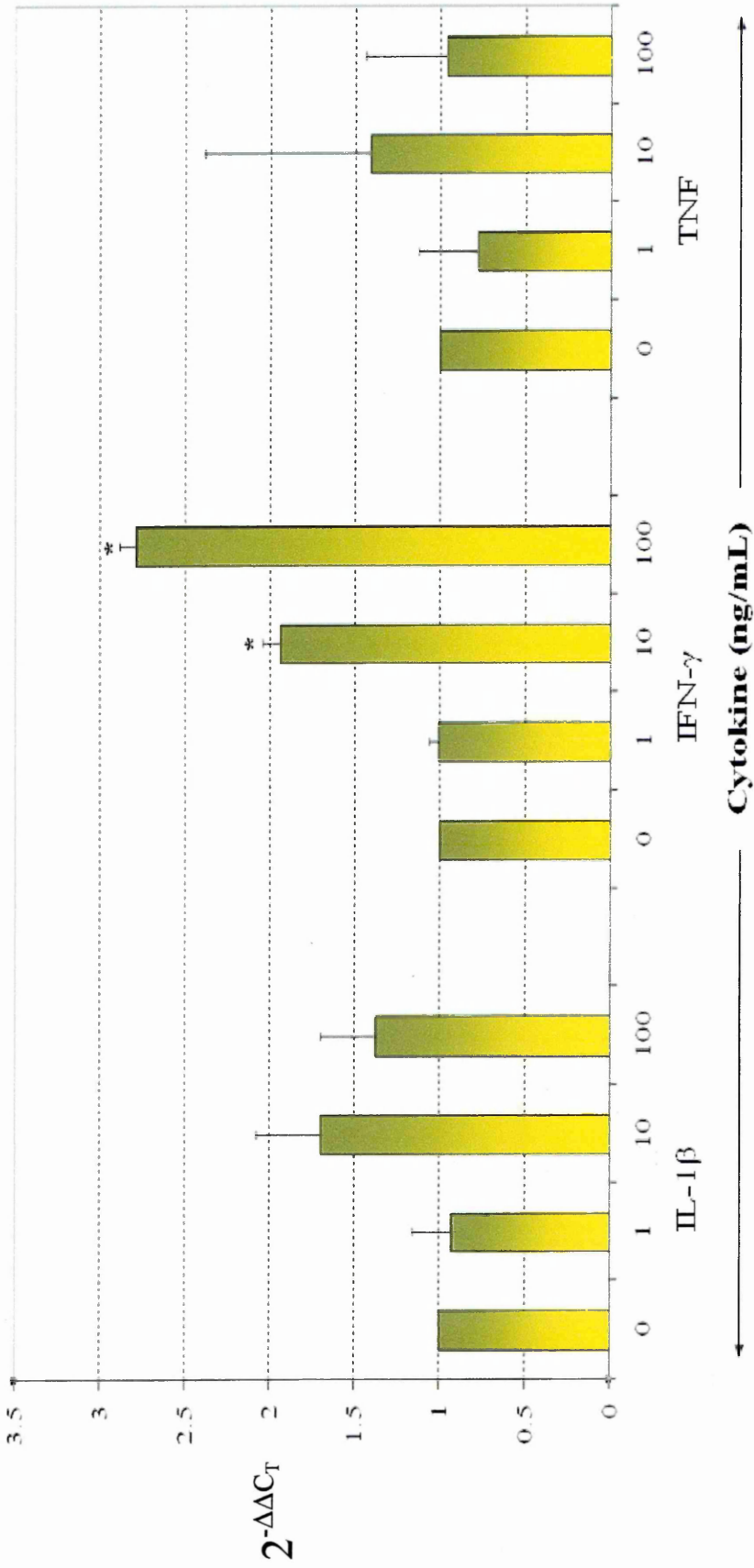
been reported. Our laboratory has previously shown that U373-MG, U87-MG, B327-01 and CHME3 microglial cells express ADAMTS-1, -4 and -5 (Cross *et al*, 2006; Haddock *et al*, 2003), however it is unknown whether SHSY-5Y neuroblastoma cells express these proteoglycanases. ADAMTS-9 has also not been studied in neuronal cells, therefore, an analysis of ADAMTS-1, -4, -5 and -9 mRNA expression levels in SHSY-5Y cells was conducted by real-time RT-PCR.

Generally, the intracellular signalling that occurs in neurones results in transcription of genes encoding for protective factors promoting growth and regeneration. The NTFs have been extensively implicated in triggering such signalling by binding to NTF-receptors on neurones (Allen & Dawbarn, 2006). Many of the genes up-regulated by RetA during differentiation of neurones are those that encode for NTF receptors (Clagett-Dame *et al*, 2005). NGF is an NTF, heavily implicated in promoting axonal outgrowth of neurones by binding to NTF receptors (Connor & Dragunow, 1998; Williams *et al*, 2006; Allen & Dawbarn, 2006). Therefore, the effects of NGF on *Adamts9*, expression in SHSY-5Y cells (differentiated or undifferentiated with RetA) was analysed. Also, the direct effect of RetA treatment on ADAMTS-9 mRNA expression levels was investigated under basal conditions by comparison with undifferentiated SHSY-5Y cells using real-time RT-PCR.

The effect of cytokines on neurones has not been as extensively studied as NTFs, largely due to the fact that glial cells have been shown to be the main responders to such mediators. However, neurones do express cytokine receptors, e.g. TGF-βRII is expressed predominantly in neuronal cells and decreased levels of the receptor correlated with increased neurodegeneration in AD (Tesseur *et al*, 2006). Neurones are the target of many destructive inflammatory pathways initiated in acute and chronic brain disorders. However, they also have the potential to contribute to such processes by intercellular interactions with other cell-types. To further characterise the expression of ADAMTS-9 in the brain, an analysis of mRNA expression by real-time RT-PCR was conducted in SHSY-5Y following treatment with a cohort of pro- and anti-inflammatory cytokines.

4.4.2 Results

4.4.2.1 Comparison of Aggrecanase ADAMTS mRNA Expression in SHSY-5Y Cells under Basal Conditions

Real-time RT-PCR analysis demonstrated that the SHSY-5Y cell line expressed ADAMTS-4, -5 and -9 but not ADAMTS-1 under basal conditions. Average relative expression of *Adamts9* ($2^{-\Delta C_T}$ = 0.05) was ~28-times greater than *Adamts4* (0.002) and 150 times greater than *Adamts5* (0.0003) (Fig. 4.7).

4.4.2.2 Effect of RetA Differentiation of SHSY-5Y Cells on Morphology and ADAMTS-9 mRNA Expression Levels

Culturing of SHSY-5Y in the presence of 10^{-5} M RetA impacted on the morphology of the cells. Microscopic analysis of RetA-treated cells (Fig 4.8ii) appeared to have differentiated when compared to untreated (Fig. 4.8Ai). RetA-treated cells had branched neurite outgrowths and had an elongated morphology when compared to untreated cells, indicating that they were more differentiated (Clagett-Dame *et al*, 2005). Furthermore, there was a marked decrease in proliferation of the differentiated cells, which remained at the same confluency without the requirement for passaging following seven days of RetA treatment (as described previously by Encinas *et al*, 2000). In contrast, undifferentiated cells displayed a high rate of proliferation and required passaging regularly.

Figure 4.8B demonstrates that culturing SHSY-5Y cells in the presence of RetA triggered a statistically ($p<0.05$) significant increase in *Adamts9* expression when compared to omitting RetA from the culture medium as detected by real-time RT-PCR. Expression of *Adamts9* in RetA-treated cells ($2^{-\Delta C_T}$ = ~0.7) was ~2-fold higher than in untreated cells ($2^{-\Delta C_T}$ = ~0.4).

4.4.2.3 Effects of Treatment of SHSY-5Y Cells with Cytokines and Growth Factors on *Adamts9* Expression

No statistically ($p>0.05$) significant effects on ADAMTS-9 mRNA expression were observed in SHSY-5Y cells (cultured +RetA and –RetA) following 0-100 ng/mL of

Figure 4.7 Comparison of Aggrecanase ADAMTS mRNA Expression in Neuroblastoma SHSY-5Y Cell Line
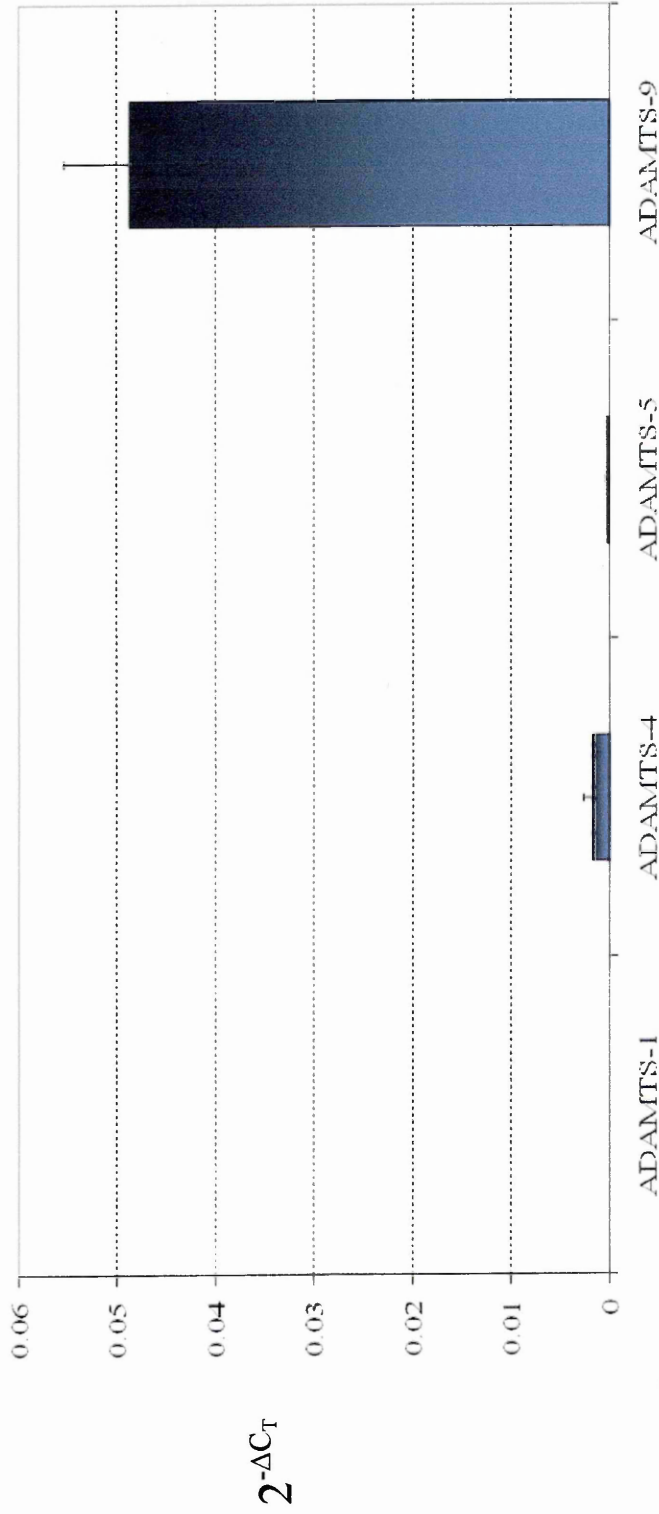
Real-time RT-PCR analysis of ADAMTS-1, -4, -5 and -9 relative steady-state mRNA expression levels ($2^{-\Delta C_T}$) in SHSY-5Y cells under basal conditions (untreated with stimulus). Cells were cultured for 7 days in the presence of 10^{-5} M RetA in T-75 flasks prior to the extraction of RNA from cells with TRI Reagent. Real-time RT-PCR was performed following cDNA synthesis. Real-time RT-PCR was performed in duplicate, normalised to GAPDH housekeeping gene expression. Results expressed as ± SEM from 2 independent experiments.

Figure 4.8 Effect of RetA-Treatment on SHSY-5Y Neuroblastoma Cell Morphology and ADAMTS-9 mRNA Expression Levels
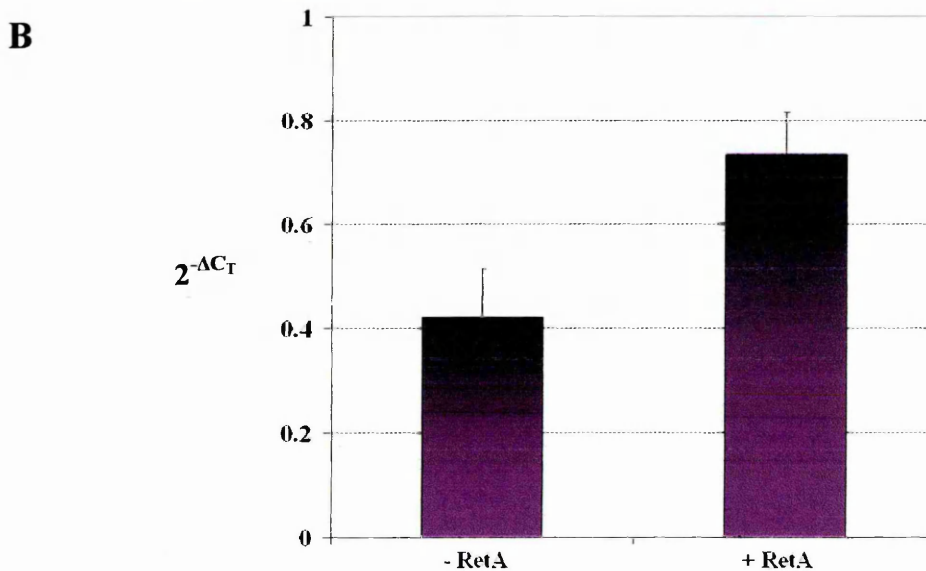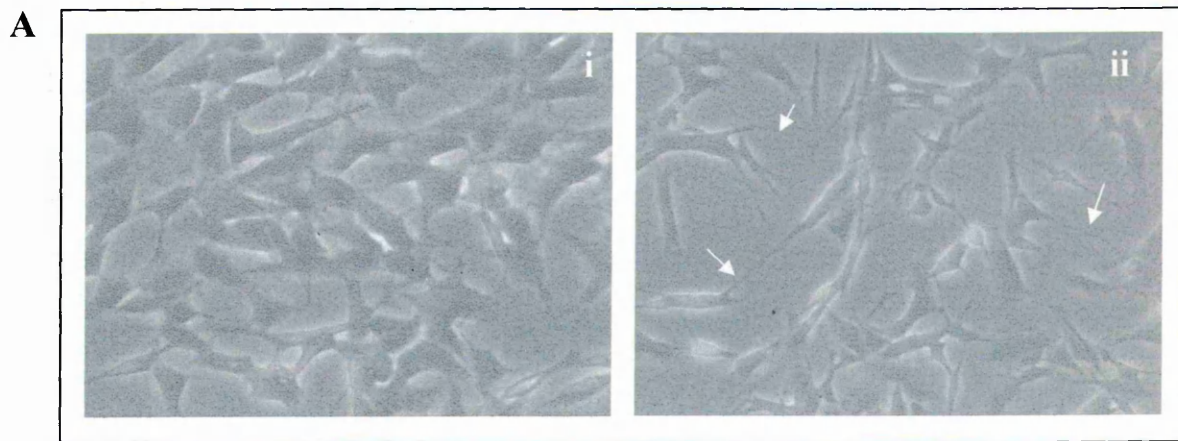
A: Equal numbers of SHSY-5Y cells were cultured in a T-75 flask with (Aii) or without (Ai) 10^{-5} M RetA for 7 days prior to capturing of images (note treated cells have decreased proliferation compared to untreated). Arrows indicate neurite outgrowth processes. Images captured on a light microscope (Leica) (x200). B: Real-time RT-PCR analysis of the effect of RetA on relative steady-state *Adamts9* expression levels ($2^{-\Delta C_T}$) in SHSY-5Y cells. Cells were cultured for 7 days with or without 10^{-5} M RetA prior to seeding cells at a density of 1×10^5 cells/well into chamber slides (with or without 10^{-5} M RetA) where they were left for 48 h (1st 24 h with serum-rich medium, 2nd 24 h in serum-free medium) prior to extraction of RNA with TRI Reagent and cDNA synthesis. Real-time RT-PCR was performed in duplicate normalised to YWHAZ housekeeping gene expression. Results expressed as ± SEM from 21 independent experiments. Statistically significant difference of *Adamts9* expression between -RetA and +RetA cells expressed as * = p<0.05 (unpaired, 2-tailed T-test).

treatment with IL-1β, IFN-γ, TNF, TGF-β1 and NGF (not shown). Also, the treatment of SHSY-5Y cells (cultured +RetA and –RetA) with both TNF and IL-1β combined did not display a synergistic effect to increase or decrease *Adamts9* expression to a statistically (p>0.05) significant level (not shown). Cells were cultured for seven days with or without 10^{-5} M RetA prior to seeding cells at a density of $1x10^5$ cells/well into chamber slides ($+10^{-5}$ M RetA or -RetA) where they were left to adhere for 24 h in serum-rich medium prior to treatment of factors for 24 h in serum-free medium. RNA was extracted with TRI Reagent and cDNA synthesised prior to performing real-time RT-PCR in duplicate normalised to YWHAZ housekeeping gene expression. Experiments were repeated independently three times.

4.5 Discussion

The study presented in this chapter is the first reported comprehensive analysis of ADAMTS-9 expression and modulation in brain-derived cells *in vitro*. ADAMTS-9 mRNA was expressed by all the cells that were cultured in the study by detection with specific real-time RT-PCR primers. Furthermore, the treatment of cell cultures with various factors showed differential modulation of *Adamts9* expression as summarised in Table 4.1.

4.5.1 Astrocyte Characterisation Discussion

The characterisation of the B327-01 and U373-MG cells demonstrated they were of astrocytic origin. The B327-01 astrocytes were not derived from a glioma and were extracted and isolated from an epilepsy patient without further modifications. However, the cells have been frozen and passaged (upto passage 6) and therefore are classified as a 'cell line'. The problems encountered in attempting to achieve characteristic GFAP ICC staining of these astrocytes was likely due to the fact that the cells have become more differentiated since the extraction process. However, the strong S100β staining and GFAP western blot confirms the B327-01 cells are a viable astrocytic cell population. The conclusions of the astrocytic characterisation would perhaps have been strengthened by performing an IgG negative control ICC, to confirm that staining was not a result of non-specific primary antibody binding. IgG controls were not conducted because of the highly characteristic astrocytic intermediate filamental staining observed with the GFAP and S100β primary antibodies.

Table 4.1 Summary of CNS-Derived Cell Culture *Adamts9* Expression Levels following Treatment with Cytokines and Growth Factors

	IL-1β	IFN-γ	TNF	TNF/IL-1	IL-1/TNF	TGFβ1	NGF
U373-MG	↑	-	↑	NT	NT	NT	NT
U87-MG	-	-	-	NT	NT	NT	NT
B327-01	↑	↓	-	NT	NT	NT	NT
CHME3	-	↑	-	NT	NT	NT	NT
SHSY-5Y (+ RetA)	-	-	-	-	-	-	-
SHSY-5Y (- RetA)	-	-	-	-	-	-	-

The table demonstrates which factors modulated a significant statistical change in *Adamts9* expression in CNS-derived cells following treatment with 0-100 ng/mL. TNF/IL-1β, IL-1β/TNF represents dual treatments with both cytokines. A significant increase in *Adamts9* expression is represented by; '↑', a significant decrease in *Adamts9* is represented by; '↓' and no significant change in *Adamts9* expression is represented by; '-'. Note the statistically significant increase of *Adamts9* expression following direct treatment with RetA on SHSY-5Y cells is not depicted in this table. NT = not tested.

4.5.2 Discussion of the Effects of Factors on ADAMTS-9 mRNA Expression in CNS-Derived Cells

The cloning of an isoform of ADAMTS-9 from an astrocyte cDNA library previously demonstrated that the peptidase was expressed by such cells in the rat (Clark *et al*, 2000). These data in this study demonstrate that ADAMTS-9 was also expressed by human astrocytes because the mRNA was detected in three different astrocytic cultures with higher levels present in B327-01 cells. Real-time RT-PCR also confirmed that ADAMTS-9 mRNA was expressed by CHME3 microglia and SHSY-5Y neuroblastoma cells under basal conditions. Overall, these data suggest that glial cells and neurones in the human CNS have the potential to constitutively express ADAMTS-9 *in vivo*. Under basal conditions, ADAMTS-9 is the dominant ADAMTS proteoglycanase mRNA expressed by SHSY-5Y neuroblastoma cells, whereas it was demonstrated that SHSY-5Y cells do not express *Adamts1*. This finding is in contrast to that obtained in another neuroblastoma cell line (N1E-115), in which ADAMTS-1 expression was detected by Sasaki *et al* (2001). The difference in ADAMTS-1 expression profile between the two neuroblastoma cell lines is likely attributed to the fact that SHSY-5Y cells are of human origin, whereas the N1E-115 cells are derived from mice.

In glial cells the effect of each pro-inflammatory cytokine on *Adamts9* expression levels was variable. This was highlighted by IFN-γ, which had no impact on *Adamts9* expression levels in U373-MG but significantly down-regulated expression in B327-01 astrocytes as well as being the only cytokine to modulate an increase in the CHME3 microglia cell line. In U373-MG, IL-1β and TNF significantly increased *Adamts9* expression over control. IL-1β also significantly up-regulated *Adamts9* in B327-01 astrocytes but TNF had no significant effect on these cells. In support of these findings, modulation of *Adamts9* expression by IL-1β and TNF has been reported previously by Demircan *et al* (2005) in chondrocytes and by TNF in an RPE-derived cell line by Bevitt *et al*, 2003. *Adamts1* has also been shown to be up-regulated by IL-1β in rat chondrocytes (Gouze *et al*, 2006) and in a mouse colon adenocarcinoma cell line (Kuno *et al*, 1997).

Data generated by our group previously in the same glial cell cultures suggests to a certain extent that ADAMTS-9 modulation is comparable to that of other ADAMTS aggrecanases in the CNS. IL-1β had a similar effect on *Adamts1* in U373-MG and

142

B327-01 as it did on *Adamts9* by triggering an up-regulation of expression. In CHME3, IL-1β had the same effect on ADAMTS-1, -4 or -5 mRNA expression as it did on ADAMTS-9 in that no modulation was detected. Furthermore, TNF modulated an increase in ADAMTS-1, -4 and -5 mRNA in U373-MG in a similar fashion to ADAMTS-9. In contrast to data obtained with ADAMTS-9, TNF also modulated transcription of *Adamts1* and *Adamts4* in CHME3 and B327-01 astrocytes (Cross *et al*, 2006).

Expression of *Adamts9* was not altered by treatment with any cytokines in the U87-MG cell line. This result adds to previous data from our laboratory with IL-1β and TNF, in that neither cytokines influenced ADAMTS-1, -4 or -5 mRNA expression levels in this cell line (Haddock *et al*, 2003). In contrast, TGF-β1 was shown in the same study to significantly down-regulate *Adamts1* expression levels in U87-MG. U87-MG cells have responded previously to treatment with IL-1β (Lai *et al*, 2005), IFN-γ (Hotfilder *et al*, 2007) and TNF (Sawada *et al*, 2004) by up-regulating expression of other factors suggesting that the necessary cytokine receptors are expressed.

The concentrations of cytokines required to induce a statistically significant modulation of *Adamts9* expression in glial cells were: 1 ng/mL (both IL-1β and TNF) in U373-MG cells, 100 ng/mL (IL-1β) and 1 ng/mL (IFN-γ) in B327-01 cells and 10 ng/mL (IFN-γ) in CHME3 cells. These concentrations are likely to exceed physiological concentrations (Gouze *et al*, 2006) that are present in the normal brain but exposure to a full repertoire of cytokines during CNS inflammation potentially has a combined effect on the regulation of ADAMTS-9 *in vivo*. Cells were only tested following treatment with cytokines for 24 h in this study, whereas *in vivo*, cytokine exposure is a more persistent phenomenon thus regulation of ADAMTS-9 is potentially more marked. A reason for not seeing modulation of ADAMTS-9 mRNA expression by factors in certain cell lines was perhaps because the incorrect time-point was studied. Unfortunately, due to time constraints, the effect of treating cells with cytokines/GFs at different time-points could not be analysed. It would be important to ascertain whether the regulation of ADAMTS-9 expression is a transient or long-term effect. Therefore, a future direction of the study would be to treat cells for a shorter (6, 12 h) and longer (48 h to a week) period of time.

4.5.3 Potential Implications for Cancer

A potential contributing factor for the varying results between the two astrocytoma cell lines is how advanced the tumours were from which the cells were derived. U373-MG cells were obtained from a grade 3 tumour (poorly differentiated) whereas the U87-MG cells were from a more advanced grade 3/4 tumour (poorly differentiated/undifferentiated). Hence, the U87-MG cells are likely to be less astrocytic than the U373-MG cells, which may explain the lower basal *Adamts9* levels and lack of cytokine-induced modulation of expression in U87-MG. A more detailed study of ADAMTS-9 with such cell lines could perhaps be undertaken from a cancer perspective. Nakada *et al* (2005), showed that U87-MG cells transfected with ADAMTS-5 were more invasive through a gel containing brevican than cells transfected with a control vector. It would be useful to ascertain whether ADAMTS-9-transfected cells displayed similar migratory properties by degrading aggrecan, versican or other ECM components.

Alternatively, there is evidence from studies in oesophageal cancer to suggest that *Adamts9* is potentially a tumour suppressor gene, despite the mechanism for this property being unknown. ADAMTS-9 was shown to be down-regulated in carcinoma cell lines and primary tumours. In addition, *Adamts9* was identified in a tumour suppressive critical region of chromosome 3 (Lo *et al*, 2006). The finding that ADAMTS-9 protein was expressed in the nucleus in this study is perhaps linked to a role in tumour suppression by influencing cell fate such as transcriptional regulation and cellular proliferation/differentiation via breakdown of DNA-binding proteins. However, nuclear expression of ADAMTS-9 protein was surprising because it is has previously been shown to be localised at the cell surface (Koo *et al*, 2007). In support of the ICC data in this study, the shorter (118 kDa) ADAMTS-9 isoform (cloned by Clark *et al*, 2000) was detected in the nucleus of mammary ECs during an extensive proteomics screen (Desrivières *et al*, 2007). In the study, nuclear extraction was performed on a) cells maintained in a proliferative stage, b) competent cells or those differentiated for c) one or d) four days. Following electrophoresis-separation of the extracts, mass spectrometry was performed prior to a BLAST search. ADAMTS-9 was only detected in the nucleus following four days of differentiation of the cultured ECs. A future direction would be to assess how the localisation of ADAMTS-9 protein is influenced by treating cells with factors such as pro-inflammatory cytokines.

ADAMTS-9 protein was also detected in the cytoplasm in this study where punctate staining suggested its location in vesicles, such as those in the secretory pathway. However, the ICC study of ADAMTS-9 in U373-MG cells is subject to conjecture because a) the species of ADAMTS-9 being detected is unknown because a number of bands were observed with the ADAMTS-9L2 antibody as shown by western blotting in Section 3.5 (a future direction would be to ascertain the identity of these bands by sequencing or mass spectrometry), b) a rabbit IgG negative control was not conducted to ascertain that the antibody is specific and c) the experiment was not repeated due to a having a finite quantity of the antibody. Therefore, the conclusion that ADAMTS-9 is expressed in the nucleus and cytoplasm of U373-MG cells cannot be made with 100% certainty.

4.5.4 Discussion of the Effects of Factors on ADAMTS-9 mRNA Expression in SHSY-5Y Cells

In contrast to the results using glial cells, no modulation of *Adamts9* expression was observed in the SHSY-5Y neuroblastoma cell line with any of the pro- or anti-inflammatory cytokines or TGF-β1 and NGF. TGF-β1 had a different effect on SHSY-5Y than had previously been shown with ECs, where the GF up-regulated ADAMTS-9 mRNA expression (Keating *et al*, 2006). A future direction would be to assess a positive control gene that at least one of these stimuli would have induced to confirm that the cells possess the necessary receptors and intracellular signalling pathways. Detection of IL-8 modulation would be suitable because the mRNA of this chemokine has been shown to be up-regulated in SHSY-5Y cells following treatment with IL-1β (Tixier *et al*, 2005). It was surprising to note that the effects of pro-inflammatory cytokines on *Adamts9* expression were not increased following differentiation with RetA because many pro-inflammatory pathways in the CNS are triggered by the retinoid (Mey, 2005). The lack of a synergistic effect of a combined treatment with IL-1β and TNF was in contrast to the modulation of *Adamts9* expression by both cytokines in chondrosarcoma cells (Demircan *et al*, 2005).

ADAMTS-9 mRNA levels were significantly raised in SHSY-5Y cells treated with RetA when compared to untreated cells. In cartilage explants, East *et al* (2007) detected an increase in ADAMTS-5 mRNA but not ADAMTS-9 in response to RetA treatment. However, explants were only exposed to RetA for a maximum of three days whereas

differentiated SHSY-5Y cells were cultured permanently in the presence of RetA in this study. The implication of ADAMTS-9 mRNA expression being up-regulated by RetA in SHSY-5Y is that it points to a potential role for the proteinase in response to RetA signalling cascades in both the normal brain and pathology. RetA signalling is a key response to nerve injury resulting in regeneration, inflammation modulation and glial cell responses, processes in which ADAMTS-9 could be involved (Mey *et al*, 2005).

The role of RetA in the developing and adult CNS is critical, especially in neurogenesis by promoting neurite outgrowth from which axons and dendrites are formed (Clagett-Dame *et al*, 2005). ADAMTS-9 has been shown to be expressed in foetal brain tissue (Clark *et al*, 2000; Somerville *et al*, 2003; Jungers *et al*, 2005) and reports have implicated the peptidase in having a role in development and embryogenesis (Llamazares *et al*, 2003; Hesselson *et al*, 2004). Consequently, these data suggests that ADAMTS-9 is potentially a gene which is triggered in response to RetA during differentiation and growth of neurones during embryogenesis (as well as in adult tissue).

4.5.5 Limitations of *In Vitro* Cell Culture Study

The study presented in this chapter has a number of limitations including the fact that cells *in vivo* respond to many extracellular factors, which are difficult to recreate *in vitro* such as matrix components, interactions with other cell-types and fluctuations in environment (e.g. blood composition) and the presence of innate and humoral immune factors.

Due to problems with commercial antibody quality and only having finite amounts of the effective ADAMTS-9L2 antibody, analysis of ADAMTS-9 at the protein level was limited to ICC analysis of the cellular localisation in U373-MG. Future work with an effective antibody would involve repeating this work (with an IgG control) as well as analysing ADAMTS-9 protein levels within cell extracts as well as in the culture media (to assess secreted levels) by western blotting. This would prove useful to ascertain whether protein levels correlated with the real-time RT-PCR data presented here. Furthermore, comparative real-time RT-PCR data are only a relative value which allows one to compare expression levels between the samples studied. It is not a reflection of actual copy number (which would require known amounts of RNA standards to calculate) within the cell.

4.5.6 Summary

In summary, these data presented in this chapter provide evidence that a) ADAMTS-9 is expressed at the mRNA level by CNS-derived cells *in vitro* under basal conditions, b) ADAMTS-9 mRNA expression is modulated in glial cells by pro-inflammatory cytokines *in vitro*, c) ADAMTS-9 mRNA expression is up-regulated by RetA in the SHSY-5Y cell line *in vitro* and d) ADAMTS-9 protein potentially has a role within the cell nucleus. Consequently, this work provides preliminary evidence that ADAMTS-9 is involved in normal physiological processes and CNS inflammatory disorders.

Chapter 5

ADAMTS-9 Expression and Modulation in Cerebral Ischaemia

5.1 Background

These data in Chapter 4 indicate that IL-1β was a potent inducer of *Adamts9* expression (especially in astrocytes). IL-1β has been heavily implicated as a mediator of inflammation following cerebral ischaemia to the point that IL-1ra has been successfully tested therapeutically in human stroke clinical trials (Emsley *et al*, 2005). Furthermore, a previous study by our laboratory showed that proteoglycanases ADAMTS-1 and ADAMTS-4 were up-regulated following tMCAo, in the rat (Cross *et al*, 2006). Therefore, a study of ADAMTS-9 in stroke was conducted by utilising the tMCAo rat model of cerebral ischaemia. In addition, a bioinformatical screen of the human ADAMTS-9 potential promoter region was conducted to assess whether it contained the binding site for HIF-1, a transcription factor heavily implicated in stroke.

5.2 ADAMTS-9 Expression in tMCAo Rat Model of Focal Cerebral Ischaemia

5.2.1 Overview of Approach

Many of the characteristics of human stroke i.e. necrosis, infarction, time-delayed responses, reperfusion and recovery can be modelled in animals. MCAo (transient or permanent) in rodents is the most widely used model of stroke with the technique offering many advantages including: a) it does not require craniotomy, b) focal occlusion in the large cerebral artery mimics the most common cause of stroke in humans and c) the technique is well established and routinely performed (Garcia *et al*, 1995). The main limitation of the model is that rodents can have difficulty eating because the technique involves cutting the external carotid artery (ECA) in order to access the MCA with the thread. Following MCAo, cell death has been shown to follow a time-course highly similar to that in humans with infarction occurring early in the striatum prior to delayed infarction in the dorsolateral cortex involving BBB opening (Garcia *et al*, 1995). The early stages are characterised by expression of hypoxia-induced genes whereas in the progressive phase neutrophils are present and many inflammatory mediators can be detected such as TNF and IL-1β (Carmichael, 2005).

Analysing ADAMTS-9 protein (by western blotting) and mRNA (by real-time RT-PCR) levels at 6, 24 and 120 h following reperfusion allows the assessment of whether the peptidase is up-regulated in the early necrotic phase or in the latter inflammatory stage of stroke. It also gives a clue as to whether ADAMTS-9 expression correlates with recovery of neuronal function i.e. when symptoms lessen after a number of days. The ADAMTS-9L2 antibody was utilised for western blotting, unfortunately, due to limited quantities (and a lack of a suitable commercial antibodies), IHC on tMCAo tissue sections could not be performed to analyse protein localisation in this study.

ISH was performed to determine the cellular origin of ADAMTS-9 by comparison with IHC of known cellular markers (e.g. GFAP, NeuN, ED1, vWF) utilising serial sections. Furthermore, *ISH* enabled the assessment of the morphology of the cells expressing *Adamts9*, providing additional evidence as to cell-type. Unfortunately, this technique could not be used to compare changes in the localisation of *Adamts9* expression between tMCAo and sham brains due to variations in tissue quality between samples (i.e. some samples had degraded over time). Also, the technique was not used to quantify expression levels (e.g. by a grading system) because the comprehensive real-time RT-PCR study was a more sensitive and quantitative method.

5.2.2 Results

5.2.2.1 Analysis of ADAMTS-9 mRNA Expression Levels in tMCAo Tissue

6 Hours

At 6 h, ADAMTS-9 mRNA was up-regulated in the ipsilateral hemispheres (IHs) of all five animals subjected to tMCAo when compared to the contralateral hemispheres (CHs) of the same brain (front and back regions combined for each hemisphere) (Fig. 5.1). The relative increases in expression were statistically significant. The means of the relative levels ($2^{-\Delta C_T}$) of ADAMTS-9 mRNA expression for the IHs (front and back combined) of the tMCAo brains were 0.004, 0.049, 0.026, 0.024 and 0.017 compared to the respective CH means of the same brains; 0.002, 0.024, 0.005, 0.010 and 0.008. No statistically significant differences between the IHs and CHs were detected in the brains of the two sham operated animals at 6 h post-procedure as shown in Figure 5.1.

Real-time RT-PCR analysis of relative steady-state ADAMTS-9 mRNA levels ($2^{-\Delta C_T}$) between 4 hemispheres from 7 rat brains subjected to sham operation or tMCAo at 6 h post-procedure. Following surgical procedures, brains were dissected into ipsilateral (occluded in tMCAo) and contralateral hemispheres prior to each hemisphere being cut in half again coronally. RNA was extracted from 5 x 30 µm sections of each quarter of each brain with TRI Reagent prior to cDNA synthesis. Real-time RT-PCR was performed in duplicate and normalised to GAPDH housekeeping gene expression. Results are expressed as mean ± SEM, n = 3 independent experiments. Significant differences between the mean values of the contralateral and ipsilateral hemispheres from each brain (following calculation of mean from front and back regions) are expressed as *** = p<0.001, ** = p<0.01 and * = p<0.05 (2 sample T-test assuming unequal variance). Regions of the same brain are in matching colours.

C = contralateral hemisphere, I = ipsilateral hemisphere, B = back of the brain, F = front of the brain.

Figure 5.1 Relative Levels of ADAMTS-9 mRNA Expression in Rat Brains 6 H Post-tMCAo or Sham-Operation
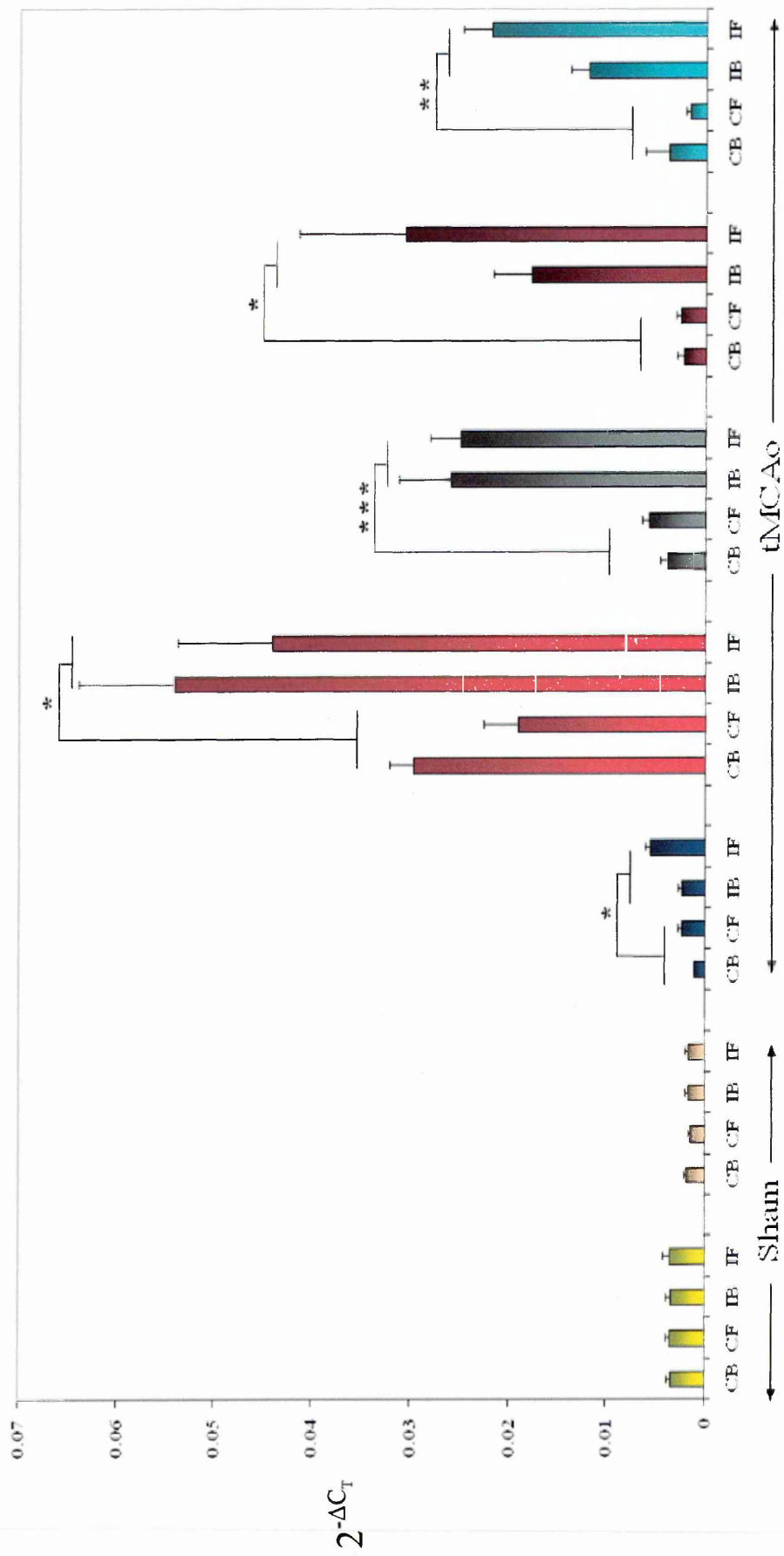
24 Hours

Figure 5.2 shows that in all four rat brains analysed at 24 h post-tMCAo, ADAMTS-9 mRNA expression was up-regulated in the IHs when compared to the CHs of the same brain. The increases were statistically significant. The means of the $2^{-\Delta C_T}$ values of ADAMTS-9 mRNA expression for the IHs of the tMCAo brains were 0.037, 0.034, 0.028 and 0.009 compared to the respective CH means of the same brains; 0.008, 0.007, 0.003 and 0.002. In contrast, no statistically significant differences between the IHs and CHs were detected in any of the brains of the four sham-operated animals at 24 h post-procedure (Fig. 5.2).

120 Hours

At 120 h post-tMCAo, all three brains analysed displayed a statistically significant up-regulation of ADAMTS-9 expression in the IHs when compared to the CHs of the same brain as shown in Figure 5.3. The means of $2^{-\Delta C_T}$ values of ADAMTS-9 mRNA expression for the IHs of the tMCAo brains were 0.013, 0.003 and 0.003 compared to the respective CH means of the same brains; 0.004, 0.001 and 0.001. Similarly to the results at 6 and 24 h post-procedure, no statistically significant differences between the IHs and CHs were observed in sham-operated animals after 120 h (Fig. 5.3).

All Time-Points (Pooled Data)

The pooled data from all the time-points studied (as shown in Figure 5.4) demonstrates that ADAMTS-9 mRNA was up-regulated significantly at 6, 24 and 120 h post-tMCAo. At 6 h, ADAMTS-9 mRNA levels were significantly increased ~3-fold ($p<0.001$) in the IHs ($2^{-\Delta C_T} = 0.024$) of tMCAo brains when compared to the CHs ($2^{-\Delta C_T} = 0.008$) of tMCAo brains. In addition, *Adamts9* expression was significantly ($p<0.001$) up-regulated ~ 9-fold in the IHs of tMCAo brains at 6 h post-operation when compared to the sham-operated ($2^{-\Delta C_T} = 0.003$) animals (all regions pooled) at the same time-point. Also, the CHs of tMCAo brains expressed ~3-fold higher levels (statistical significance = $p<0.01$) of ADAMTS-9 mRNA when compared to sham-operated tissue (IHs and CHs combined) (Fig. 5.4).

Real-time RT-PCR analysis of relative steady-state ADAMTS-9 mRNA levels ($2^{-\Delta C_T}$) between 4 hemispheres from 7 rat brains subjected to sham operation or tMCAo at 24 h post-procedure. Following surgical procedures, brains were dissected into ipsilateral (occluded in tMCAo) and contralateral hemispheres prior to each hemisphere being cut in half again coronally. RNA was extracted from 5 x 30 μm sections of each quarter of each brain with TRI Reagent prior to cDNA synthesis. Real-time RT-PCR was performed in duplicate and normalised to GAPDH housekeeping gene expression. Results are expressed as mean ± SEM, n = 3 independent experiments. Significant differences between the mean values of the contralateral and ipsilateral hemispheres from each brain (following calculation of mean from front and back regions) are expressed as *** = p<0.001 and ** = p<0.01 (2 sample T-test assuming unequal variance). Regions of the same brain are in matching colours. C = contralateral hemisphere, I = ipsilateral hemisphere, B = back of the brain, F = front of the brain.

154

Figure 5.2 Relative Levels of ADAMTS-9 mRNA Expression in Rat Brains 24 H Post-tMCAo or Sham-Operation
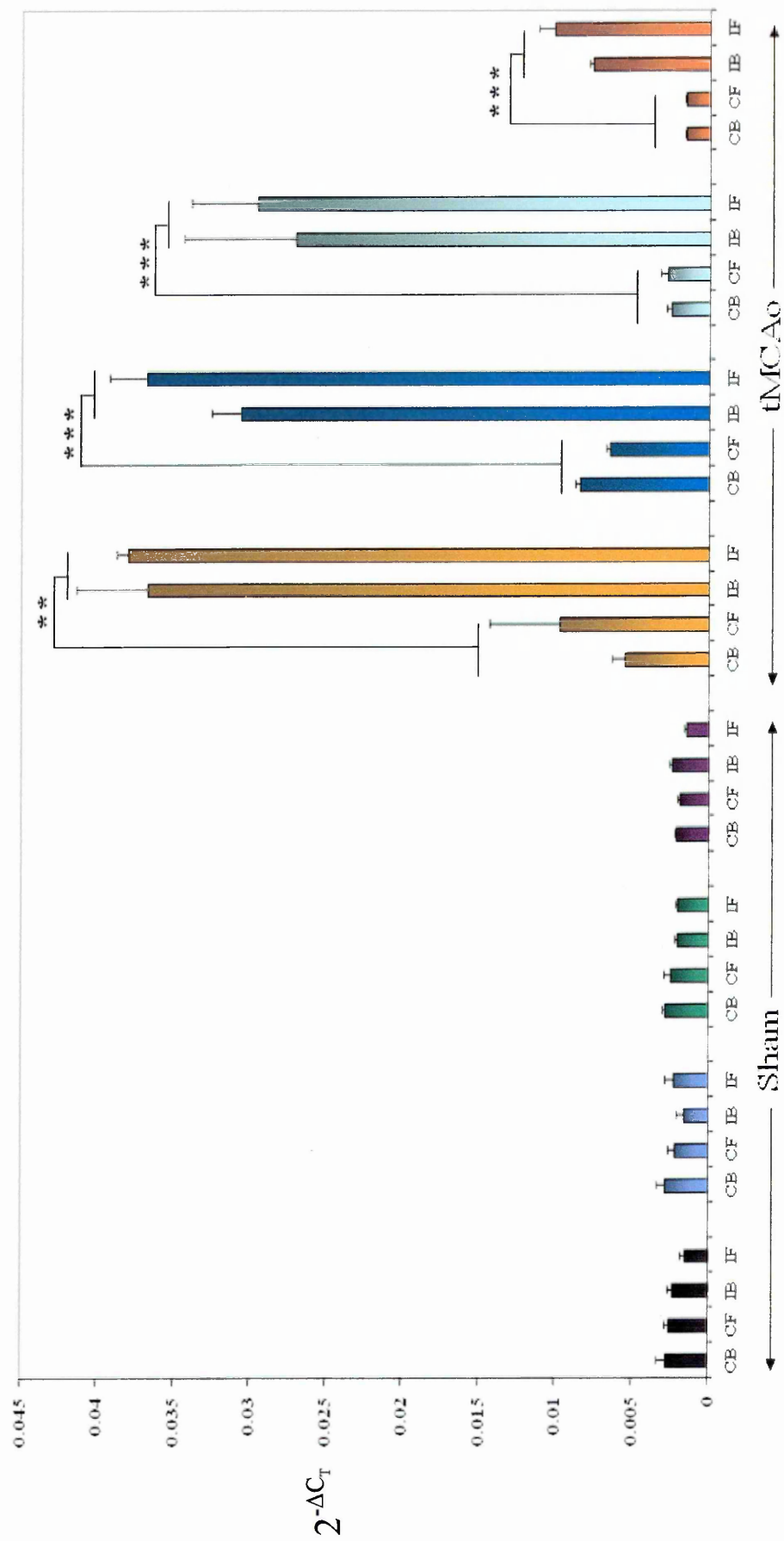
155

Real-time RT-PCR analysis of relative steady-state ADAMTS-9 mRNA levels ($2^{-\Delta C_T}$) between 4 hemispheres from 7 rat brains subjected to sham operation or tMCAo at 120 h post-procedure. Following surgical procedures, brains were dissected into ipsilateral (occluded in tMCAo) and contralateral hemispheres prior to each hemisphere being cut in half again coronally. RNA was extracted from 5 x 30 µm sections of each quarter of each brain with TRI Reagent prior to cDNA synthesis. Real-time RT-PCR was performed in duplicate and normalised to GAPDH housekeeping gene expression. Results are expressed as mean ± SEM, n = 3 independent experiments. Significant differences between the mean values of the contralateral and ipsilateral hemispheres from each brain (following calculation of mean from front and back regions) are expressed as *** = $p < 0.001$ and * = $p < 0.05$ (2 sample T-test assuming unequal variance). Regions of the same brain are in matching colours. C = contralateral hemisphere, I = ipsilateral hemisphere, B = back of the brain, F = front of the brain.

Figure 5.3 Relative Levels of ADAMTS-9 mRNA Expression in Rat Brains 120 H Post-tMCAo or Sham-Operation
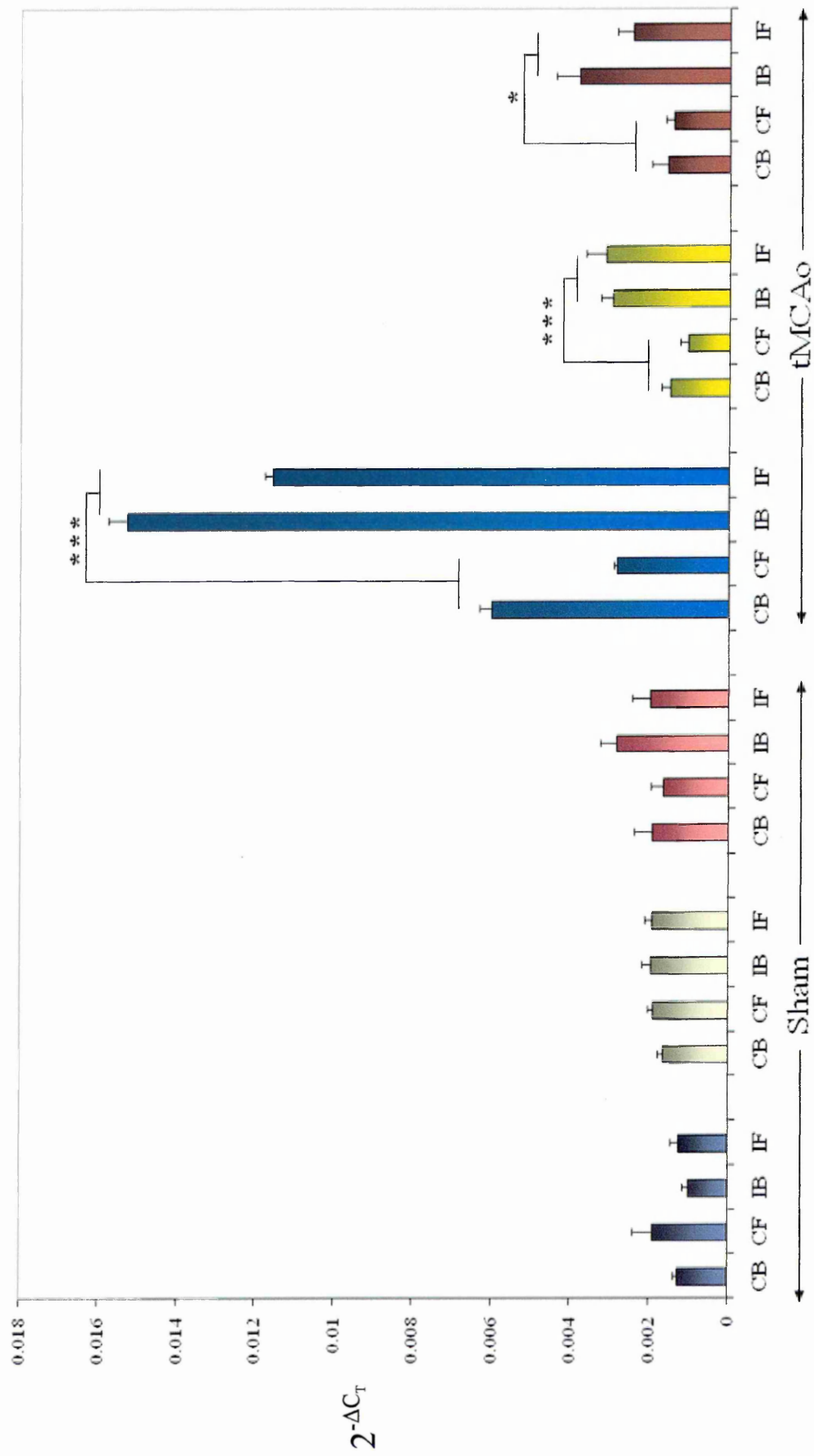
Real-time RT-PCR analysis of steady-state relative ADAMTS-9 mRNA expression levels ($2^{-\Delta C_T}$) at 6, 24 and 120 h post-tMCAo or sham-operation. Following surgical procedures, brains were dissected into ipsilateral (occluded in tMCAo) and contralateral hemispheres prior to each hemisphere being cut in half again coronally. RNA was extracted from 5 x 30 μm sections of each quarter of each brain with TRI Reagent prior to cDNA synthesis. Real-time RT-PCR was performed in duplicate and normalised to GAPDH housekeeping gene expression. The mean $2^{-\Delta C_T}$ values from each region of each brain at all time-points (see Figs 5.1-5.3) were pooled to calculate an overall mean, which is represented in this figure ± SEM, n = 12-32 (depending on number of animals at each time-point). Note: data from the front and back regions for each hemisphere following either tMCAo or sham operation at each time-point were combined and presented as 'C' or 'I'. Significant differences between hemispheres from the same treatment (tMCAo) or tMCAo hemispheres (ipsilateral and contralateral combined) are expressed as *** = p<0.001 and ** = p<0.01 (2 sample T-test assuming unequal variances). C = contralateral, I = ipsilateral hemisphere.

158

Figure 5.4 Relative Levels of ADAMTS-9 mRNA Expression in Rat Brains at all Time-Points following tMCAo or Sham-Operation
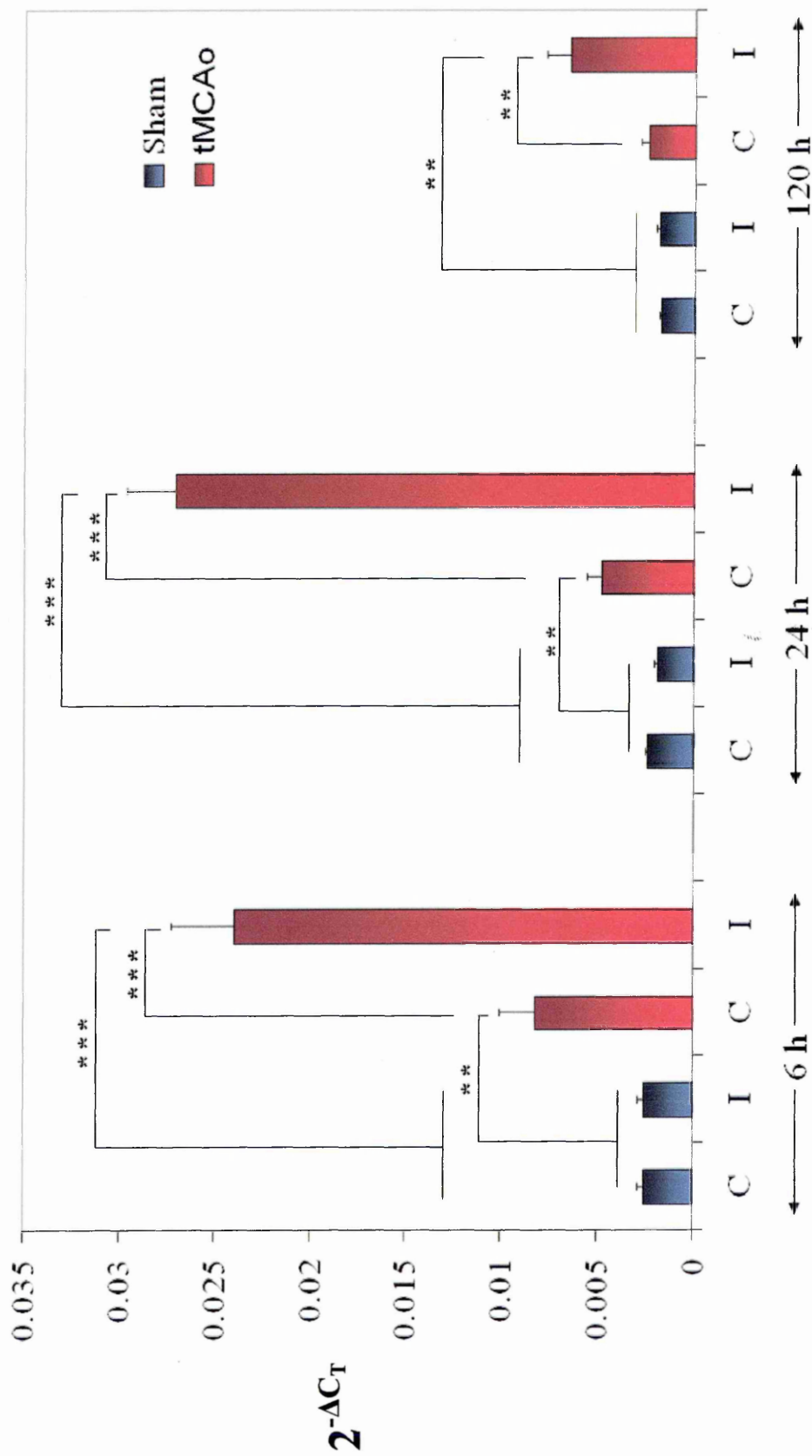
At 24 h, the pooled data shown in Figure 5.4 demonstrates that ADAMTS-9 mRNA expression was significantly raised in the IHs ($2^{-\Delta C_T}$ = 0.027) of tMCAo brains whencompared to the CHs ($2^{-\Delta C_T}$ = 0.005) from tMCAo and sham-operated hemispheres ($2^{-\Delta C_T}$ = 0.002). The statistically significant (p<0.001) difference in expression between both tMCAo hemispheres was ~6-fold whereas a 13-fold increase was observed between IHs of tMCAo brains compared to sham (p<0.001). In addition, the CHs of tMCAo brains expressed ~2-fold higher levels (statistical significance = p<0.01) of ADAMTS-9 mRNA when compared to sham-operated tissue (IHs and CHs combined) at 24 h (Fig. 5.4).

Although mean relative expression levels were lower than those detected after 6 and 24 h, statistically significant increases in ADAMTS-9 mRNA were observed in the IHs of tMCAo when compared to CHs of tMCAo brains and sham-operated brains (both p<0.01) at 120 h as demonstrated in Figure 5.4. The tMCAo IHs (0.007) displayed ~3-times higher ADAMTS-9 mRNA expression than the tMCAo CHs (0.002) and 4-times more than sham brain hemispheres (0.002). In contrast to data at 6 and 24 h, the CHs of tMCAo brains expressed no statistically significant (p>0.05) differences in ADAMTS-9 mRNA levels when compared to sham-operated tissue (IHs and CHs combined) at 120 h (Fig. 5.4).

5.2.2.2 Analysis of ADAMTS-9 Protein Expression Levels in tMCAo Tissue

The representative image in Figure 5.5 of western blotting with anti-β-actin antibody demonstrates that equal protein levels (6 μg) were loaded between samples in the tMCAo study. At 6 h post-tMCAo/sham-operation, five main bands were detected with the ADAMTS-9L2 antibody at ~98, 62, 49, 39 and 35 kDa as shown in Figure 5.6i. Densitometrical analysis demonstrated that the sum of the IODs of all the ADAMTS-9 protein bands detected were lower in CHs of sham brains when compared to IHs of sham brains and tMCAo brains (Fig 5.6ii).

At 24 h post-procedure, a ~188 kDa band was observed in tMCAo samples but not in sham-operated brains as shown by the western blot in the Figure 5.7i. Densitometrical analysis indicated that higher levels of the ~188 kDa protein were present in the CHs of tMCAo brains when compared to the IHs (Fig 5.7ii). Bands at ~80 (faint) and 50 kDa were also observed with slightly higher levels of the former in tMCAo IH samples when

Fig. 5.5 Legend: Western blotting analysis of tMCAo and sham-operated rat brains with anti-β-actin antibody as a protein loading control. Protein was extracted from tissue with TRI Reagent prior to determination of protein concentration by BCA assay. SDS-PAGE (10%) was performed with 6 μg protein/well before transferring separated proteins to nitrocellulose membrane and western blotting. Neg. = western blotting whereby the primary antibody was omitted from the protocol (replaced by TBS), which served as a control for assessment of non-specific binding of the secondary antibody. Image is representative of all western blotting in this study. Note: protein levels were comparable across the samples.

Fig. 5.6 Legend: Western blotting analysis of tMCAo and sham-operated rat brains at 6 h post-procedure with ADAMTS-9L2 antibody (5.6i). Protein was extracted from tissue with TRI Reagent prior to determination of protein concentration by BCA assay. SDS-PAGE (10%) was performed with 6 μg protein/well before transferring separated proteins to nitrocellulose membrane and western blotting. Peptide blocking was performed with the ADAMTS-9L2 'immunising peptide' to assess non-specific binding of the primary antibody (PB). NC (negative control) = western blotting whereby the primary antibody was omitted from the protocol (replaced by TBS), which served as a control for assessment of non-specific binding of the secondary antibody. Densitometry was performed on detected bands using the LabWorks Image Acquisition and Analysis Software to semi-quantify expression levels by measuring the IODs. The sum of the IODs of the three bands (~98, 62, 49, 39 and 35 kDa) detected in each hemisphere for sham and tMCAo brains are presented in graphical form (front and back regions combined) (5.6ii).

Figure 5.5 Protein Loading Control for tMCAo Western Blotting Study
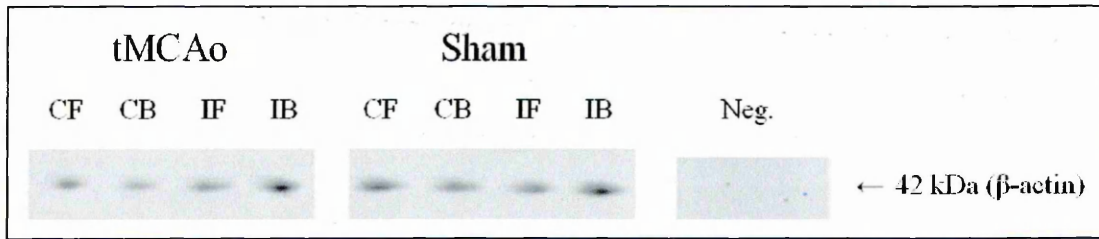
Figure 5.6 Expression of ADAMTS-9 Protein in Rat Brains at 6 H Post-tMCAo or Sham-Operation
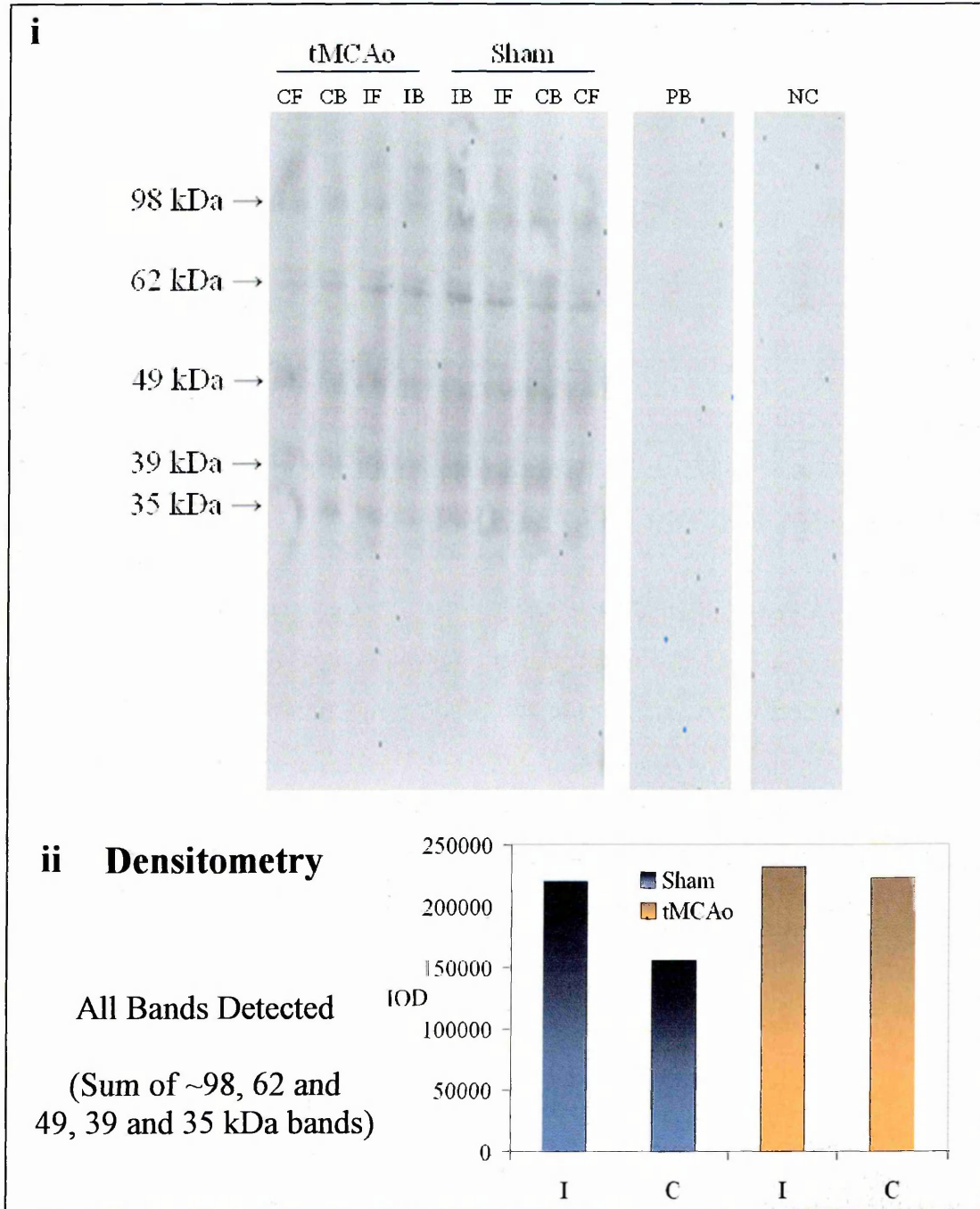
Western blotting analysis of tMCAo and sham-operated rat brains at 24 h post-procedure with ADAMTS-9L2 antibody (5.7i). Protein was extracted from tissue with TRI Reagent prior to determination of protein concentration by BCA assay. SDS-PAGE (10%) was performed with 6 µg protein/well before transferring separated proteins to nitrocellulose membrane and western blotting. Peptide blocking was performed with the ADAMTS-9L2 'immunising peptide' to assess non-specific binding of the primary antibody (PB). NC (negative control) = western blotting whereby the primary antibody was omitted from the protocol (replaced by TBS), which served as a control for assessment of non-specific binding of the secondary antibody. Densitometry was performed on detected bands using the LabWorks Image Acquisition and Analysis Software to semi-quantify expression levels by measuring the IODs. The sum of the IODs of the three bands (~188, 80 and 50 kDa) detected in each hemisphere for sham and tMCAo brains are presented in graphical form (front and back regions combined) as well as the IODs for the individual ~188 and 80 kDa bands (5.7ii).

Figure 5.7 Expression of ADAMTS-9 Protein in Rat Brains at 24 H Post-tMCAo or Sham-Operation

ii **Densitometry**

~188 kDa Band

~80 kDa Band
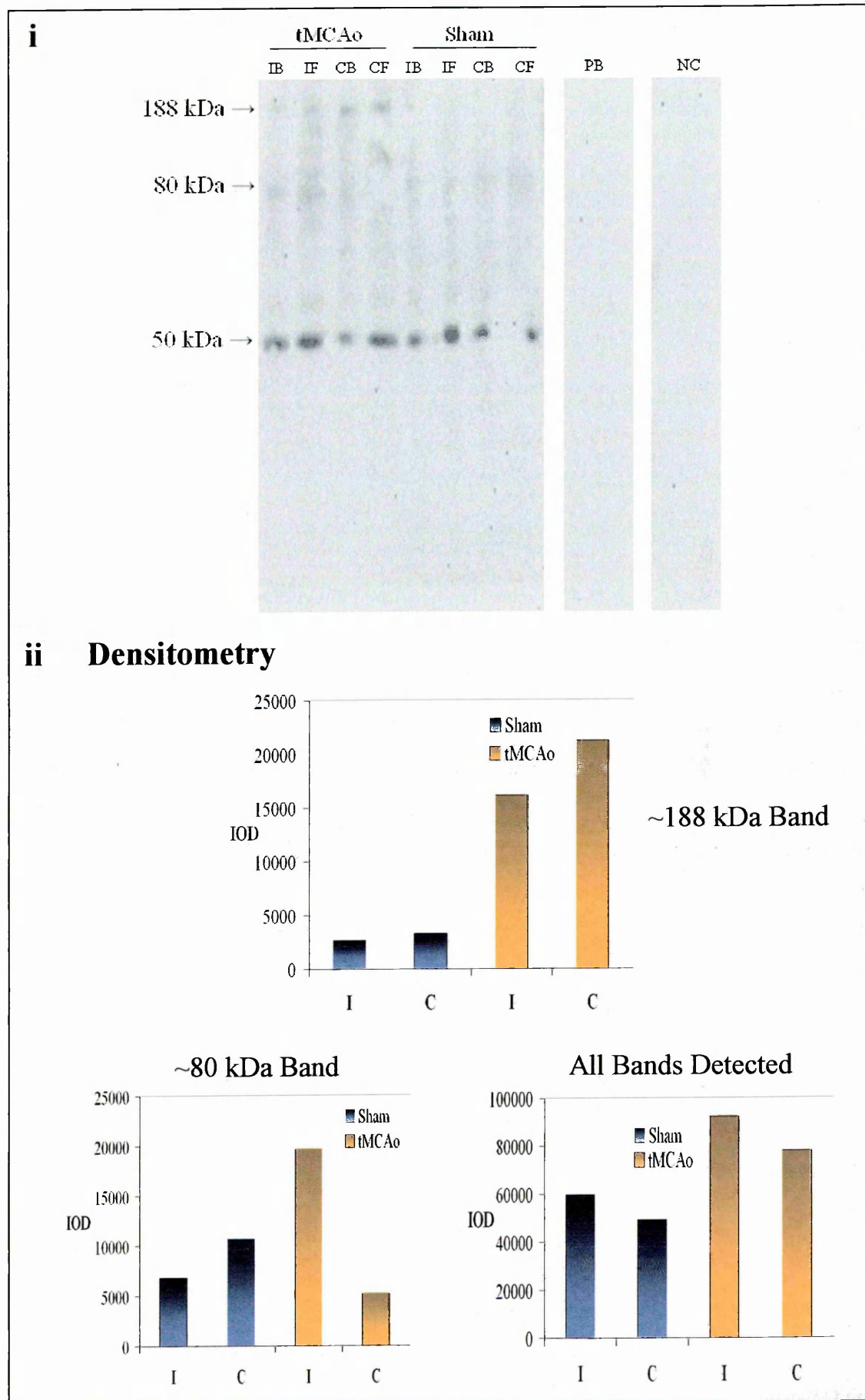
All Bands Detected

compared to sham as detected by densitometry (Fig. 5.7ii). The sum of the IODs of all the bands detected with the ADAMTS-9L2 antibody were higher for tMCAo brains when compared to sham as shown by the densitometry graph in Figure 5.7ii.

Five days (120 h) post-procedure, bands were observed at ~140, 64 and 38 kDa in both tMCAo and sham-operated samples (Fig 5.8i). The densitometry shown in Figure 5.8ii indicates that the sum of the IODs of all the bands observed with the ADAMTS-9L2 antibody were higher in IHs of sham brains compared to IH and CHs of tMCAo tissue. Whereas, the CHs of sham-operated brains had less ADAMTS-9 protein than the IH and CHs of tMCAo tissue (Fig. 5.8ii).

5.2.2.3 Cellular Origin of ADAMTS-9 mRNA in tMCAo Tissue

Identification and characterisation of ADAMTS-9-positive cells was performed with the kind assistance of neuropathologist Dr. Stephen Wharton (The University of Sheffield/Royal Hallamshire Hospital, Sheffield, UK).

Intense ADAMTS-9 mRNA expression in large cells of the cerebral cortex, thalamus and the dentate gyrus/Cornu Ammonis (CA3) of the hippocampus of tMCAo tissue sections is demonstrated in Figures 5.9A, C and E). The localisation of NeuN expression in large cells (neurones) was comparable to that of ADAMTS-9 mRNA expression described above as shown by IHC (Fig. 5.9B, D and F). Furthermore, ADAMTS-9 mRNA was detected in smaller cells of the same regions as shown in Figures 5.9A, C and E. The H&E stains in Figures 5.9M and N confirmed which regions of the brain were being studied.

ADAMTS-9 mRNA expression was not detected in cells which were positive for vWF (detected by IHC and shown in Fig. 5.9J) i.e. blood vessels. Figure 5.9H shows representative GFAP staining localised around the blood vessels of the leptomeninges whereas Figure 5.9I demonstrates that expression of this protein was localised globally in the hippocampus. GFAP protein and ADAMTS-9 mRNA did not appear to be localised in exclusively the same regions. The smaller cells, possibly glial cells, expressing *Adamts9* potentially also express GFAP.

165

Western blotting analysis of tMCAo and sham-operated rat brains at 120 h post-procedure with ADAMTS-9L2 antibody (5.8i). Protein was extracted from tissue with TRI Reagent prior to determination of protein concentration by BCA assay. SDS-PAGE (10%) was performed with 6 μg protein/well before transferring separated proteins to nitrocellulose membrane and western blotting. Peptide blocking was performed with the ADAMTS-9L2 'immunising peptide' to assess non-specific binding of the primary antibody (PB). NC (negative control) = western blotting whereby the primary antibody was omitted from the protocol (replaced by TBS), which served as a control for assessment of non-specific binding of the secondary antibody. Densitometry was performed on detected bands using the LabWorks Image Acquisition and Analysis Software to semi-quantify expression levels by measuring the IODs. The sum of the IODs of the three bands (~140, 64 and 38 kDa) detected in each hemisphere for sham and tMCAo brains are presented in graphical form (front and back regions combined) (5.8ii).

Figure 5.8 Expression of ADAMTS-9 Protein in Rat Brains at 120 H Post-tMCAo or Sham-Operation

*IS*H detection of *Adamts9* (antisense probe) (A, C, E) and IHC detection of NeuN (B, D, F), GFAP (H, I) and vWF (J) in tMCAo (24 h) tissue sections. Images M and N are H&E stains. *IS*H with the sense probe served as a control of ADAMTS-9 riboprobe specificity (G). IHC negative controls (omission of primary antibody from protocol as control for non-specific binding of the secondary antibodies) for GFAP (K) and vWF (L) are included. A, B, H, J, L and M are serial sections of the same region (leptomeninges [LM]/cerebral cortex [CC]/thalamus [T]). C, D and G are taken from the same region as A, B, H, J, L and M but showing more cerebral cortex (view shifted up). E, F, I, K and N are serial sections from the same region (hippocampus). Black Arrows represent *Adamts9*-positive large cells (neurones). Red arrows represent *Adamts9*-positive small cells (potentially glia). BV = blood vessel, DG = dentate gyrus, Cornu Ammonis field 3 = CA3. Images were taken on an Olympus BX60 microscope in fluorescent mode (IHC) or bright-field mode (*IS*H and H&E) (x100).

Figure 5.9 Cellular Expression of ADAMTS-9 mRNA Expression in tMCAo Tissue Sections

*IS*H detection of *Adamts9* (antisense probe) (A, C, E) and IHC detection of NeuN (B, D, F), GFAP (H, I) and vWF (J) in tMCAo (24 h) tissue sections. Images M and N are H&E stains. *IS*H with the sense probe served as a control of ADAMTS-9 riboprobe specificity (G). IHC negative controls (omission of primary antibody from protocol as control for non-specific binding of the secondary antibodies) for GFAP (K) and vWF (L) are included. A, B, H, J, L and M are serial sections of the same region (leptomeninges [LM]/cerebral cortex [CC]/thalamus [T]). C, D and G are taken from the same region as A, B, H, J, L and M but showing more cerebral cortex (view shifted up). E, F, I, K and N are serial sections from the same region (hippocampus). Black Arrows represent *Adamts9*-positive large cells (neurones). Red arrows represent *Adamts9*-positive small cells (potentially glia). BV = blood vessel, DG = dentate gyrus, Cornu Ammonis field 3 = CA3. Images were taken on an Olympus BX60 microscope in fluorescent mode (IHC) or bright-field mode (*IS*H and H&E) (x100).

Figure 5.9 cont. Cellular Expression of ADAMTS-9 mRNA Expression in tMCAo
Tissue Sections
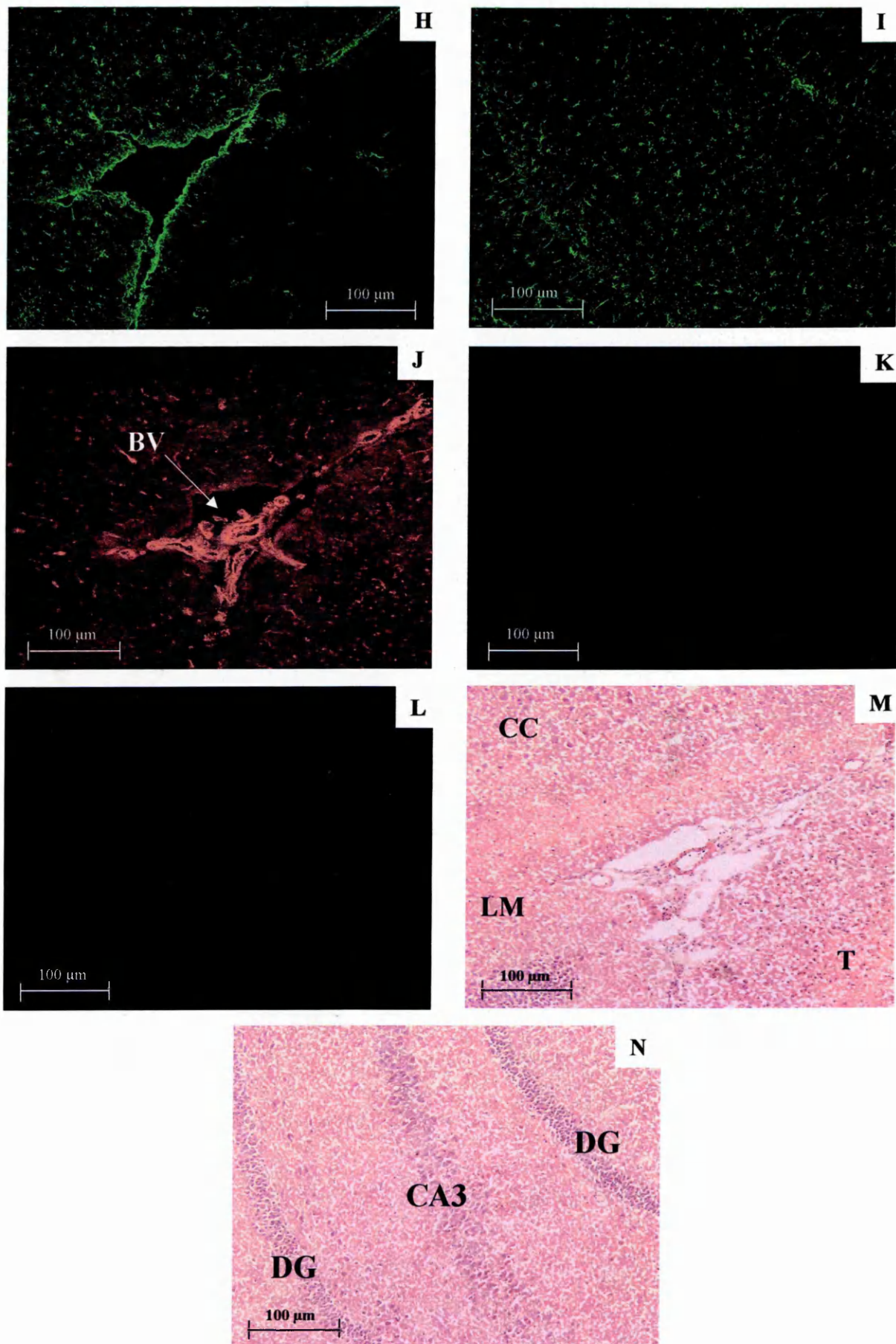
Identification of specific brain regions was achieved by analysis of H&E staining, IHC (of cellular markers) and *IS*H signal. Sections incubated with the sense strand (Fig. 5.9G) and no probe displayed only background *IS*H signals. IHCs performed without the incubation of the primary antibodies (replaced by PBS) showed no fluorescent signal (Fig. 5.9K and L). Therefore, these data suggest that neurones and potentially glial cells express ADAMTS-9 mRNA in tMCAo tissue.

5.2.2.4 Morphological Analysis of *Adamts9*-Positive Cells in tMCAo Tissue

Expression of ADAMTS-9 mRNA was detected in pyramidal neurones of the cerebral cortex (Fig. 5.10A), dentate gyrus of the hippocampus (Fig. 5.10B) and CA3 of the hippocampus (Fig. 5.10C). The cells were large and triangular/conical in morphology, characteristic of pyramidal neurones (López-Gallardo & Prada, 2001). *Adamts9* was also detected in the densely arranged granular neuronal cells of the dentate gyrus (Fig. 5.10B). Smaller cells also expressed *Adamts9* as shown in Figure 5.10A, B and C. Such cells were not as morphologically distinct as the neuronal cells but they are likely to be glia based on the size. Sections incubated with the sense strand (Fig. 5.10D) displayed only faint background signals. Consequently, these data strongly suggest that different neuronal cell-types express ADAMTS-9 mRNA and indicates that glial cells are potentially also expressing the peptidase.

5.4 Discussion

These data presented in this chapter represents the first study of ADAMTS-9 in a CNS inflammatory disorder. It demonstrates that ADAMTS-9 is up-regulated at the mRNA level following tMCAo and that the mature-form (~188 kDa) is present 24 h post-occlusion, although the absence of this species at 6 and 120 h may be due to the protein extraction method (see Section 3.5.3). Furthermore, these data shows that *Adamts9* is expressed by neurones and potentially glia *in vivo* as shown by *IS*H analysis of tMCAo tissue sections.

The real-time RT-PCR data provide strong evidence that the transcription of *Adamts9* is modulated by pathological conditions mimicking those that occur in response to cerebral ischaemia in humans. Statistically significant increases in ADAMTS-9 mRNA expression were detected in all tMCAo IHs when compared to tMCAo CHs and sham-

Figure 5.10 Neuronal expression of ADAMTS-9 mRNA
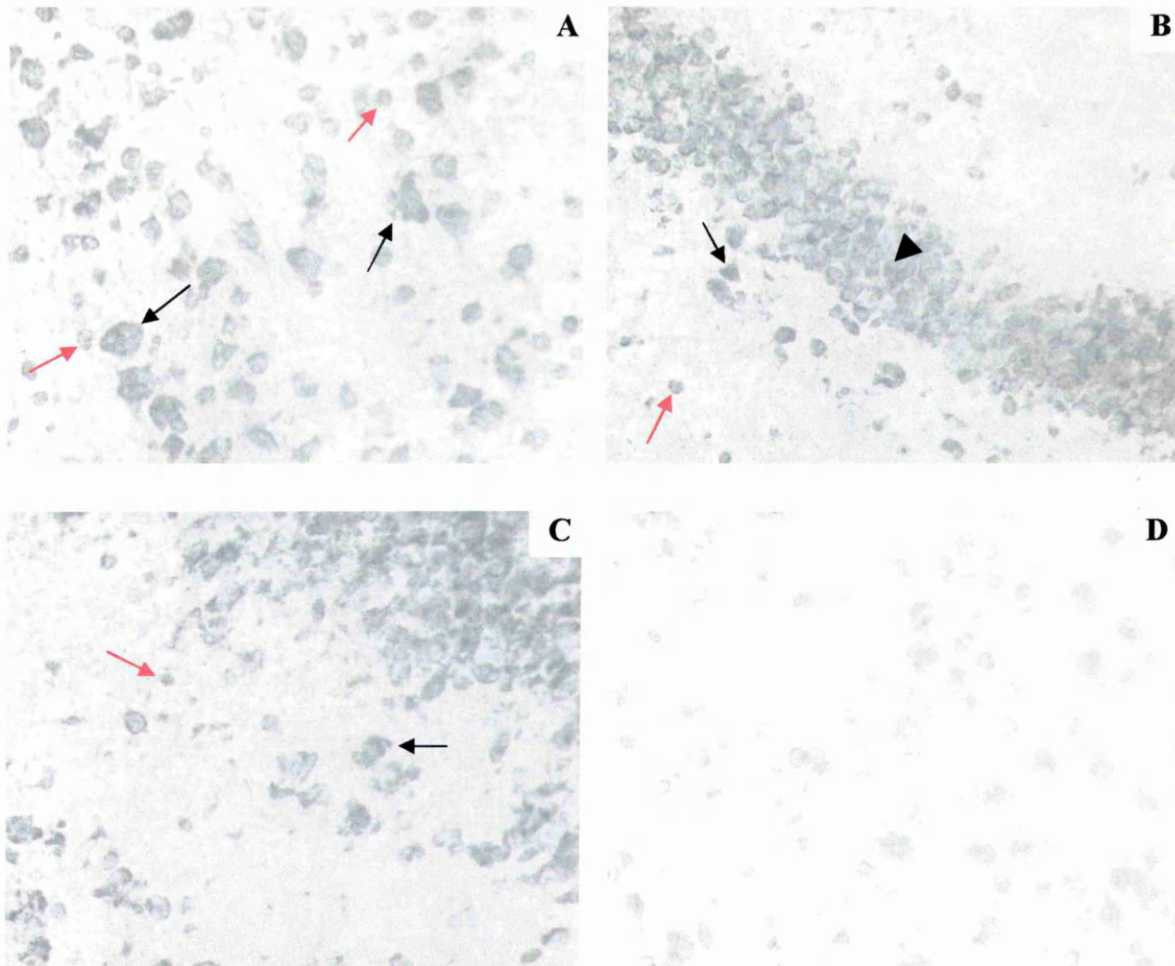
*IS*H detection of *Adamts9* (antisense probe) in A) cerebral cortex, B) dentate gyrus of the hippocampus and C) CA3 of the hippocampus of tMCAo (24 h) tissue sections. Full black arrows represent *Adamts9*-positive pyramidal neurones. Arrowheads represent *Adamts9*-positive granular neurones. Red arrows represent smaller *Adamts9*-positive cells (potentially glia). *IS*H with the sense probe served as a control of ADAMTS-9 riboprobe specificity (D). Images A and D are from the same brain region. Images were taken on an Olympus BX60 microscope in bright-field mode (x 400).

operated animals at all time-points post-procedure (twelve tMCAo brains versus nine sham brains). These data are in contrast to ADAMTS-5 mRNA expression levels, which were generally not altered in the tMCAo model as shown previously by our laboratory (Cross *et al*, 2006).

5.4.1 Implications of ADAMTS-9 mRNA and Protein Data at 6 Hours Post-tMCAo

A rapid increase in ADAMTS-9 mRNA expression at 6 h post-tMCAo was detected. The initial hypoxic stages of stroke involve the up-regulation of transcription factors such as HIF-1 and NF-κB (Dirnagl *et al*, 1999), a process which involves IL-1β (Yao *et al*, 2006; Jung *et al*, 2003). There is evidence that IL-1β is important in the early stages following stroke because IL-1ra was only effective when administered 3 h post-MCAo as opposed to 8-12 h (Toulmond & Rothwell, 1995). As shown in Chapter 4, IL-1β up-regulated ADAMTS-9 expression in CNS-derived cells *in vitro*. Therefore, such IL-1β-mediated modulation is potentially responsible for the increased levels of *Adamts9* expression shown in brains at 6 h post-tMCAo *in vivo*.

However, the increase in ADAMTS-9 mRNA expression did not correlate with an increase in protein expression in tMCAo brains at 6 h. Western blotting with ADAMTS-9L2 antibody detected no variation in the intensity of bands between tMCAo and sham-operated protein extracts. The detected bands at ~98, 62, 49, 39 and 35 kDa were not present following western blotting with the peptide-blocked antibody or negative control (no primary antibody) suggesting that they represent ADAMTS-9 fragments as opposed to being a result of non-specific binding. However, given that Demircan *et al* (2005) reported non-specific binding of the antibody (albeit with no evidence for this i.e. peptide blocking experiments were not performed), it cannot be said with 100% confidence that the antibody is entirely specific. Given the fact that the proteins are considerably smaller than the ~188 kDa mature form (Somerville *et al*, 2003) of the enzyme, the bands are likely to be a result of ADAMTS-9 processing (see Fig. 1.5). The band at ~98 kDa could potentially correspond to the 100 kDa band described previously as representing ADAMTS-9 following cleavage of the prodomain, GON domain and TSP-1s 9-15 (Koo *et al*, 2007). However, Demircan *et al* (2005) previously detected a band at 100 kDa with the ADAMTS-9L2 antibody but dismissed it as being a result of non-specific binding to proteins other than ADAMTS-9. The small

size of the proteins at ~62, 49, 39 and 35 kDa detected at 6 h are likely to represent ADAMTS-9 fragments containing the 2nd linker domain (to which the antibody is raised) but lacking most domains N- and C-terminus to it (including the metalloproteinase domain) i.e. in-active forms.

The fact that ADAMTS-9 expression is raised at the mRNA level but not the protein level after 6 h is probably a result of insufficient time elapsing for protein translation to have occurred to a detectable level. However, another potential explanation is translational (post-transcriptional) control of gene expression, which has been compared to (pre-) transcriptional control (e.g. cytokine modulation) in terms of importance (Mata *et al*, 2005). Post-transcriptional control involves the suppression of protein synthesis by a number of mechanisms including mRNA turnover (decay) and repression of translation (Wouters *et al*, 2005).

Pertinent to the 6 h ADAMTS-9 data is the widely reported finding that hypoxia can cause a rapid inhibition of the initiation step of mRNA translation. Hypoxia suppresses translation by triggering phosphorylation (and inhibition) of eukaryotic initiation factors (eIF2α and eIF4F), which are critical for facilitating the recruitment of the ribosomal subunit prior to loading onto the mRNA (Wouters *et al*, 2005; van den Beucken *et al*, 2006). Therefore, the rapid depletion of oxygen following tMCAo may have led to the increase in ADAMTS-9 mRNA levels via pro-inflammatory mediators, whereas ADAMTS-9 protein synthesis was potentially inhibited by hypoxia-induced inhibition of translation.

5.4.2 Implications of ADAMTS-9 mRNA and Protein Data at 24 Hours Post-tMCAo

At 24 h post-tMCAo, ADAMTS-9 mRNA expression was comparable to those detected at 6 h. This was in contract to ADAMTS-1 (~4-fold) and ADAMTS-4 (2-fold), mRNA levels of which were higher at 24 h than at 6 h post-tMCAo as detected by our laboratory previously (Cross *et al*, 2006). Importantly, the mature-form of ADAMTS-9 protein was only detected by western blotting (~188 kDa band) in tMCAo brains and not in sham-operated tissue at 24 h. The deduced M_r of the mature form of ADAMTS-9, lacking the prodomain is 184 kDa but this is likely to be higher (>185 kDa) given that there are nine consensus sites for *N*-linked glycosylation (Somerville *et al*, 2003). The

175

~188 kDa band observed in this study was the same size as that detected by western blotting previously with the ADAMTS-9L2 antibody (Demircan *et al*, 2005). The finding that the CHs of tMCAo brains contained higher levels of mature ADAMTS-9 protein than the IHs was surprising given that ADAMTS-9 mRNA levels were higher in the IHs when compared to CHs (discussed further in Section 5.4.4).

Bands at ~80 and 50 kDa were detected by western blotting in tMCAo and sham-operated brains at 24 h, which suggests they represent ADAMTS-9 fragments containing the 2nd linker domain as they were absent following blocking of the antibody with the immunising peptide. However, it cannot be ruled out that the presence of the detected bands may be due to non-specific binding of the antibody to proteins other than ADAMTS-9 (Demircan *et al*, 2005). The ~80 kDa band was slightly more intense in the IHs of tMCAo brains than sham-operated brains perhaps a result of there being more overall ADAMTS-9 protein in the tissue prior to processing. The band at ~50 kDa is likely to represent the same fragment detected at 6 h (~49 kDa).

5.4.3 Implications of ADAMTS-9 mRNA and Protein Data at 120 Hours Post-tMCAo

ADAMTS-9 mRNA levels were decreased by 120 h post-stroke when compared to earlier time-points. However, despite levels being lower than at 6 and 24 h, *Adamts9* levels remained significantly higher in tMCAo IHs when compared to tMCAo CHs and sham-operated brains at 120 h. This is in contrast to ADAMTS-1 and ADAMTS-4 levels in tMCAo IHs, which were not significantly higher than sham-operated or tMCAo CHs at 120 h (Cross *et al*, 2006).

No difference in ADAMTS-9 protein levels were detected between tMCAo and sham-operated brains at 120 h by western blotting with ADAMTS-9L2 antibody. The three bands detected by western blotting of brain protein extracts at 120 h were at ~140, 64 (both faint) and 38 kDa. The bands were not present following peptide blocking or western blotting with the omission of the primary antibody. However, the bands may still have been a result of the antibody binding to non-ADAMTS-9 proteins (Demircan *et al*, 2005). The ~64 kDa band is likely to represent the same ADAMTS-9 fragment observed at ~62 kDa in the 6 h brains whereas the ~38 kDa band potentially represents an ADAMTS-9 species following further processing. Neither the ~64 kDa nor ~38 kDa

forms of ADAMTS-9 will have retained their metalloproteinase domain because the fragments are too small (see Fig. 1.5), thus they are likely to be proteolytically inactive. However, the very faint band observed at ~140 kDa is potentially important because it is likely to still contain the metalloproteinase. The ~140 kDa protein is ~48 kDa less than the reported mature-form, which was detected in tMCAo brains at 24 h suggesting that further C-terminal processing has occurred. The finding that the ~188 kDa form of ADAMTS-9 was not detected at 120 h, but processed forms were, suggests that the half-life of the protein is quite short and it has been broken down.

5.4.4 Overall Discussion of tMCAo Real-Time RT-PCR and Western Blotting Data

The early stages post-stroke are the most crucial with many clinical trials failing because administration occurred outside the 'temporal window of efficacy' (Dirnagl *et al*, 1999). Therefore the findings in this study that ADAMTS-9 mRNA is up-regulated rapidly following tMCAo (6 h and 24h) and the mature enzyme (protein) is expressed at 24 h in tMCAo brains is important. Many of the mediators of stroke have well-defined time courses of increasing, peaking and decreasing expression levels following ischaemia, which may or may not correlate with the pattern of ADAMTS-9 expression (by modulating expression) observed in this study. Experiments in the rat have shown that TNF (which up-regulated *Adamts9* in U373-MG) expression started to increase at 2 h post-ischaemia prior to peaking at 12 h and remaining high for 24 h before returning to normal levels at 120 h. Whereas IL-1β levels started to rise at 4 h, peaked at 24 h before returning to normal at 120 h (Perera *et al*, 2006). Furthermore, our laboratory has shown previously that IL-1β and TNF mRNA were increased in tMCAo IHs when compared to tMCAo CHs and sham brains at 24 h. However, the impact of IL-1β may be nullified by IL-1ra levels, which were also higher in tMCAo at the mRNA level at a statistically significant level (Cross *et al*, 2006).

The finding that ADAMTS-9 mRNA expression was raised in the CHs of tMCAo brains when compared to both hemispheres of sham-operated tissue (at 6 and 24 h) was important because it suggests that the ischaemia had a systemic effect. This was potentially a result of decreased blood-flow to the CHs caused by tMCAo or a consequence of activated cells (and therefore pro-inflammatory mediators) migrating from the IHs to the CHs. Such responses may explain to a certain extent why higher

levels of the mature-form of ADAMTS-9 protein were detected in the CHs when compared to the IHs in tMCAo brains at 24 h. Furthermore, ADAMTS-9 protein potentially had a shorter half-life in the IHs because of its breakdown by up-regulated proteinases e.g. MMPs, whereas the ~188 kDa was still readily detectable in the CHs. To confirm this theory, intervening time-points would need to be studied such as 12, 16 and 20 h post-operation.

It is likely that TIMP-3 is the natural inhibitor of ADAMTS-9 *in vivo* (Hashimoto *et al*, 2001). Previous studies in our laboratory showed that TIMP-3 levels remained constant between tMCAo IHs, tMCAo CHs and sham-operated brains at all time-points post-procedure (Cross *et al*, 2006). Therefore, the increase in mature-ADAMTS-9 detected at 24 h was potentially not counteracted by an increase in TIMP-3, thus the enzyme could be contributing to the pathological consequences of a stroke or aiding in recovery.

5.4.5 Cellular Origin of ADAMTS-9 Discussion

The *IS*H study provided strong evidence that neurones are the predominant cell-type expressing ADAMTS-9 in tMCAo rat brains because the distribution of ADAMTS-9 mRNA expression was comparable with NeuN expression (shown by IHC). High-magnification morphological analysis of *IS*H and the fact that specific neuronal populations are characteristically present in distinct brain regions confirmed that pyramidal neurones and granular neurones were *Adamts9*-positive. The finding that *Adamts9* is expressed in the cerebral cortex is supported by Jungers *et al* (2005), who also detected (with a radiolabeled version of the riboprobe used in this study) the mRNA in the cerebral cortex of embryonic mouse brains, however, no cell-types were identified.

In addition to neurones, there were smaller cells which were positive for *Adamts9* but NeuN-negative and therefore are likely to be glia. Although GFAP was expressed in the regions of *Adamts9*-positive small cells it was difficult to determine whether the *IS*H signal was from astrocytes. This is because whereas NeuN is particularly useful for deducing co-localisation with mRNA because it is a marker for neuronal nuclei, whereas GFAP is an intermediate filament protein that is present in processes which are distant from the cell nucleus. Therefore, it cannot be confirmed that these *Adamts9*-

178

positive cells were astrocytes but it cannot be ruled out especially given that such cells express *Adamts9 in vitro* as shown in Chapter 4.

As well as astrocytes, the small cells could potentially be microglia/macrophages or infiltrating inflammatory cells. It was demonstrated that a microglia cell line (CHME3) expressed ADAMTS-9 *in vitro* (Chapter 4), therefore an antibody against ED1 (microglia/macrophage marker) was used for IHC of tMCAo tissue sections in an attempt to confirm this finding *in vivo*. Unfortunately, despite using varying dilutions of primary and three separate secondary antibodies and attempting both AP-BCIP/NBT and fluorescent detection (see Table 2.6), non-specific binding (high-background staining) was a major problem (not shown). Therefore, a comparison of ADAMTS-9 *IS*H and ED1 IHC could not be performed. Future work would involve performing GFAP *IS*H and ED1 *IS*H to determine whether the mRNA was co-localised with *Adamts9* in glial cell nuclei.

The comparison of *Adamts9 IS*H and vWF IHC successfully ruled out ECs as a predominant source of ADAMTS-9 expression in tMCAo. Areas of vWF expression (blood vessels) displayed negligible expression of *Adamts9*. This data is in contrast to other work, which showed that ADAMTS-9 mRNA is expressed by both human umbilical vein ECs (HUVECs) and dermal microvascular ECs (HUDMECs) (D. J. Buttle, pers commun). RT-PCR and western blotting on samples extracted from CNS-derived ECs, would confirm whether such cells express ADAMTS-9 mRNA and protein respectively. Previous studies (albeit in non-CNS-derived cultures) have shown that other ADAMTSs are expressed by ECs including ADAMTS-1 (Norata *et al*, 2004) and ADAMTS-13 (Turner *et al*, 2006). IgG negative control IHCs were not conducted in the tMCAo study because highly characteristic NeuN, GFAP and vWF staining were observed.

5.4.6 Limitations and Future Directions of tMCAo Study

It would be important to repeat the western blotting of tMCAo proteins following separation with SDS-PAGE gels containing a lower percentage of acrylamide (4%). This would enable better resolution of the higher M_r species and perhaps enable the detection of the zymogen, which is potentially more active than the mature form (Koo *et al*, 2007). To further interpret the western blotting data in this study, future work

would involve identifying proteins detected by blotting on PVDF membranes prior to excising the detected bands and performing protein sequencing. Alternatively, tMCAo protein extracts could be subjected to 2-D SDS-PAGE, which separates proteins on the basis of isoelectrical point (pH at which a protein carries no net charge) and M_r. Following 2-D SDS-PAGE, bands of interest would be excised and subjected to mass spectrometry to identify the protein (Lahm, & Langen, 2000). In this study, 6 µg of total protein was loaded/SDS-PAGE well prior to western blotting, which was perhaps too low a concentration to detect some sparingly expressed ADAMTS-9 species. Future work would involve loading higher levels of protein to further strength the conclusions drawn in this thesis.

The ADAMTS-9 conclusions drawn from the real-time RT-PCR and western blotting tMCAo data would have been made with increased confidence if the analysis of ADAMTS-1, -4 or -5 expression was performed as an internal positive control. The detection of comparable expression levels to those published previously (Cross *et al*, 2006) would have further validated the methods applied in this study. This approach would not have been available to validate the *IS*H because this technique has not been performed previously in our laboratory on ADAMTSs in tMCAo tissue. Despite, these controls not being performed, these data in this study was considered to be highly valid because of the inclusion of stringent negative controls e.g. omission of primary antibodies for western blotting, no RT samples for real-time RT-PCR and sense probes for *IS*H.

A limitation with the tMCAo study was the small number (twenty-one) of animals analysed. Two additional animals were subjected to tMCAo but no symptoms were observed and were therefore not included in the study. Tissue was obtained from The University of Manchester and unfortunately due to time and cost restraints, only twenty-three animals could be utilised for this study. Limitations of studying a small sample size were emphasised by the fact that data obtained from animals subjected to tMCAo at identical time-points were variable. In contrast, data obtained from across the sham-operated animals were highly comparable, suggesting that tMCAo initiated different responses between animals. Variation in post-ischaemic responses is a phenomenon that occurs in humans, no one stroke is identical and symptom severity varies between patients (Dirnagl *et al*, 1999). Therefore, the rat model would likely be unrepresentative of human stroke if all these data were identical following tMCAo. The fact that

statistically significant modulation of *Adamts9* expression was detected in all animals subjected to tMCAo, whilst no modulation was detected in all sham brains enabled conclusions to be drawn with confidence despite the small sample size.

5.4.7 Summary

To summarise this chapter, these data indicate that a) ADAMTS-9 mRNA is up-regulated in response to tMCAo at 6, 24 and 120 h post-procedure, b) the mature form of ADAMTS-9 protein is expressed at 24 h post-tMCAo and c) pyramidal and granular neurones are the predominant cells expressing ADAMTS-9 mRNA in tMCAo tissue Thus, ADAMTS-9 is potentially implicated in the brain's response to cerebral ischaemia and possibly other CNS inflammatory disorders.

Chapter 6

Analysis of Putative ADAMTS-9 Promoter Region for Transcription Factor Binding Sites

6.1 Background

This thesis has demonstrated that human ADAMTS-9 mRNA expression is modulated by pro-inflammatory cytokines in glial cells *in vitro*. Furthermore, expression of the rat species of ADAMTS-9 was shown to be modulated at the mRNA level in response to tMCAo *in vivo*. One potential mechanism for up-regulation of ADAMTS-9 mRNA expression is through the activation of transcription factors, which are proteins that bind to specific DNA sequences (transcription factor response elements) through DNA-binding domains. Transcription factors bound to upstream promoter regions are required for RNA polymerase II activation of transcription of eukaryotic genes (Turner *et al*, 2001). Many transcription factors are activated by factors pertinent to CNS inflammation e.g. as a result of intra-cellular signalling cascades activated by binding of cytokines to cell-surface receptors.

To provide evidence as to which transcription factors potentially activate the expression of ADAMTS-9 in human and rat, a bioinformatical screening of the putative promoter regions for these species was conducted. The software adopted for this analysis was MatInspector (http://www.genomatix.de/cgibin/matinspector_prof/mat_fam.), which locates transcription factor binding sites in DNA sequences. The tool utilises an extensive library of matrix descriptions for the transcription factor binding sites and assigns a 'quality rating' for each match as described by Quandt *et al* (1995) and Cartharius *et al* (2005). The software gives a 'matrix similarity' value, which expresses how close the input sequence is to the matrix of a particular transcription factor. It takes into account how highly conserved nucleotides are within a particular position of the matrix sequence e.g. mismatches in highly conserved positions decrease the matrix similarity score. A perfect match = 1.00, whereas a good match is considered to be >0.80 (Quandt *et al*, 1995).

6.2 Bioinformatical Approach

The human (NM_182920) and rat (NM_001107877) ADAMTS-9 sequences were obtained from the Entrez nucleotide database (http://www.ncbi.nlm.nih.gov/sites/entrez?db=Nucleotide&itool=toolbar) and were subjected to nucleotide BLAST searches. As expected ADAMTS-9 sequences were 100% matched. From the 'query result screen',

183

the NCBI Map Viewer (http://www.ncbi.nlm.nih.gov/mapview) option was chosen for the ADAMTS-9 sequence, which enabled the location of the gene on the corresponding chromosome to be visualised. In Map Viewer, the ADAMTS-9 gene was selected on the chromosome and the 'sequence viewer' option was chosen from the drop-down menu. The ADAMTS-9 plus strand sequence and the sequence upstream of the gene were visualised in NCBI Sequence Viewer v2.0 (http://www.ncbi.nlm.nih.gov/entrez/viewer. fcgi?view=graph&val=NT_022517.17&_gene=ADAMTS9) in 'graph' mode. The putative ADAMTS-9 promoter sequence (4 kb) immediately upstream (to the 5'-end) of the ADAMTS-9 gene was exported from the Sequence Viewer in FASTA format and imported into the MatInspector input form. From the Library Selection menu, 'Transcription factor binding sites' was chosen. Next, Matrix Library 7.0 was selected and only 'vertebrate' matrix groups were searched for in the query. Identified transcription factor binding sites of relevance to this study were highlighted in the putative ADAMTS-9 promoter regions in Microsoft Word.

6.3 Results

6.3.1 Analysis of Putative Human ADAMTS-9 Promoter Region for Transcription Factor Binding Sites

The BLASTn search of the human ADAMTS-9 gene confirmed it was located on chromosome 3. MatInspector identified 824 sequences in the putative human ADAMTS-9 promoter region (4 kb), which matched consensus transcription factor binding sites in the software matrix library. Figure 6.1 illustrates the locations of the consensus sequences for transcription factors pertinent to CNS inflammation e.g. those that are regulated by cytokines. Three NFκB binding sites were located at bp: 1324-1336, 3336-3348 and 3565-3577 upstream of the human ADAMTS-9 gene in the putative promoter region. The matrix similarity scores for the three sites were 0.84, 0.90 and 0.92 respectively. In addition, one consensus binding site for transcription factor activator protein 1 (AP-1) was identified in the putative promoter sequence by MatInspector (Fig. 6.1), 3703-3713 bp from the start of the ADAMTS-9 gene. The matrix similarity score for the site was 0.95. Also, an IRF-1 consensus site was shown to be present in the putative promoter region, located 3221-3241 bp 5' to the start of the ADAMTS-9 gene sequence (Fig 6.1), with a matrix similarity of 0.88.

Figure 6.1 Map of Putative Human ADAMTS-9 Promoter Region Showing Consensus Binding Sites of Transcription Factors Pertinent to CNS Inflammation

```
CCCCCCTCCCTCCTGCCCTCCTTGGCTGCGGCGGCGACGCGAGGCAGCGGCCGTGGAGAGCGCGCGGAGCCCGGCGCCCGCCG
CCAACTTTTGACTTTAGGAGTCGCTGAGGTCTCGCTGCGAGGGTCCCGTCTGCGCTCGGCTGAGCAACGCCGCCGCCTGCCGA
GAGCTGAGCCGCTCGGGCCGCAGGAGGAGCCGGAGGAGCAGGAGGAGGAGGAGGACTGGGGCTCGGCTGCTTGGCCGCATAAT
GCCCAGCGAGCGGGCAGGAGAAGGCGAGGAACTTGCGCTCCGAGGCGCGCCGGGCGCCCTGTGCTGGCCGGGATAGCTGAGCG
GCTTCTTGAATGGGGGGGCTGGGGGGGCGGAGGCGGGGGGGCCGCGGGTCCACAGCCTCTCAAATGCCCCGGTGCACGCCTCT
AAGAGGAGGAGAGGGGAGGAGAAAGCGAGACGAACGGGGACCGCCTCCTTCCAGACCATGTCCCCTCCTCGGCCGGCCCGTGC
GGGACTCGCAGCCGGAGGCCCTGCCGGCTGCAAGAGGCGGAGGCCAGAGGCGTCACCAGCGCCGGGGCAGCTGTTCCTGGTCC
CCGCCACCTCGCTGAAGTGGGGTTTTCTGAGATTCCCTGCCCCGGGGAGGGAAAGCAGGGAAAGTTCTCTCCCTTTCCTGGCG
CGCGTGCAGCCACTTCCCCTCTCGTCTTTTTCCTCTCCTCTCCTCTCTCTCCTCCCTTCCGAGTCTCTTTTTCCTCCTCCCCC
TTGTCTCTCTGCTGCCTCTCGGACTCTGTCCCTTCTCCCCATTTCCCCTGTGATGTCTGTCTTCTCCCCGCCCCACC
GTGTCCCTGTCTGTTTCTCACATTTCTCCTTTTCCTTTCCTTTCTCTTTCCGTCCCCATCTCTTGCCACCAGTCCCCATCTTTT
GGTTTCTTACAAGTGAAAGTGGCCCAGCGCCGGAGCGCCTTCCCTTCCTACACTTTTTCATTCGGGAAGAGATTTGGCACCTG
AGCTCCGCTCTCGATTTAATCACCCCAAGTCAAGAGTTTTAGAAATGGGGTTCTTAATCCTGCAGGTCGGAGTGTGTTTCTAA
TACGTGGTCTCTTGAAAATTTCGCAAAATATTTAAGCTGTGCTTTCCACCAACCTCTGTCACCATTCATGGAGGGTCCATAGC
ATTCTGTAGGTCCCCTGCCCCAAAAAAGGTTAAGAACAAATTTTGGCAGCAAGAAGGGGCGGGGACTCTGGCGCCCCTCACTA
CCAGGGGGTTTAGAGATGGGAGGGGAAGGGGGGATGGAGTGTAAAGTTGTAGATCCCTGTGGGAGGCACCAGTCCCTGGAGGG
ATTTCTCAATCACTTCCGCTTGCTTTCAGCCTGAGAGATGCTTGGAAAGACTGGGAAAGACTGAAAGCAGGCGCTTCAAGCTA
CACCTTCGTGTGTGTGTGTGTGTGTGTGTGTGTGTGTGTGTGAATTGTTCAATCTTGGGTGGTTCAGTGGCGCCTTTTC
TTTAACCAGCCCTCAGGAAGATAGAATTTCAAGATAATTTCAAGAGGAAAGACATGACAATATCGTTAAAAATATATAAATAT
ATGACTAATAAATATATATTTGCCCAAGTATCCTAGAACGGGGGTTGAGGTTCTGTTGCGTGGTAGGTTAGCACTCAGGACTA
GAAATACCAAAGATTGCCAACACCAGGAACCAAATCGCAATATGCTAGCAATGTCAACTATTCTTGAGATACTAATACATATA
TTTCTTCTGGTGAAGGGTAAAAATGACTTGGCAAGACGAATTTGCTAAATAATTGTTAACCCAAATTGATAATGTTACCATCG
TCTTATTACTGGAATTTCATAATGGATATGTAAAATGTAAGGATGGAAAAATAACATCTGTATTGTGCACAATTAGAGATTTT
TAGAGAATGGCATTTAAACCTTGAACCTCCAAATTAATTCACTAAAATACGTTTCTTCTAATACACAATCTTTCTTTTTATTA
TAACAACATTCCCCACAATCACAGTGTCTGGGAGTTGCTGAAAATTTAGTAAGGAACAGAAAAATATCAAGAAATCAATCTAT
TGGCTGATTCCTGTGGAAAATATTCCAGTACTTCCATTGTAAAATTACTCAAAAATATAGCACTTTCCAGTATTTCCCATTAA
ATCTTTTTTTCTCTTTCAGTTCAAATCCTTCCTGACAAAGAGAAGTTAACTAATGGTATAGAAATTACGATATGTAGGGACAG
AAGCCTCCTTTGTGTACTCTCTCTCCTTTGCTTTCTTTCTAGGACTTTGCTTGAAGAATGAACTTTGTCTACAGTTTTAAAAA
ATTGATCCACAAGAGCTGATAGGCCAGAAAGATACAAAATATCTCTTGGTGAACTCCTGAGGTGACCAAGAACCTAGGTTTAT
GAATTTCTCATCCTTAGTGAGTCTACCCATCTTTTCTTCAGTGTATTAGCTGGCTTCTGCATTTACATCTGTAAAAAAGTCTT
AAAGAATCTTAGGAAAATGTCTTTTAAATCGTGAGACATGAAAAAGACAGTTGAGCTAACTAAGCAAGTCAGGCAAAAATCTT
TTGTCTGAATAATTACTCTTTGTCTAAATAAGTACTCTTATTCAGTACTTACCATGGGGTAACATATAGCATTTAATTTAATT
CTCAAAACAGCTCTTTCAGGAAGTCAGTGTCAGTAATCTCATTTTACCAATAAGGATACCGAGATCTGAATAAGTGAAATAAT
TTGACCCCCCTCAATCCAGTAAGTGAGAGACACGATTCAAACTCCGTTTCAGTCGTTCAATCCAAGTTCATAACTATTATCAT
ATGTCATGAATAACTGATTAATCAGAAGCACTGCTAGATTTTTGGAGGGTTGCTTTGTGGGAAAATGGCTAAAATCATTCAGA
GAATTGCCTCAAGCTTTTATTGCATGTATAACTTTTCTTTAGCTCTCTCTTATTCTTCTCATGCAAAGTATTTAATGAAAATC
ATGTCAGCGATTTCATTGATATTTCACAGCTTTTCCCTCAGCAGTTAGAAGAGATCTGGCACATAGTAGGTAGTCAATAAGTA
TTTATTAAGACTAGGCATGGTGGCTCACACCTGTAATCCTAGCACTTTGGAAGGTTGAGGTGGGAGGATTGCATGAGGTCAGT
TCAGCGGTTCAAGACCAGCCTTGGCAACATAGCAACCCCTTGTCTCTACAAAAAAAGAGAAAAGAAATAATAAAATGAAATAA
AATAAATTGGCCCCTCATAAAAATTTGCTCTGAAAGAAGCAAACCTTTTCAAGGTCACCTGGAGTTAAAGGAGGGACAGTTTT
TAGCCCGTTTTCTTCGTGGGACTTTACTGGAATTGAATGGTATTGTAGGTTAAGTGGAAGTATTCATTGGCTGATTCGTCATG
AAAATTAGATCCCAGAGGAGTGATGAATGATATTAGTCACTAGGGAGAGATAATCCGGCCAATGGAAATGACAGTGATGACAT
CACAAATGACTCTGTTTGCCTAATGCCACTGGAAACAGCAGGAAGGAGACTTGAAGCAAAGCCATCAATTTCCACAGAAAGGG
GAAACCCACACCCAAATGGTAGGGAGGGCCCAGGAGCCAGAATTCAAGTGAATAGTTTCCTGAGTGGTCAGCAGCGTCAGGTG
ATTTGGGGAACAGATAAGCCCCTGGTACTTGGTAGCACTGCATTCTGGTCAGTGAATCACCAAGCTGGGACCTGGTGCTGGCT
GAGCTCTGTGACCTTGGGCCTAAAGAATCTTAGGGAGATGTGTTTTACATGACAAGAAATGAAAAGGACAATTGTGCTAACTA
AATAATTTGGGTTCCAATCTTTTGTCTGAATAATAATAATGAGAATCTTTTCTTGAGTACTTACTATGTACCAGACCATGTGT
ACTATGTCCTCTCTGATCCGGTTTCCTATTTGCAGACTGCAGCAGGTAGAAACTGTGTTGTCTTTGTTTGCCCTGTGAGTGAA
TGACCTTAGTGTATTT
```

The putative promoter sequence (4 kb) immediately upstream of human ADAMTS-9 was obtained using Sequence Viewer v2.0. Transcription factor binding sites within the putative promoter sequence on chromosome 3 were identified using MatInspector software. Consensus binding sites of transcription factors pertinent to CNS inflammation are highlight in colur and underlined as follows: Blue = NFκB, Brown = AP-1 and Orange = IRF-1.

6.3.2 Analysis of Putative Rat ADAMTS-9 Promoter Region for Transcription Factor Binding Sites

Chromosome 4 was identified as the location of the rat ADAMTS-9 gene within the rat genome as confirmed by a BLASTn search of the peptidase DNA sequence. MatInspector matched 507 sequences within the ADAMTS-9 putative promoter region with the matrices of transcription factors. Within the putative rat ADAMTS-9 promoter region, two NFκB consensus binding sites were identified by MatInspector as illustrated in Figure 6.2. The sites were located at 2231-2243 (matrix similarity = 0.86) and 3336-3348 (0.90) bp from the start of the ADAMTS-9 gene. An AP-1 site was also identified in the putative promoter sequence, 208-218 bp upstream of the ADAMTS-9 gene (Fig 6.3), with a matrix similarity score of 0.88. Furthermore, the putative rat promoter sequence of ADAMTS-9 contained two sequences where IRF-1 could bind 343-363 and 2626-2646 bp from the ADAMTS-9 gene. The matrix similarity ratings were 0.87 and 0.89 respectively. In contrast to the putative human ADAMTS-9 promoter, the rat sequence contained a consensus HIF-1 binding motif (matrix similarity = 0.96) at 3314-3330 bp 5'to the gene (Fig 6.2).

6.4 Discussion

6.4.1 Implications for *In Vitro* ADAMTS-9 Glial Cell Study

The bioinformatical analysis presented in this chapter provides preliminary evidence that ADAMTS-9 gene expression is potentially a target of transcription factor activation in human and rat. The findings that three NFκB and one AP-1 consensus binding sites are present in the putative human promoter region suggest that pro-inflammatory cytokines could up-regulate ADAMTS-9 expression by activating these transcription factors. It is well established that binding of both IL-1β and TNF to cell-surface receptors trigger intracellular signalling cascades, resulting in the activation of NFκB and AP-1 transcription factors. A study by Kordula *et al* (2000) demonstrated that such mechanisms occur in astrocytes to trigger gene expression. Therefore, the up-regulation of ADAMTS-9 mRNA expression in glial cells by IL-1β and TNF as demonstrated in Chapter 4 was potentially a result of transcription factor NFκB and/or AP-1 activation.

Figure 6.2 Map of Putative Rat ADAMTS-9 Promoter Region Showing Consensus Binding Sites of Transcription Factors Pertinent to CNS Inflammation

```
TAGCATTATCATCATCAATATGATTCTCCAAACTCTTTTTAATGGGGCCAATTTACTTCCAAGTCTGTAAGCAAGGCACAGAT
CCCTTGTCTTCTGTTCAGCAGCCATTAGACATCAGTAAGGCAGAGTCAAGCCCTTTCAGCTCTAAATCTGATCTTGAGCTTTT
CCAACAGTTACTTTATCCACCCGGCAAACCCCCCATTAAACTCTGATTCAGACGGCAAAGCTTCAATTGCTTCCATGACACAT
GTTGCTCATAGCGCTTCTTTTCATGAGCGGAGTTTTCAAAGCGATTCCCAGAGACGTTGCTTATACAAATGGTTCCAGCACAC
CTAGATAAAACATCAAAAACGAAATGCTGTGTTGTGGATAAGAGCATGGAGCAGTGCCTGGGTTGGAAACCCCAGCATCCACA
TAAGCTAAAATTGGATGTGCGCGCCTGTTACTCTGGCAGTGTGCCCCGACTTGCCAGCCTAGCACAAAGATGAGCTTCCATTG
ATTTTAGGGATCTTGTTACAAGCAGAGAGCAACAGGGAAGACACTGGATGTGCTGCCCCTCTGGCCTCTGCATGACATTCACA
GAAGGACACACCNNNACACNCANNCACATATACACAAACACACACACNNCACACCACACACNNNNNNNNNNCACACNCNNNNNA
NNNCACNNNNNNNNNNNNNNNNNNNNNNNNNNNNNNNNNNNNNNNNNNNNNNNNTACNNNNNNNNNNNNNNNNNNNNNNCACACNNNN
NNNNNNNNNNNNNNNCNNNCANNNNNNNNNNNNNNNACNNNNNNNNNNNNNNNNNNNNNNNNNNNNNNNNNNNNNNNNNNNNNNNN
NNNNCCCNNNTANNNNNNNNNNNNNNNNNNNNNNNNNNNNNNNNNNNNNNNNNNNNNNNNNNNNNNNNNNNNNNNNNNNNNNNNNN
NNNNNNNNNNNNNNNNNNNNNNNNNNNNNNNNNNNNNNNNNNNNNNNNNNNNNNNNNNNNNNNNNNNNNNNNNNNNNNNNNNNNNN
NNNNNNNNNNNNNNNNNNNNNNNNNNNNNNNNNNNNNNNNNNNNNNNNNNNNNNNNNNNNNNNNNNNNNNNNNNNNNNNNNNNNNN
NNNNNNNNNNNNNNNNNNNNNNNNNNNNNNNNNNNNNNNNNNNNNNNNNNNNNNNNNNNNNNNNNNNNNNNNNNNNNNNNNNNNNN
NNNNNNNNNNNNNNNNNNNNNNNNNNNNNNNNNNNNNNNNNNNNNNNNNNNNNNNNNNNNNNNNNNNNNNNNNNNNNNNNNNNNNN
NNNNNNNNNNNNNNNNNNNNNNNNNNNNNNNNNNNNNNNNNNNNNNNNNNNNNNNNNNNNNNNNNNNNNNNNNNNNNNNNNNNNNN
NNNNNNNNNNNNNNNNNNNNNNNNNNNNNNNNNNNNNNNNNNNNNNNNNNNNNNNNNNNNNNNNNNNNNNNNNNNNNNNNNNNNNN
NNNNNNNNNNNNNNNNNNNNNNNNNNNNNNNNNNNNNNNNNNNNNNNNNNNNNNNNNNNNNNNNNNNNNNNNNNNNNNNNNNNNNN
NNNNNNNNNNNNNNNNNNNNNNNNNNNNNNNNNNNNNNNNNNNNNNNNNNNNNNNNNNNNNNNNNNNNNNNNNNNNNNNNNNNNNN
NNNNNNNNNNNNNNNNNNNNNNNNNNNNNNNNNNNNNNNNNNNNNNNNNNNNNNNNNNNNNNNNNNNNNNNNNNNNNNNNNNNNNN
NNNNNNNNNNNNNNNNNNNNNNNNNNNNNNNNNNNNNNNNNNNNNNNNNNNNNNNNNNNNNNNNNNNNNNNNNNNNNNNNNNNNNN
NNNNNNNAGCCCAGAAACAGACTTTTAGAGTACCATCCAATACCTTAGAGTTCTAGAAGTCAAAAGTCTGGGCAGCCTCAGTA
AGCTTCTCTACTTAGGGCTTTAGTGACTGAAACAAGGTTTCAGCCTGCCTGGGCATTCTGGACAAGTCTGCTTTGAGTCCACT
CTGGTTGCTGACAAATTTCCGTTCTTGCAAGTCTGGAATGGAGCTTCCTTGTACTTGGTGGATTTTTTTCCGATATGTTTTTG
ATGCCTTTCCTCACCAAGCCATCTTGTCTTCATCTATTTGTCCCTAGAAAAGATTGCTGCTTATGCGCGTCCCATGGGAGTCC
CTGCAATGTCATTTCAAAGCCAGCGATGGAGTGTCCGTCCCTTTGCACTGAACCGCTTTGTATTTTTGTGGTGTTGCAGGGGT
CTGTCTCACTCTCCGGTTTGAGATTGGTCTCAATTGTAGCATCCTCCTGCTTCAGCCATGTAGGTGGGCCCACCAGCGTGCGG
CCTCTACCTCACACTGTAGTCTCACGTATTTCCTCGTCCCGCACCACCTCCAGTGCCTGTGACTGAGCTGGGCCTCCAGATAG
TCTGCCGTGAAGTCTACAAATCAGTGACCTTAATTTCACCTACACAGTCTGATATACCACAGATCCTTGGAAGTAACGCCGGA
AGGCAAAGCCGAAGGGGCCATCTTCGAATTTGCTTCTTGTACCCTGCTCCTCGGCTTAAAGGGAAACAATGGTTAAACAATCA
GCTGGCCTGAGCAGCTCCTCTGTTTGTAGAAGATGGGTGGATTTGAGAAGACGGGAGGGGCAGAGACAAGATTTAAGCCGGTG
CGTGAGCAGTACTCTTTCCGTAGCCTTGTGCGCTTTCTTGGCGGGCAAGCCTGCAGACCACACATGGCATCATCTGTTACAGG
AAGCCTTGCAGGCTTGACGGGTATCCAGACAAAATGGCATCCAGAAGCCTAACTGAAGAGGCTGTGTTGCAGATTGAGAAGGG
CCCGTTTCCTCTGTCCAACCATTCTCACGTCAACCTCAGTGTATTGTTTGCTGTCCTTTAAGAAGACTGCTGTTTGTCTGGAA
AGATCGGCATAGTTCTGGCAGATTTGTTCCTCCTTTAACAAATCACTAAGTCCATAAACGTTTAGTAAGAGTCAGTTTTACTC
CAGGCCCTGAATTAGGTATAAAACATCATATCTGTCCTCTGAGAGCCTCTAGCTGTAGATACTCCTGTCCTTTCACCAGATGA
CTTAAAAGGAGGACCGAAAATGAGGTGGGAATGACTAGCGGTGACATTCAGAAACCTCAGTGGTAGCTGTGGCCAAAGGAGAG
ACTTTCATTCCCCAGGTGTTTCCACTAGAATGTTCTATGAGGACATGTGTAAATCCACACTGTCCAATCGAGAAGCCAGGCCC
ACGTGTAGCTATTGAATGGGACTGACCAGTGGGAGGCAGATTGGATTACATTTTACTTAATTTTAATTTTAAATATTAACTGC
TACGTGCAACCCCTGTATTATACAGCTCAGAAAATACATACTCTGGAACCATTCATTCATTTTTTTCAATGTGTGTGTATGTG
TTCCTGCATGTGTGTTTACATGTGCATGGGAATGGGGGGGGCAGGTCCATGTCAATTACATGCATCATTCATTCTCCATCTTG
GTTTTTGATTGCTGAGCCTTGAGCTCACCAGTTTGGCTGATCTGGCTGTCAGAAGACTCCAGTGTCTCTGCCATCTCCCCAGG
AAAGGGGTTATAGAGAGGCACTGCCCTACCTGGCTTATTTAAGTAGGTTCTGGGGATTGAATTCAGATCTGAAAGTTTGCATA
GCAGGCTCTCAGCTGACTGGGCCATCCACCCCCCTCCAGCCTTCCCATTGTTCATTCGTTGGTTACTTTTAATTCCTCCATG
ATCTTCTGTTCTTCAGCTTCGAAAGGTGTTTAAAATCTAACATCTGAATCACCTTCTCATGTAACTTAATTCTCTCTGATTAAT
TTCTAGCATCAACATTAAGATAATGCAAGCCAAAGAGTTTTTAGAGGTAGATGCAAAAAGCAAAACTACATAAAATTTATTAT
TGTATAGAAATACAAG
```

The putative promoter sequence (4 kb) immediately upstream of rat ADAMTS-9 was obtained using Sequence Viewer v2.0. Transcription factor binding sites within the putative promoter sequence on chromosome 4 were identified using MatInspector software. Consensus binding sites of transcription factors pertinent to CNS inflammation are highlight in colur and underlined as follows: Blue = NFκB, Aqua = HIF-1, Brown = AP-1 and Orange = IRF-1. Note: the full chromosome 4 sequence downstream of the ADAMTS-9 gene was not fully available hence the undetermined bases (N).

6.4.2. Implications for ADAMTS-9 in Response to Cerebral Ischaemia

Consensus binding sites for NFκB (two sites) and AP-1 (one site) were also identified in the putative rat ADAMTS-9 promoter region. Consequently, pro-inflammatory cytokine-mediated activation of these transcription factors in the rat *in vivo* may have been important contributing factors in the up-regulation of ADAMTS-9 mRNA expression detected following tMCAo, as shown in Chapter 5. Further evidence that transcriptional activation of ADAMTS-9 is a feature of cerebral ischaemia comes from the finding that IRF-1 consensus binding sites were present in the human (one site) and rat (two sites) putative promoter regions. IRF-1 is a transcription factor, which has been implicated in inflammation and apoptosis (Vaughan *et al*, 1997). A study by Iadecola *et al* (1999) provided evidence that IRF-1 is important in cerebral ischaemia. IRF-1 gene expression was up-regulated within 12 h of MCAo in mice, with levels peaking at 4 days. Furthermore, the volume of ischaemic injury was decreased by $23 \pm 3\%$ in IRF-1$^{-/+}$ and by $46 \pm 9\%$ in IRF$^{-/-}$ mice with less severe neurological defects than WT. Therefore, in both humans and rats, IRF-1 activation potentially up-regulates ADAMTS-9 expression following cerebral ischaemia.

The role of HIF-1 as a 'master transcription factor' (Hirato, 2002) in response to hypoxia following cerebral ischaemia has been well documented. To date it has been shown that HIF-1 regulates the expression of over 100 target genes (Ke & Costa, 2006) including ~5% of all genes in arterial ECs in hypoxic conditions (Manalo *et al*, 2005). Therefore, the presence of a HIF-1 binding site in the putative rat ADAMTS-9 promoter sequence is a potential explanation for the up-regulation of *Adamts9* expression detected at 6 and 24 h following tMCAo in the rat. This is substantiated by the decreased levels of *Adamts9* expression 120 h post-tMCAo, when the brain would have returned to normoxic conditions.

6.4.3. Limitations of Bioinformatical Approach

The bioinformatical study presented in this chapter is limited because it is not known a) exactly where the promoter sequence of ADAMTS-9 on chromosome 3 (in human) or chromosome 4 (in rat) is located and b) what size the promoter region is. Therefore, the identified consensus sequences may be located outside the promoter region thus binding of the transcription factor would not trigger expression of ADAMTS-9. There are a

number of approaches which can be applied to confirm and identify the promoter region of a particular gene. The most widely used experimental procedure is to clone a segment of DNA, upstream of the gene, in a vector carrying a reporter gene. The expression of the reporter gene can be determined in appropriate host cells. To further analyse the location of the promoter region, deletion mutants can be constructed to assess the importance of the different regions of the identified promoter in terms of initiating transcription. Deletion mutants can be generated using *exonuclease III*, which progressively cleaves dsDNA generating multiple sequences from within the potential gene regulatory region (Strachan & Read, 1999). The mutants can be cloned into a vector, which has a reporter gene downstream of the MCS prior to transfection into human cells, pertinent to the study of interest i.e. glial or neuronal cells. The reporter gene must a) code for a protein which is not endogenous to the transfected cells and b) be easily detected. A commonly used reporter gene is luciferase, which encodes for a protein that emits light. Consequently, constructs which contain the promoter region of ADAMTS-9 will trigger the expression of the reporter gene in the cells following transfection. Following this 'mapping' approach, one can deduce whether the transcription factor binding sites are within the ADAMTS-9 promoter region.

6.4.4 Summary

This chapter demonstrated using a bioinformatics-based approach that NFκB, AP-1 and IRF-1 transcription factor matrices matched sequences in both the human and rat putative ADAMTS-9 promoter regions. In addition, a HIF-1 binding domain was identified in the rat ADAMTS-9 'promoter'. Therefore, ADAMTS-9 gene expression has the potential to be activated by transcription factors, which are implicated in CNS inflammatory disorders. Such mechanisms may have contributed to the modulation of ADAMTS-9 expression detected in the CNS inflammatory models studied in this thesis, *in vivo* (tMCAo) and *in vitro* (glial cells treated with cytokines).

Chapter 7

General Discussion

7.1 Implications of the Study

ADAMTS-9 is a recently discovered peptidase which has been studied mainly in embryogenesis because it has a highly similar structure to *C. elegans* gonadal morphogenesis proteinase GON-1 (Somerville *et al*, 2003; Llamazares *et al*, 2003) and cartilage because it cleaves the major structural component; aggrecan (Somerville *et al*, 2003). Despite ADAMTS-9 being expressed in the developing and adult CNS and having the ability to cleave CSPGs present in brain ECM, it has not been studied in this tissue.

The findings in Chapter 4 that ADAMTS-9 mRNA is expressed under basal conditions by human astrocytic, neuronal and microglial cell lines *in vitro* suggests that the peptidase is constitutively expressed in the brain. Therefore, ADAMTS-9 could potentially play a part in normal ECM remodelling following expression by endogenous CNS cells via cleavage of lecticans particularly versican and aggrecan (Somerville *et al*, 2003) and potentially brevican. In support of this hypothesis that ADAMTS-mediated proteoglycanolysis is occurring *in vivo* in the brain, our laboratory has shown previously that brevican and phosphacan were colocalised with ADAMTS-4 on astrocytes (by IHC) in tMCAo tissue (Haddock *et al*, 2007). Similar experiments with ADAMTS-9 would be important to confirm activity.

As well as being constitutively expressed by cells *in vitro*, there is evidence stemming from this study showing that ADAMTS-9 expression is regulated by external factors as summarised in Figure 7.1. Each of the factors had differential effects on ADAMTS-9 mRNA expression across the cell-types suggesting that *in vivo* modulation of the peptidase is complex. Three of the factors that modulated *Adamts9* expression were pro-inflammatory cytokines, heavily implicated in CNS inflammation (reviewed by Viviani *et al*, 2004; Owens *et al*, 2004). As well as being a key event in acute disorders such as trauma or stroke, inflammation is also a feature of chronic diseases such as MS and PD (reviewed by Lucas *et al*, 2006), thus ADAMTS-9 has the potential to be modulated in response to a host of CNS pathologies. Support for this hypothesis was demonstrated in Chapter 5, in an animal model of cerebral ischaemia, an acute inflammatory insult, highly prevalent in humans. *Adamts9* mRNA expression was shown to be significantly raised in rat brains subjected to tMCAo (compared to sham-operated tissue). Such modulation *in vitro* and *in vivo* was potentially a result of activation of ADAMTS-9

191

Based on the results generated in this study, modulation of ADAMTS-9 mRNA expression in the brain is likely to be complex and multi-factorial as represented by the figure opposite (not to scale). In addition to being expressed under basal conditions in the cells cultured *in vitro* in this study, *Adamts9* expression was modulated to a certain extent by IL-1β, TNF, IFN-γ and RetA, which are all factors shown to be important in CNS inflammation thus providing preliminary evidence that the peptidase could be involved in acute and chronic brain pathologies. This hypothesis was supported by *in vivo* studies demonstrating that ADAMTS-9 mRNA was up-regulated in rats subjected to tMCAo when compared to sham-operated animals. Bioinformatical analysis of the putative promoter region of ADAMTS-9 provided evidence that IL-1β and TNF could potentially up-regulate ADAMTS-9 in these models by activating transcription factors NFκB and/or AP-1, consensus sites of which were present in the rat and human sequences. More specifically, in response to cerebral ischaemia, transcription could potentially be activated by IRF-1 (in human and rat) and/or HIF-1 (in rat) because consensus sites for these transcription factors shown to be heavily implicated in stroke are present in the ADAMTS-9 'promoter' sequences. Red arrows indicate up- or down-regulation of ADAMTS-9 (TS-9) expression. Note: the neurone in the figure is of pyramidal morphology but other neuronal types such as granular neurones also express ADAMTS-9 (as shown in this study by *ISH*).

192

Figure 7.1 Modulation of ADAMTS-9 Expression in the CNS
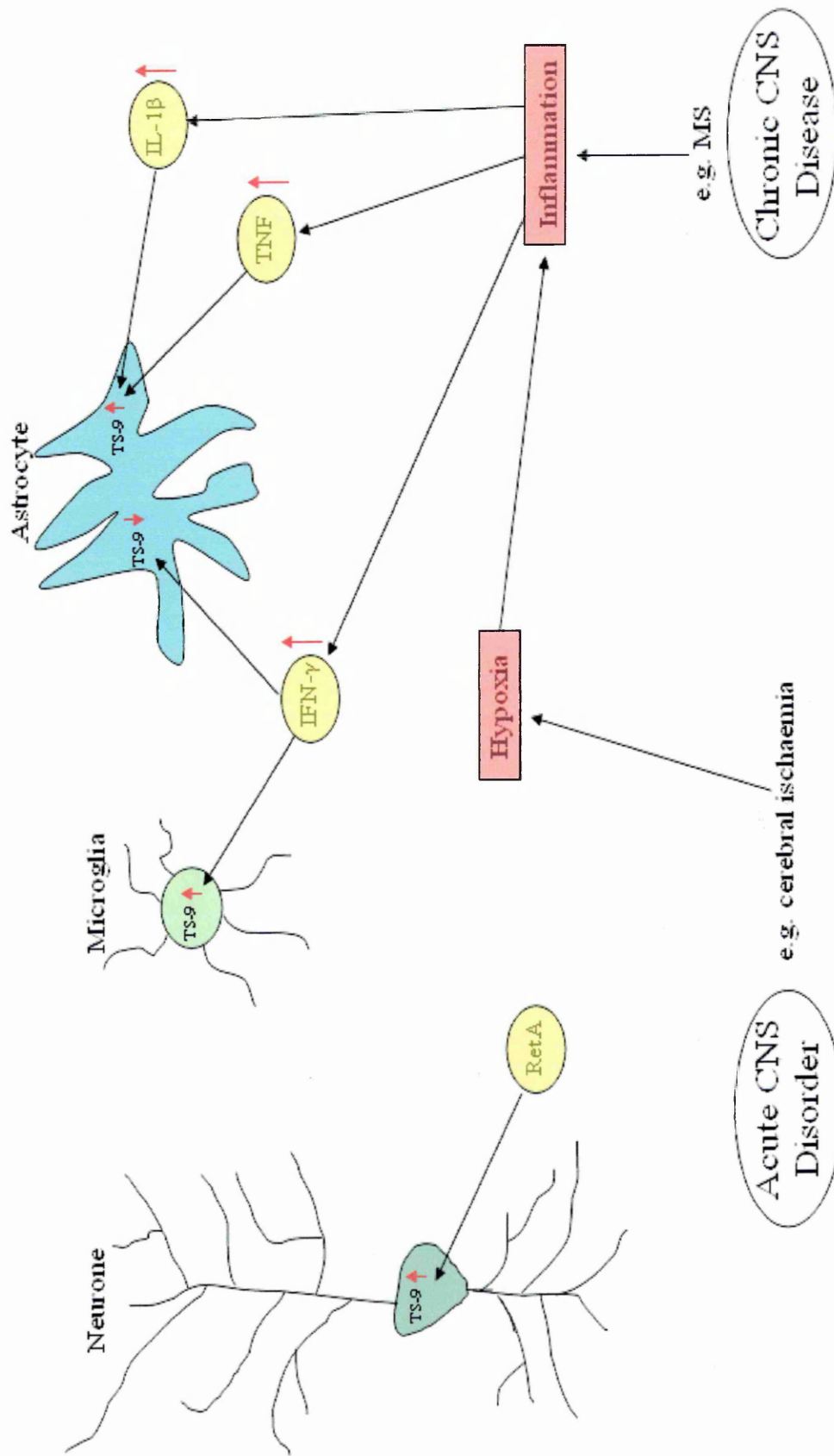
gene expression by transcription factors through binding to consensus sequences shown to be present in the putative promoter regions as demonstrated in Chapter 6.

Given the finding that the potentially active-form (~188 kDa) of ADAMTS-9 was expressed in tMCAo brains and not in sham-operated tissue, it is tempting to postulate that ADAMTS-9 has a destructive role in the CNS. However, from these initial studies it is not possible to ascertain whether ADAMTS-9 up-regulation is damaging or protective and could potentially be both in different pathologies. These data showing that RetA increased the expression of ADAMTS-9 mRNA in SHSY-5Y cells suggests the peptidase has a protective role in the CNS because RetA has been shown to promote neurite outgrowth and regeneration post-CNS damage (Mey *et al*, 2005). Further evidence that ADAMTS-9 is potentially implicated in the neuronal response to injury came from data demonstrating that granular and pyramidal neurones were the predominant cells expressing *Adamts9* in tMCAo tissue sections.

To further understand the role of ADAMTS-9 within the CNS, it would be important to answer the question of where the protein is localised *in vivo*. Unfortunately, IHC analysis of ADAMTS-9 protein could not be performed in this study due to limited quantities of the ADAMTS-9L2 antibody. ICC of U373-MG cells demonstrated that ADAMTS-9 was localised within the nucleus and intracellular vesicles but not the ECM. However, this result may have been because ICC was performed on monolayer 24 h (post-seeding on chamber slides) cultures, which were unlikely to have synthesised ECM within the time frame of the experiment. Other studies have suggested that though ADAMTS-9 is secreted, it remains localised at or near the cell surface, potentially in the pericellular matrix (glycocalyx), which is a region of ECM closely associated with the plasma membrane (Somerville *et al*, 2003; Koo *et al*, 2006; Koo *et al*, 2007).

Following up-regulation, ADAMTS-9 could be contributing to neuronal regeneration by two potential mechanisms: 1) promotion of neuronal differentiation/proliferation by enzymatic activity in the nucleus or 2) operating as a peptidase on the cell-surface of migrating CNS cells and clearing a path through the ECM or glial scar by degradation of known substrates aggrecan and versican (Somerville *et al*, 2003), enabling neuronal outgrowth and/or migration of neuronal precursor cells. Alternatively, the breakdown of CSPGs by ADAMTS-9 could have a damaging effect on the CNS by allowing the migration of inflammatory cells and activated microglia to susceptible neurones.

The efficiency by which ADAMTS-9 cleaves CSPGs does not appear to be as high as ADAMTS-1, -4 or -5, perhaps limiting the impact of the peptidase as a proteoglycanase *in vivo* (Somerville *et al*, 2003). Therefore, the up-regulation of ADAMTS-9 expression following stroke is not necessarily a bad thing because it is unlikely that the normal ECM structure will be significantly degraded by the peptidase.

7.2 Future Directions

To further elucidate the role of ADAMTS-9 in CNS inflammation, it would be important to focus on functional studies. An ADAMTS-9 knock-out animal would be a useful tool to assess the role of the enzyme not just in the CNS but also in general physiology. Pertinent to this study would be to subject ADAMTS-9$^{-/-}$ mice to tMCAo and compare symptom-severity with ADAMTS-9$^{+/+}$ animals. This would give a clearer indication as to whether the higher levels of *Adamts9* in tMCAo (shown in this study) correlate with destructive or protective responses. To date KO mice have increased our understanding of the functions of ADAMTS-1, -2, -4 and 5 (reviewed by Flannery, 2006).

To augment the studies in this thesis a continuous source of efficacious/specific anti-ADAMTS-9 antibodies would be highly useful, particularly ones recognising different domains of the peptidase e.g. the prodomain. This would enable the determination of whether the zymogen, potentially the most active species (Koo *et al*, 2007) or processed forms were present in protein extracts, as detected by western blotting (based on the size of the protein). This was not possible with the ADAMTS-9L2 antibody, which detected active and latent protein. Effective antibodies would enable semi-quantification of proteins in extracts by performing densitometry on western blot bands or by development of a quantitative enzyme-linked immunosorbent assay (ELISA). The antibodies would also be used to determine whether protein levels correlated with mRNA levels, as determined by real-time RT-PCR in the cell culture protein extracts. Furthermore, in disease models such as tMCAo, a better understanding of whether the protein was active or not could be gained. The antibody would also be utilised for IHC, analysing the cellular localisation of the ADAMTS-9 protein in tMCAo tissue. This would support the *ISH* study which showed that neurones were the predominant cell-type expressing ADAMTS-9 mRNA. Performing IHC with cellular markers and

conducting co-localisation analysis with ADAMTS-9 IHC would be a better approach to confirm glial cell association than comparing IHC with *ISH*. Also, ICC would be conducted with the antibody to ascertain whether the localisation of ADAMTS-9 protein is intracellular in all cell-types used in this thesis, which appeared to be the case in U373-MG (although this experiment needs repeating).

Many of the inflammatory mechanisms seen following cerebral ischaemia are common to other CNS pathologies. Therefore, it would be illuminating to compare the responses of ADAMTS-9 observed in the tMCAo model with other brain disorders/diseases. The techniques developed, optimised and validated in this study can be applied to other disorders such as MS by utilising MS post-mortem tissue or the EAE model (Cross *et al*, 2005; Haddock *et al*, 2006).

It is likely that the substrate profile of ADAMTS-9 is not yet complete. The expression of the purified, full-length ADAMTS-9 protein would provide a useful tool to further investigate potential substrates for the enzyme. Also, a range of deletion mutant-forms of ADAMTS-9 would provide a better understanding as to which domains are important in proteolytic activity and activation. It was originally planned to express ADAMTS-9 in High Five insect cells (Invitrogen) as part of this study as was achieved previously with ADAMTS-1, -4 and -5 (Vankemmelbeke *et al*, 2003) but due to time constraints this was not possible. Somerville *et al* (2003) stated that 'given its complex domain structure and cell surface localisation, a purified ADAMTS-9 is not yet available'. Therefore, it is likely that the generation of recombinant ADAMTS-9 will be difficult to achieve but the rewards would be to vastly improve our understanding of the peptidase.

7.3 Conclusion

The study documented in this thesis provides evidence that ADAMTS-9 has the potential to be implicated in normal physiology and pathology in the CNS. Functional studies are required to further elucidate the role of ADAMTS-9 within the brain before considering whether the peptidase is a candidate for therapeutic intervention to treat CNS inflammatory disorders.

Aarum, J, Sandberg, K, Haeberlein, SLB, Persson, MAA (2003). Migration and Differentiation of Neuronal Precursor Cells can be directed by Microglia. Proceeding of the National Academy of Sciences **100**; 15983-15988

Abbaszade, I, Liu, R-Q, Yang, F, Rosenfeld, SA, Ross, OH, Link, JR, Ellis, DM, Tortorella, MD, Pratta, MA, Hollis, JM, Wynn, R, Duke, JL, George, HJ, Hillman Jr, MC, Murphy, K, Wiswall, BH, Copeland, RA, Decicco, CP, Bruckner, R, Nagase, H, Itoh, Y, Newton, RC, Magolda, RL, Trzaskos, JM, Hollis, GF, Arner, EC, Burn, TC (1999). Cloning and Characterization of *ADAMTS11*, an Aggrecanase from the ADAMTS Family. Journal Biological Chemistry **274**; 23443-23450

Aidinis, V, Carninci, P. Armaka, M, Witke, W, Harokopos, V, Pavelka, N, Koczan, D, Argyropoulos, C, Thwin, M-M, Möller, S, Kazunori, W, Gopalakrishnakone, P, Ricciardi-Castagnoli, P, Thiesen, H-J, Hayashizaki, Y, Kollias, G (2005). Cytoskeletal Rearrangements in Synovial Fibroblasts as a Novel Pathopysiological Determinant of Modeled Rheumatoid Arthritis. Public Library of Science Genetics **1**; 455-466

Aktas, O, Ullrich, O, Infante-Duarte, C, Nitsch, R, Zipp, F (2007). Neuronal Damage in Brain Inflammation. Clinical Implications of Basic Neuroscience Research **64**; 185-189

Allan, SM, Rothwell, NJ (2003). Inflammation in Central Nervous System Injury. Philosophical Transactions of the Royal Society London Biological Sciences **358**; 1669-1677

Allen, SJ, Dawburn, D (2006). Clinical Relevance of the Neurotrophins and their Receptors. Clinical Science **110**; 175-191

Ambrosini, E, Remoli, ME, Giacomini, E, Rosicarelli, B, Serafini, B, Lande, R, Aloisi, F, Coccia, EM (2005). Astrocytes Produce Dendritic Cell-Attracting Chemokines In Vitro and In Multiple Sclerosis Lesions. Journal of Neuropathology & Experimental Neurology **64**; 706-715

Andreini, C, Banci, L, Bertini, I, Elmi, S, Rosato, A (2005). Comparative Analysis of the ADAM and ADAMTS Families. Journal of Proteome Research **4**; 881-888

Aono, S, Oohira, A (2006). Chondroitin Sulphate Proteoglycans in the Brain. Advances in Pharmacology **53**; 323-336

Arner, EC (2002). Aggrecanase-Mediated Cartilage Degradation. Current Opinion in Pharmacology **2**; 322-329

Asahi, M, Asahi, K, Jung, JG, del Zoppo, GJ, Fini, ME, Lo, EH (2000). Role for Matrix Metalloproteinase 9 after Focal Cerebral Ischemia: Effects of Gene Knockout and Enzyme Inhibition with BB-94. Journal of Cerebral Blood Flow Metabolism **20**; 1681-1689

Ayers, MM, Hazelwood, LJ, Catmull, DV, Wang, D, McKormack, Q, Bernard, CCA, Orian, JM (2004). Early Glial Responses in Murine Mouse Models of Multiple Sclerosis. Neurochemistry International **45**; 409-419

Ballabh, P, Braun, A, Nedergaard, M (2004). The Blood-Brain Barrier: an Overview Structure, Regulation, and Clinical Implications. Neurobiology of Disease **16**; 1-13

Bandtlow, CE, Zimmermann, DR (2000). Proteoglycans in the Developing Brain: New Conceptual Insights for Old Proteins. Physiological Reviews **80**; 1267-1290

Bar-Or, A, Oliveira, E. M. L, Anderson, D. E, Hafler, D. A (1999). Molecular Pathogenesis of Multiple Sclerosis. Journal of Neuroimmunology **100**; 252-259

Barritt, AW, Davies, M, Marchand, F, Hartley, R, Grist, J, Yip, P, McMahon, SB, Bradbury, EJ (2006). Chondroitinase ABC Promotes Sprouting of Intact and Injured Spinal Systems after Spinal Cord Injury. Journal of Neuroscience **26**; 10856-10867

Batchelor, PE, Porritt, MJ, Martinello, P, Parish, CL, Liberatore, GT, Donnan, GA, Howells, DW (2002). Macrophages and Microglia Produce Local Trophic Gradients that Stimulate Axonal Sprouting toward but not beyond the Wound Edge. Molecular and Cellular Neuroscience **21**; 436-453

Bear, MF, Connors, BW, Paradiso, MA (2001). Neuroscience - Exploring the Brain, 2nd Edition. Lippincott Williams & Wilkins **4**; 74-84

Bellail, AC, Hunter, SB, Brat, DJ, Tan, C, Van Meir, EG (2004). Microregional Extracellular Matrix Heterogeneity in Brain Modulates Glioma Cell Invasion. International Journal of Biochemistry & Cell Biology **36**; 1046-1069

Berg, JM, Tymoczko, JL, Stryer, L. Biochemistry, 5th Ed (WH Freeman and Company, 2002)

Bevitt, DJ, Mohamed, J, Catterall, JB, Li, Z, Arris, CE, Hiscott, C, Sheridan, C, Langton, KP, Barker, MD, Clarke, MP, McKie, N (2003). Bev Expression of ADAMTS metalloproteinases in the retinal pigment epithelium derived cell line ARPE-19: transcriptional regulation by TNFα. Biochemica et Biophysica Acta **1626**; 83-91

Block, ML, Hong, J-S (2005). Microglia and Inflammation-Mediated Neurodegeneration: Multiple Triggers with a Common Mechanism. Progress in Neurobiology **76**; 77-98

Bocci, G, Francia, G, Man, S, Lawler, J, Kerbal, RS (2003). Thrombospondin 1, a Mediator of the Antiangiogenic Effects of Low-Dose Metronomic Chemotherapy. Proceedings of the National Academy of Sciences **100**; 12917-12922

Bode, W, Gomis-Ruth, FX, Stockler, W (1993). Astacins, Serralysins, Snake Venom and Matrix Metalloproteinases Exhibit Identical Zinc-Binding Environments (HEXXHXXGXXH and Met-Turn) And Topologies and should be Grouped into a Common Family, the Metzincins. FEBS Letters **331**; 134-140

Bornstein, P (2001). Thrombospondins as Matricellular Modulators of Cell Function. Journal of Clinical Investigation **107**; 929-934

Boutin, H, Lefeuvre, RA, Horai, R, Asano, M, Iwakura, Y, Rothwell, NJ (2001). Role of IL-1α and IL-1β in Ischemic Brain Damage. Journal of Neuroscience **21**; 5528-5534

Boyd, JG, Gordon, T (2003). Neurotrophic Factors and Their Receptors in Axonal Regeneration and Functional Recovery After Peripheral Nerve Injury. Molecular Neurobiology **27**; 277-324

Bracken, CP, Whitelaw, ML, Peet, DJ (2003). The Hypoxia-Inducible Factors: Key Transcriptional Regulators of Hypoxic Responses. Cellular and Molecular Life Sciences **60**; 1376-1393

Brakebusch, C, Seidenbecher, CI, Asztely, F, Rauch, U, Matthies, H, Meyer, H, Krug, M, Böckers, TM, Zhou, X, Kreutz, MR, Montag, D, Gundelfinger, ED, Fässler, R (2002). Brevican-Deficient Mice Display Impaired Hippocampal CA1 Long-Term Potentiation but Show No Obvious Deficits in Learning and Memory. Molecular and Cellular Biology **22**; 7417-7427

Bresnahan, PA, Leduc, R, Thomas, L, Thorner, J, Gibson, HL, Brake, AJ, Barr, PJ, Thomas, G (1990). Human *fur* gene Encodes a Yeast KEX2-like Endoprotease that Cleaves Pro-β-NGF In Vivo. Journal of Cell Biology **111**; 2851-2859

Burridge, JH, Elessi, K, Pickering, RM, Taylor, PN (2007). Walking on an Uneven Surface: The Effect of Common Peroneal Stimulation on Gait Parameters and Relationship Between Perceived and Measured Benefits in a Sample of Participants With a Drop-Foot. Neuromodulation: Technology at the Neural Interface **10**; 59-67

Bush, TG, Puvanachandra, N, Horner, CH, Polito, A, Ostenfeld, T, Svendsen, CN, Mucke, L, Johnson, MH, Sofronview, MV (1999). Leukocyte Infiltration, Neuronal Degeneration, and Neurite Outgrowth after Ablation of Scar-Forming, Reactive Astrocytes in Adult Transgenic Mice. Neuron **23**; 297-308

Bustin, SA (2000). Absolute Quantification of mRNA using Real-Time Reverse Transcription Polymerase Chain Reaction Assays. Journal of Molecular Endocrinology **25**; 169-193

Bustin, SA (2002). Quantification of mRNA using Real-Time Reverse Transcription PCR (RT-PCR): Trends and Problems. Journal of Molecular Endocrinology **28**: 23-39

Butte, AJ, Dzau, VJ, Glueck, SB (2001). Further Defining Housekeeping, or "Maintenance," Genes. Focus on "A Compendium of Gene Expression in Normal Human Tissues". Physiological Genomics **7**; 95-96

Cal, S, Obaya, AJ, Llamazares M, Garabaya, C, Quesada, V, López-Otín, C (2002). Cloning, Expression Analysis, and Structural Characterization of Seven Novel Human ADAMTSs, a Family of Metalloproteinases with Disintegrin and Thrombospondin-1 Domains. Gene **283**; 49-62

Cao, J, Hymowitz, M, Conner, C, Bahou, WF, Zucker, S (2005). The Propeptide Domain of Membrane Type 1-Matrix Metalloproteinase Acts as an Intramolecular Chaperone when Expressed in *Trans* with the Mature Sequence in COS-1 Cells. Journal of Biological Chamistry **38**; 29648-29653

Capila, I, Linhardt, RJ (2002). Heparin-Protein Interactions. Angewandte Chemie International Edition **41**; 391-412

Carmichael, ST (2005). Rodent Models of Focal Stroke: Size, Mechanism, and Purpose. Journal of the American Society for Experimental NeuroTherapeutics **2**; 396-409

Carroll-Anzinger, D, Al-Aharthi, L (2006). Gamma Interferon Primes Productive Human Immunodeficiency Virus Infection in Astrocytes. Journal of Virology **80**; 541-544

Cartharius, K, Frech, K, Grote, K, Klocke, B, Haltmeier, M, Klingenhoff, A, Frisch, M, Bayerlein, M, Werner, T (2005). MatInspector and Beyond: Promoter Analysis based on Transcription Factor Binding Sites. Bioinformatics **21**; 2933-2942

Chan, EY (2005). Advance in Sequencing Technology. Mutation Research **573**; 13-40

Chen, Y-G, Hata, A, Lo, RS, Wotton, D, Shi, Y, Pavletich, N, Massagué, J (1998). Determinants of Specificity in TGF-β Signal Transduction. Genes & Development **12**; 2144-3298

Choi, J-W, Park, SC, Kang, GH, Liu, JO, Youn, H-D (2004). Nur77 Activated by Hypoxia-Inducible Factor-1α Overproduces Proopiomelanocortin in von Hippel-Lindau-Mutated Renal Cell Carcinoma. Cancer Research **64**; 35-39

Cipriani, B, Chen, L, Hiromatsu, K, Knowles, H, Raine, CS, Battistini, L, Porcelli, SA, Brosnan, CF (2003). Upregulation of Group 1 CD1 Antigen Presenting Molecules in

Guinea Pigs with Experimental Autoimmune Encephalomyelitis: an Immunohistochemical Study. Brain Pathology **13**; 1-9

Clagett-Dame, M, McNeill, EM, Muley, PD (2005). Role of All-Trans Retinoic Acid in Neurite Outgrowth and Axonal Elongation. Journal of Neurobiology **66**; 739-756

Clark, ME, Kelner, GS, Turbeville, LA, Boyer, A, Arden, KC, Maki, RA (2000). ADAMTS9, a Novel Member of the ADAM-TS/Metallospondin Gene Family. Genomics **67**; 343-350

Collins-Racie, LA, Flannery, CR, Zeng, W, Corcoran, C, Annis-Freeman, B, Agostino, MJ, Arai, M, DiBlasio-Smith, E, Dorner, AJ, Georgiadis, KE, Jin, M, Tan, X-Y, Morris' EM, LaVallie, ER (2004). ADAMTS-8 Exhibits Aggrecanase Activity and is Expressed in Human Articular Cartilage. Matrix Biology **23**; 219-230

Compston, A (2004). The Pathogenesis and Basis for Treatment in Multiple Sclerosis. Clinical Neurology and Neurosurgery **106**; 246-248

Connor, B, Dragunow (1998). The Role of Neuronal Growth Factors in Neurodegenerative Disorders of the Human Brain. Brain Research Reviews **27**; 1-39

Cross, NA, Chandrasekharan, S, Jokonya, N, Fowles, A, Hamdy, FC, Buttle, DJ, Eaton, CL (2005a). The Expression and Regulation of ADAMTS-1, -4, -5, -9, and -15 and TIMP-3 by TGFβ1 in Prostate Cells: Relevance to the Accumulation of Versican. The Prostate **63**; 269-275

Cross, AK, Haddock, G, Surr, J, Plumb, J, Bunning, RAD, Buttle, DJ, Woodroofe, MN (2005b). Differential Expression of ADAMTS-1, -4, -5 and TIMP-3 in Rat Spinal Cord at different Stages of Acute Experimental Autoimmune Encephalomyelitis. Journal of Autoimmunity **26**; 16-23

Cross, AK, Haddock, G, Stock, CJ, Allan, S, Surr, J, Bunning, RAD, Buttle, DJ, Woodroofe, MN (2006). ADAMTS-1 and -4 are Up-Regulated following Transient Middle Cerebral Occlusion in the Rat and their Expression is Modulated by TNF in Cultured Astrocytes. Brain Research **1088**; 19-30

Davidson, RK, Waters, JG, Kevorkian, L, Darrah, C, Cooper, A, Donell, ST, Clark, IM (2006). Expression Profiling of Metalloproteinases and their Inhibitors in Synovium and Cartilage. Arthritis Research & Therapy **8**; R124

del Zoppo, GJ, Milner, R, Mabuchi, T, Hung, S, Wang, X, Berg, GI, Koziol, JA (2007). Microglial Activation and Matrix Protease Generation during Focal Cerebral Ischemia. Stroke **38**; 646-651

De Fraipont, F, Nicholson, AC, Feige, JJ, Van Meir, EG (2001). Thrombospondins and Tumour Angiogenesis. Trends in Molecular Medicine **7**; 401

Demircan, K, Hirohata, S, Nishida, K, Hatipoglu, OF, Oohashi, T, Yonezawa, T, Apte, SS, Ninomiya, Y (2005). ADAMTS-9 is Synergistically Induced by Interleukin-1β and Tumor Necrosis Factor α in OUMS-27 Chondrosarcoma Cells and in Human Chondrocytes. Arthritis & Rheumatism **52**; 1451-1460

Desrivières, S, Kuhn, K, Müller, J, Gläser, M, Laria, NC-P, Korder, J, Sonnentag, M, Neumann, T, Schwarz, J, Schäfer, J, Hamon, C, Groner, B, Prinz, T (2007). Comparison of the Nuclear Proteomes of Mammary Epithelial Cells at different Stages of Functional Differentiation. Proteomics **7**; 2019-2037

Dirnagl, U, Iadecola, C, Moskowitz, MA (1999). Pathobiology of Ischaemic Stroke: an Integrated View. Trends in Neurosciences **22**; 391-397

Dronne, M-A, Greiner, E, Dumont, T, Hommel, M, Boissel, J-P (2007). Role of Astrocytes in Grey Matter During Stroke: A Modelling Approach. Brain Research **1138**; 231-242

Dunn, R, Reed, JE, du Plessis, DG, Shaw, EJ, Reeves, P, Gee, AL, Warnke, P, Walker, C (2006). Expression of *ADAMTS-8*, a Secreted Protease with Antiangiogenic Properties. is Downregulated in Brain Tumours. British Journal of Cancer **94**; 1186-1193

East, CJ, Stanton, H, Golub, SB, Rogerson, FM, Fosang, AJ (2007). ADAMTS-5 Deficiency does not Block Aggrecanolysis at Prefferred Cleavage Sites in the

Chondroitin Sulphate-Rich Region of Aggrecan. Journal of Biological Chemistry **282**; 8632-8640

Elston, GN (2003). Cortex, Cognition and the Cell: New Insights into the Pyramidal Neuron and Prefrontal Function. Cerebral Cortex **13**; 1124-1138

Emsley, HCA, Smith, CJ, Gavin, CM, Georgiou, RF, Vail, A, Barberan, EM, Hallenbeck, JM, del Zoppo, GJ, Rothwell, NJ, Tyrrell, PJ, Hopkins, SJ (2003). An Early and Sustained Peripheral Inflammatory Response in Acute Ischaemic Stroke: Relationships with Infection and Atherosclerosis. Journal of Neuroimmunology **139**; 93-101

Emsley, HCA, Smith, CJ, Georgiou, RF, Vail, A, Hopkins, SJ, Rothwell, NJ, Tyrrell, PJ (2005). A Randomised Phase II Study of Interleukin-1 Receptor Antagonist in Acute Stroke Patients. Journal of Neurology, Neurosurgery & Psychiatry **76**; 1366-1372

Encinas, M, Iglesias, M, Liu, Y, Wang, H, Mihaisen, A, Ceňa, V, Gallego, C, Comella, JX (2000). Sequential Treatment of SH-SY5Y Cells with Retinoic Acid and Brain-Derived Neurotrophic Factor gives Rise to Fully Differentiated, Neurotrophic Factor-Dependent Human Neuron-Like Cells. Journal of Neurochemistry **75**; 991-1003

Esiri, MM (2007). The Interplay between Inflammation and Neurodegeneration in CNS Disease. Journal of Neuroimmunology **184**; 4-16

Farina, C, Aliosi, F, Meinl, E (2007). Astrocytes are Active Players in Cerebral Innate Immunity. Trends in Immunology **28**; 138-145

Farkas, E, Luiten, PGM (2001). Cerebral Microvascular Pathology in Aging and Alzheimer's Disease. Progress in Neurobiology **64**; 575-611

Flannery, CR, Zeng, W, Corcoran, C, Collins-Racie, LA, Chockalingham, PS, Hebert, T, Mackie, SA, McDonagh, T, Crawford, TK, Tomkinson, KN, LaVallie, ER, Morris, EA (2002). Autocatalytic Cleavage of ADAMTS-4 (Aggrecanase-1) Reveals Multiple Glycosaminoglycan-Binding Sites. Journal of Biological Chemistry **277**; 42775-42780

Flannery, CR (2006). MMPs and ADAMTSs: Functional Studies. Frontiers in Bioscience 11; 544-569

Flynn, G, Maru, S, Loughlin, J, Romero, IA, Male, D (2003). Regulation of chemokine receptor expression in human microglia and astrocytes. Journal of Neuroimmunology **136**; 84-93

Galtrey, CM, Fawcett, JW (2007). The Role of Chondroitin Sulfate Proteoglycans in Regeneration and Plasticity in the Central Nervous System. Brain Research Reviews **54**; 1-18

Gao, G, Westling, J, Thompson, VP, Howell, TD, Gottschall, PE, Sandy, JD (2002). Activation of the Proteolytic Activity of ADAMTS4 (Aggrecanase-1) by C-terminal Truncation. The Journal of Biological Chemistry **277**; 11034-11041

Gao, G, Plaas, A, Thompson, VP, Jin, S, Zuo, F, Sandy, JD (2004). ADAMTS4 (aggrecanase-1) Activation on the Cell Surface involves C-terminal Cleavage by Glycosylphosphatidyl Inositol-Anchored Membrane Type 4-Matrix Metalloproteinase and Binding of the Activated Proteinase to Chondroitin Sulfate and Heparan Sulfate on Syndecan-1. Journal of Biological Chemistry **279**; 10042-10051

Garcia, JH, Liu, K-F, Ho, K-L (1995). Neuronal Necrosis After Middle Cerebral Artery Occlusion in Wistar Rats Progresses at Different Time Intervals in the Caudoputamen and the Cortex. Stroke **26**; 636-643

GeneDetect.com Ltd (2007). Oligonucleotide Probe Information Sheet. http://www.genedetect.com/Merchant2/OligoHandling.pdf at SHU 7/8/07

Germann, S, Juul-Jensen, T, Letarnec, B, Gaudin, V (2006). DamID, a New Tool for Studying Plant Chromatin Profiling *in vivo*, and its use to Identify Putative LHP1 Target Loci. Plant Journal **48**; 153-163

Gibson, RM, Rothwell, NJ, Le Feuvre, RA (2004). CNS Injury: The Role of the Cytokine IL-1. Veterinary Journal **168**; 230-237

Ginzinger, DG (2002). Gene Quantification using Real-Time Quantitative PCR: An Emerging Technology hits the Mainstream. Experimental Hematology **30**; 503-512

Glasson, SS, Askew, R, Sheppard, B, Carito, BA, Blanchet, T, Ma, H-L, Flannery, CR, Kanki, K, Wang, E, Peluso, D, Yang, Z, Majumdar, MK, Morris, EA (2004). Characterization and Osteoarthritis Susceptibility in ADAMTS-4-Knockout Mice. Arthritis & Rheumatism **50**; 2547-2558

Glasson, SS, Askew, R, Sheppard, B, Carito, B, Blanchet, T, Ma, H-L, Flannery, CR, Peluso, D, Kanki, K, Yang, Z, Majumdar, MK, Morris, EA (2005). Deletion of ADAMTS5 Prevents Cartilage Degradation in a Murine Model of Osteoarthritis. Nature **434**; 644-648

Goertsches, R, Comabella, M, Navarro, A, Perkal, H, Montalban, X (2005). Genetic association between polymorphisms in the *ADAMTS14* gene and multiple sclerosis. Journal of Neuroimmunology **164**; 140-147

Goldsmith, JG, Ntuen, EC, Goldsmith, EC (2007). Direct Quantification of Gene Expression using Capillary Electrophoresis with Laser-Induced Fluorescence. Analytical Biochemsitry **360**; 23-29

Gosselin, D, Rivest, S (2007). Role of IL-1 and TNF in the Brain: Twenty Years of Progress on a Dr. Jekyll/Mr. Hyde Duality of the Innate Immune System. Brain, Behaviour and Immunity **21**; 281-289

Gouze, J-N, Gouze, E, Popp, MP, Bush, ML, Dacanay, EA, Kay, JD, Levings, PP, Patel, KR, Saran, J-PS, Watson, RS, Ghizzani, SC (2006). Exogenous Glucosamine Globally Protects Chondrocytes from the Arthritogenic Effects of IL-1β. Arthritis Research & Therapy **8**; R173

Gregersen, R, Lambertsen, K, Finsen, B (2000). Microglia and Macrophages are the Major Source of Tumor Necrosis Factor in Permanent Middle Cerebral Artery Occlusion in Mice. Journal of Cerebral Blood Flow & Metabolism **20**; 53-65

Guidance on the Operation of the Animals (Scientific Procedures) Act 1986 (c.14), London, The Stationary Office

Gunson, RN, Collins, TC, Carman, WF (2006). Practical Experience of High Throughput Real Time PCR in the Routine Diagnostic Virology Setting. Journal of Clinical Virology **35**; 355-367

Haddock, G, Cross, AK, Surr, J, Buttle, DJ, Bunning, RAD, Woodroofe, MN (2003). Expression of ADAMTS-1, -4, -5 and TIMP-3 in Central Nervous System Cell Lines: Possible Role in CNS Physiology and Pathology. Proceedings of the 6th European Meeting on Glial Cell Function in Health and Disease, Berlin, Germany. Glia **2**; 33-33

Haddock, G, Cross, AK, Plumb, J, Surr, J, Buttle, DJ, Bunning, RAD, Woodroofe, MN (2006). Expression of ADAMTS-1, -4, -5 and TIMP-3 in Normal and Multiple Sclerosis CNS White Matter. Multiple Sclerosis **12**; 386-396

Haddock, G, Cross, AK, Sharrack, B, Callaghan, J, Bunning, RAD, Buttle, DJ, Woodroofe, MN (2007). Brevican and Phosphacan Expression and Localization following Transient Middle Cerebral Artery Occlusion in the Rat. Biochemical Society Transactions 35; 692-694

Hafler, DA (2004). Multiple Sclerosis. Journal of Clinical Investigation **113**; 788-794

Halder, RC, Jahng, A, Maricic, I, Kumar, V (2006). Mini Review: Immune Responses to Myelin-Derived Sulfatide and CNS-Demyelination. Neurochemical Research **32**; 257-262

Hamatani, T, Faloc, G, Carter, MG, Akutsu, H, Stagg, CA, Sharov, AA, Dudekula, DB, VanBuren, V, Ko, MSH (2004). Age-Associated Alteration of Gene Expression Patterns in Mouse Oocytes. Human Molecular Genetics **13**; 2263-2278

Hashimoto, G, Aoki, T, Nakamura, H, Tanzawa, K, Okada, Y (2001). Inhibition of ADAMTS4 (Aggrecanase-1) by the Tissue Inhibitors of Metalloproteinases (TIMP-1, 2, 3 and 4). FEBS Letters **494**; 192-195

Hashimoto, G, Shimoda, Okada (2004). ADAMTS4 (Aggrecanase-1) Interaction with the C-Terminal Domain of Fibronectin Inhibits Proteolysis of Aggrecan. Journal of Biological Chemistry **279**; 32483-32491

He, F, Sun, YE (2007). Glial Cell More than Support Cells? International Journal of Biochemistry & Cell Biology **39**; 661-665

Hedbom, E, Häuselmann, HJ (2002). Molecular Aspects of Pathogenesis in Osetoarthritis: the Role of Inflammation. Cellular and Molecular Life Sciences **59**; 45-53

Hesselson, D, Newman, C, Kim, KW, Kimble (2004). GON-1 and Fibulin have Antagonistic Roles in Control of Organ Shape. Current Biology **14**; 2005-2010

Hicks, DG, Longoria, G, Pettay, J, Grogan, T, Tarr, S, Tubbs, R (2004). *In Situ* Hybridization in the Pathology Laboratory: Genereal Principles, Automation, and Emerging Research Applications for Tissue-Based Studies of Gene Expression. Journal of Molecular Histology **35**; 595-601

Higuchi, R, Dollinger, G, Walsh, PS, Griffith, R (1992). Simultaneous Amplification and Detection of Specific DNA Sequences. Biotechnology (NY) **10**; 413-417

Hijova, E (2005). Matrix Metalloproteinases: Their Biological Functions and Clinical Implications. Bratislavské Lekárske Listy **106**; 127-132

Hirota, K (2002). Hypoxia-Inducible Factor 1, a Master Transcription Factor of Cellular Hypoxic Gene Expression. Journal of Anesthesia **16**; 150-159

Hoek, RM, Ruuls, SR, Murphy, CA, Wright, GJ, Goddard, R, Zurawski, SM, Blom, B, Homola, ME, Streit, WJ, Brown, MH, Barclay, AN, Sedgwick, JD (2000). Down-Regulation of the Macrophage Lineage through Interaction with OX2 (CD200). Science **290**; 1768-1771

Honisch, C, Chen, Y, Mortimer, C, Arnold, C, Schmidt, O, van den Boom, D, Cantor, CR, Shah, HN, Gharbia, SE (2007). Automated Comparative Sequence Analysis by Base-Specific Cleavage and Mass Spectrometry for Nucleic Acid-based Microbial Typing. Proceedings of the National Academy of Sciences **104**; 10649-10654

Hortega, P, del Rio, P (1921). Estudios Sobre La Neuroglia. La Glia de Escasas Radiciones (Oligodendroglia). Boletin de la Real Sociedad Espanola de la Historia Natural **21**; 63-92

Hosomi, N, Ban, CR, Naya, T, Takahashi, T, Guo, P, Song, XY, Kohno, M (2005). Tumour Necrosis Factor-Alpha Neutralization Reduced Cerebral Edema through Inhibition of Matrix Metalloproteinase Production after Transient Focal Cerebral Ischemia. Journal of Cerebral Blood Flow Metabolism **25**; 959-967

Hotfilder, M, Knupfer, H, Mohlenkamp, G, Pennekamp, P, Knupfers, M, Van Gool, S, Woolff, JE (2007). Interferon-Gamma Increases IL-6 Production in Human Glioblastoma Cell Lines. Anticancer Research **20**; 4445-50

Huang, T.-F (1998). What have Snakes Taught us about Integrins? Cellular and Molecular Life Sciences **54**; 527-540

Huang, J, Upadhyay, UM, Tamargo, RJ (2006). Inflammation in Stroke and Focal Cerebral Ischemia. Surgical Neurology **66**; 232-245

Hui, W, Barksby, HE, Young, DA, Cawston, TE, McKie, N, Rowan, AD (2005). Oncostatin M in Combination with Tumour Necrosis Factor α Induces a Chondrocyte Membrane Associated Aggrecanase that is Distinct from ADAMTS Aggrecanase-1 or - 2. Annals of the Rheumatic Diseases **64**; 1624-1632

Hurskainen, TL, Hirohata, S, Seldin, MF, Apte, SS (1999). ADAM-TS5, ADAM-TS6 and ADAM-TS7, Novel Members of a New Family of Zinc Metalloproteinases. Journal of Biological Chemistry **274**; 25555-25563

Iadecola, C, Salkowski, CA, Zhang, F, Aber, T, Nagayama, M, Vogel, SN, Ross, ME (1999). The Transcription Factor Interferon Regulatory Factor 1 is Expressed after Cerebral Ischemia and Contributes to Ischemic Brain Injury. Journal of Experimental Medicine **189**; 719-727

International Brain Injury Association (IBIA) (2007). Brain Injury Facts. http://www.internationalbrain.org/content.php?pages=facts at SHU 14/6/07

Janabi, N, Peudenier, S, Héron, B, NG, KH, Tardieu, M (1995). Establishment of Human Microglial Cell Lines after Transfection of Primary Cultures of Embryonic Microglial Cells with SV40 Large T Antigen. Neuroscience Letters **195**; 105-108

Jensen, MB, Hegelund, IV, Lomholt, ND, Finsen, B, Owens, T (2000). IFNgamma Enhances Microglial Reactions to Hippocampal Axonal Degeneration. Journal of Neuroscience **20**; 3612-3621

Jones, GC, Riley, GP (2005). ADAMTS Proteinases: A Multi-Domain, Multi-Functional Family with Roles in Extracellular Matrix Turnover and Arthritis. Arthritis Research & Therapy **7**; 160-169

Jongeneel, C.V., Bouvier,J. & Bairoch,A (1989). A Unique Signature Identifies a Family of Zinc-Dependent Metallopeptidases. FEBS Letters **242**; 211-214

Jung, Y-J, Isaacs JS, Lee, S, Trepel, J, Neckers, L (2003). IL-1β-Mediated Up-Regulation of HIF-1α via an NFκB /COZ-2 Pathway Identifies HIF-1 as a Critical Link between Inflammation and Oncogenesis. Journal of the Federation of American Societies for Experimental Biology **17**; 2115-2117

Jungers, KA, Le Goff, C, Somerville, RP, Apte SS (2005). *Adamts9* is Widely Expressed in Mouse Embryo Development. Gene Expression Patterns **5**; 609-17

Kashiwagi, M, Tortorella, M, Nagase, H, Brew, K (2001). TIMP-3 is a Potent Inhibitor of Aggrecanase 1 (ADAM-TS4) and Aggrecanase 2 (ADAM-TS5). Journal of Biological Chemistry **276**; 12501-12504

Kashiwagi, M, Enghild, JJ, Gendron, C, Hughes, C, Caterson, B, Itoh, Y, Nagase, H (2004). Altered Proteolytic Activities of ADAMTS-4 Expressed C-Terminal Processing. Journal of Biological Chemistry **279**; 10109-10119

Ke, Q, Costa, M (2006). Hypoxia-Inducible Factor-1 (HIF-1). Molecular Pharmacology **70**; 1469-1480

Keating, DT, Sadlier, DM, Patricelli, A, Smith, SM, Walls, D, Egan, JJ, Doran, PP (2006). Microarray Identifies ADAM Family Members as Key Responders to TGF-β1 in Alveolar Epithelial Cells. Respiratory Research **7**; 114-130

Kern, CB, Twal, WO, Mjaatvedt, CH, Fairey, SE, Toole, BP, Iruela-Arispe, ML, Argraves, WS (2007). Proteolytic Cleavage of Versican during Cardiac Cushion Morphogenesis. Developmental Dynamics **235**; 2238-2247

Kessler, E, Safrin, M (1994). The Propeptide of Pseudomonas aeruginosa Elastase Acts an Elastase Inhibitor. Journal of Biological **36**; 22726-22731

Kim, J, Kim, H, Lee, S-J, Choi, YM, Lee, SJ, Lee, JY (2005). Abundance of ADAM-8, -9, -10, -12, -15 and -17 and ADAMTS-1 in Mouse Uterus during the Oestrous Cycle. Reproduction, Fertility and Development **17**; 543-555

Kim, SU, de Vellis, J (2005). Microglia in Health and Disease. Journal of Neuroscience Research **81**; 302-313

Knudson, CB, Knudson, W (2001). Cartilage Proteoglycans. Cell & Development Biology **12**; 69-78

Komminoth, P, Merk, FB, Leav, I, Wolfe, HJ, Roth, J (1992). Comparison of 35S- and Digoxigenin-Labeled RNA and Oligonucleotide Probes for In Situ Hybridization Expression of mRNA of the Seminal Vesicle Secretion Protein II and Androgen Receptor Genes in the Rat Prostate. Histochemistry **98**; 217-28

Koo, B-H, Longpré, J-M, Somerville, RPT, Alexander, JP, Leduc, R, Apte, SS (2006). Cell-Surface Processing of Pro-ADAMTS9 by Furin. Journal of Biological Chemistry **281**; 12485-12494

Koo, B-H, Longpré, J-M, Somerville, RPT, Alexander, JP, Leduc, R, Apte, SS (2007). Regulation of ADAMTS9 Secretion and Enzymatic Activity by its Propeptide. Journal of Biological Chemistry **282**; 16146-16154

Kordula, T, Bugno, M, Rydel, RE, Travis, J (2000). Mechanism of Interleukin-1- and Tumour Necrosis Factor α-Dependent Regulation of the α₁-Antichymotrypsin Gene in Human Astrocytes. Journal of Neuroscience 20; 7510-7516

Kricka, LJ (1991). Chemiluminescent and Bioluminescent Techniques. Clinical Chemistry **37**; 1472-1481

Kuno, K, Kanada, N, Nakashima, E, Fujiki, F, Ichimura, F, Matsushima, K (1997). Molecular Cloning of a Gene Encoding a New Type of Metalloproteinase-Disintegrin Family Protein with Thrombospondin Motifs as an Inflammation Associated Gene. Journal of Biological Chemistry **272**; 556-562

Kuno, K, Terashima, Y, Matsushima, K (1999). ADAMTS-1 Is an Active Metalloproteinase Associated with the Extracellular Matrix. Journal of Biological Chemistry **274**; 18821-18826

Kuno, K, Okada, Y, Kawashima, H, Nakamura, H, Miyasaka, M, Ohno, H, Matsushima, K (2000). ADAMTS-1 Cleaves a Cartilage Proteoglycan, Aggrecan. FEBS Letters **478**; 241-245

Lahm, H-W, Langen, H (2000). Mass Spectrometry: A Tool for the Identification of Proteins Separation by Gels. Electrophoresis **21**; 2105-2114

Lai, J-P, Douglas, SD, Wang, Y-J, Ho, W-Z (2005). Real-Time Reverse Transcription-PCR Quantitation of Substance P Receptor (NK-1R) mRNA. Clinical and Diagnostic Laboratory Immunology **12**; 537-541

Lambert, E, Dassé, Emilie, Haye, B, Petitfrère, E (2004). TIMPs as Multifacial Proteins. Critical Reviews in Oncology/Hematology **49**; 187-198

Lee, DM, Weinblatt, ME (2001). Rheumatoid Arthritis. Lancet 358; 903-911

Lee, YB, Nagai, A, Kim, SU (2002). Cytokines, Chemokines, and Cytokine Receptors in Human Microglia. Journal of Neuroscience Research **69**; 94-103

Lee, KJ, Kim, H, Rhyu, IJ (2005). The Roles of Dendritic Spine Shapes in Purkinje Cells. Cerebellum **4**; 97-104

LeWinn, EB (1984). The Steroidal Actions of Digitalis. Perspectives in Biology and Medicine. **27**; 183-99

Little, CB, Mittaz, L, Belluoccio, D, Rogerson, FM, Campbell, IK, Meeker, CT, Bateman, JF, Pritchard, MA, Fosang, AJ (2005). ADAMTS-1-Knockout Mice do not Exhibit Abnormalities in Aggrecan Turnover In Vitro or In Vivo. Arthritis & Rheumatism **52**; 1461-1472

Liu, Y-L, Xu, Y, Yu, Q (2005). Full-Length ADAMTS-1 and the ADAMTS-1 Fragments display Pro- and Antimetastatic Activity, respectively. Oncogene **2005**; 1-16

Liu, W, Furuichi, T, Miyake, M, Rosenberg, GA, Liu, KJ (2007). Differential Expression of Tissue Inhibitor of Metalloproteinase-3 in Cultured Astrocytes and Neurons Regulates the Activation of Matrix Metalloproteinase-2. Journal of Neuroscience Research **85**; 829-836

Livak, KJ, Schmittgen, TD (2001). Analysis of Relative Gene Expression Data using Real-Time Quantitative PCR and the $2^{-\Delta\Delta C_T}$ Method. Methods **25**; 402-408

Llamazares, M, Cal, S, Quesada, V, López-Otín, C (2003). Identification and Characterization of ADAMTS-20 Defines a Novel Subfamily of Metalloproteinases-Disintegrins with Multiple Thrombospondin-1 Repeats and a Unique GON Domain. Journal of Biological Chemistry **278**; 13382-13389

Lo, PHY, Leung, ACC, Kwok, CYC, Cheung, WSY, Ko, JMY, Yang, LC, Law, S, Wang, LD, Li, J, Stanbridge, EJ, Srivastava, G, Tang, JCO, Tsao, SW, Lung, ML (2007). Identification of a Tumor Suppressive Critical Region Mapping to 3p14.2 in Esophageal Squamous Cell Carcinoma and Studies of a Candidate Suppressor Gene, *ADAMTS9*. Oncogene **26**; 148-157

Longa, EZ, Weinstein, PR, Carlson, S, Cummins, R (1989). Reversible Middle Cerebral Artery Occlusion without Craniectomy in Rats. Stroke **20**; 84-91

Longré, J-M and Leduc, R (2004). Identification of Prodomain Determinants Involved in ADAMTS-1 Biosynthesis. Journal of Biological Chemistry **279**; 33237-33245

López-Castejón G, Sepulcre, MP, Porca, FJ, Castellana, B, Planas, JV, Meseguer, J, Mulero, V (2007). The type II Interleukin-1 Receptor (IL-1RII) of the Bony Fish Gilthead Seabream *Sparus aurata* is Strongly Induced after Infection and Tightly Regulated at Transcriptional and Post-Transcriptional Levels. Molecular Immunology **44**; 2772-2780

López-Gallardo, M, Prada, C (2001). Spatial and Temporal Patterns of Morphogenesis of Hippocampal Pyramidal Cells: Study in the Early Postnatal Rat. Hippocampus **11**; 118-131

Lucas, S-M, Rothwell, NJ, Gibson, RM (2006). The Role of Inflammation in CNS Injury and Disease (2006). British Journal of Pharmacology **147**; S232-S240

Luehrsen, KR, Davidson, S, Lee, YJ, Rouhani, R, Soleimani, A, Raich, T, Cain, CA, Collarini, EJ, Yamanishi, DT, Pearson, J, Magee, K, Madlansacay, MR, Bodepudi, V, Davoudzadeh, D, Schueler, PA, Mahoney, W (2000). High-density Hapten Labeling and HRP Conjugation of Oligonucleotides for Use as In Situ Hybridization Probes to Detect mRNA Targets in Cells and Tissues. Journal of Histochemistry & Cytochemistry **48**; 113-145

Mackay, IM, Arden, KE, Nitsche, A (2002). Real-Time PCR in Virology. Nucleic Acids Research **30**; 1292-1305

Mackay, IM (2004). Real-Time PCR in the Microbiology Laboratory. Clinical Microbiology and Infection **10**; 190-212

Malfait, A-M, Liu, R-Q, Ijiri, K, Komiya, S, Tortorella, MD. (2002). Inhibition of ADAM-TS4 and ADAM-TS5 Prevents Aggrecan Degradation in Osteoarthritic Cartilage. Journal of Biological Chemistry **277**; 22201-8

Manalo, DJ, Rowan, A, Lavoie, T, Natarajan, L, Kelly, BD, Ye, SQ, Garcia, JGN, Semenza, GL (2005). Transcriptional Regulation of Vascular Endothelial Cell

Responses to Hypoxia by HIF-1. Hemostasis, Thrombosis and Vacular Biology *105*; 659-669

Markovic-Plese, S, Pinilla, C, Martin, R (2004). The Initiation of the Autoimmune Response in Multiple Sclerosis. Clinical Neurology and Neurosurgery **106**; 218-222

Mata, J, Marguerat, S, Bähler, J (2005). Post-Transcriptional Control of Gene Expression: a Genome-Wide Perspective. Trends in Biochemical Sciences **30**; 506-514

Matthews, RT, Gary, SC, Zerillo, S, Pratta, M, Solomon, K, Arner, EC, Hockfield, S (2000). Brain-enriched Hyaluronan Binding (BEHAB)/Brevican Cleavage in a Glioma Cell Line Is Mediated by a Disintegrin and Metalloproteinase with Thrombospondin Motifs (ADAMTS) Family Member. Journal Biological Chemistry **275**; 22695-22703

Mbele, GO, Deloulme, JC Benoît, Gentil, J, Delphin, C, Ferro, M, Garin, J, Takahashi, M, Baudier, J (2002). The Zinc- and Calcium-binding S100B Interacts and Co-localizes with IQGAP1 during Dynamic Rearrangement of Cell Membranes. Journal of Biological Chemistry **277**; 49998-500007

McNicol, AM, Farquharson, MA (1997). *In Situ* Hybridisation and its Diagnostic Applications in Pathology. Journal of Pathology **182**; 250-261

Mey, Jörg (2005). New Therapeutic Target for CNS Injury? The Role of Retinoic Acid Signalling after Nerve Lesions. Journal of Neurobiology **66**; 757-779

Miguel, RF, Pollak, A, Lubec, G (2005). Metalloproteinase ADAMTS-1 but not ADAMTS-5 is Manifold Overexpressed in Neurodegenerative Disorders as Sown Syndrome, Alzheimer's and Pick's Disease. Molecular Brain Research **133**; 1-5

Mulcahy, NJ, Ross, J, Rothwell, NJ, Loddick, SA (2003). Delayed Administration of Interleukin-1 Receptor Antagonist Protects against Transient Cerebral Ischaemia in the Rat. British Journal of Pharmacology **140**; 471-476

Munoz-Fernandez, MA, Fresno, M (1998). The Role of Tumor Necrosis Factor, Interleukin-6, Interferon-γ and Inducible Nitric Oxide Synthase in the Development and Pathology of the Nervous System. Progress in Neurobiology **56**; 307-340

Nakada, M, Miyamori, H, Kita, D, Takahashi, T, Yamashita, J, Sato, H, Miura, R, Yamaguchi, Y, Okada, Y (2005). Human Glioblastomas Overexpress ADAMTS-5 that Degrades Brevican. Acta Neuropathologica 110; 239-246

Nakamura, H, Fujii, Y, Inoki, I, Sugimoto, K, Tanzawaw, K, Matsuki, H, Miura, R, Yamaguchi, Y, Okada, Y (2000). Brevican is Degraded by Matrix Metalloproteinases and Aggrecanse-1 (ADAMTS4) at Different Sites. Journal of Biological Chemistry **275**; 38885-38890

Nakayama, K (1997). Furin: a Mammalian Subtilisin/Kex2p-Lie Endprotease involved in Processing of a Wide Variety of Precursor Proteins. Biochemical Journal **327**; 625-635

Nardi, JB, Gao, C, Kanost, MR (2001). The Extracellular Matrix Protein Lacunin is Expressed by a Subset of Hemocytes involved in Basal Lamina Morphogenesis. Journal of Insect Physiology **47**; 997-1006

National Statistics (2006). News Release, Heart Disease Leading Cause of Death in England & Wales. http://www.statistics.gov.uk/pdfdir/hsq0506.pdf at SHU 14/6/07

Nilsson, SK, Hulspas, R, Weier, HU, Quesenberry, PJ (1996). In Situ Detection of Individual Transplanted Bone Marrow Cells using FISH on Sections of Paraffin-Embedded Whole Murine Femurs. Journal of Histochemistry & Cytochemistry **44**; 1069-1074

Nimmerjahn, A, Kirchoff, F, Helmchen, F (2005). Resting Microglial Cells are Highly Dynamic Surveillants of Brain Parenchyma In Vivo. Science **27**; 1314-8

Norata, GD, Björk, H, Hamsten, A, Catapano, AL, Eriksson (2004). High-Density Lipoprotein Subfraction 3 Decreases ADAMTS-1 Expression Induced by

Lipopolysaccharide and Tumour Necrosis Factor-α in Human Endothelial Cells. Matrix Biology **22**; 557-560

O'Keefe, J (1999). Do Hippocampal Pyramidal Cells Signal Non-Spatial as well as Spatial Information? Hippocampus **9**; 352-364

Owens, T, Babcock, AA, Millward, JM, Toft-Hansen (2004). Cytokine and Chemokine Inter-Regulation in the Inflamed or Injured CNS. Brain Research Reviews **48**; 178-184

Parish, CR (2006). The Role of Heparan Sulphate in Inflammation. Nature Reviews Immunology **6**; 633-643

Perera, MN, Ma, HK, Arakawa, S, Howells, DW, Markus, R, Rowe, CC, Donnan, GA (2006). Inflammation following Stroke. Journal of Clinical Neuroscience 13; 1-8

Petty, MA, Lo, EH (2002). Junctional Complexes of the Blood-Brain Barrier: Permeability Changes in Neuroinflammation. Progress in Neurobiology **68**; 3110323

Pfefferkorn, T, Rosenberg, GA, (2003). Closure of the Blood-Brain Barrier by Matrix Metalloproteinase Inhibition Reduces rtPA-Mediated Mortality in Cerebral Ischemia with Delayed Reperfusion. Stroke **34**; 2025-2030

Plumb, J, Cross, AK, Surr, J, Haddock, G, Smith, T, Bunning, RAD, Woodroofe, MN (2005). ADAM-17 and TIMP3 Protein and mRNA Expression in Spinal Cord White Matter of Rats with Acute Experimental Autoimmune Encephalomyelitis. Journal of Neuroimmunology **164**; 1-9

Porter, S, Clark, IM, Kevorkian, L, Edwards, DR (2005). The ADAMTS Metalloproteinases. Biochemical Journal **386**; 15-27

Properzi, F, Asher, RA, Fawcett, JW (2003). Chondroitin Sulphate Proteoglycans in the Central Nervous System: Changes and Synthesis after Injury. Biochemical Society Transactions **31**; 335-336

Purves, D, Augustine, GJ, Fitzpatrick, D, Katz, LC, LaMantia, A-S, McNamara, JO, Williams, SM (2001). Neuroscience, 2nd Edition. Sinauer Associates, Inc

Quandt, K, Frech, K, Karas, H, Wingender, E, Werner, T (1995). MatInd and MatInspector: New Fast and Versatile Tools for Detection of Consensus Matches in Nucleotide Sequence Data. Nucleic Acids Research **23**; 4878-84

Rauch, U, Zhou, X-H, Roos, G (2005). Extracellular Matrix Alterations Lacking Four of its Components. Biochemical and Biophysical Research Communications **328**; 608-617

Rawlings, N.D., Morton, F.R. & Barrett, A.J. (2006) *MEROPS*: the Peptidase database. Nucleic Acids Research **34**; D270-D272

Relton, JK, Rothwell, NJ (1992). Interleukin-1 Receptor Antagonist Inhibits Ischaemic and Excitotoxic Neuronal Damage in the Rat. Brain Research Bulletin **29**; 243-246

Rheinhardt, JM, Finkbeiner, WE (2001). Protease XXIV Increases Detection of Mucin Gene Expression during In Situ Hybridization in Archival Tissue. Journal of Histochemistry & Cytochemistry **49**; 923-924

Rhodes, KE, Fawcett, JW (2004). Chondroitin Sulphate Proteoglycans: Preventing Plasticity or Protecting the CNS? Journal of Anatomy **204**; 33-48

Rodríguez-Manzaneque, JC, Milchanowski, AB, Dufour, EK, Leduc, R, Iruela-Arispe, ML (2000). Characterization of METH-1/ADAMTS-1 Processing Reveals Two Distinct Active Forms. Journal of Biological Chemistry **275**; 33471-33479

Rodríguez-Manzaneque, JC, Westling, J, Thai, SN.-M, Luque, A, Knauper, V, Murphy, G, Sandy, JD, Iruela-Arispe, ML (2002). ADAMTS1 Cleaves Aggrecan at Multiple Sites and is Differentially Inhibited by Metalloproteinase Inhibitors. Biochemical and Biophysical Research Communications **293**; 501-508

Rosenberg, GA, Cunningham, LA, Wallace, J, Alexander, S, Estrada, EY, Grossetete, M, Razhagi, A, Miller, K, Gearing, A (2001). Immunohistochemistry of Matrix

Metalloproteinases in Reperfusion Injury to Rat Brain: Activation of MMP-9 Linked to Stromelysin-1 and Microglia in Cell Cultures. Brain Research **893**; 104-112

Roughley, PJ (2006). The Structure and Function of Cartilage Proteoglycans. European Cells and Materials **12**; 92-101

Rubin, LL, Staddon, JM (1999). The Cell Biology of the Blood-Brain Barrier. Annual Reviews Neuroscience **22**; 11-28

Rucker, HK, Wynder, HJ, Thomas, WE (2000). Cellular Mechanism of CNS Pericytes. Brain Research Bulletin **51**; 363-369

Saito, K, Suyama, K, Nishida, K, Sei, Y, Basile, AS (1996). Early Increase in TNF-α, IL-6 and IL-1β Levels in Transient Cerebral Ischemia in Gerbil Brain. Neuroscience Letters **206**; 149-152

Sandy, JD, Neame, PJ, Boynton, RE, Flannery, CR (1991). Catabolism of Aggrecan in Cartilage Explants. Journal of Biological Chemistry **266**; 8683-8685

Sandy, JD, Verscharen, C (2001). Analysis of Aggrecan in Human Knee Cartilage and Synovial Fluid indicates that Aggrecanase (ADAMTS) Activity is Responsible for the Catabolic Turnover and Loss of whole Aggrecan whereas other Protease Activity is Required for C-terminal Processing In Vivo. Biochemical Journal **358**; 615-626

Sandy, JD, Westling, J, Kenagy, RD, Iruela-Arispe, ML, Verscharen, C, Rodriguez-Mazaneque, JC, Zimmermann, DR, Lemire, JM, Fischer, JW, Wight, TN, Clowes, AW (2001). Versican V1 Proteolysis in Human Aorta *In Vivo* occurs at the Glu^{441}-Ala^{442} Bond, a Site that is Cleaved by Recombinant ADAMTS-1 and ADAMTS-4. Journal of Biological Chemistry 276; 13372-13378

Santos, PC, Gottfried, C, Gehlen, G, Gonçalves, C-A, Achaval, M (2005). Distribution and Ontogeny of Gial Fibrillary Acidic Protein in the Snail *Megalobulimus Abbreviatus*. Comparative Biochemistry and Physiology, Part A **141**; 140-145

Sasaki, M, Seo-Kiryu, S, Kato, R, Kita, S-i, Kiyama, H (2001). A Disintegrin and Metalloprotease with Thrombospondin Type I Motifs (ADAMTS-1) and IL-1 Receptor

Type I mRNAs are Simultaneously Induced in Nerve Injured Motor Neurons. Molecular Brain Research **89**; 158-163

Sawada, M, Kiyono, T, Nakashima, S, Shinoda, J, Naganawa, T, Hara, S, Iwama, T, Sakai, N (2004). Molecular Mechanisms of TNF-α-Induced Ceramide Formation in Human Glioma Cells: P53-Mediated Oxidant Stress-Dependent and -Independent Pathways. Cell Death and Differentiation **11**; 997-1008

Schechter, I, Berger, A (1967). On the Size of the Active Site in Proteases. I. Papain. Biochemical and Biophysical Research Communications **27**; 157-62

Semenza, GL, Jiang, B-H, Leung, SW, Passantino, R, Concordet, J-P, Maire, P, Giallongo (1996). Hypoxia Response Elements in the Aldolase A, Enolase 1, and Lactate Dehydrogenase A Gene Promoters Contain Essential Binding Sites ofr Hypoxia-Inducible Factor 1. Journal of Biological Chemistry **271**; 32529-32537

Siegel, GJ, Agranoff, BW, Albers, RW, Fisher, SK, Uhler, MD (1999). Basic Neurochemistry, Molecular, Cellular, and Medical Aspects, 6th Edition. Lippincott, Williams & Wilkins

Silver, J, Miller, JH (2004). Regeneration Beyond the Glial Scar. Nature Reviews Neuroscience **5**; 146-156

Soejima, K, Matsumoto, M, Kokame, K, Yagi, H, Ishizashi, H, Maeda, H, Nozaki, C, Miyata, T, Fujimura, Y, Nakagaki, T (2003). ADAMTS-13 Cysteine-Rich/Space Domains are Functionally Essential for Von Willebrand Factor Cleavage. Blood **102**; 3232-3237

Sohn, M, Tan, Y, Wang, B, Klein, RL, Trojanowska, M, Jaffa, AA (2005). Mechanisms of Low-Density Lipoprotein-Induced Expression of Connective Tissue Growth Factor in Human Aortic Endothelial Cells (2006).American Journal of Physiology - Heart and Circulatory Physiology **290**; H1624-H1634

Somerville, RPT, Longpre, J-M, Jungers, KA, Engle, JM, Ross, M, Evanko, S, Wight, TN, Leduc, R, Apte, SS (2003). Characterization of ADAMTS-9 and ADAMTS-20 as a

distinct ADAMTS Subfamily Related to Caenorhabitis elegans GON-1. Journal of Biological Chemistry **278**; 9503-9513

Somerville, RPT, Longpre, J-M, Apel, ED, Lewis, RM, Wang, LW, Sanes, JR, Leduc, R, Apte, SS (2004). ADAMTS7B, the Full-Length Product of the *ADAMTS7* Gene, Is a Chondroitin Sulfate Proteoglycan Containing a Mucin Domain. Journal of Biological Chemistry **279**; 35159-35175

Song, R-H, Tortorella, MD, Malfait, A-M, Alston, JT, Yang, Z, Arner, EC, Griggs, DW (2007). Aggrecan Degradation in Human Articular Cartilage Explants is Mediated by Both ADAMTS-4 and ADAMTS-5. Arthritis & Rheumatism **56**; 575-585

Sospedra, M, Martin, R (2005). Immunology of Multiple Sclerosis. Annual Reviews Immunology **23**; 683-747

Stangel, M, Hartung, H-P (2002). Remyelinating Strategies for the Treatment of Multiple Sclerosis. Progress in Neurobiology **68**; 361-376

Stanton, H, Rogerson, FM, East, CJ, Golub, SB, Lawlor, KE, Meeker, CT, Little, CB, Last, K, Farmer, PJ, Campbell, IK, Fourie, AM, Fosang, AJ (2005). ADAMTS5 is the Major Aggrecanase in Mouse Cartilage *in vivo* and *in vitro*. Nature **434**; 648-652

Strachan, T, Read, AP (1999). Human Molecular Genetics 2, 2nd Edition. BIOS Scientific Publishers Ltd

Tada, M, Diserens, AC, Desbaillets, I, de Tribolet, N (1994). Analysis of Cytokine Messenger RNA Expression in Human Glioblastoma Cells and Normal Astrocytes by Reverse-Transcription Polymerase Chain Reaction. Journal of Neurosurgery **80**; 1063-73

Tang, BL (2001). ADAMTS: A Novel Family of Extracellular Matrix Proteases. International Journal of Biochemistry & Cell Biology **33**; 33-44

Tao, Zhenyin, Peng, Y, Nolasco, L, Cal, S, Lopez-Otin, C, Li, R, Moake, JL, Lopez, JA, Dong, J-f (2005). Recombinant CUB-1 Domain Polypeptide Inhibits the Cleavage of

ULVWF Strings by ADAMTS13 under Flow Conditions. Hemostasis, Thrombosis and Vascular Biology **106**; 4139-4145

Tesseur, I, Zou, K, Esposito, L, Bard, F, Berber, E, Van Can, J, Lin, AH, Crews, L, Tremblay, P, Mathews, P, Mucke, L, Masliah, E, Wyss-Coray, T (2006). Deficiency in Neuronal TGF-ß Signaling Promotes Neurodegeneration and Alzheimer's Pathology. Journal of Clinical Investigation **116**; 3060-3069

Thomas, G (2002). Furin at the Cutting Edge: From Protein Traffic to Embryogenesis and Disease. Nature Reviews Molecular Cell Biology **3**; 753-766

Tixier, E, Lalanne, F, Just, I, Galmiche, JP, Neunlist, M (2005). Human Mucosa/Submucosa Interactions during Intestinal Inflammation: Involvement of the Enteric Nervous System in Interleukin-8 Secretion. Cellular Microbiology **7**; 1798-1810

Tortorella, MD, Pratta, M, Liu, R-Q, Austin, J, Ross, OH, Abbaszade, I, Burn, T, Arner, E (2000). Sites of Aggrecan Cleavage by Recombinant Human Aggrecanase-1 (ADAMTS-4). Journal of Biological Chemistry **275**; 18566-18573

Tortorella, MD, Arner, EC, Hills, R, Easton, A, Korte-Sarfaty, J, Fok, K, Wittwer, AJ, Liu, R-Q, Malfait, A-M (2004). α_2-Macroglobulin is a Novel Substrate for ADAMTS-4 and ADAMTS-5 and Represents an Endogenous Inhibitor of these Enzymes. Journal of Biological Chemistry **279**; 17554-17561

Tortorella, MD, Arner, EC, Hills, R, Gormley, J, Fok, K, Pegg, L, Munie, G, Malfait, A-M (2005). ADAMTS-4 (aggrecanase-1): N-Terminal activation mechanisms. Archives of Biochemistry and Biophysics **444**; 34-44

Toulmond, S, Rothwell, NJ (1995). Interleukin-1 Receptor Antagonist Inhibits Neurological Damage Caused by Fluid Percussion Injury in the Rat. Brain Research **671**; 261-266

Tran, EH, Prince EN, Owens, T (2000). IFN-γ Shapes Immune Invasion of the Central Nervous System via Regulation of Chemokines. Journal of Immunology **164**; 2759-68

Trendelenburg, G, Dirnagl, U (2005). Neuroprotective Role of Astrocytes in Cerebral Ischemia: Focus on Ischemice Preconditioning. Glia **51**; 307-320

Tsiola, A, Hamzei-Sichani, F, Peterlin, Z, Yuste, R (2003). Quantitative Morphologic Classification of Layer 5 Neurons from Mouse Primary Visual Cortex. Journal of Comparative Neurology **461**; 415-428

Turner, PC, McLennan, AG, Bates, AD, White, MRH (2001). Molecular Biology: Instant Notes, 2nd Ed. BIOS Scientific Publishers Ltd

Turner, N, Nolasco, L, Tao, Z, Dong, JF, Moake, J (2006). Human Endothelial Cells Synthesize and Release ADAMTS-13. Journal of Thrombosis and Haemostasis **4**; 1396-1404

Uno, H, Matsuyama, T, Akita, H, Nishimura, H, Sugita, M (1997). Induction of Tumor Necrosis Factor-α in the Mouse Hippocampus following Transient Forebrain Ischemia. Journal of Cerebral Blood Flow & Metabolism **17**; 491-499

Vaccarino, FM, Fagel, DM, Ganat, Y, Maragnoli, ME, Ment, LR, Ohkubo, Y, Schwartz, ML, Silbereis, J, Smith, KM (2007). Astroglial Cells in Development, Regeneration, and Repair. Neuroscientist **13**; 173-185

Van den Beucken, T, Koritzinsky, M, Wouters, BG (2006). Translational Control of Gene Expression during Hypoxia. Cancer Biology and Therapy **5**; 749-55

Van Wart, HE, Birkedal-Hansen, H (1990). The cysteine switch: A principle of regulation of metalloproteinase activity with potential applicability to the entire matrix metalloproteinase gene family. Proceedings of the National Academy of Sciences USA **87**; 5578-5582

Vandesompele, J, De Preter, K, Pattyn, F, Poppe, B, Van Roy, N, De Paepe, A, Speleman, F (2002). Accurate Normalisation of Real-Time Quantitative RT-PCR Data by Geometric Averaging of Multiple Internal Control Genes. Genome Biology **3**; 0034.1-0034.11

Vankemmelbeke, MN, Jones, GC, Fowles, C, Ilic, MZ, Handley, CJ, Day, AJ, Knight, CG, Mort, JS, Buttle, DJ (2003). Selective Inhibition of ADAMTS-1, -4 and -5 by Catechin Gallate Esters. European Journal of Biochemistry **270**; 2394-2403

Vaughan, PC, van Wijnen, AJ, Stein, JL, Stein, GS (1997). Interferon Regulatory Factors: Growth Control and Histone Gene Regulation – It's Not Just Interferon Anymore. Journal of Molecular Medicine **75**; 348-359

Vázquez, F, Hastings, G, Ortega, M-A, Lane, TF, Oikemus, S, Lombardo, M, Iruela-Arispe, ML (1999). METH-1, a Human Ortholog of ADAMTS-1, and METH-2 are Members of a New Family of Proteins with Angio-Inhibitory Activity. Journal of Biological Chemistry **274**; 23349-23357

Viapiano, MS, Matthews, RT (2006). From Barriers to Bridges: Chondroitin Sulphate Proteoglycans in Neuropathology **12**; 488-496

Vilhardt, F (2005). Microglia: Phagocyte and Glia Cell. International Journal of Biochemistry & Cell Biology **37**; 17-21

Viviani, B, Bartesaghi, S, Corsini, E, Galli, CL, Marinovich, M (2004). Cytokines Role in Neurodegenerative Events. Toxicology Letters **149**; 85-89

Wahl, S (2007). Transforming Growth Factor-β: Innately Bipolar. Current Opinion in Immunology **19**; 55-62

Wallenstein, S, Zucker, CL, Fleiss, JL (1980). Some Statistical Methods Useful in Circulation Research. Circulation Research **47**; 1-9

Wang, S, Sdrulla, AD, diSibio, G, Bush, G, Nofziger, D, Hicks, C, Weinmaster, G, Barres, BA (1998). Notch1 Receptor Activation Inhibits Oligodendrocyte Differentiation. Neuron **21**; 63-75

Wang, CX, Shuaib, A (2002). Involvement of Inflammatory Cytokines in Central Nervous Injury. Progress in Neurobiology **67**; 161-172

Wang, H, Ubll, JJ, Stricker, R, Reiser, G (2002). Thrombin (PAR-1)-induced proliferation in astrocytes via MAPK involves multiple signaling pathways. American Journal of Cell Physiology **283**; C1351-64

Wang, P, Tortorella, M, England, K, Malfait, A-M, Thomas, G, Arner, EC, Pei, D (2004). Proprotein Convertase Furin Interacts with and Cleaves Pro-ADAMTS-4 (Aggrecanase-1) in the *Trans*-Golgi Network. Journal of Biological Chemistry **279**; 15434-15440

Wang, LW, Dlugosz, M, Somerville, RPT, Raed, M, Haltiwanger, RS, Apte, SS (2007). O-Fucosylation of Thrombospondin Type 1 Repeats in ADAMTS Like-1/Punctin-1 Regulates Secretion: Implications for the ADAMTS superfamily. Journal of Biological Chemistry **23**; 17024-17031

Wang, Q, Tang, XN, Yenari, MA (2007). Inflammatory Response in Stroke. Journal of Neuroimmunology **184**; 53-68

Werner, P, Pitt, D, Raine, CS (2001). Multiple Sclerosis : Altered Glutamate Homeostasis in Lesions Correlates with Oligodendrocytes and Axonal Damage. Annals of Neurology **50**; 169-180

Westling, J, Gottschall, PE, Thompson, VP, Cockburn, A, Perides, G, Zimmermann, DR, Sandy, JD (2004). ADAMTS4 (Aggrecanase-1) Cleaves Human Brain Versican V2 at Glu405-Gln406 to Generate Glial Hyaluronate Binding Protein. Biochemical Journal **377**; 787-795

Williams, BJ, Eriksdotter-Jonhagen, M, Granholm, A-C (2006). Nerve Growth Factor in Treatment and Pathogenesis of Alzheimer's Disease. Progress in Neurobiology **80**; 114-128

Wong, ML, Medrano, JF (2005). Real-Time PCR for mRNA Quantitation. International Journal of Life Science Methods **39**; 75-85

Wouters, BG, van den Beucken, T, Magagnin, MG, Koritzinsky, M, Fels, D, Koumenis, C (2005). Control of the Hypoxic Response through Regulation of mRNA Translation. Seminars in Cell & Developmental Biology **16**; 487-501

Yamaguchi, Y (2000). Lecticans: Organizers of the Brain Extracellular Matrix. Cellular and Molecular Life Sciences **57**; 276-289

Yamaji, N, Nishimura, K, Abe, K, Ohara, O, Nagase, T, Nomura, N (2004). Metalloproteinase having Aggrecanase Activity. US Patent 6,716,613

Yamasaki, T, Kawaji, K, Ono, K, Bito, H, Hirano, T, Osumi, N, Kengaku, M (2001). *Pax6* Regulates Granule Cell Polarization during Parallel Fiber Formation in the Developing Cerebellum. Development **128**; 3133-3144

Yao, J, Kim, TW, Qin, J, Jiang, Z, Qian, Y, Xiao, H, Lu, Y, Wen, Q, Gulen, MF, Sizemore, N, DiDonato, J, Sato, S, Akira, S, Su, B, Li, X (2006). Interleukin-1 (IL-1)-induced TAK1-dependent *Versus* MEKK3-dependent NFκB Activation Pathways Bifurcate at IL-1 Receptor-associated Kinase Modification. Journal Biological Chemistry **282**; 6075-6089

Yiallouros, I, Berkhoff, EG, Stöcker, W (2000). The Roles of Glu93 and Tyr149 in Astacin-Like Zinc Peptides. FEBS Letters **484**; 224-228

Yin, K-J, Cirrito, JR, Yan, P, Hu, X, Xiao, Q, Pan, X, Bateman, R, Song, H, Hsu, F-F, Turk, J, Xu, J, Hsu, CY, Mills, JC, Holtzman, DM, Lee, J-M (2006). Matrix Metalloproteinases Expressed by Astrocytes Mediate Extracellular Amyloid-β Peptide Catabolism. Journal of Neuroscience **26**; 10939-1-948

Yu, W-H, Yu, S-sC, Meng, Qi, Brew, K, Woessner Jr., JF (2000). TIMP-3 Binds to Sulfated Glycosaminoglycans of the Extracellular Matrix. Journal of Biological Chemistry **275**; 31226-31232

Zeng, W, Corcoran, C, Collins-Racie, LA, LaVallie, ER, Morris, EA, Flannery, CR (2006). Glycosaminoglycan-Binding Properties and Aggrecanase Activities of Truncated ADAMTSs: Comparative Analyses with ADAMTS-5, -9, -16 and -18. Biochemica et Biophysica Acta **1760**; 517-524

Zhang, Z, Chopp, M, Powers, C (1997). Temporal Profile of Microglial Response following Transient (2h) Middle Cerebral Artery Occlusion. Brain Research **744**; 189-198

Zheng, X, Chung, D, Takayama, TK, Majerus, EM, Sadler, JE, Fujikawa, K (2001). Structure of von Willebrand Factor-Cleaving Protease (ADAMTS13), a Metalloprotease Involved in Thrombotic Thrombocytopenic Purpura. Journal of Biological Chemistry **276**; 41059-41063